TECHNISCHE UNIVERSITÄT DARMSTADT

Development and Characterization of a FKBP51FK1 Affinity Matrix for Protein-Protein Interaction Studies

Entwicklung und Charakterisierung einer FKBP51FK1 Affinitätsmatrix für Protein-Protein-Interaktionsstudien

Vom Fachbereich Chemie
der Technischen Universität Darmstadt

zur Erlangung des Grades
Doctor rerum naturalium (Dr. rer. nat.)

Dissertation von
Stephanie Katharina Merz, Dipl.-Chem.

Erstgutachter: Prof. Dr. Felix Hausch
Zweitgutachter: Prof. Dr. Alexander Löwer

Darmstadt 2022

Überarbeitete Version vom 04.12.2022

Tag der Einreichung: 11. Januar 2022

Tag der mündlichen Prüfung: 11. April 2022

Merz, Stephanie Katharina: Development and Characterization of a FKBP51FK1 Affinity Matrix for Protein-Protein Interaction Studies
Darmstadt, Technische Universität Darmstadt,
Jahr der Veröffentlichung der Dissertation auf TUprints: 2022
URN: urn:nbn:de:tuda-tuprints-229587
Tag der mündlichen Prüfung: 11.04.2022

Erklärungen laut Promotionsordnung

§8 Abs. 1 lit. c PromO

Ich versichere hiermit, dass die elektronische Version meiner Dissertation mit der schriftlichen Version übereinstimmt und für die Durchführung des Promotionsverfahrens vorliegt.

§8 Abs. 1 lit. d PromO

Ich versichere hiermit, dass zu einem vorherigen Zeitpunkt noch keine Promotion versucht wurde und zu keinem früheren Zeitpunkt an einer in- oder ausländischen Hochschule eingereicht wurde. In diesem Fall sind nähere Angaben über Zeitpunkt, Hochschule, Dissertationsthema und Ergebnis dieses Versuchs mitzuteilen.

§9 Abs. 1 PromO

Ich versichere hiermit, dass die vorliegende Dissertation selbstständig und nur unter der Verwendung der angegebenen Quellen verfasst wurde.

§9 Abs. 2 PromO

Die Arbeit hat bisher noch nicht zu Prüfungszwecken gedient.

Darmstadt, 11.01.2022

Table of Content

Zusammenfassung

Das FK506 bindende Protein FKBP51 spielt eine Rolle bei psychischen Erkrankungen wie zum Beispiel Depression und Angststörung. Zudem wird FKBP51 auch bei metabolischen Erkrankungen wie Fettleibigkeit und Diabetes sowie im Kontext von Krebserkrankungen und chronischem Schmerz beschrieben. Jedoch sind die zugrunde liegenden zellulären Funktionen und biologischen Mechanismen kaum bekannt.

Die FKBP-Familie umfasst eine Vielzahl von Mitgliedern mit großen strukturellen Ähnlichkeiten, wodurch die Entwicklung von maßgeschneiderten Liganden zu einer Herausforderung wird. Dennoch ist FKBP51 ein interessantes Zielprotein für die Wirkstoffforschung. Zwei Leitstrukturen, SAFit1 und SAFit2, die eine hohe Selektivität für FKBP51 im Vergleich zu dem biologischen Gegenspieler FKBP52 aufweisen, wurden von der Arbeitsgruppe von Herrn Professor Felix Hausch entwickelt. Beide Substanzen interagieren mit der Bindungstasche innerhalb der FK1 Domäne von FKBP51.

Die Charakterisierung des FKBP51 Proteininteraktionsnetzwerks ist ein Ansatz zur Untersuchung der biologischen Funktionen von FKBP51. Zudem können anhand von Proteininteraktionspartnern Rückschlüsse auf die zugrunde liegenden molekularen Mechanismen und Signaltransduktionswege gezogen werden. Während der Doktorarbeit wurde eine FKBP51FK1 Affinitätsmatrix zur Anreicherung von möglichen Proteinbindungspartnern, die mit der FK1 Domäne interagieren, entwickelt. Dabei wurde das Herstellungsverfahren für die Affinitätsmatrix optimiert. Zur Charakterisierung der FKBP51FK1 Affinitätsmatrix wurde ein fluoreszenzbasierter Bindungsassay entwickelt. Hierbei wurde die Integrität der Bindungstasche durch die Bindung und kompetitive Elution eines mit Fluorescein markierten FKBP Liganden gezeigt. Zur Anreicherung von potentiellen FKBP51 Interaktionspartnern aus Zelllysaten, die mit der Bindungstasche der FK1 Domäne wechselwirken, wurden Pull-Down Assays mit FKBP51 als „Köder“ entwickelt. Die Proteinanreicherung wurde mittels „Peptidmassenfingerprinting“ in Kooperation mit SINTEF Industry in Trondheim untersucht.

Zudem wurden neu entwickelte FKBP Liganden mittels Fluoreszenzpolarisationsassay charakterisiert. Hierbei wurden hoch affine FKBP Liganden mit Dissoziationskonstanten im pikomolaren Bereich identifiziert. Weiterhin wurde eine makrozyklische chemische Substanz mit Selektivität für FKBP51 im Vergleich zu FKBP12 identifiziert.

Abstract

The FK506 binding protein 51 (FKBP51) plays a role in psychiatric diseases such as major depression and anxiety. Several studies indicated that FKBP51 is also related to cancer, chronic pain and metabolic disorders such as obesity and diabetes. However, the underlying cellular and molecular biological mechanisms are poorly understood.

FKBP51 belongs to the FKBP protein family that includes several FK506 binding proteins sharing structural identities. In the last years, FKBP51 has emerged as a drug target, even though the structural similarity of FKBPs makes the development of selective FKBP ligands still challenging. Two FKBP lead compounds, SAFit1 and SAFit2, showing selectivity for FKBP51 in comparison with the biological counterpart FKBP52, were developed by the Hausch research group some years ago. Both compounds interact with the binding pocket of the FK1 domain. Unfortunately, the biological function of FKBP51 and the cellular effects of FKBP ligands are hardly understood until now.

The aim of the PhD project was to gain insights into the FKBP51 protein interaction network. The identification of FKBP51 binding partners is a good starting point for elucidating cellular functions, the underlying signal transduction and signaling pathways of FKBP51. The project was focused on the enrichment of potential FKBP51 binding proteins interacting with the binding pocket of the FK1 domain. For this purpose, a FKBP51FK1 affinity matrix was developed and the affinity matrix preparation protocol was optimized. A fluorescence-based binding assay was developed to characterize the FKBP51FK1 affinity matrix. The binding pocket integrity was shown by the binding and competitive elution of a fluorescein-labeled FKBP ligand. A pull-down assay applying FKBP51FK1 as bait was developed to enrich potential FKBP51 binding proteins from cell lysates. The protein enrichment was assessed by a bottom-up proteomic approach in cooperation with SINTEF Industry in Trondheim.

Another part of the PhD thesis dealt with the characterization of new FKBP ligands by competitive fluorescence polarization assays. Here, high affinity ligands showing dissociation constants in the picomolar range were discovered. In addition to that, a macrocyclic compound showing selectivity for FKBP51 in comparison with FKBP12 was identified.

1. Introduction

1.1. The FK506 Binding Protein (FKBP) Family

The FK506 binding proteins (FKBPs) and the cyclosporin A-binding cyclophilins belong to the family of immunophilins named and characterized by the binding of immunosuppressant drugs. The immunosuppressive FKBP ligands FK506 (Tacrolimus), a natural macrolide, and Rapamycin (Sirolimus) were focused in several studies. Various FKBP family members have been described: FKBP12, FKBP12.6, FKBP13, FKBP25, FKBP38, FKBP51 and FKBP52 [37].

FKBP51 was related to various disease such as psychiatric, stress-related (depression, anxiety post-traumatic stress disorder) and metabolic disorders (obesity and diabetes) [37] as well as chronic pain [60] and cancer [75].

Different molecular functions, biological processes and pathways have been related to FKBPs and FKBP-drug complexes. The T-cell activation is inhibited by the binding of the immunosuppressive drug FK506 to the FKBP12 binding pocket for example [39, 82, 95]. In short, calcineurin, a Ca^{2+}- and calmodulin dependent serine/threonine phosphatase interacts with the FK506/FKBP12 complex inhibiting the dephosphorylation of the nuclear factor of activated T-cells (NF-AT) [56, 56, 57] causing immunosuppression [63]. The binding of Rapamycin to FKBP12 inhibits the serine/threonine kinase activity of FRAP (FKBP12-Rapamycin associated protein)/mTOR (mammalian target of rapamycin) [14, 15, 76]. FKBP12 and FKBP12.6 play also a role in ryanodine receptor regulation and signaling [2, 5, 9, 22, 45, 86, 92, 92, 97, 105, 107]. FKBP51 and FKBP52 are described as Hsp90 co-chaperones and as part of the steroid hormone receptor complexes. Several studies indicated the involvement of FKBP51 in the AKT and NFκB pathway [3, 7, 13, 26, 37, 47, 50, 59, 68, 74].

1.2. Structure of FKBP51

FKBP51 is consisting of three domains (Figure 1): (1) the *N*-terminal located FK1 (a FKBP-type) domain showing peptidyl-prolyl *cis-trans* isomerase (PPIase), (2) the FK2 (a FKBP-like) domain, (3) the *C*-terminal located three unit repeat of the tertratricopeptide repeat (TPR) domain exhibiting the major Hsp90 binding site for the MEEVD motif [37, 77, 83]. The FK1 domain exhibiting structural similarities with FKBP12 is built by 5 antiparallel β-strands that are curved around a central α-helix [83]. The TPR domain comprises 7 α-helices [37, 83]. The binding of the natural ligands FK506 and Rapamycin inhibits the PPIase activity [37].

48% sequence identity and 60% similarity were found for FKBP12 and the FK1 domain as well as 26% sequence identity and 44% similarity for the FK2 domain and FKBP12 [83]. FKBP51 and its close homologue FKBP52 share a sequence identity of 60% and a similarity of 75% but the relative orientation of the domains is different [37, 104].

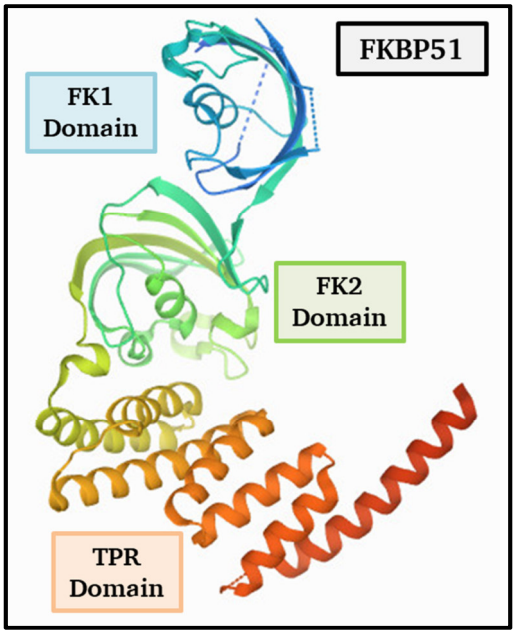

Figure 1: Crystal Structure of FKBP51.

FKBP51 is consisting of three domains: (1) *N*-terminal located FK1 domain (blue), (2) FK2 domain (green) and (3) *C*-terminal located three unit repeat of the TPR domain (yellow-red). Image from RCSB PDB (rcsb.org) of PDB ID 1KT0 [83].

1.3. FKBP Interacting Proteins

1.3.1. Hsp90

FKBP51 has been described as Hsp90 co-chaperone. Hsp90 regulates the folding and formation of large protein-protein complexes [21]. The FKBP51/Hsp90 interaction is well characterized. The binding of FKBP51 to Hsp90 mediated by its *C*-terminal MEEVD motif was demonstrated [37, 37, 54, 83]. Other studies suggest the involvement of additional interaction sites beside the MEEV motif including the FK1 and FK2 domain [17, 37, 64]. A mass spectrometry based study by Ebong *et al.* indicated a FKBP51 driven displacement of Hsp70 and Hop from the GR/Hsp90 complex [25, 37].

1.3.2. Steroid Hormone Receptors

FKBP51 and FKBP52 interact with steroid hormone receptor (SHR) complexes [37]. The glucocorticoid (GR), the progesterone (PR), the androgen (AR), the estrogen (ER) and the mineralcorticoid receptor (MR) belong to the SHR family. Schülke *et al.* studied the effect of FKBP51, FKBP52 and other TPR containing proteins on steroid hormone receptors by reporter gene and co-immunoprecipitation assays [78]. The GR, MR, PR and AR were inhibited by FKBP51 in contrast to FKBP52. No effect on ER was observed [78]. In another study, the association of FKBP51 with the GR and the PR was shown [8].

The *fkbp5* gene, encoding FKBP51, is induced by glucocorticoids [12, 99]. Experimental evidence for a negative feedback regulation of the GR by FKBP51 was shown [73]. The transcriptional activity of the GR is lowered by increased FKBP51 expression. FKBP51 and FKBP52 have antagonistic effects on steroid hormone receptor function. The steroid hormone receptor signaling is reduced by FKBP51 [72] and enhanced by FKBP52. The study by Reynolds *et al.* indicated glucocorticoid resistance by FKBP51 overexpression in squirrel monkeys showing high circulating cortisol levels and reduced GR hormone-binding affinity. The incorporation of FKBP51 into the GR complex was inhibited by FK506 [72].

1.3.3. AKT

FKBP51 might serve as a scaffolding protein in the AKT pathway and act as a negative regulator. FKBP51 is supposed to recruit PHLPP (PH domain leucine-rich repeat-containing protein phosphatase) to AKT resulting in its dephosphorylation [7, 68]. Experimental evidence for the direct interaction between the FK1 domain of FKBP51 was given but the interaction was not affected by FKBP ligands [26]. The deubiquitinase USP49 was described as a regulator of the AKT pathway by deubiquitinating FKBP51 [37, 59].

1.3.4. NFκB Signaling

Various FKBP51 interaction partners involved in the NFκB pathway have been reported but the findings are controversial and under discussion. The most often described FKBP51 binding partners are the members of IKK complex: IKKα, IKKβ and IKKγ [3, 13, 47, 50, 74].

1.4. FKBP Ligands

The key compounds SAFit1 and SAFit2 show a high selectivity towards FBP51 in comparison with FKBP52. Upon binding to FKBP51 phenylalanine 67 is switched from the binding site to an outward conformation [27]. A cellular effect of SAFit1 was shown by a neurite outgrowth assay. The neurite outgrowth was stimulated by the FKBP ligand SAFit1 in a dose-dependent manner but the underlying mechanisms are still unclear [28].

1.5. Proteomics

1.5.1. Application

Mass spectrometry (MS) based proteomics enables the identification, characterization and quantification of proteins in complex biological samples [24, 38, 58, 69]. The method is used in the basic protein research to analyze the proteome of biological specimens such as cells, cellular compartments, tissues and body fluids (e.g. blood) under different conditions or in a disease related context [24, 38]. MS based proteomics is a useful tool for studying protein-protein interactions, the expression levels of proteins and post-translational protein modifications (PTMs) such as phosphorylation and glycosylation as well as for peptide sequencing [24, 38, 49, 69, 103]. Proteomic studies provide a good starting point to gain insights into cellular functions, cellular processes, signal transduction, pathways and cell signaling.

1.5.2. Bottom-Up and Top-Down Proteomics

Bottom-up proteomics aims at the proteome analysis by peptide sequencing [38]. In short, proteins in a sample are digested by a protease and the resulting peptides are analyzed by MS [23, 24, 38, 69]. The MS data are converted and processed for peptide identification [24, 38]. The MS spectra are matched with peptides and finally proteins are assigned to the identified peptides [23, 24, 38, 96]. The peptide and protein identification relies on different bioinformatics algorithms, search engines and data bases [24, 38, 96] (Figure 2). Analyzing peptides instead of complete proteins by MS offers the following advantages. In most cases, soluble peptides that are compatible with the ionization method can be generated from proteins whereas parent proteins might show a low solubility [23]. The sensitivity for MS based peptide detection is higher than for protein detection [23].

Intact proteins are analyzed and characterized by a top-down proteomic approach [69]. This method is used to investigate PTMs or splice variations [69]. The progress in the field might

contribute to the identification of new biomarkers and protein drug targets [24]. MS based proteomics plays also an important role in clinical diagnostics [24].

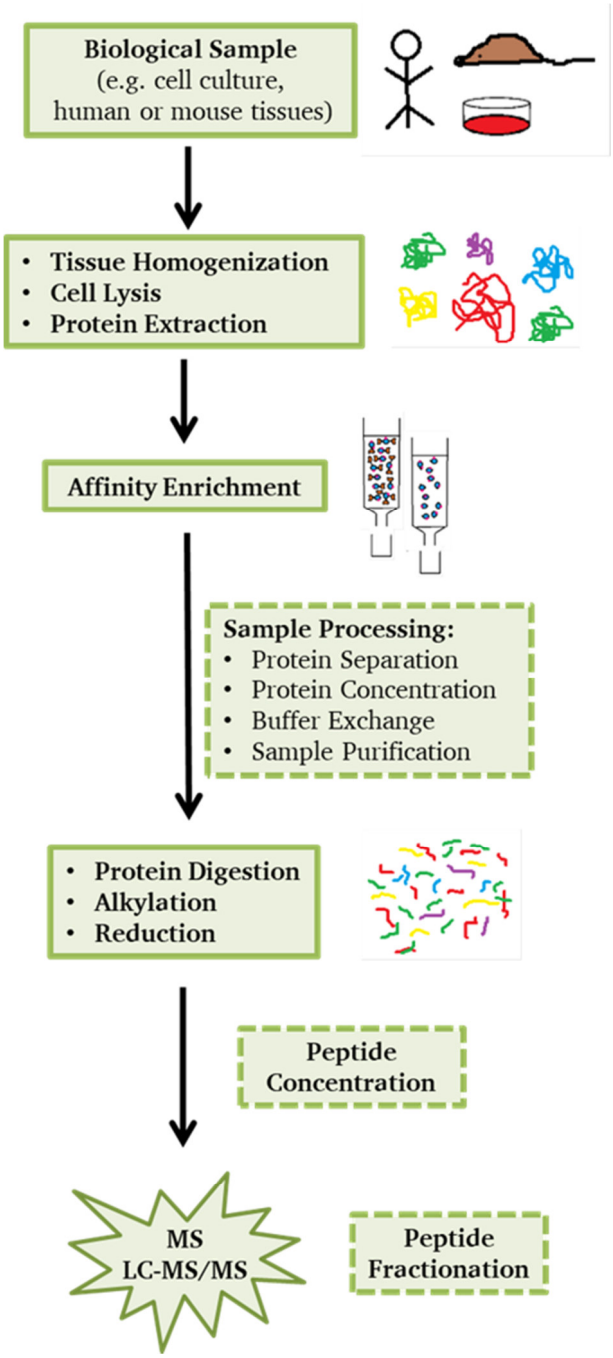

Figure 2: Sample Preparation for a Bottom-Up Proteomic Approach.

1.5.3. Sample Preparation for a Bottom-Up Proteomic Approach

Buffer Exchange, Protein Fractionation and Concentration

Desalting, buffer exchange, the removal of impurities and detergents interfering with the subsequent MS analysis as well as protein fractionation and sample concentration are crucial steps prior MS analysis. Several technical methods have been described for this purpose. The sample preparation method should be selected on the basis of the sample complexity, the abundance of the target protein(s), the sample buffer compatibility with the subsequent MS analysis, the sensitivity of the mass spectrometer and the complexity of the data analysis. The availability of the required equipment and the costs are limiting factors.

Protein precipitation with organic solvents such as acetone, methanol or ethanol is a less expensive, simple method for desalting and sample concentration [24].

Protein separation by (gel) electrophoresis or size exclusion chromatography (SEC) could be beneficial to reduce the sample complexity prior MS analysis. However, protein fractionation might be unlikely due to sample loss. As an advantage of (gel) electrophoretic methods the removal of salts or detergents and the protein separation are enabled in one step [24].

Detergent Compatibility

Biological assays or the sample collection for downstream MS analysis can include the use of detergents. Cell lysis buffers are supplemented with non-ionic detergents (e.g. Triton X-100, digitonin, CHAPS, Nonidet P40 substitute) to solubilize membrane proteins for example [24, 58]. Strong denaturing agents (e.g. urea, guanidine hydrochloride, sodium dodecyl sulfate, sodium deoxycholate) can also be used for cell lysis [24, 33, 58] depending on the downstream application. Moreover, detergents are required for protein solubilization [58] and degradation ensuring the accessibility of proteolytic cleavage sites in the digestion step [24, 79]. Detergents such as sodium dodecyl sulfate (SDS) are used to address hydrophilic and hydrophobic proteins [58]. Detergents carrying polyethylene glycol units (e.g. Nonidet P40 substitute, Triton-X 100, Tween) are eluted during liquid chromatography and suppress peptide based signals [24]. The strong ionic detergent SDS used for protein denaturation can also cause signal suppression at low levels of 0.01% [24]. Alternatively, the detergents *N*-octyl-beta glucoside or octylthioglucoside can be used [24]. In addition to that, detergents that are degraded by heating or at a low pH level have been developed for MS based applications (e.g. ProteasMax™ by Promega [79], *Rapi*Gest SF Surfactant by Waters [33], PPS

Silent® Surfactant by expedeon, Progenta™ Anionic Acid Labil Surfactants by Protea Biosciences) [24]. The digestion methods suspension-trapping (S-Trap) or filter aided sample preparation (FASP) enabling the removal of SDS provide a possibility to exploit the advantages of lysis/assay buffers supplemented with SDS and to overcome the negative effects on the LC-MS analysis caused by amphiphilic detergents [38, 58].

Protein Digestion

The protease trypsin showing a high catalytic activity is most commonly applied for protein digestion [23, 24]. The protein cleavage leads to the generation of peptides with *C*-terminal located arginine or lysine residues that are beneficial for collision-induced dissociation (CID) tandem mass spectrometry [24].

Various digestion methods (Figure 3) including in-solution, in-gel and on bed digestion as well as filter based methods such as S-Trap and FASP have been described [24, 35, 38, 58, 80].

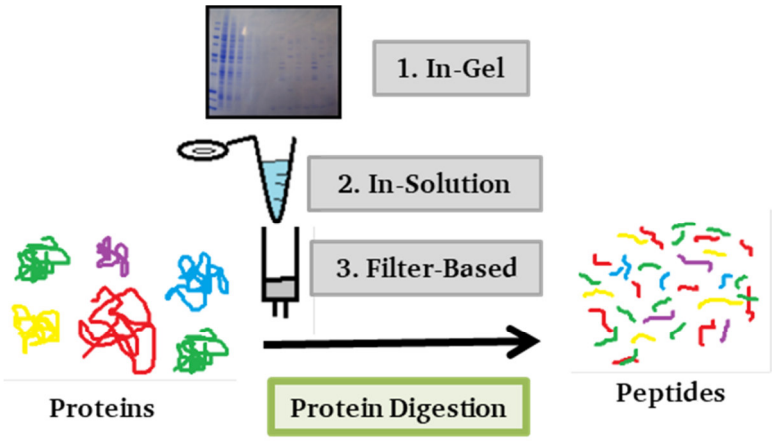

Figure 3: Protein Digestion Methods.

The S-Trap protocol is compatible with up to 5% SDS. The principle relies on the preparation of a particulate protein suspension by adding phosphoric acid and a buffer made of methanol (90%) and triethylammonium bicarbonate (100 mM) [38, 58]. The protein suspension is trapped by a stack of filters [38, 58]. FASP includes the following steps. Firstly, samples supplemented with SDS are loaded on a filter and washed with urea (8 M) to remove SDS [58]. Secondly, additional wash steps are performed to remove urea [58]. Thirdly, the protease is added to the filter membrane for protein digestion [58]. Ludwig *et al.* compared in-solution digestion with S-Trap and FASP in combination with SDS and/or urea based cell lysis [58]. In contrast to in-solution digestion, S-Trap and FASP enabled SDS based cell lysis

in combination with LC-MS analysis [58]. Their findings showed that the total number of identified proteins and the enrichment of distinct proteins are affected by the applied digestion method [58]. In-solution digestion was the best choice regarding to the preparation time and the costs but the method resulted in a lower number of identified proteins and showed the lowest reliability [58]. S-Trap is highlighted as a fast digestion method showing a high reproducibility by Ludwig *et al.* and HaileMariam *et al.* [38, 58].

Unanticipated cleavages, peptide modifications in the reduction and alkylation step, deamidation and methionine oxidation can impede the peptide identification by MS [23]. Especially the analysis of very complex samples including low and high abundant proteins can be impaired by these issues [23].

Peptide Fractionation

Standard methods used for proteomic studies comprise a liquid chromatography system connected with a mass spectrometer (LC-MS) [24]. Peptides are fractionated by (high-pH) reverse-phase, ion-exchange or size exclusion chromatography to increase the number of identified peptides [24, 58]. Co-eluting peptides cause signal suppression [24]. Nano-LC/UPLC (Ultra-Performance Liquid Chromatography) or silica-based monolithic capillaries are more likely for the analysis of small sample amounts [24].

1.5.4. Instrument

Using a liquid chromatography system in combination with electrospray ionization tandem mass spectrometry (MS/MS) [38, 69] is common for this approach [23, 24, 69]. Matrix-assisted laser desorption ionization (MALDI) MS can offer another possibility [23]. A mass spectrometer comprises several components – an ion source for sample ionization, a mass analyzer measuring the mass/charge ratio (m/z) and a detector counting the number of ions with a distinct m/z ratio [24]. Various mass analyzers are available for proteomic based MS analysis such as ion trap, quadrupole, time of flight (TOF) and Fourier transform ion cyclotron (FT-MS) [24]. Combining two mass analyzers might be beneficial [24]. Several dissociation methods leading to further peptide fragmentation such as collision-induced dissociation (CID), electron-capture dissociation (ECD), electron-transfer dissociation (ETD) and higher-energy collisional dissociation (HCD) are applied [24].

1.5.5. MS Data Analysis

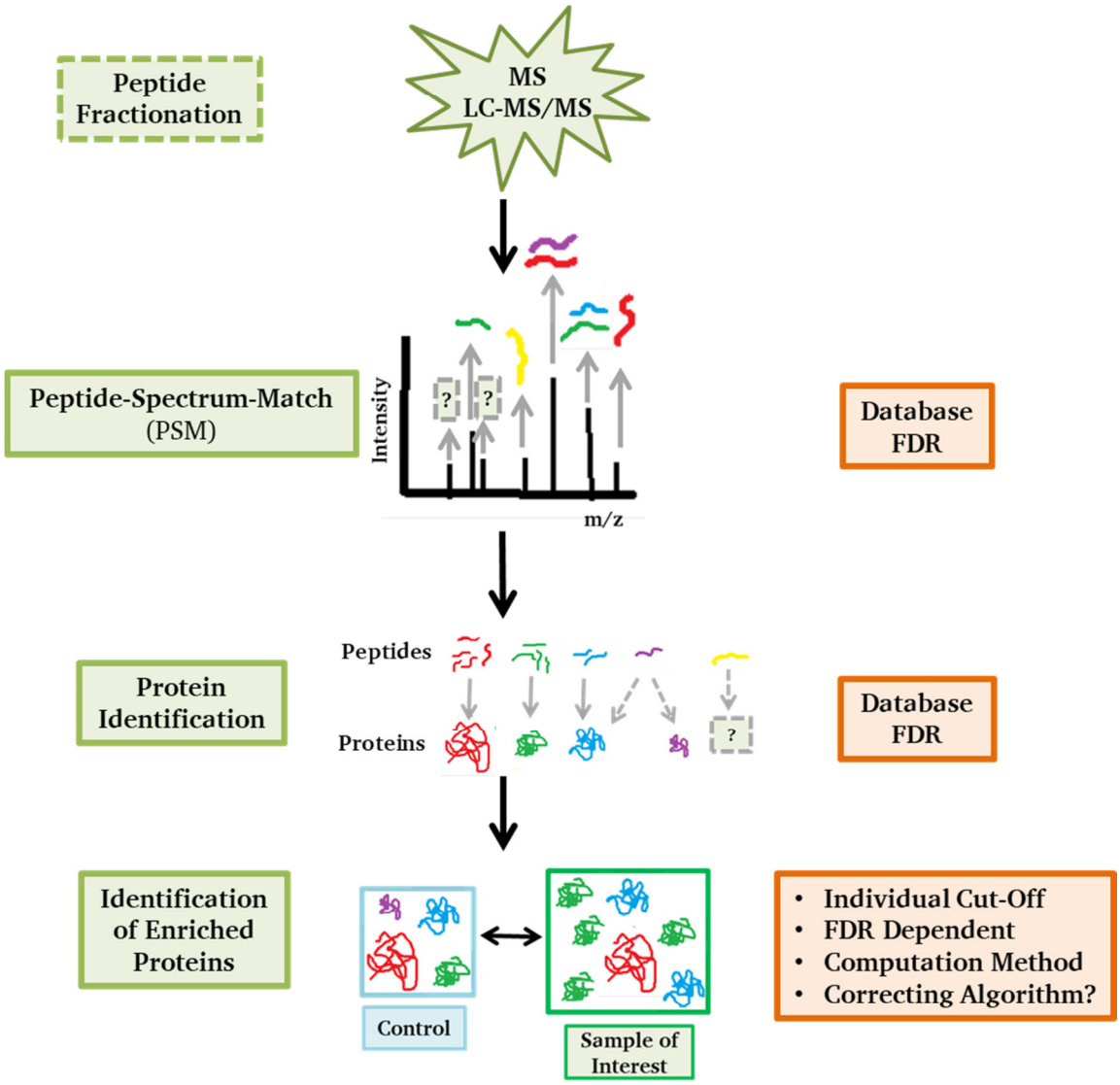

Figure 4: Identification of Enriched Proteins by a MS-Based Proteomic Approach.

Peptide and Protein Identification

Normally, the raw data generated in a proteomic MS analysis are converted for the upcoming analysis [24, 69]. Comparing MS data with theoretical peptide sequences in a target data base to identify peptide-spectrum matches (PSMs) is a popular approach [23, 24, 69, 88]. PSMs are subjected to a protein sequence database for protein inference [23, 24, 69] (Figure 4).

The identification of PSMs is affected by spectra quality, the interference of different precursor ions in tandem mass spectrometry and peptide modifications such as oxidation, reduction, nitration and phosphorylation [23]. Poor spectra quality, sample impurities able to

ionize, peptide modifications not included in the database search or peptides missed in the applied database can lead to unmatched spectra [23]. The protein digestion can generate peptides that can be originated from different proteins and thus cannot be assigned specifically to a distinct protein [23, 24]. Furthermore, databases do not contain all proteins, protein variants or modifications that are present in the analyzed sample [23]. For that reason, including multiple databases in the analysis might be beneficial [23, 24].

The database dependent processes for peptide and protein identification are error-prone [24, 88]. Therefore the results should be assessed to estimate the confidence into the peptide-spectrum matches and especially into the protein assignment as final experimental read-out. The False Discovery Rate (FDR) is a scoring system addressing this approach that can be related to the peptide or protein stage [24, 88]. Different FDR definitions have been described [24, 88]. The FDR can be defined for example as a ratio between the number of false PSMs and the total number of PSMs [24]. In this context, the FDR can be determined by various methods such as target-decoy search strategy (TDS) and mixture model-based methods [24]. The TDS based method includes the generation of artificial decoy peptides by reversing or shuffling protein sequences from the target data base [24]. A protein-level FDR can be related to proteins identified on the basis of incorrect peptide-spectrum matches (PSMs) [88]. Another protein-level FDR definition is based on the identification of proteins that are not present in the sample [88].

PeptideShaker, a proteomics informatics software, can be used for peptide and protein identification enabling the combination of results from different search engines [69, 96]. This approach results in an increased number of protein identifications [69]. A bottom-up proteomic approach using automated sequence database searching can lead to the identification of 4,000 up to 8,000 proteins in a sample [23].

Label Free Proteomics – Relative Protein Quantitation

Label-free proteomics relies on the comparison of MS signal intensities for identified peptides in the samples of interest or on spectral counting [23, 69]. Spectral counting means comparing the total number of spectra assigned to a distinct protein in different samples [23]. Label free proteomics is a fast, cost-efficient method for relative peptide and protein quantitation [23, 24]. An internal peptide standard with a known concentration can be added to the samples prior MS analysis as a quality control for relative protein quantitation [24]. External peptide standards can be analyzed between the samples [24] to verify or estimate the precision and accuracy of the instrument. However, peptides having different physical and

chemical properties affecting the mass spectrometric analysis cannot be quantified exactly [24].

Absolute Protein Quantitation

Several methods for stable isotope protein labeling have been developed and applied for MS-based protein quantitation. The principle is based on the detection of labeled and unlabeled peptide forms by MS and the comparison of the corresponding signal intensities [69]. Various metabolic and chemical labeling techniques including stable isotope labeling by amino acids in cell culture (SILAC), isotope-coded affinity tag (ICAT), $^{15}N/^{14}N$ metabolic labeling, $^{18}O/^{16}O$ enzymatic labeling, isotope coded protein labeling (ICPL), tandem mass tags (TMT) as well as isobaric tags for relative and absolute quantification (iTRAQ) have been described [23, 24, 69]. Protein quantitation methods can be error-prone due to incomplete peptide labeling [24].

1.6. Objective

The main part of the PhD project aimed on the identification of FKBP51 binding proteins interacting with the FK1 domain. The identification and further characterization of FKBP51FK1 interaction partners might give insights into the poorly understood cellular role of FKBP51. Most recently, the stimulation of neurite outgrowth by the key FKBP ligand SAFit1 was shown [28] but the underlying cellular mechanisms are still unclear. The identification of proteins interacting with the binding pocket of the FK1 domain might contribute to the understanding of FKBP ligand dependent cellular effects as well as to the discovery of unknown effects.

The study focusing on the identification of FKBP51 interaction partners can be divided into two parts. Firstly, a FKBP51FK1 affinity matrix was developed and characterized. In detail, a FKBP51FK1 domain mutant, exhibiting a *C*-terminal located mono cysteine residue, was expressed and purified. The purified FK1 domain was covalently coupled to activated agarose beads carrying iodoacetyl groups. The coupling reaction was optimized with regard to the buffer system, the reaction time and the protein density on the beads. A fluorescence based binding assay addressing the binding pocket of the FK1 domain was developed to analyze the FKBP51FK1 affinity matrix. The integrity of the binding pocket was shown by the binding of a fluorescein labeled FKBP51 ligand (tracer) to the affinity matrix and the competitive elution with FKBP ligands.

The second part included the development of a pull-down assay using covalently coupled FKBP51FK1 as bait to capture FKBP51 binding proteins from N2a (murine neuroblastoma) and HEK293 (human embryonic kidney) cell lysates. SAFit1 and another FKBP ligand (PPU339) were applied for competitive elution to enrich potential FKBP51 binding partners interacting with the binding pocket of the FK1 domain. Especially FKBP51-protein interactions inhibited by FKBP ligands should be addressed by this approach. The protein elution profile, the sample complexity and the sample purity were analyzed by SDS-PAGE and silver staining. Subsequently, the pull-down assay samples were analyzed by a bottom-up proteomic approach in cooperation with SINTEF Industry (Trondheim, Norway) to identify enriched proteins. The findings were assigned to cellular compartments and protein classes by PANTHER [4, 16, 61, 89]. In the beginning, HEK293 cell lysates were used to develop the FKBP51FK1 pull-down assay and to test different assay conditions since culturing HEK293 cells was easy and time-saving. Finally, N2a cell lysates were applied to address FKBP ligand dependent effects on the basis of the neurite outgrowth assay [28].

Another part of the thesis dealt with the characterization of new FKBP ligands by robot based competitive fluorescence polarization assays. SAFit analogues, bicycles [51], macrocycles [11, 100] and small molecule FKBP51 degraders [91] were developed by members of the Hausch research group in the context of structure based drug discovery. Increasing the binding affinity and improving the selectivity within the FKBP protein family were parts of the objectives. The binding affinities of various chemical compounds were determined for FKBP12, FKBP12.6, FKBP51FK1 and FKBP52FK1. The fluorescence polarization assays were performed in close cooperation with Tianqi Mao, Jürgen Kolos, Michael Bauder, Andreas Voll, Patrick Purder, Tim Heymann, Christian Meyners and Claudia Sippel.

2. Materials

2.1. Commercially Available Chemicals and Kits

Table 1: Commercially Available Chemicals, Resins and Kits.

Chemical/Enzyme	Supplier
Acetic acid	Carl Roth
Agar-Agar Kobe I, powder, for Microbiology	Carl Roth
$AgNO_3$	Carl Roth
Ammonium bicarbonate BioUltra ≥ 99.5%	Sigma
Ammonium peroxydisulphate (APS)	Carl Roth
Ampicillin sodium salt ≥ 99%, for molecular biology and biochemistry	Carl Roth
Pierce® BCA assay kit (# 23227)	Thermo Scientific
Bromphenole blue	Carl Roth
Buffer solution for the pH meter: pH 4.01, 7.01, 10.01	HANNA instruments
Coomassie Brilliant Blue R250	Carl Roth
cOmplete, Mini, EDTA-free Protease Inhibitor Cocktail Tablets # 04 693 159 001	Roche
1,4-Dithiothreitol (DTT) ≥ 99% p.a.	Carl Roth
Dimethyl sulfoxide (DMSO), ROTIPURAN®≥ 99.8% p.a	Carl Roth
DNAseI, Desoxyribonuclease I from bovine pancreas, lyophilized powder, protein ≥ 85%, ≥ 400 Kunitz units/mg	Sigma Aldrich
Ethanol, ROTIPURAN® ≥ 99.8% p.a.	Carl Roth
Ethanol ≥ 99,8 %, denatured	Carl Roth
Ethylenediaminetetraacetic acid disodium salt dehydrate (EDTA $2Na^+ \cdot 2H_2O$)	Sigma Aldrich
Fluorescein sodium salt	Fluka
Formalin	Carl Roth
Glycerol, 86% (v/v)	Carl Roth
Glycine	Carl Roth
Hydrochloric acid	Carl Roth
Hepes PUFFERAN® ≥ 99.5 % p.a.	Carl Roth
Imidazole	Fluka Chemica
Isopropyl-β-D-1-thiogalacto-pyranosid (IPTG) ≥ 99% for Biochemistry	Carl Roth
Kanamycin sulfate ≥ 750 I.U./mg	Carl Roth
K_2CO_3	Alfa Aesar
LB-media (Luria/Miller), pH 7.0 ± 0.2: 10 g/L Tryptone, 5 g/L Yeast extract, 10 g/L NaCl	Carl Roth
Lysozyme ≥ 35000 FIP U/mg Bioscience-Grade, Lyophilized, M=14 kDa	Carl Roth
2-Mercaptoethanol/ß-Mercaptoethanol (ß-Me)	Sigma Life Science
$Na_2S_2O_2$	Sigma
Nonidet® P40	Sigma
Phenyl methylsulfonyl fluoride (PMSF) ≥ 99% for Biochemistry	Carl Roth
Protino® Ni-NTA Agarose (50% (v/v) aqueous suspension, containing 30% (v/v) ethanol)	Macherey-Nagel
Rotiphorese® Gel 30 (37.5:1, 30% Acrylamide, 0.8% Bisacrylamide)	Carl Roth
Sodium dodecyl sulfate (SDS)	Carl Roth

Sodium chloride (NaCl) ≥ 99.5% p.a.ACS, ISO	Carl Roth
Sodium hydroxide (NaOH)	Carl Roth
N, N, N', N'-Tetramethylethylenediamine (TEMED)	Carl Roth
Tris(2-carboxyethyl)phosphine TCEP·HCl	trc canada
Tris PUFFERAN® ≥ 99.9% p.a.	Carl Roth
Tris-hydrochloride PUFFERAN® ≥ 99% p.a.	Carl Roth
Triton X-100, pure	Carl Roth
Tween 20	Carl Roth

Table 2: Marker SDS-PAGE.

PageRuler™ and PageRuler™ Plus Prestained Protein Ladder were used for gels stained with Coomassie and for Western blotting. PageRuler™ Unstained Broad Range Protein Ladder was used for gels analyzed by Coomassie and silver staining.

Marker	Supplier/Item Number	Range
PageRuler™ Prestained Protein Ladder	Thermo Scientific, # 26616	10 kDa-180 kDa
PageRuler™ Plus Prestained Protein Ladder	Thermo Scientific, # 26619	10 kDa-250 kDa
PageRuler™ Unstained Broad Range Protein Ladder	Thermo Scientific, # 26630	5 kDa-250 kDa

The marker PageRuler™ Unstained Broad Range Protein Ladder was diluted 1:5 in 1x laemmli-buffer supplemented with 28 μL 2-mercaptoethanol per 1 mL buffer for silver staining. The diluted marker was not boiled.

2.2. FKBP Ligands and Tracer Made by the Hausch Laboratory

20 mM DMSO (ROTIPURAN®≥ 99.8% p.a, Carl Roth) stocks of all compounds were prepared. 40 μM DMSO aliquots of the tracer MTQ238 were prepared. One tracer aliquot was used up to 10 times. DMSO stocks were stored with argon at -20°C. Tracers were excluded from light if possible.

Tracer

The tracer MTQ238 (Figure 5, right, [70]) was used for active-site-titrations to determine the concentration of purified FKBPs showing an intact binding pocket. MTQ238 was also applied for binding assays and competitive fluorescence polarization (FP) assays to determine the dissociation constant Kd of new FKBP ligands. MTQ238 was synthesized by Tianqi Mao (MTQ). The tracer CK182 (Figure 5, [53]) was used to characterize the FKBP51FK1 affinity matrix by a binding assay. CK182 was also applied for competitive FP-assays.

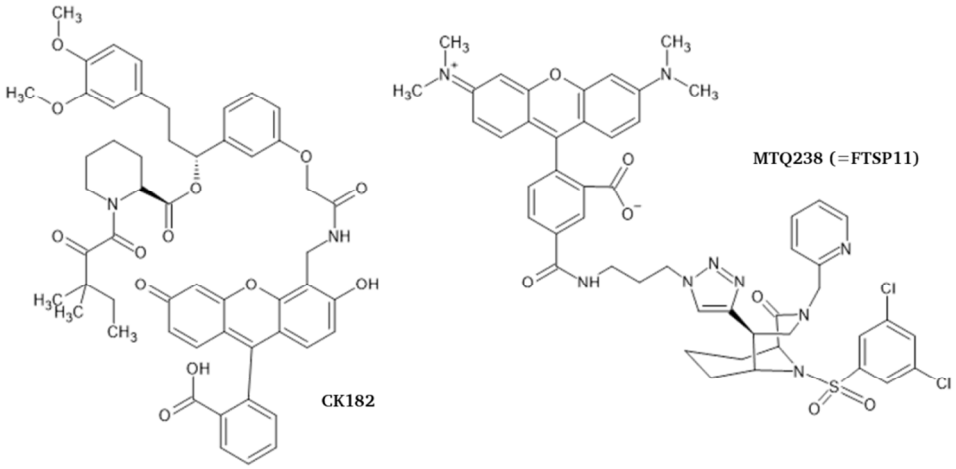

Figure 5: Tracer Made by the Hausch Laboratory.

Left: Structure of the tracer CK182 made of a FKBP ligand and the fluorophore fluorescein [53]. Right: Structure of the tracer MTQ238 (= FTSP11) consisting of a bicyclic FKBP ligand and the fluorescent dye 5-TAMRA [70].

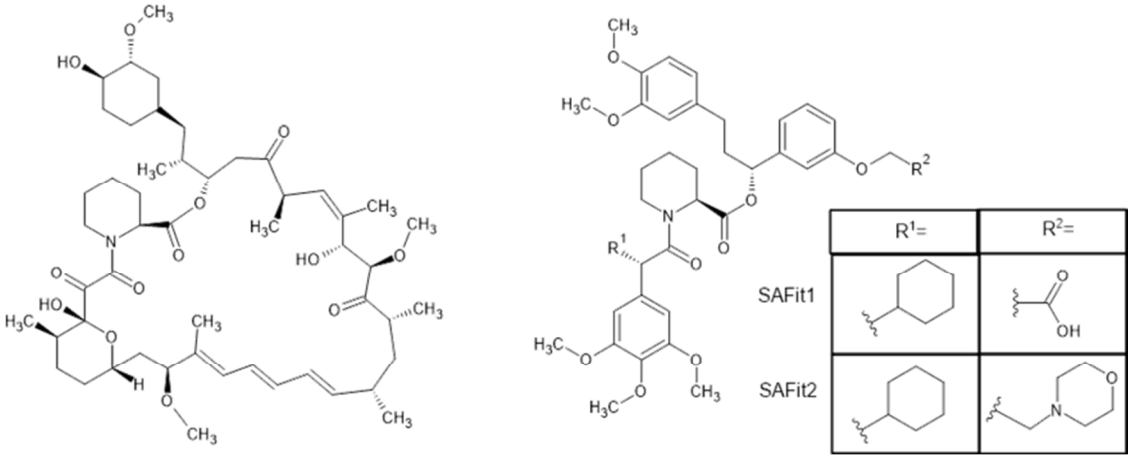

Figure 6: Chemical Structure of the FKBP Ligands Rapamycin, SAFit1 and SAFit2.

Left: Chemical structure of rapamycin [52]. Right: Chemical structure of SAFit1 and SAFit2 [28].

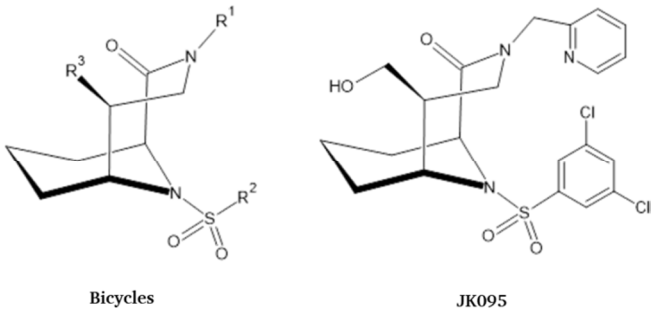

Figure 7: Structure of Bicyclic Compounds.

Left: Core structure of bicyclic compounds [70] such as PPU339 (not published).
Right: Structure of JK095 (= Compound 16 h in [70]).

FKBP51FK1 Affinity Matrix Binding Assay

The compounds used for FKBP51FK1 affinity matrix binding assays are listed below (Table 3). The corresponding compound batch is indicated. The origin of CK182 is unknown. JK095 was synthesized by Jürgen Kolos. SAFit1 was synthesized by Michael Bauder (MBA) and Tim Heymann. Rapamycin was purchased from Alfa Aesar.

Table 3: Tracer and Compounds Used for the FKBP51FK1 Affinity Matrix Binding Assay.

20 mM DMSO stocks of CK182, JK095, Rapamycin and SAFit1 were prepared. The stocks were diluted with assay buffer. Fluorescein sodium salt was dissolved in the corresponding assay buffer.

Compound	Binding Assay	Batch
CK182 (Tracer)	SMe62, SMe64, SMe69	origin unknown, aliquot 8 (08/17/2017) an aliquot with an additional freeze cycle was used for SMe69
	SMe450 (Aliquot 2) SMe456 (Aliquot 4)	origin unknown, Aliquots from 04/24/2020
Fluorescein sodium salt	SMe62, Serial dilution of the fluorescent dye	Fluka, Lot & Filling Code: 456103/1, 43305018
JK095	SMe69	Stock from 03/06/2018
Rapamycin 99%	SMe62	Alfa Aesar powder, #J62473, Lot.: 502DO51
SAFit1	SMe64	MBA053
	SMe450, SMe456	THE104

FKBP51FK1 Pull-Down Assay

SAFit1 and THE212P were synthesized and purified by Tim Heymann. PPU339 was prepared by Patrick Purder. All compounds were analyzed by HPLC, mass spectrometry and FP-assay. The HPLC and MS-analysis was run by Tim Heymann and Patrick Purder. PPU339 was characterized by FP-assay by Patrick Purder.

Table 4: Compounds Applied for Elution in a FKBP51FK1 Pull-Down Assay.

SAFit1 and PPU339=FKBP ligands. THE212P=Non-binding SAFit1 analogue.

Compound	Batch	FKBP51FK1 Pull-Down Assay	MS Run
PPU339		SMe382	3rd
SAFit1	THE104	SMe289	1st
		SMe305	2nd
		SMe382	3rd
THE212P		SMe382	3rd

2.3. Consumables

2.3.1. Plastic Materials

- **Assay plates**
  - 96-well assay plate (Greiner Bio-One, flat bottom, clear, polystyrene, non-sterile)
  - 384-well assay plate (Corning #3575, non-binding surface, black, polystyrene, flat bottom, no lid)
  - 384-well assay ABGene Plate (AB-1056, Thermo Fisher)
- **Dishes**
  - Petri dishes (with cam, 92 x 16 mm, Sarstedt)
  - TC-dish 150 (Sarstedt, Order No.: 83.3903, Growth area: ~ 152 cm2)
  - TC-dish 100 (Sarstedt, 83.3902, Growth area: ~ 58.8 cm2)
- **Empty chromatography columns**
  - 1 mL (Mobicol "Classic", MoBiTec, without filters, #M1002)
  - 1 mL (Mobi Spin Column "F" with fixed outlet plug, inserted 10 μm filter, MoBiTec, #M105010S)
  - 1 mL (Mobicol "F" with fixed outlet plug, inserted 35 μm filter, MoBiTec, #M105035F)
  - 2.5 mL (inserted 90 μm filter, MoBiTec, #S10129)
  - 10 mL (inserted 10 μm filter, MoBiTec, #S10141)
  - 2 mL (Poly-Prep®) and 20 mL (Econo-Pac®) empty gravity flow column (Bio-Rad)
- **Pipette tips**
  - 10 μL, 20 μL, 200 μL, 1000 μL (Sarstedt)
  - 10 μL, 20 μL, 200 μL, 1000 μL filter tips (Sarstedt, Biosphere® plus)
  - BiomekFX^P Robot: P30 and P30XL pipette tips Biomek AP384® (Beckman Coulter)

- **Serological pipettes**
    - 5 mL, 10 mL, 25 mL, 50 mL (sterile) Greiner Bio-one
- **Tubes**
    - 1.5 mL, 2 mL LB (protein low binding) tubes (Sarstedt)
    - 1.5 mL, 2 mL tubes (Sarstedt)
    - 5 mL ProteinLoBind Tubes (Eppendorf)
    - 15 mL, 50 mL tubes (Greiner Bio-One, TPP)
    - 1.5 mL cryo tube (Sarstedt)
    - Tubes for bacteria culture (14 mL, sterile, Greiner Bio-One)
- **Cuvettes:** SEMI-Micro, 10x10x45 (Greiner Bio-One)

2.3.2. Filtration

Table 5: Filter Applied for Microbiological and Protein Biochemical Approaches.

Filter	Supplier	Application
MILLEX®GV Filter Unit 0.22 μm, Durapore® PVDF Membrane	Merck Millipore, SLGU033RS	Sterile filtration of water-based stocks (IPTG, Kan, Amp)
Steritop® Millipore Express™ Plus, 0.22 μm	Merck Millipore, # SCGPT02RE	Sterile filtration of buffer stocks, filtration and degassing of buffers used for the ÄKTA pure system

2.3.3. Protein Concentration and Dialysis

Table 6: Materials for Protein Concentration and Dialysis.

Material	Supplier	Application
Amicon® Ultra-0.5 Centrifugal filter devices, 3K device	Millipore	Protein concentration Buffer exchange Sample volume: up to 500 μL Final concentrated sample volume: 15 μL up to 20 μL
Amicon® Ultra-2 mL centrifugal filters (Ultracel®-10 K), Regenerated cellulose 10,000 NMWL	Merck Millipore, Ireland	Protein concentration Buffer exchange Sample volume: up to 2 mL
Cenricon-10 (Ultracel YM-10), Regenerated cellulose 10,000 MWCO, # 4205 (not available anymore)	Amicon® Bioseperations	Protein concentration Buffer exchange Sample volume: up to 2 mL
Slide-A-Lyzer Mini Dialysis Device 3.5K MWCO, 2 mL # 88403	Thermo Scientific	Protein dialysis, Sample volume: 2 mL Reservoir volume: 44.5 mL

2.4. Plasmid and *E.* Coli Strain for Bacterial Expression

Plasmid for the Expression of HsFKBP51FK1MonoCys C103A/C107I/E140C (HG653, aa 1-140)

A codon optimized plasmid encoding a mutant of human FKBP51FK1 (amino acids 1-140, mutation: C103A/C107I/E140C) was purchased from Thermo Fisher. The mutant contains a 6x histidine-taq at the *N*-terminus for affinity based protein purification and a *C*-terminal located mono cysteine residue for covalent protein immobilization. The insert was analyzed by Sanger sequencing (Eurofins: Primer seq T7-terminator (5'-3'): GCT AGT TAT TGC TCA GCG G). The DNA sequence was translated into the amino acid sequence with Gentle. The molecular weight, the molecular extinction coefficient and the isoelectric point (pI) were determined with the ExPASy Prot-Param tool [29, 81]. The mutant is also named Hs51FK1MonoCys (HG653).

Hs51FKBP51FK1MonoCys was expressed in *E. coli* BL21(DE3)pLys.

- **Amino Acid Sequence:**
  MSYYHHHHHHDYDIPTTENLYFQGAPMTTDEGAKNNEESPTATVAEQGEDITSKKDRGVLKIV
  KRVGNGEETPMIGDKVYVHYKGKLSNGKKFDSSHDRNEPFVFSLGKGQVIKAWDIGVATMKKG
  EIAHLLIKPEYAYGSAGSLPKIPSNATLFFEIELLDFKGC
- **Total number of amino acids:** 166
- **Theoretical molecular weight:** 18.5 kDa
- **Theoretical molecular extinction coefficient:** 17420 M^{-1} cm^{-1} (at 280 nm, in water)
- **Theoretical pI:** 6.3

2.5. Protein Biochemistry

2.5.1. SDS-PAGE

- Gels: Empty gel cassettes (mini, 1.0 mm, NC2010, Invitrogen™, Thermo Fisher Scientific), Gradient gels (4% - 20%, wedge well, Thermo Scientific)
- Gel electrophoresis chamber: XCell SureLock, Novex & Mini Gel tank Invitrogen (Thermo Fisher Scientific), Mini-PROTEAN® Tetra System (Bio-Rad)
- Electrophoresis power supply: EPS3501XL (Amersham Biosciences), EPS600 (Pharmacia), EPS301/EPS601/EP1001 (Amersham Pharmacia Biotech), Power PAC 300 & 3000 (Bio-Rad)
- Gel drying frame (Carl Roth)
- Cellophane sheets for gel drying (Carl Roth, Sigma)

2.5.2. Preparation of the FKBP51FK1 Affinity Matrix

SulfoLink® coupling resin (Thermo Fisher, product number: 20401 (10 mL)), carrying 19 μmol iodoacetyl groups per milliliter resin (cp. certificate of analysis from Thermo Fisher for the corresponding batch), was used to prepare FKBP51FK1 affinity matrices (cp. p. 44). The resin was made of 6% crosslinked beaded agarose and supplied as 50% slurry in storage buffer (10 mM EDTA, 0.05% (w/v) NaN_3, 50% (v/v) glycerol) (cp. Instructions 0527.3 SulfoLink® Coupling Resin, Thermo Scientific, USA). SulfoLink® coupling resin batch SD250987 was used in SMe49. Batch SK259724 was used in SMe162, SMe182, SMe225, SMe249 and SMe303.

2-mercaptoethanol (Sigma Life Science) was used as a blocking reagent after HsFKBP51FK1MonoCys was immobilized on SulfoLink® coupling resin. Lot BCBF9538V (Pcode: 101099762) was used in SMe162, SMe182, SMe225. Lot SHBD8455V (Pcode: 1001742777) was used in SMe249, SMe303.

2.5.3. Protein Purification

Size exclusion column applied for protein purification: HiLoad 26/600 Superdex 200 pg (GE Healthcare).

2.6. Cell Culture

2.6.1. Media and Additives

Table 7: Cell Culture Media and Supplements.

Material	Supplier/Item Number	Application
Heat Inactivated FBS, Fetal Bovine Serum, sterile Origin: South America	Gibco life technologies, # 10500	Cell culture media
Poly-L-lysine solution mol wt 70,000-150,000 0.01% sterile filtered (= 50x stock)	SIGMA Life Science	Coating of tissue culture plates used for culturing N2a cells
0.25% Trypsin-EDTA (1x), sterile	Gibco, # 25200-56	Detachment of adherent cells (HEK293 and N2a)
Sterile water	Carl Roth, #9186.1	Coating of tissue culture plates with poly-L-lysine
Dulbecco´s Phosphate Buffered Saline (DPBS) -$CaCl_2$, -$MgCl_2$	Gibco, life technologies, #14190-169	Cell passaging
DMEM (Dulbecco´s Modified Eagle Medium) ([+] 4.5 g/L D-Glucose, L-Glutamin, [+] Pyruvat)	Gibco Invitrogen, #41966-029	Cell culture
Penicillin/Streptomycin (10 000 Units/mL Penicillin, 10 000 μg/mL Streptomycin)	Gibco, #15140-122	Cell culture
Trypan Blue Stain 0.4%	Gibco, life technologies, #15250-61	Cell counting

2.6.2. Mammalian Cell Lines

N2a (RG Hausch), HEK293 (RG Hausch)

2.7. Instruments and Equipment

Table 8: Centrifuges.

Centrifuge	Temp.	Rotor
Biofuge pico Heraeus	RT	Tabletop centrifuge
Biozym Table Mini Centrifuge	RT	Tabletop centrifuge
Eppendorf Centrifuge 5804 R	4°C-RT	F34-6-38, F45-30-11, A-2-DWP
SIGMA 6-16 KS	4°C-RT	12269, 12449, 12600
Sorvall RC-5B Refrigerated Superspeed Centrifuge	4°C-RT	SS-34, GS3

Table 9: Instruments and Equipment.

Device	Supplier	Application
ÄKTA pure	GE Healthcare	Protein purification
Analytical balance	Sartorius	
Balance	KERN EMB 500-1	
BRANSON Sonifier 450		Protein purification
Canon MG3550 Scanner/Printer	Canon	Gel documentation
DS11+ Spectrophotometer	DeNovix, Biozym	OD, Protein concentration
innova™ 4000 Incubator Shaker	New Brunswick Scientific	Bacterial culture
IXUS 180 Digital Camera	IXUS	Gel documentation
LABWIT ZWY-211C Orbital shaking incubator	LABWIT	Bacterial culture
Magnetic stirrer	Heidolph	Mixing
Milli-Q® Ultrapure Lab Water System	Merck	Buffer preparation
Plate Reader TECAN Genios Pro/Spark	TECAN	Binding assays
pH Meter HI2212 pH/ORP Meter	HANNA instruments	Buffer preparation
Robot, Biomek FX^{P}	Beckman Coulter	Liquid handling
Rocking platform	Heidolph DUOMAX 1030	Mixing, shaking
Rolling device: RM5 Assistant 348 Phoenix Instrument RS-TR05	Biozym -	Mixing
Thermomixer	Biozym	Warming of tubes and assay plates
Variomag Monoshaker		Shaking assay plates
Vortex	Heidolph	
Water bath	GFL	Warming of buffers, stocks and chemicals

2.8. Software and Database

Chemical structures were drawn with ACD/ChemSketch (Freeware) 2020.2.1. Self-made figures were prepared with Paint and PowerPoint 2010. Size exclusion chromatograms were exported from the Unicorn 7.1 software (GE Healthcare). Venn diagram matrices were calculated with Perseus or received from Hanne Haslene-Hox (SINTEF Industry, Trondheim, Norway). Venn diagrams were prepared with InteractiVenn and Venn Diagram Plotter. Pictures, figures and Venn diagrams were edited with PowerPoint 2010.

Table 10: Applied Software and Tools.

Software & Supplier	Application
ACD/ChemSketch (Freeware) 2020.2.1 [1]	Drawing chemical structures
Biomek® (Beckman Coulter)	Robot, Biomek FX^P
Citavi 6	Reference management software
ExPASy – ProtParam tool [29, 81]	Calculation of chemical and physical parameters of purified proteins based on the amino acid sequence: • Theoretical molecular weight • Theoretical molecular extinction coefficient (at 280 nm, in water) • Theoretical isoelectric point (pI) • Number of amino acids
Gene Ontology [4, 6, 30, 89, 90], PANTHER [61]	Proteomic analysis
Gentle (developed by Magnus Manske, University of Cologne)	Creation and analysis of plasmid maps
GraphPad Prism 9.4.1	Data Analysis, Graphic Presentation
InteractiVenn [42]	Drawing Venn diagrams (not quantitative) Calculation of overlapping areas
Microsoft Excel 2010	Data analysis, Calculation
Microsoft PowerPoint 2010	Figure editing
Microsoft Word 2010	Thesis writing
Paint	Drawing
Perseus Version 1.6.15.0 [93]	Proteomic data analysis
Unicorn 7.1 (GE Healthcare)	ÄKTA pure, System operation and data analysis
UniProtKB [90, 94]	Protein reference database
Venn Diagram Plotter Version 1.6.7458.27187 (June 2, 2020) by Kyle Littlefield and Matthew Monroe (PNNL, Richland, WA)	Drawing quantitative Venn diagrams

3. Methods

All experiments were labeled with an internal number (SMe) in order to allocate different runs and assay conditions to the corresponding results.

3.1. Micro and Molecular Biology

3.1.1. Preparation of Media, Stocks and Flasks

Flasks up to 500 mL or tubes (1.5 mL and 2 mL) were sterilized in a pressure cooker. 2 L flasks used for protein expression were rinsed with 80% (v/v) ethanol.

To prepare LB-media for bacterial cultures, 12.5 g powdered LB-media premix (10 g/L tryptone, 5 g/L yeast extract, 10 g/L NaCl, pH 7.0 ± 0.2, Carl Roth) were dissolved in 500 mL desalted water and boiled in a pressure cooker. Ampicillin sodium salt (c_{final} = 0.1 mg/mL) or kanamycin sulfate (c_{final} = 0.05 mg/mL) were added to the chilled media.

To prepare LB-agar plates, 6.3 g LB-media premix were mixed with 5 g Agar-Agar Kobe I (Carl Roth) dissolved in 250 mL desalted water and boiled in a pressure cooker with a stirring bar. After cooking the mix was stirred at RT and the corresponding antibiotics were added to the chilled (= warm to the touch) mix. The media was poured carefully into petri dishes (with cam, Sarstedt) without air bubbles. To reduce contaminations with microorganisms present in the air, LB-agar plates were prepared in the environment of a camping stove.

Kanamycin sulfate (c_{stock} = 50 mg/mL = 1000x) or ampicillin sodium salt (c_{stock} = 100 mg/mL = 1000x) were dissolved in desalted water. The applied water was filtered (0.22 μm PES Membrane Steritop® Filter, Millipore Express™ Plus, Merck) and sterilized in a pressure cooker before use. To maintain the selective pressure during bacteria growth, antibiotics were added freshly to LB-media or liquid LB-agar. Kanamycin, ampicillin and IPTG stocks were filtered (MILLEX® GV Filter Unit 0.22 μm Durapore® PVDF, Merck), aliquoted and stored at -20°C up to 6 months. Kanamycin and IPTG stocks were stored up to 3 days and ampicillin stocks up to 24 h at 4°C.

3.1.2. Transformation of *E. Coli* Cells

Plasmid DNA (10 ng up to 100 ng) was thawed on ice and added carefully to chemically competent *E. coli* cells (100 µL). The DNA and the bacteria cells were mixed by snipping. After incubating for 15 min on ice, heat shock was performed (incubation for 45 s at 42°C). Afterwards, the bacteria cells were incubated on ice for 1 min. 800 µL pre-warmed LB-media were inoculated with 100 µL *E. coli* cells and incubated for 30 min (selection by ampicillin resistance) or 40 min (selection by kanamycin resistance) at 37°C on an orbital shaker or thermomixer. A LB-agar plate supplemented with the required antibiotic was inoculated by dilution plating.

3.1.3. Preparation of Glycerol Stocks

To prepare a 45% (v/v) glycerol stock, glycerol (86% (v/v), Carl Roth) was diluted with either desalted, filtered water (0.22 µm PES Membrane Steritop® Filter, Millipore Express™ Plus, Merck) or with Millipore water and boiled in a pressure cooker. 500 µL of a bacterial overnight culture ($OD_{600} \geq 1$) were transferred into a cryo tube (1.5 mL Sarstedt). 250 µL 45% (v/v) glycerol were dropped into the tube and the tube was carefully inverted. To ensure a uniform distribution of glycerol, the tube was inverted once again immediately before freezing and storing at -80°C.

3.1.4. Sequencing

The insert of plasmid HP653 (glycerol stock: HG653) was verified by Sanger sequencing (Eurofins). Primer seq T7-terminator (5'-3'): GCT AGT TAT TGC TCA GCG G.

3.2. Protein Biochemistry

3.2.1. Expression of Recombinant HsFKBP51FK1MonoCys

The optimized protein expression protocol for HsFKBP51FK1MonoCys is described below. To prepare an overnight culture, 20 mL up to 50 mL LB-media supplemented with 20 µL up to 50 µL 1000x kanamycin sulfate (c_{final} = 50 µg/mL) or 1000x ampicillin (sodium salt) (c_{final} = 100 µg/mL) were inoculated with *E. coli* cells, carrying the plasmid for protein expression, scrapped from a glycerol stock. The bacteria culture was incubated at 30°C for 14 h up to 16 h on an orbital shaker (220 rpm). The main culture was inoculated with the overnight culture (OD_{600} = 0.1) and incubated at 35°C up to 37°C on an orbital shaker. Up to 50 mL of the pre-culture were used to inoculate 1 L bacteria culture. The protein expression

was induced with 0.6 mM IPTG (c_{stock} = 1 M) at OD_{600} = 0.4 - 0.6. The bacteria culture was incubated for 4 h at 35°C up to 37°C on an orbital shaker. To harvest the cells, the bacteria culture was centrifuged (6000 rcf, 20 min, 4°C) and the supernatant discarded. To evaluate the protein expression, 300 µL up to 500 µL of the bacteria culture were collected before as well as after inducing the protein expression. The samples were spun (6000 rcf, 3 min, RT) and the supernatant was discarded. Depending on the cell pellet size a corresponding volume of 10 mM Tris (pH 8) was used to dissolve the cell sediment. The volume of both samples, before and after induction, was normalized to OD_{600}. For example, the cell sediment prepared from 500 µL bacteria culture at OD_{600} = 0.5 was dissolved in 20 µL 10 mM Tris (pH 8). The cell pellet collected after induction at OD_{600} = 2.5 was dissolved in 100 µL 10 mM Tris (pH 8). After adding an equal volume of 4x laemmli buffer supplemented with 2-mercaptoethanol (recipe: cp. chapter 3.2.6, p. 38) the samples were boiled at 95°C for 10 min and subjected to SDS-PAGE. Possible breakpoints included freezing the cell sediments up to 7 weeks and the boiled samples mixed with laemmli-buffer at -20°C. The culture volume was about 30% up to 50% of the total flask volume. To increase the bacteria growth rate baffled flasks were used if available.

The expression of HsFKBP51FK1MonoCys was supported by Johanna Bartmuß (protein batch: JBa 3.3, Bachelor thesis [10]) and Steffen Hartmann (protein batch: SMe34/141, research internship).

3.2.2. Purification of Recombinant HsFKBP51FK1MonoCys

The purification of recombinant HsFKBP51FK1MonoCys, carrying a *N*-terminal located histidine-tag, included the following steps: enzymatic cell lysis by lysozyme, mechanical cell lysis by sonication, semi-batch affinity purification by Protino® Ni-NTA agarose (Macherey-Nagel), protein polishing and buffer exchange by size exclusion chromatography (SEC). SEC was also applied to estimate the purity and the molecular weight of the purified protein (cp. p. 36). The efficiency of the purification steps and the purity of the purified protein were analyzed by SDS-PAGE and Coomassie staining (cp. p. 38-39). For that purpose, samples (20 µL up to 30 µL) were collected from each purification step. The concentration and dialysis of purified HsFKBP51FK1MonoCys is described in chapter 3.2.4 (cp. p. 37). The optimized purification protocol for HsFKBP51FK1MonoCys is described below.

The purification of HsFKBP51FK1MonoCys was supported by Johanna Bartmuß (protein batch: JBa3.3, Bachelor thesis [10]).

Plastic Ware and Buffer Preparation

Plastic tubes with a protein low binding surface were used for all purification steps: 15 mL/50 mL tubes (TPP), 15 mL/50 mL protein LoBind tubes (Eppendorf), 1.5 mL/2 mL protein low binding tubes (Sarstedt).

All buffers (Table 11) were pre-chilled. 1 M Hepes stocks were filtered (Steritop® Millipore Express™ Plus, 0.22 μm, Merck Millipore, # SCGPT02RE). DTT stocks were prepared daily to prevent oxidation and stored at 4°C excluded from light. DNAseI, thawed at RT, and lysozyme were added freshly to the pre-chilled lysis buffer components. The lysis buffer was stirred slowly on ice until a clear solution was obtained. The irreversible serine protease inhibitor PMSF (phenylmethylsulfonyl fluoride) unstable in water based buffers was added by dropping immediately before use.

Table 11: Protein Purification Buffers.

Chemical	c_{stock}	Solvent	Storage Temp. Stocks	Buffer c_{final}			
				Lysis	Equili-bration	Wash	Elution
Hepes, (pH 8)	1 M	VE-H_2O	RT	20 mM	20 mM	20 mM	20 mM
NaCl	3 M	VE-H_2O	RT	300 mM	300 mM	20 mM	20 mM
Imidazole	3 M	VE-H_2O	RT	10 mM	–	10 mM	300 mM
Glycerin	86% (v/v)	H_2O	RT	–	–	5% (v/v)	–
DTT	1 M	VE-H_2O	Freshly prepared	1 mM	–	1 mM	10 mM
Lysozyme	Solid		-20°C	2 mg/mL	–	–	–
PMSF	200 mM	EtOH p.a. grade	-20°C up to 2 months	1 mM	–	1 mM	–
DNAseI	20 mg/mL	0.15 M NaCl	-20°C	0.1 mg/mL	–	–	–

Enzymatic and Mechanical Cell Lysis

The cell sediments were always handled on ice. Each cell pellet prepared from 1 L bacteria culture was transferred into a 50 mL tube, a cross stirring bar and 20 mL lysis buffer were added. The mix was stirred at 4°C for 30 min and vortexed (1x vortexed at RT for 30 s, stirred at 4°C for 5 min, 1x vortexed for 30 s, stirred at 4°C for 25 min). To disrupt the bacterial cell membrane the mix was treated with ultrasound (Branson sonifier 450: 3x 3 min, Duty cycle: 40%, Output-control: 4) on ice. The mix was inverted carefully after each step to ensure the contact of not disrupted cells with the surface of the probe tip. After centrifugation (20000 rcf, 4°C, 30 min) the supernatant was incubated with equilibrated Protino®

Nickel-NTA beads (Macherey-Nagel). 1 mL settled bead volume was used for a cell pellet made from 1 L bacteria culture.

Semi-Batch Affinity Purification Using Nickel-NTA Agarose

The Protino® Nickel-NTA slurry was transferred into a tube (= double amount of the settled bead volume). The beads were spun-down (500 rcf, 5 min, RT) and the storage buffer was discarded. VE-H_2O was added (double volume of the settled bead volume), the beads were suspended and spun-down (500 rcf, 5 min, RT). The supernatant was discarded. This step was repeated two times with VE-H_2O and equilibration buffer. The equilibrated beads were added to the cell lysate and carefully suspended by inverting. The mix was incubated on a rolling device for 1 h at 4°C. The mix was centrifuged (500 rcf, 3 min, 4°C) and the supernatant was transferred into a new tube. The beads were resuspended with a part of the supernatant (= double volume of the settled bead volume) and transferred into an empty column (Bio-Rad: 20 mL or 2 mL, MoBiTec: 5 mL). The empty columns were washed with VE-H_2O and equilibration buffer before use. The residual supernatant was loaded on the packed column. The flow-through was collected on ice and added a second time to increase the protein yield. The column was washed two times with 4 CV wash buffer. About 2.5 CV elution buffer were added and the eluates were collected on ice. The elution step was monitored by a Bradford assay. 90 μL 1x ROTI®Nanoquant (Carl Roth, 1x ROTI®Nanoquant = 1 part 5x ROTI®Nanoquant + 4 parts VE-H_2O) and 5 μL of each eluate were mixed in a 96-well assay plate (Greiner Bio-One, flat bottom, clear, polystyrene, non-sterile) for the Bradford assay. A high protein concentration in the sample was indicated by dark blue coloring. The UV protein concentration of the eluates was determined by a spectrophotometer (A280). The fractions containing the highest protein concentration were pooled and subjected to size exclusion chromatography (SEC). To avoid protein precipitation in the elution buffer, SEC was started on the same day.

3.2.3. Size Exclusion Chromatography (SEC)

A size exclusion column (HiLoad 26/600 Superdex 200 pg, GE Healthcare) was connected to an ÄKTA pure system (GE Healthcare), equipped with a superloop (sample volume up to 10 mL), a UV detector (A280), a conductivity detector and a F9-C fraction collector. The system was placed in a cooling cabinet (4°C). All buffers were prepared with MP-H_2O, pre-chilled, filtered (0.22 μm, Merck Millipore) and degassed on ice before use.

The column was washed with 2 CV MP-H_2O and 2 CV running buffer (either 50 mM Tris, 5 mM EDTA, ±510 μM up to 950 μM TCEP, pH 8 or 20 mM Hepes, 20 mM NaCl,

5% (v/v) glycerin, 1 mM DTT, pH 8) before use. The complete system was also primed with MP-H_2O and running buffer.

All samples were centrifuged (20,000 rcf, 4°C, 20 min) and loaded on the column via a superloop. The centrifugation step was repeated if protein precipitation was observed. The flow rate was about 1.3 mL/min during sample load and elution. The fractions were collected in either 15 mL or 50 mL tubes (peak based fractionation, limit: about 40 mAU).

3.2.4. Protein Dialysis and Concentration

Besides size exclusion chromatography, dialysis and ultrafiltration (Amicon® Ultra centrifugal filters) were applied to exchange the storage buffer of protein samples. Furthermore, Amicon® Ultra centrifugal filters were used for protein concentration.

Slide-A-Lyzer® mini dialysis devices (#88403, 3.5K MWCO, Thermo Scientific, sample volume: 2 mL, reservoir volume: 44.5 mL) were used for protein dialysis. The dialysis was performed according to the manufacturer's instructions. About 44.5 mL of the new buffer were filled into the dialysis tube and a small stirring bar was added. The membrane unit of the device was washed with the new buffer and carefully taped on a tissue to remove residual drops. The protein solution was added immediately. The dialysis membrane was always wetted during the procedure. Air bubbles at the boarder of the dialysis membrane and the new buffer were removed. The buffer was stirred slowly and the dialysis was performed overnight at 4°C. The buffer of the reservoir was exchanged four times (e.g. after 150 min, 4 h, 5 h and 19 h).

Amicon® Ultra-2 mL centrifugal filters (Ultracel®-10 K, regenerated cellulose, 10,000 NMWL, Millipore) or Centricon-10 filters (Ultracel YM-10, regenerated cellulose, 10,000 MWCO, # 4205, Amicon® Bioseparations, Merck Millipore) were used to concentrate HsFKBP51FK1MonoCys. The filters were utilized according to the manufacture´s recommendation. After the membrane was wetted the first time, it was not dried out. The contact time of the sample was as short as possible to avoid sample loss due to unspecific protein interactions with the membrane. To prevent sample precipitation in the filter, the sample was resuspended carefully during the centrifugation step (e.g. after 10 min and 30 min). The reuse of the centrifugal filters is not recommend since 20% of purified HsFKBP51FK1MonoCys (SMe142) were lost by applying the centrifugal filter a second time.

3.2.5. **Casting Polyacrylamide Gels for SDS-PAGE**

The recipe for two self-made polyacrylamide gels is described below. A mixture consisting of Rotiphorese® Gel 30 (37.5:1, 30% Acrylamide, 0.8% Bisacrylamide, Carl Roth), VE-H_2O, 5.34 mL 1 M Tris (pH 8.8), 280 μL 5% (w/v) SDS, 84 μL 10% (w/v) APS and 17 μL TEMED was prepared. The Rotiphorese® Gel 30/VE-H_2O ratio was adjusted for different separation gels (Table 12).

Table 12: Separation Gel Recipe for SDS-PAGE.

Rotiphorese® Gel 30 was mixed with VE-H_2O, 5.34 mL 1 M Tris (pH 8.8), 280 µL 5% (w/v) SDS, 84 µL 10% (w/v) APS and 17 µL TEMED to cast two gels (empty gel cassette mini, 1.0 mm, NC2010, Invitrogen™, Thermo Fisher Scientific). The required volumes of Rotiphorese® Gel 30 and VE-H_2O are indicated.

Ingredient	Separation Gel				
	8%	10%	12%	14%	16%
Rotiphorese® Gel 30	3.8 mL	4.75 mL	5.7 mL	6.65 mL	7.6 mL
VE-H_2O	4.8 mL	3.8 mL	2.8 mL	1.9 mL	0.9 mL

APS and TEMED were added as last to induce the radical polymerization. The mixture was poured into empty gel cassettes (mini, 1.0 mm, NC2010, Invitrogen™, Thermo Fisher Scientific). The separation gels were layered with 0.5 mL up to 1 mL 2-propanol preventing gel drying. After the polymerization was completed, 2-propanol was carefully removed, the stacking gel (recipe for 250 mL: 44 mL Rotiphorese® Gel 30, 186 mL VE-H_2O, 15 mL Tris-HCl (pH 6.8), 5 mL 5% (w/v) SDS) was casted and the combs were added immediately. The gels were wrapped with wet tissues and stored at 4°C.

3.2.6. **Sample Preparation for SDS-PAGE**

Either 3 parts of a sample were mixed with 1 part 4x laemmli buffer (320 mM Tris, 40% (v/v) glycerol, 8% (w/v) SDS, 0.04% (w/v) bromphenol blue, 2.8% (v/v) 2-mercapto-ethanol) or 2 parts of a sample were mixed with 2 parts 4x laemmli buffer. A final concentration of 1x laemmli buffer was used for all samples that were subjected to silver staining since the lowered SDS concentration led to a reduced background. To prepare viscous samples (e.g. made from bacterial cell sediments) for SDS-PAGE, a final concentration of 2x laemmli buffer was applied. 2-mercaptoethanol was freshly added (28 μL per 1 mL 4x laemmli buffer). The sample/laemmli-buffer mix was incubated for 10 min at 95°C. The samples were spun down and loaded on a gel. The boiled samples were stored at 4°C or -20°C.

3.2.7. Running SDS-PAGE

One gel up to four gels was/were placed into a gel electrophoresis chamber according to the manufacturer´s guideline (XCell SureLock, Novex & Mini Gel tank Invitrogen, Thermo Fisher Scientific: up to 2 gels, Mini-PROTEAN® Tetra System Bio-Rad: up to 4 gels). The chamber was filled with 1x SDS running buffer, the samples were loaded and the electrophoresis was run keeping the current constant (1x gel: I = 15 mA for the stacking gel, I = 25 mA for the separation gel; 2x gels: I = 25 mA for the stacking gel, I = 45 mA for the separation gel). The upper limit of the voltage was set at 350 V. 1 part 10x SDS running buffer (30 g Tris, 144 g glycine, 10 g SDS per 1 L, dissolved in VE-H_2O) was diluted with 9 parts VE-H_2O.

3.2.8. Coomassie Staining

Gels were incubated in the staining solution (40% (v/v) EtOH, 10% (v/v) acetic acid, 1 g/L Coomassie Brilliant Blue R250, Carl Roth) for at least 30 min up to 48 h on a shaking platform at RT. The staining time was adjusted to the expected protein amount per band. The staining solution was removed and the destaining solution was added (40% (v/v) EtOH, 10% (v/v) acetic acid). The incubation time in the destaining step was as long as the staining time. To improve the destaining procedure the solution was changed 2 up to 4 times. The destaining step was continued with VE-H_2O overnight if no protein bands were visible.

Gel drying is described in chapter 3.2.10 (p. 40).

3.2.9. Silver Staining

All containers used for the staining procedure were cleaned with 70% (v/v) EtOH, acetone, 70% (v/v) EtOH and MP-H_2O before use. The silver staining was performed at RT. All buffers were freshly prepared.

The gels were incubated in fixation solution (30% (v/v) EtOH, 10% (v/v) acetic acid) for at least 18 h up to 24 h on a shaker to remove carrier ampholytes. The solution was exchanged 3 times. The gels were washed 2 times for 10 min with 20% (v/v) EtOH and MP-H_2O. For sensitizing, each gel was soaked in 0.8 mM $Na_2S_2O_3$ and washed 2 times for 1 min with MP-H_2O. All gels were impregnated with 12 mM $AgNO_3$ and incubated for 20 min up to 2 h on a shaker. Afterwards, each gel was dipped in a water bath for 10 s, transferred into developer solution (3% (w/v) K_2CO_3, 250 μL Formalin/L, 125 μL 10% (w/v) $Na_2S_2O_3$) and incubated for 30 min up to 40 min on a shaker. To interrupt the development step, the gels were transferred into stop solution (4% (w/v) Tris, 2% (v/v) acetic acid) and incubated for

30 min up to 2 h on a shaker. Finally, the gels were washed 2 times with MP-H_2O for 30 min [18].

Silver stained gels were fixed in a gel drying frame (3.2.10) and pictures were taken. The figures were edited in Microsoft PowerPoint 2010.

An error occurred during the staining of the gels shown in Figure 24 a. The $Na_2S_2O_3$ or the $AgNO_3$ solution was not well prepared probably. The gels were stored in MP-H_2O for five days at RT. The gels were stained a second time. The second trial was started with the sensitizing step.

3.2.10. **Gel Drying**

To dry gels, a sandwich consisting of 2 cellophane sheets, the gel and a gel drying frame was prepared. 2 cellophane sheets were immersed in water. One cellophane sheet was placed on the gel drying frame, the gel was placed in the center and excess gel pieces were cut. A second sheet of cellophane was added by wetting the gel surface with water. Air bubbles were removed gently. The second part of the gel drying frame was mounted and the frame was fixed with clamps. Remaining air bubbles led to tears in the drying gels.

3.2.11. **Spectrophotometric Based Protein Quantitation**

The protein concentration based on the absorption at 280 nm was determined with a DS11+-spectrophotometer (DeNovix). The absorption at 280 is mainly caused by the amino acids tryptophan, tyrosine and phenylalanine [43]. The concentration c of a purified protein is proportional to the absorption at 280 nm within a distinct range depending on the instrument´s specification (Equation 1). The molecular extinction coefficient ε that depends on the solvent and the path length d of the spectrophotometric measurement unit are constants. The molecular extinction coefficient ε of a purified protein was calculated based on the amino acid sequence with ExPASy (cp. chapter 2.8, [29, 81]). Water was assumed as solvent for the calculation of the molecular extinction coefficient by ExPASy.

$$A = \varepsilon * c * d$$

Equation 1: Calculation of the Protein Concentration Based on the Absorption at 280 nm.

A = absorption at 280 nm. c = protein concentration. d = path length of the micro volume unit. ε = molecular extinction coefficient.

To estimate the protein concentration of samples containing a protein mix an approximation equation was applied.

$$1\,A = 1\ \mathrm{mg/mL}$$

Equation 2: Approximation of the Protein Concentration.
A = absorption at 280 nm.

To determine the UV concentration of a protein mix or a purified protein, 1 μL or 2 μL were added to the micro volume unit of the spectrophotometer. Each measurement was performed in duplicate or triplicate. The sample buffer was used as blank.

3.2.12. **Active-Site Titration (AST)**

An active-site titration was performed to quantify purified FKBPs exhibiting an intact binding pocket for protein or compound interactions [53, 70]. For this purpose, a serial dilution of the protein was mixed with a tracer consisting of a FKBP ligand and a fluorophore (chapter 2.2, p. 22). The binding of the tracer to the protein was determined by fluorescence polarization (FP). Here, the tracer MTQ238 [70], binding to the FK1 domain of FKBP51 and FKBP52 as well as to FKBP12 and FKBP12.6, was used. MTQ238 is made of a bicyclic FKBP ligand and 5-Tamra as fluorophore (Figure 5).

The protein stock was diluted in FP-assay buffer (20 mM Hepes, 0.002% (v/v) Triton X-100, pH 8) based on the UV concentration (c_{final}(Protein, 1st well)=2 μM up to 5 μM). 20 mM MTQ238 DMSO stocks were pre-diluted 1:500 in DMSO (c_{stock}(MTQ238)=40 μM) to prevent compound precipitation in the following step. The 40 μM tracer stock was pre-diluted 1:67 in FP-assay buffer (c(4x MTQ238)=600 nM). 30 μL FP-assay buffer were transferred into a 384-well assay plate (Corning #3575, non-binding surface, black). 60 μL of the pre-diluted protein stock were transferred and a serial dilution (15 up to 16 steps) was performed. 10 μL 4x tracer (=MTQ238) were added (c_{final}(MTQ238)=150 nM per well). 30 μL buffer mixed with 10 μL 4x tracer and 40 μL buffer were included as controls. The assay plate was incubated for at least 30 min up to 45 min at RT on a monoshaker. The fluorescence polarization was measured with the plate reader TECAN GENios Pro (Excitation: 535 nm ± 25 nm, Emission: 590 nm ± 20 nm, Gain: 71, Mirror: Dichroic 2, Temperature: 32°C up to 40°C). Protein low binding tubes were used for all steps. All assays were performed at least twice and in a technical duplicate. EC50 and Hillslope were determined by 4-Parameter fit (Equation 3).

$$y = min + \frac{(max - \min)}{1 + \left(\frac{x}{EC50}\right)\text{^}(-Hillslope)}$$

Equation 3: 4-Parameter Fit.

Min = lower plateau. Max = upper plateu.
EC_{50} = half maximal effective concentration.

The protein active-site-concentration was determined by Equation 4.

$$cAST = \frac{cUV}{EC50} * [\frac{cfinal(Tracer)}{2} + Kd(Tracer)]$$

Equation 4: Determination of the Protein Concentration by Active-Site Titration.

AST = Active-site-concentration. c_{UV} = Protein concentration determined on the basis of the UV absorption at 280 nM. EC_{50} = half maximal effective concentration. Kd = Dissociation Constant.

3.2.13. **FKBP Ligand-Binding Assay**

Binding assays were performed to determine the dissociation constant (Kd) of the tracer for FKBPs. The pipetting protocol is similar to the protocol for active-site-titrations. A serial dilution of the protein (15 dilution steps) was performed and an equal tracer concentration was added to each well. In contrast to the AST lower tracer and protein concentrations were applied. Final protein concentration in the 1st well: 1 μM up to 5 μM. Equal tracer concentrations were used in the ligand binding and the competitive fluorescence polarization assay (Table 13, p. 43). The fluorescence polarization was measured with the plate reader TECAN GENios Pro (Excitation: 535 nm ± 25 nm, Emission: 590 nm ± 20 nm, Gain: 100, Mirror: Dichroic 2, Temperature: 32°C up to 40°C). All assays were performed at least in technical duplicates. The Kd was determined as described by Wang *et al.*[102].

FP-Assay Buffer: 20 mM Hepes, 0.002% (v/v) Triton X-100, pH 8.

3.2.14. **Competitive Fluorescence Polarization Assays**

Robot-based competitive fluorescence polarization assays were performed to characterize chemical compounds and to calculate binding affinities. The chemical compounds (20 mM DMSO stock) were pre-diluted in DMSO (final compound concentration: 10 μM up to 5 mM depending on the expected Kd). A serial compound dilution (1:2) was performed with DMSO (assay plate: 384-well, ABGene; final volume per well: 6 μL up to 8 μL). The assay plate was

centrifuged (180 rcf, 2 min, RT) and 2 μL of the serial compound dilution were added to 10.5 μL of 11.9x tracer (diluted in FP-assay buffer) in another 384-well assay plate (ABGene). 5 μL of the compound/tracer mix were added to 45 μL 1.1x FKBP, pre-diluted in FP-assay buffer, in a 384-well assay plate (Corning #3575, non-binding surface). The assay plate was centrifuged (180 rcf, 2 min, RT) and the compound/protein/mix was incubated in the dark for 15 min. The following controls were applied: (1) "no protein" (45 μL FPA buffer + 5 μL DMSO/tracer mix), (2) "no tracer" (45 μL FKBP + 5 μL DMSO/FPA buffer mix), (3) "DMSO" (45 μL protein + 5 μL DMSO/FPA buffer mix, (4) "high protein" (protein excess about factor 10,000 + 5 μL tracer/DMSO mix). The final tracer and protein concentrations are given in Table 13. The fluorescence polarization was measured by a plate reader (TECAN GENios Pro, Excitation: 535 nm ± 25 nm, Emission: 590 nm ± 20 nm, Gain: 100, Mirror: Dichroic 2, Temperature: 32°C up to 40°C). The final compound dilution factor is 62.5. The assays were performed in technical duplicates.

Table 13: Competitive Fluorescence Polarization Assay – Protein and Tracer Concentration.

The amino acid sequence of the applied FKBP constructs is indicated by the HG number (glycerol stock number). Tracer: MTQ238.

Protein	c_{final} (FKBP)	c_{final} (MTQ238)
FKBP51FK1 HG633	15 nM	1 nM
FKBP52FK1 HG92	10 nM	1 nM
FKBP12 HG21	1 nM	0.5 nM
FKBP12.6 NoCys HG707	10 nM	1 nM

The Kd for the compounds was determined by cubic fit as described by Wang *et al.* [101].

3.2.15. **BCA Assay (Bicinchoninic Acid Assay)**

The Pierce® BCA assay kit (Thermo Scientific, #23227) was applied to calculate the total protein concentration in HEK293 and N2a cell lysates. The assay was performed regarding to the manufacturer´s instruction. The cell lysate samples were pre-diluted in NETN cell lysis buffer (100 mM NaCl, 20 mM Tris, 0.5 mM EDTA, 0.5% (v/v) Nonidet-P40 substitute, 1 mM PMSF, 1 mM DTT, protease inhibitor cocktail (cOmplete mini, Roche, 1 tablet per 10 mL cell lysis buffer)). 25 μL of each sample were mixed with 200 μL working solution (reagents provided by the manufacturer) in a 96-well assay plate (clear, flat bottom, Greiner). The assay plate was incubated for 30 min at 37°C on a thermomixer. The absorbance was measured with a plate reader (TECAN GENios Pro) at 540 nm.

3.2.16. **FKBP51FK1 Affinity Matrix Preparation**

FKBP51FK1 Affinity Matrix

To prepare a FKBP51FK1 based affinity matrix, the HsFKBP51FK1 mono cysteine mutant was covalently coupled to SulfoLink® coupling resin (Thermo Scientific) carrying iodoacetyl groups via a nucleophilic substitution (S_N2 reaction). Residual reactive groups of the resin were blocked with 2-mercaptoethanol (Figure 8).

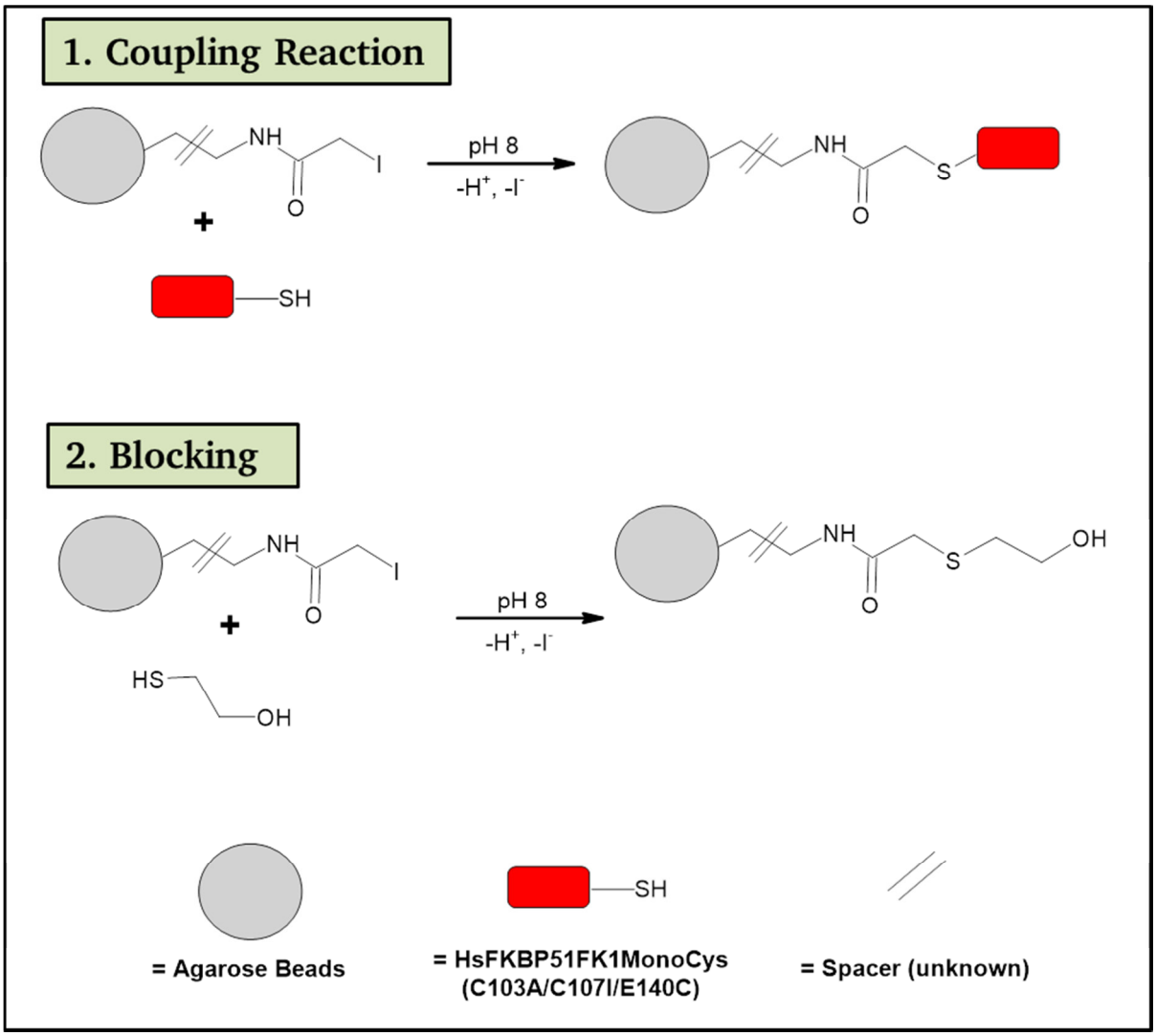

Figure 8: Immobilization of HsFKBP51FK1MonoCys on SulfoLink® Coupling Resin.

1. Coupling Reaction: HsFKBP51FK1MonoCys C103A/C107I/E140C carrying a *C*-terminal located mono cysteine residue (red box) was covalently coupled to SulfoLink® coupling resin (Thermo Scientific, grey circle) exhibiting reactive iodoacetyl groups via a S_N2 reaction. 2. Blocking: Residual reactive groups were blocked with 2-mercaptoethanol. The characteristic features of the 12-atom spacer are unknown.

The preparation of the FKBP51FK1 affinity matrix can be divided into five parts:

1. Equilibration of the SulfoLink® coupling resin
2. Coupling of HsFKBP51FK1MonoCys
3. Washing to remove unbound HsFKBP51FK1MonoCys
4. Blocking of residual active iodoacetyl groups with 2-mercaptoethanol
5. Washing and storage.

To monitor the progress of the coupling reaction, the concentration of free HsFKBP51FK1MonoCys in the reaction mix was estimated by SDS-PAGE and Coomassie staining (Figure 9).

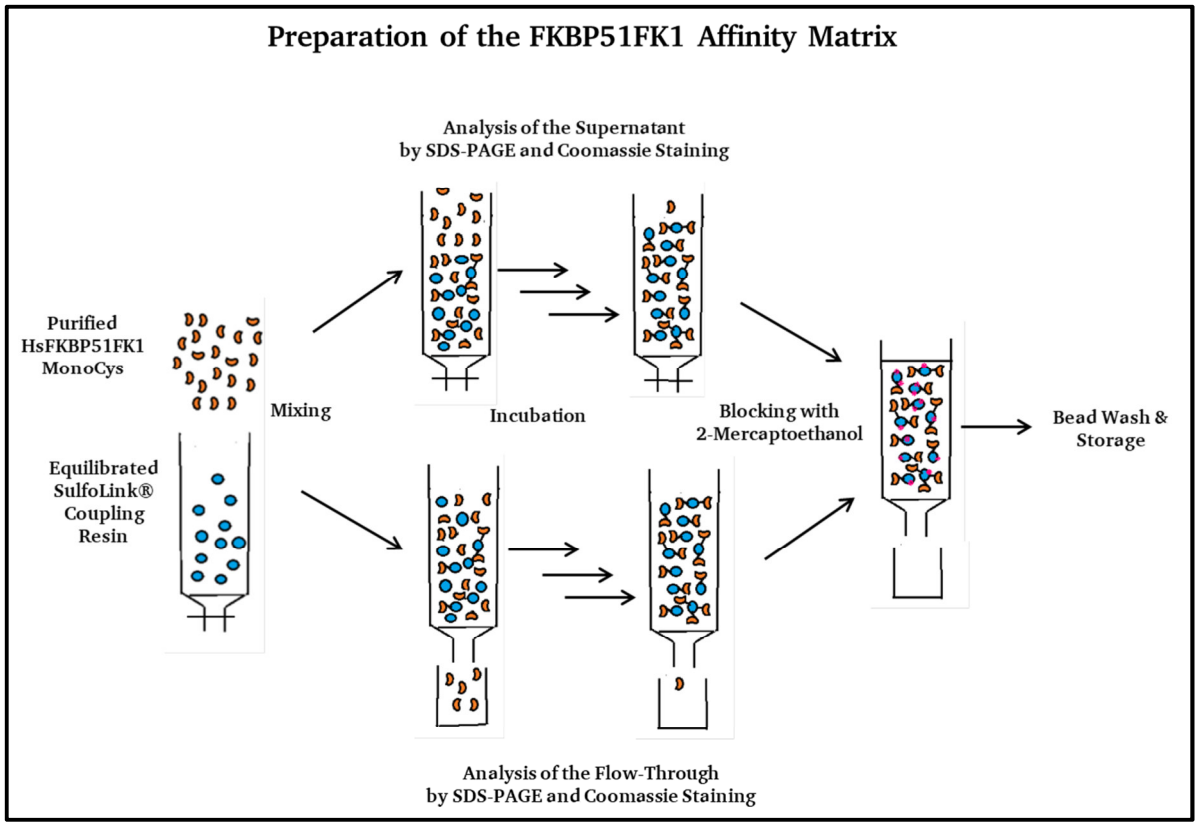

Figure 9: Preparation of the FKBP51FK1 Affinity Matrix – Experimental Setup.

HsFKBP51FK1MonoCys C103A/C107I/E140C was mixed with equilibrated SulfoLink® coupling resin (Thermo Scientific). The mix was incubated until the coupling reaction was completed. The concentration of free HsFKBP51FK1MonoCys in the reaction mix was analyzed by SDS-PAGE and Coomassie staining at different time points to evaluate the progress of protein immobilization. Samples were collected either by gravity flow (lower part) or collected from the supernatant (upper part). 2-Mercaptoethanol was added to inhibit residual active groups of the resin.

The FKBP51FK1 affinity matrix preparation protocol was optimized with regard to the coupling buffer and the incubation time. The procedure for the preparation of a FKBP51FK1 affinity matrix exhibiting a final protein density between 20 μM and 950 μM is described below. The test experiments are described in the supplement (chapter 6.1.1, p. 162 ff.). The optimized immobilization protocol was successfully applied by Jan-Philip Kahl (Master student, Intern, Batch: SMe312/JPK).

The protein immobilization was performed at RT. An HsFKBP51FK1MonoCys stock was diluted in 50 mM Tris/5 mM EDTA/equimolar TCEP/pH 8. The TCEP concentration was related to the UV based protein concentration. Comparing the settled bead volume with the protein volume the ratio was 1:1 or 1:2 (Table 14).

Table 14: Experimental Setup – FKBP51FK1 Affinity Matrix Preparation.

Different buffers were applied for protein dilution and bead equilibration. Buffer 1: 50 mM Tris, 5 mM EDTA, pH 8. Buffer 2: Buffer 1 + 20 µM TCEP, pH 8. Buffer 4: Buffer 1 + 950 µM TCEP, pH 8.

	HsFKBP51FK1 MonoCys	**SulfoLink® Coupling Resin**	**Number *N* of Independent Experiments**	**Exp. No.**
c	20 μM	19 mM	*N*=2	SMe357 SMe378
V	400 μL	400 μL		
Eq.	1	950		
Buffer	2	1		
c	950 μM	19 mM	*N*=4	SMe162 SMe182 SMe225 SMe303
V	0.8 mL - 5 mL	0.8 mL - 5 mL		
Eq.	1	20		
Buffer	4	1		
c	700 μM[1)]/770 μM[2)]	19 mM	*N*=2	SMe249[1)] SMe312/JPK[2)]
V	5.1 mL[1)]/2.5 mL[2)]	3.8 mL[1)]/2.0 mL[2)]		
Eq.	1	20		
Buffer	4	1		

SulfoLink® coupling resin (Thermo Scientific) was transferred into an empty column (MoBiTec: 2.5 mL, #S10129; 10 mL, #S10141) and equilibrated with 10 CV coupling buffer (50 mM Tris, 5 mM EDTA, pH 8). The equilibrated beads were remained in the column or transferred into a protein low binding tube (1.5 mL, 2 mL or 5 mL). HsFKBP51FK1MonoCys was added to the resin and the beads were suspended by inverting. After mixing, the column/tube was incubated standing upright for 5 min up to 10 min allowing the resin to settle down. A sample was collected immediately from the supernatant to estimate the amount of unbound HsFKBP51FK1MonoCys. The column/tube was inverted and incubated

for 1 h up to 2 h on a rolling device. Afterwards the column/tube was incubated standing upright for 5 min up to 10 min and another sample was collected from the supernatant. Samples from a tube were transferred into a column. The residual buffer was drained by gravity flow and the affinity resin was washed with 4 CV coupling buffer.

An excess of 2-mercaptoethanol (about 10x) was used to inhibit residual iodoacteyl groups of the resin. 1 CV blocking buffer (50 mM Tris, 5 mM EDTA, 10 mM 2-mercaptoethanol, pH 8) was added to the resin. The beads were suspended in the blocking buffer by inverting the column and the mix was incubated for 15 min on a rolling device. This step was repeated 5 times. Afterwards the column was placed in an upright position and the remaining blocking buffer was added. The column was washed with 20 CV coupling buffer not supplemented with TCEP. The FKBP51FK1 affinity matrix was stored in protein low binding tubes (Sarstedt) at 4°C.

Control Beads

Beads blocked with 2-mercaptoethanol (not coupled to FKBP51FK1) were prepared as a pull-down assay control. The procedure was similar to the protocol for the FKBP51FK1 affinity matrix preparation. Protein storage buffer was added to the beads instead of HsFKBP51FK1MonoCys.

3.2.17. FKBP51FK1 Affinity Matrix Binding Assay

A fluorescence based binding assay was established to assess the integrity of the FKBP51FK1 binding pocket after the protein immobilization. The binding of the tracer CK182 [53], consisting of a FKBP51 ligand interacting with the binding pocket of the FK1 domain and fluorescein as a fluorophore, was analyzed (Figure 5, p. 23: Chemical structure of CK182, Figure 10, p. 49).

The binding assay included 6 parts:

1. Estimation of the assay window by a serial dilution of CK182 or fluorescein
2. Adding a tracer excess to a column carrying the FKBP51FK1 affinity matrix and to a control column carrying naked beads (not coupled to FKBP51FK1)
3. Washing to remove not or unspecific bound tracer
4. Adding a FKBP ligand (SAFit1, JK095, Rapamycin) for the competitive elution of CK182

5. Determining the fluorescence intensity (FI) of all samples by a plate reader:
    - Initial FI=FI of CK182 loaded on both columns
    - FI of the flow-through collected while loading CK182
    - FI of the wash fractions
    - FI of the eluates
6. Comparing the initial FI of CK182 with the FI of samples containing unspecific or not bound tracer (=flow-through and wash fractions) and with samples containing competitively eluted CK182.

The binding assay was developed together with Johanna Bartmuß in the context of her Bachelor thesis. She showed the binding of CK182 to a thiol sepharose 4B based FKBP51FK1 affinity matrix and the competitive elution of the tracer with SAFit2 (Figure 6: Chemical structure of SAFit2, p. 23) [10].
Here, a SulfoLink® coupling resin based FKBP51FK1 affinity matrix was analyzed and different FKBP51 ligands (Rapamycin, SAFit1 (Figure 6, p. 23), JK095 (Figure 7, p. 24)) were tested as eluting agents.

To estimate the lower and upper detection limit of the plate reader as well as the area describing a proportional relation between the tracer concentration and the fluorescence intensity, a serial dilution of CK182 (SMe450, SMe456) or fluorescein sodium salt (Fluka) (SMe62, SMe64, SMe69) was performed with assay buffer (50 mM Tris, ± 5 mM EDTA, 0.002% (v/v) up to 0.02% (v/v) Triton X-100, 0.55% (v/v) up to 2% (v/v) DMSO, pH 8, cp. Table 15, p. 51). The first serial dilutions were run with fluorescein sodium salt instead of CK182 due to the limited availability of the tracer. However, the fluorescent properties of both chemicals might be different. Samples exceeding the upper detection limit of the plate reader or the upper saturated area were diluted with assay buffer.

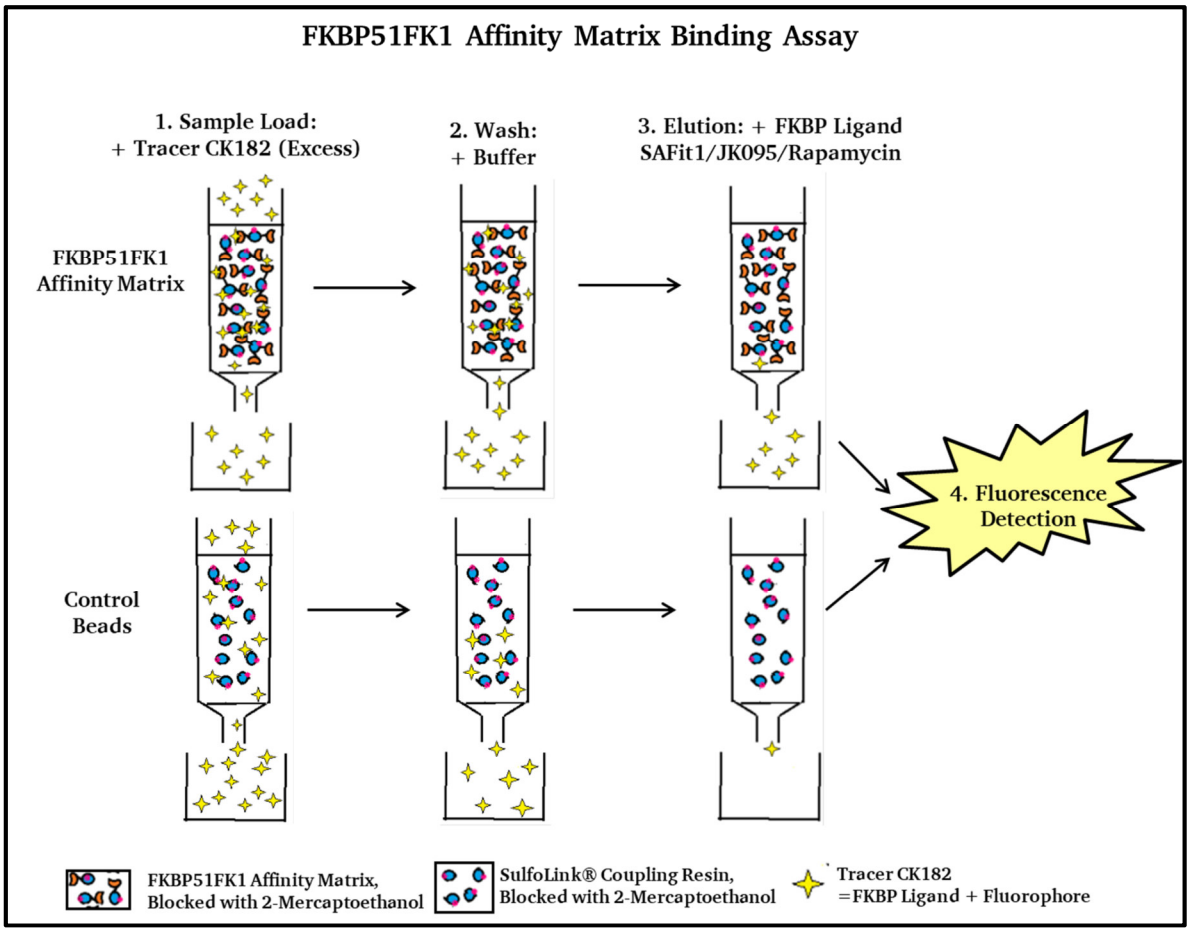

Figure 10: Fluorescence-Based FKBP51FK1 Affinity Matrix Binding Assay.

An excess (1.5x up to 2x) of the tracer CK182, consisting of a FKBP51FK1 ligand and fluorescein, was loaded on a column filled with the FKBP51FK1 affinity matrix. The column was washed with buffer to remove unbound or unspecific bound tracer. A compound (SAFit1, JK095 or Rapamycin) interacting with the binding pocket of the FK1 domain was added to elute CK182. The fluorescence intensities of the tracer added to the column, the flow-through collected during sample load, the wash fractions and the eluates were detected by a plate reader. Beads (- FKBP51FK1) only blocked with 2-mercaptoethanol were used as a control.

20 mM DMSO stocks of CK182 (Figure 5, p. 23: Chemical structure), SAFit1, Rapamycin (Figure 6, p. 23: Chemical structure) and JK095 (Figure 7, p. 24: Chemical structure) were prepared or inherited from former group members (chapter 2.2, p. 22). The use of protein low binding tubes for all CK182 dilutions is recommended to decrease or to inhibit the unspecific binding of the fluorophore to the plastic surface of the tubes. The DMSO compound stocks were diluted with assay buffer and vortexed. The assay concentration of all compounds is given in Table 15 (p. Table 15). Due to the limited compound solubility in water based buffers, compound solutions were centrifuged (15557 rcf, 20 min, RT) after diluting DMSO stocks with assay buffer. Only solutions not showing visible precipitation were used for the

binding assay. However, compound precipitation that was not visible might have been occurred.

Two empty 1 mL columns (Mobi Spin Column “F” with fixed outlet plug, inserted 10 μm filter, MoBiTec, #M105010S) were rinsed with assay buffer. One column was filled with the FKBP51FK1 affinity matrix (settled bead volume: 50 μL). A second column containing the resin with blocked active groups (not coupled to FKBP51FK1) was also prepared as a control. The columns were equilibrated with 5 CV up to 100 CV assay buffer. 1.5 up to 2 equivalents CK182 were added to both columns. The amount of CK182 was related to the calculated density of immobilized FKBP51FK1. After washing with 52 CV up to 420 CV assay buffer, a FKBP ligand (Rapamycin, SAFit1, JK095) was added for elution (Table 15). All fractions (sample load, wash and elution, Figure 10) were collected in protein low binding tubes (1.5 mL, 2 mL, Sarstedt) and stored under light exclusion. The progress of the wash and the elution step was monitored by measuring the fluorescence intensity of the corresponding fractions. The wash step was completed after the baseline of the fluorescence intensity (FI) or a low level FI was reached. The elution was stopped after detecting a decrease of the fluorescence intensity in the eluates.

To measure the fluorescence intensity, 20 μL of each sample and 20 μL of the tracer loaded on both columns were transferred twice into a 384-well assay plate (Corning, #3575, no lid, flat bottom, non-binding surface, black, polystyrene). The assay buffer and dissolved compounds added for elution were included as negative controls. The fluorescence intensity of all samples was measured by a plate reader (Tecan GENios Pro, Tecan Spark, Table 16). Fluorescein was excited at 485 nm (± 20 nm) and the emission was measured at 520 nm (± 10 nm, Tecan GENios Pro) or at 535 nm (± 25 nm, Tecan Spark).

The application of the protocol described for SMe450 and SMe456 is recommended for further assays (Table 15, Table 16).

Table 15: Experimental Setup Fluorescence-Based FKBP51 Affinity Matrix Binding Assay.

An excess of the tracer CK182 was added to an equilibrated column filled with the FKBP51FK1 affinity matrix. A column only carrying beads (- FKBP51FK1) served as a control. Settled bead volume = 50 µL (= 1 CV). The buffer volumes added for the equilibration, wash and elution step are indicated in column volumes (= CV). The experimentally estimated density of immobilized FKBP51FK1 is given. The amount of CK182 loaded on each column was divided by the estimated amount of immobilized FKBP51FK1 (= 51FK1) to calculate the CK182/51FK1 ratio. The amount of the compound (= Cpd) added for elution was divided by the estimated amount of FKBP51FK1 to calculate the Cpd/51FK1 ratio. DMSO stocks of CK182 and the compounds were diluted with assay buffer 1-4 as indicated. The final DMSO concentration in the assay buffer is given.

Buffer 1: 50 mM Tris, 5 mM EDTA, 0.002% (v/v) Triton X-100, 0.1% (v/v) DMSO, pH 8.
Buffer 2: 50 mM Tris, 5 mM EDTA, 0.02% (v/v) Triton X-100, 2% (v/v) DMSO, pH 8.
Buffer 3: 50 mM Tris, 5 mM EDTA, 0.002% (v/v) Triton X-100, 0.55% (v/v) DMSO, pH 8.
Buffer 4: 50 mM Tris, 0.02% (v/v) Triton X-100, 0.57 % (v/v) DMSO, pH 8.

Table 15a: FKBP51 Affinity Matrix Binding Assay Design.

Exp. No.	51FK1 Density	Column Equili-bration	CK182		CK182/ 51FK1 Ratio
			c(CK182)	*V (CK182)*	
SMe62	350 μM	100 CV buffer	20 μM	1.75 mL	2
SMe64	350 μM	100 CV buffer	100 μM	350 μL	2
SMe69	350 μM	100 CV buffer	84 μM	420 μL	2
SMe450	20 μM	5 CV buffer	100 μM	15 μL	1.5
SMe456	950 μM	6 CV buffer	100 μM	710 μL	1.5

Exp. No.	Wash	Elution	Cpd/ 51FK1 Ratio	Assay Buffer	c_{final} (DMSO)
SMe62	420 CV buffer	107 CV 20 μM Rapamycin	6	1	0.1% (v/v)
SMe64	333 CV buffer	36 CV 200 μM SAFit1	21	2	2% (v/v)
SMe69	130 CV buffer	20 CV 340 μM JK095	19	2	2% (v/v)
SMe450	52 CV buffer	6 CV 100 μM SAFit1	30	3	0.55% (v/v)
SMe456	100 CV buffer	120 CV 100 μM SAFit1	13	4	0.57% (v/v)

Table 15b: Fraction Volume - FKBP51 Affinity Matrix Binding Assay.

Exp. No.	Fraction Volume		
	Flow-Through	**Wash Fraction**	**Elution**
SMe62	~ 1.6 mL in total	• 1st 40 µL – 60 µL • 2nd: 120 µL • 23x 800 µL – 100 µL • last: 500 µL (+51FK1), 120 µL (-51FK1)	• 1st: 80 µL – 110 µL • 2nd to last: 700 µL – 1200 µL
SMe64	~ 350 µL in total	• 1st: 40 µL – 60 µL • 13x 1000 µL – 1500 µL • last: 200 – 500 µL	• 60 µL – 500 µL
SMe69	~ 420 µL in total	• 1st: 20 µL – 60 µL • 2nd to last: 400 µL – 1000 µL	• 50 µL – 500 µL
SMe450	1 fraction: • 40 µL/50 µL	• 7x 100 µL – 950 µL • last: 100 µL	• 3x 100 µL
SMe456	1 fraction: • 710 µL	• 10x 500 µL	• 12x 500 µL

Table 16: Binding Assay – Fluorescence Intensity Detection.

20 µL of each sample were transferred twice into a 384 well assay plate (Corning, #3575, non-binding surface, black). The fluorescence intensity was measured with a plate reader (Tecan GENios Pro or Tecan Spark). CK182 was excited at 485 nm and the emission was measured at 520 nm (Tecan GENios Pro) or at 535 nm (Tecan Spark). The filter bandwidth is indicated. Program Tecan GENios Pro: Number of reads = 10, Integration time = 40 µs, Lag time = 0 µs. Program Tecan Spark: Number of flashes = 30, Integration time = 40 µs, Lag time = 0 µs, Settle time = 0 ms, Z-Position = 20386 µm (SMe456), 20429 µm (SMe450).

Exp. No.	Plate Reader	Tracer	Wavelength	Temp.	Gain	Mirror
SMe62 SMe64 SMe69	Tecan GENios Pro	CK182	Ex: 485 ± 20 nm Em: 520 nm ± 10 nm	24°C up to 26°C	23	Dichroic 3
SMe450	Tecan Spark	CK182	Ex: 485 ± 20 nm Em: 535 nm ± 25 nm	26°C	37	Dichroic 510
SMe456				31°C	24	

3.2.18. Pull-Down Assay for the Affinity Enrichment of Potential FKBP51 Binding Proteins

Objective

A pull-down assay with a FKBP51FK1 affinity matrix was developed to enrich potential FKBP51FK1 interacting proteins from cell lysates. The aim was to catch FKBP51 binding partners by the affinity matrix. Unspecific bound proteins should be removed by washing. Especially, binding partners interacting with the binding pocket of the FKBP51FK1 domain should be addressed. For that purpose, the FKBP ligands SAFit1 and PPU339, interacting with the binding pocket, were applied for competitive elution.

Control Experiments

Three different control experiments were run to distinguish FKBP ligand dependent eluting proteins from unspecific eluting proteins. Firstly, the SAFit1 dependent elution from a high density FKBP51 affinity column was compared with the mock elution to analyze unspecific wash effects. Additional assay buffer instead of a FKBP ligand was added to a FKBP51FK1 affinity matrix for mock elution. Secondly, the effect of an organic compound on the protein elution profile should be analyzed. The presence of an organic compound such as SAFit1 or PPU339 in the assay buffer might be sufficient for the unspecific elution of proteins from the FKBP51FK1 affinity matrix due to altered buffer properties. Therefore, the SAFit1 and PPU339 dependent protein elution profile from a low density FKBP51FK1 affinity column was compared with the elution profile caused by a non-binding SAFit1 analogue (=THE212P). The aim was to differentiate between the competitive elution of proteins caused by the binding of a FKBP ligand to the binding pocket of the FK1 domain and the elution induced by altered buffer properties. Thirdly, beads not coupled to FKBP51FK1 were included as a control to assess the background caused by unspecific protein interactions with the agarose based beads.

Pull-Down Assay Procedure

In general, the pull-down assay can be divided into 6 parts (Figure 11):

1. Preparation of a column carrying either the FKBP51FK1 (C103A/C107I/E140C) affinity matrix or the control beads that were not coupled to FKBP51FK1
2. Column equilibration with assay buffer
3. Addition of HEK293 or N2a cell lysate
4. Wash with assay buffer to remove unspecific bound proteins

5. Addition of either a FKBP ligand (SAFit1 or PPU339) or the non-binding SAFit1 analogue THE212P for elution or addition of assay buffer for mock elution
6. Assay read out:
    - SDS-PAGE & silver staining
    - Bottom-up proteomic analysis

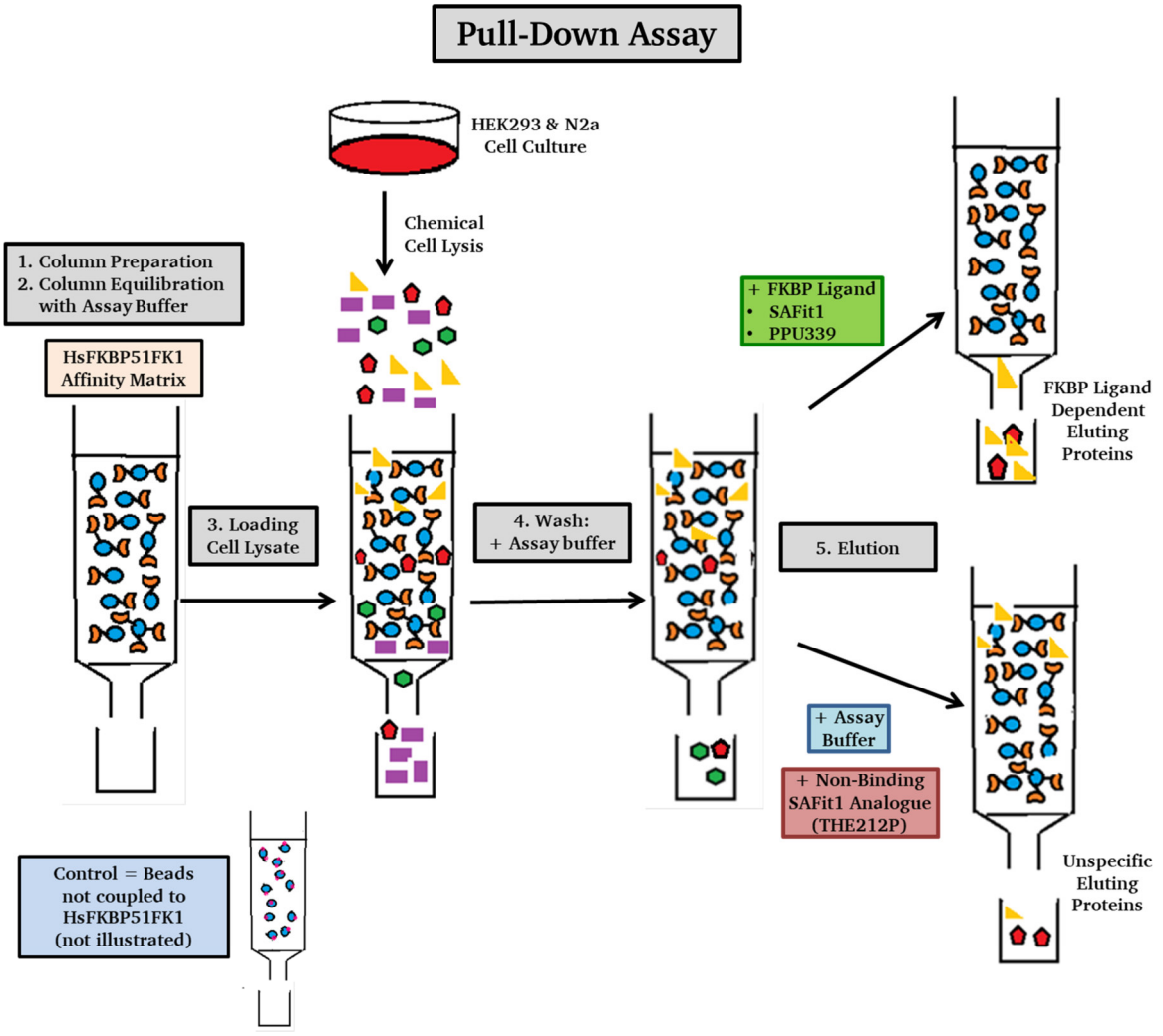

Figure 11: Experimental Setup FKBP51FK1 Pull-Down Assay.

Cell lysate (N2a or HEK293) was loaded on a column carrying the FKBP51FK1 (C103A/C107I/E140C) affinity matrix (final protein density: 20 µM or 950 µM). The column was washed with assay buffer to remove unspecific binding proteins. The FKBP ligands SAFit1 or PPU339 interacting with the FK1 domain of FKBP51 were added to elute potential protein binding partners. The non-binding SAFit1 analogue THE212P was applied as a control and assay buffer was added for mock elution to differentiate compound-dependent eluting proteins from unspecific eluting proteins. Control experiments were performed with beads not coupled to FKBP51FK1.

Four different pull-down assays were analyzed by MS-based proteomics (Table 17 a & b, p. 63). The differences are summed up below. Cell lysates originated from HEK293 (Figure 13 a) or N2a cells (Figure 13 b, Figure 14, Figure 15) were loaded on small affinity columns carrying 20 μmol (Figure 15) or 950 μmol immobilized FKBP51FK1 (Figure 13 a+b, Figure 14) per 1 L swollen settled beads to catch possible interacting proteins. The columns were washed with 50 CV assay buffer. Either compounds interacting with the binding pocket of the FKBP51FK1 domain, namely SAFit1 and PPU339, assay buffer or a non-binding SAFit1 analogue were added for elution. SAFit1 was applied for elution from the 20 μM (Figure 15) and the 950 μM FKBP51FK1 column (Figure 13 a+b, Figure 14). The mock elution with buffer from a 950 μM FKBP51FK1 column was included as a control in the 1st (Figure 13 a) and the 2nd MS run (Figure 13 b) but skipped in the 3rd MS run (Figure 14, Figure 15). However, additional controls were included in the 3rd MS run. A mock column carrying blocked beads (- FKBP51FK1) was included (Figure 14, Figure 15). Additionally, THE212P, a non-binding SAFit1 analogue was used for elution from a 20 μM FKBP51FK1 column (Figure 15). The bicyclic compound PPU339 was also added for elution from the 20 μM FKBP51FK1 column in the 3rd MS run (Figure 15).

Proteomic Pull-Down Assay Read Out

Firstly, all pull-down assay fractions were subjected to SDS-PAGE and silver staining to analyze the sample complexity and purity. Secondly, the samples were analyzed by MS-based proteomics at SINTEF industry (Norway, Trondheim). The MS-experiments were designed and run by Hanne Haslene-Hox and Anna Nordborg. The MS-data were analyzed by Hanne Haslene-Hox, Anna Nordborg [40] [41] and me (Figure 12).

Sample Preparation for Mass Spectrometry

The wash and elution fractions were pooled to reach the required protein amount per sample for the MS analysis. In a subsequent step, the samples were concentrated and the buffer was exchanged by ultrafiltration (chapter 3.2.4, p. 37). The protein concentration of the final samples was estimated spectrophotometrically based on the UV absorption at 280 nm (chapter 3.2.11, p. 40) or by SDS-PAGE (chapter 3.2.7, p. 39) and Coomassie staining (chapter 3.2.8, p. 39). The final samples were analyzed by SDS-PAGE and silver staining (chapter 3.2.9, p. 39). The samples were frozen in liquid nitrogen, stored at -80°C, thawed at room temperature and shipped on dry ice to Trondheim (in Norway). The samples were processed by Hanne Haslene-Hox and analyzed by MS-based proteomics at SINTEF Industry [40, 41]. The method is described in the supplement (Suppl. chapter 6.1.2, p. 169 ff.).

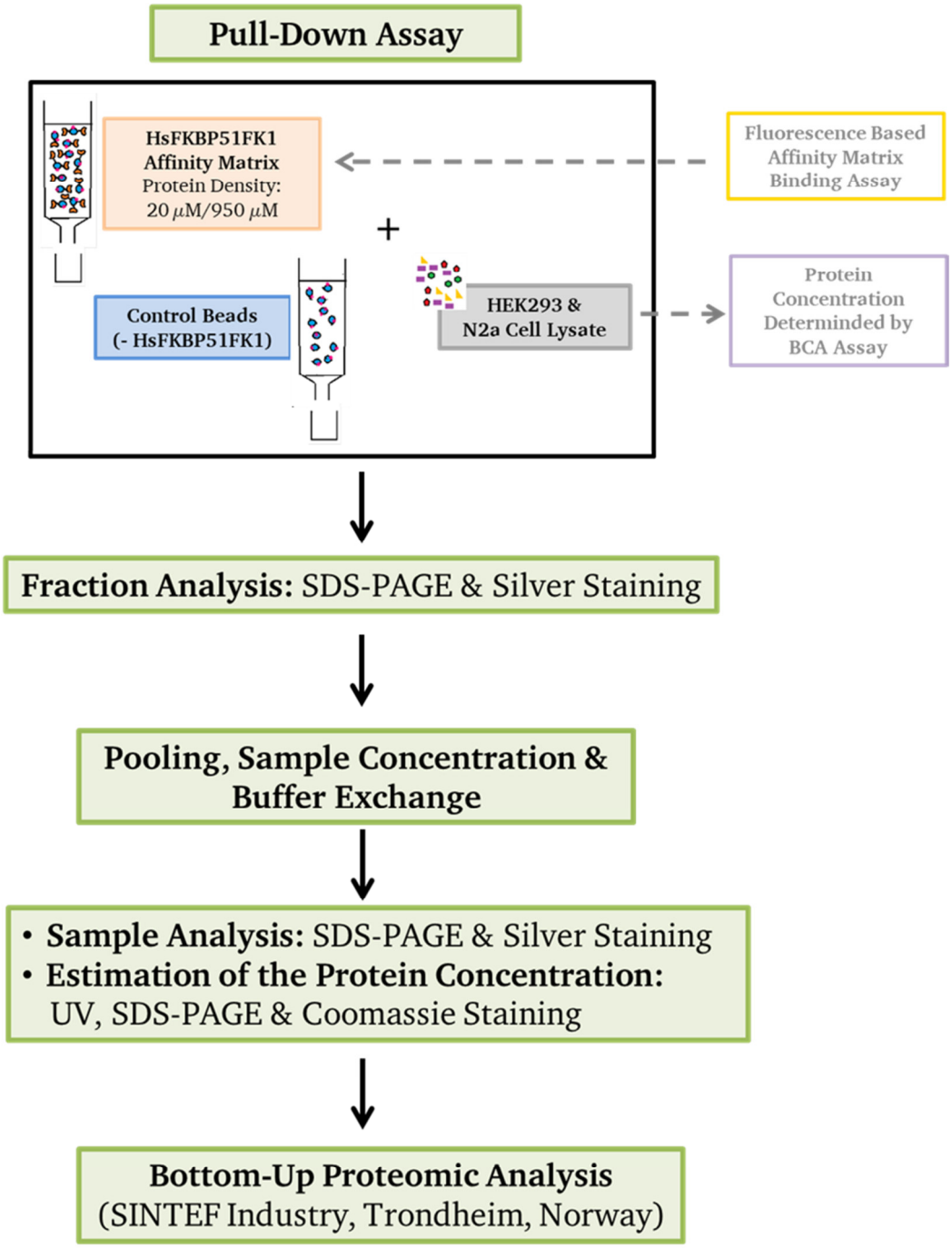

Figure 12: Workflow MS-Based Proteomic Pull-Down Assay Analysis.

A FKBP51FK1 affinity matrix was applied as a bait to enrich potential FKBP51 binding proteins from cell lysates. The samples were analyzed by MS-based proteomics.

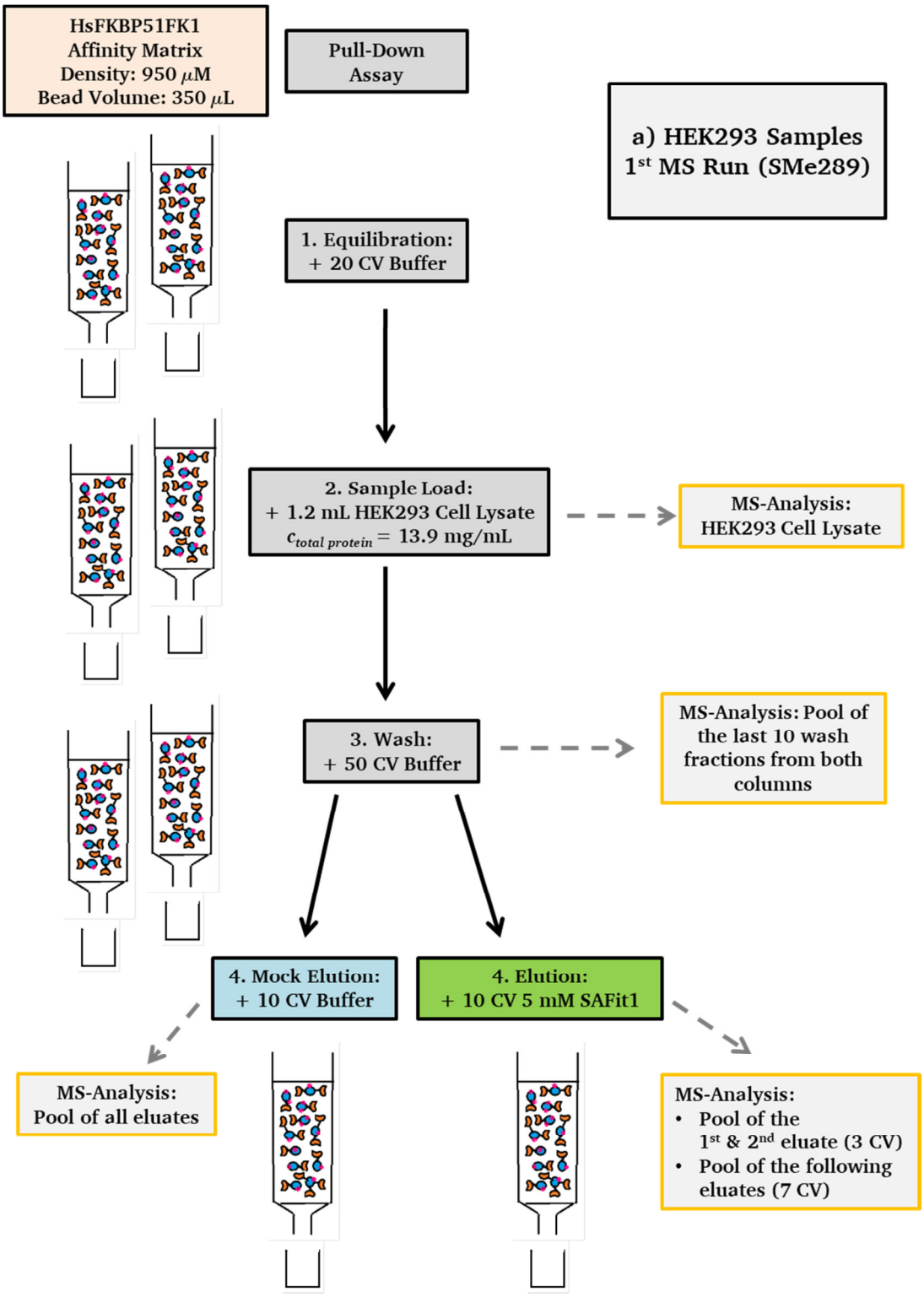

Figure 13 a: Comparing SAFit1 Dependent Elution with Mock Elution from a High Density FKBP51FK1 Affinity Column – HEK293 Samples (1st MS Run).

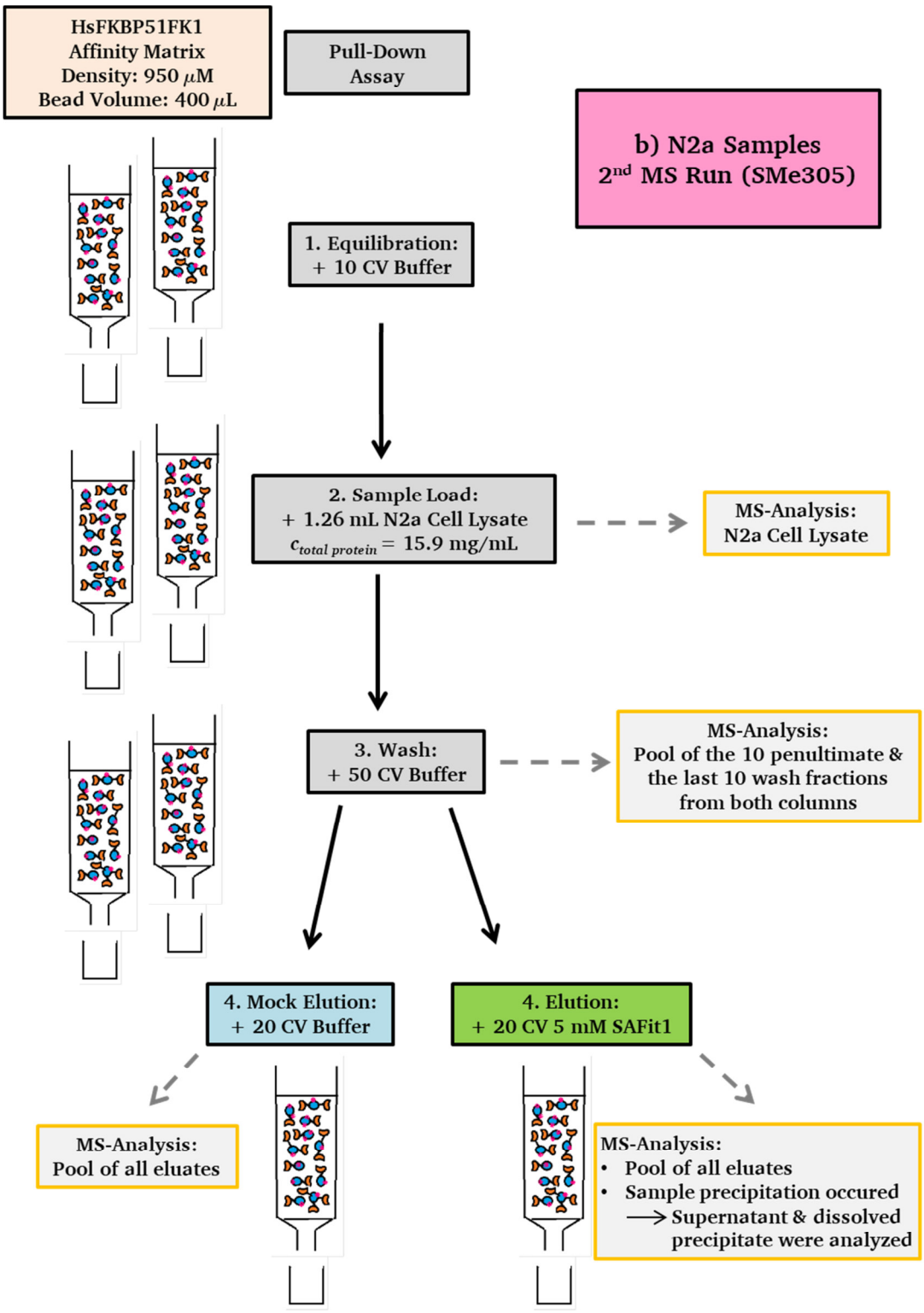

Figure 13 b: Comparing SAFit1 Dependent Elution with Mock Elution from a High Density FKBP51FK1 Affinity Column – N2a Samples (2nd MS Run).

Figure 13: Comparing SAFit1 Dependent Elution with Mock Elution from a High Density FKBP51FK1 Affinity Column.

Two columns carrying the HsFKBP51FK1 (C103A/C107I/E140C) affinity matrix (settled bead volume: 350 µL = 1 CV (Figure a), 400 µL = 1 CV (Figure b), about 332.5 nmol HsFKBP51FK1 per 350 µL settled beads) were equilibrated with 10 CV buffer. Either 1.2 mL HEK293 cell lysate (16.7 mg total protein, Figure a) or 1.26 mL N2a cell lysate (20 mg total protein, Figure b) were added to both columns. After washing both columns with 50 CV assay buffer, 10 CV (Figure a) up to 20 CV (Figure b) 5 mM SAFit1 (= FKBP ligand) were added for elution. To discriminate between SAFit1 dependent eluting proteins and unspecific eluting proteins an equal volume of assay buffer was added to the 2nd column for mock elution. The last wash fractions (Figure a + b: last 10 wash fractions, Figure b: + 10 penultimate wash fractions) and the eluates were pooled and prepared for MS-based analysis. SAFit1 dependent eluates were compared with the wash fractions and the mock eluates carrying unspecific eluting proteins. The complete HEK293 and N2a cell lysate was also analyzed as a control.

Figure a – HEK293 samples: Two pools of the SAFit1 dependent eluates were analyzed to differentiate between early and late SAFit1 dependent eluting proteins. All fractions of the mock elution were pooled.

Figure b – N2a samples: All fractions collected after adding SAFit1 or assay buffer in the elution step were pooled.

Equilibration and cell lysis buffer, pH 8: 20 mM Tris, 100 mM NaCl, 0.5 mM EDTA, 0.5% (v/v) Nonidet-P40 substitute, 1 mM PMSF, 1 mM DTT, Protease inhibitor cocktail (cOmplete mini, Roche, 1 tablet per 10 mL buffer).
Wash buffer, pH 8 = equilibration/cell lysis buffer without Nonidet-P40 substitute.
Elution buffer, pH 8 = wash buffer ± 5 mM SAFit1.

Figure 14: Comparing N2a Samples from a High Density FKBP51FK1 Affinity Column with N2a Samples from a Mock Column (3rd MS Run).

Two 400 µL columns carrying 380 nmol covalently coupled HsFKBP51FK1 (C103A/C107I/E140C) were prepared. Two 400 µL columns filled with the blocked beads (not coupled to HsFKBP51FK1) were applied as a control. After the column equilibration with 10 CV buffer, 1.6 mL N2a cell lysate carrying about 19 mg total protein were added to each column. After washing with 50 CV buffer, 20 CV 5 mM SAFit1 were added for elution. The last 20 wash fractions as well as all eluates were pooled to prepare samples for MS-based analysis. The complete N2a cell lysate was also analyzed by MS.

Equilibration and cell lysis buffer, pH 8: 20 mM Tris, 100 mM NaCl, 0.5 mM EDTA, 0.5% (v/v) Nonidet-P40 substitute, 1 mM PMSF, 1 mM DTT, Protease inhibitor cocktail (cOmplete mini, Roche, 1 tablet per 10 mL buffer).
Wash buffer, pH 8 = equilibration/cell lysis buffer not supplemented with Nonidet-P40 substitute. Elution buffer, pH 8 = wash buffer ± 5 mM SAFit1.

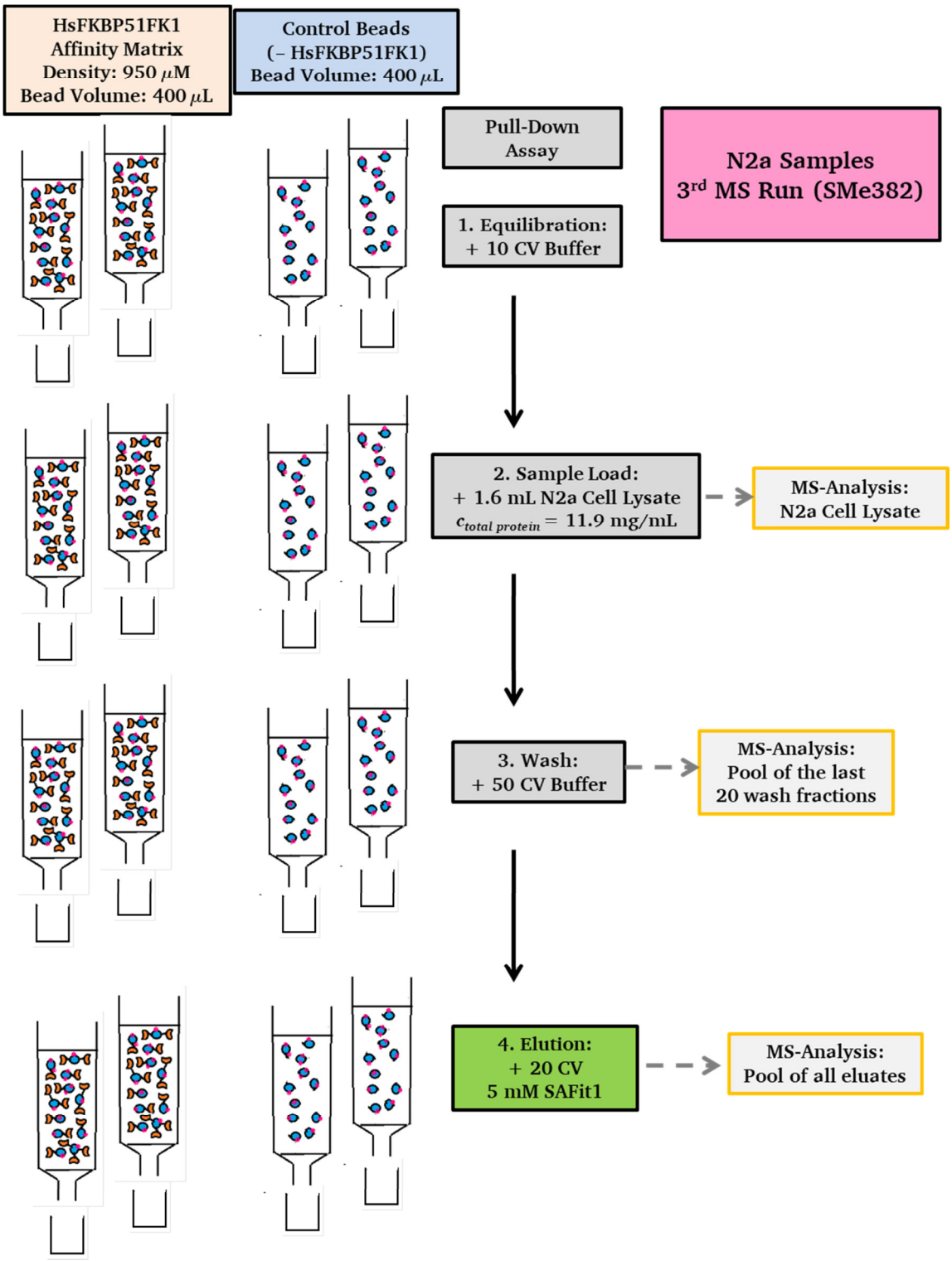

Figure 14: Comparing N2a Samples from a High Density FKBP51FK1 Affinity Column with N2a Samples from a Mock Column (3rd MS Run).

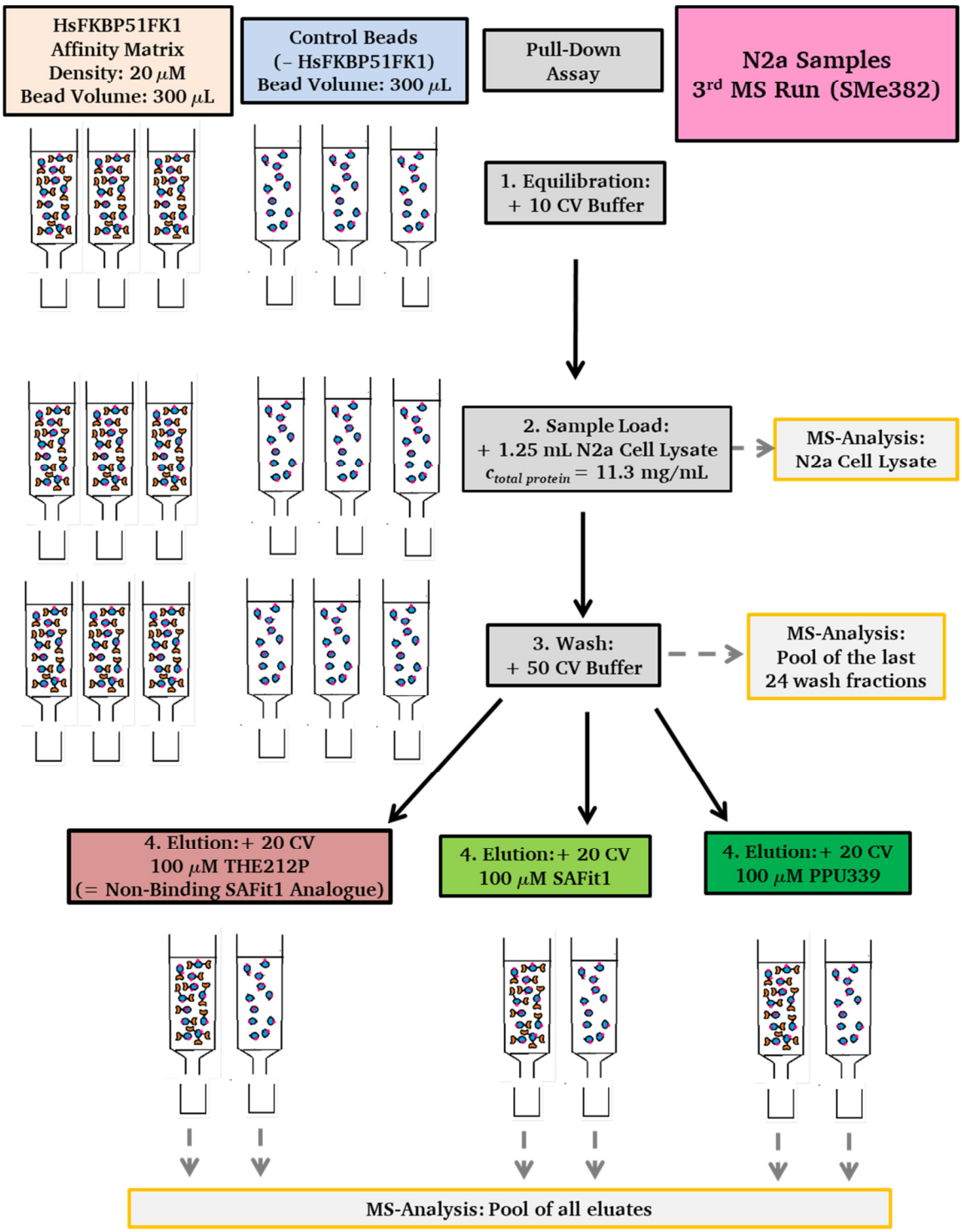

Figure 15: FKBP51FK1 Pull-Down Assays Applying a 20 µM Affinity Matrix.

Figure 15: FKBP51FK1 Pull-Down Assays Applying a 20 µM Affinity Matrix.

Three 300 µL affinity columns carrying 6 nmol covalently coupled HsFKBP51FK1 (C103A/C107I/E140C) were prepared. Three 300 µL columns filled with blocked beads (- FKBP51FK1) served as a control. After the column equilibration with 10 CV buffer, about 1.25 mL N2a cell lysate (about 14 mg total protein) were loaded on each column. All columns were washed with 50 CV buffer. Either 20 CV 100 µM SAFit1 or 100 µM PPU339 were added to elute potential binding partners interacting with the binding pocket of the FK1 domain. 20 CV 100 µM THE212P (= non-binding SAFit1 analogue) were added to another affinity column for elution to distinguish specific eluting proteins from the background.

The last 24 wash fractions and all eluates were pooled and processed for MS-based analysis. The total N2a cell lysate was also investigated.

Equilibration and cell lysis buffer, pH 8: 100 mM NaCl, 20 mM Tris, 0.5 mM EDTA, 0.5% (v/v) Nonidet-P40 substitute, 1 mM PMSF, 1 mM DTT, Protease inhibitor cocktail (cOmplete mini, Roche, 1 tablet per 10 mL buffer).
Wash buffer, pH 8 = 200 mM NaCl, 20 mM Tris, 0.5 mM EDTA, 1 mM PMSF, 1 mM DTT, Protease inhibitor cocktail (cOmplete mini, Roche, 1 tablet per 10 mL buffer).
Elution buffer, pH 8 = wash buffer + 100 µM SAFit1/100 µM PPU339/100 µM THE212P.

Table 17: Overview Samples Analyzed by Mass Spectrometry.

Samples of interest that could include enriched proteins are green colored.
[1]2nd Run (SMe305): Precipitation occurred during the concentration of the eluate. The supernatant (sample C) and the dissolved pellet (sample D) were analyzed.
[2]3rd Run (SMe382): The pull-down assay using a high density FKBP51FK1 affinity matrix and 5 mM SAFit1 for elution was performed twice.

Table 17 a: Samples Collected from a High Density (950 µM) FKBP51FK1 Affinity Column.

Affinity Matrix			Wash	Elution					Buffer		Sample ID		
Control Beads: – HsFKBP51FK1	20 µ HsFKBP51FK1	950 µM HsFKBP51FK1	+ Buffer	Mock Elution: + Buffer	+ 100 µM The212P	+ 100 µM SAFit1	+ 5 mM SAFit1	+ 100 µM PPU339	c(NaCl) = 100 mM	c(NaCl) = 200 mM	1st Run (SMe289)	2nd Run (SMe305)	3rd Run (SMe382)
–	–	+	+	–	–	–	–	–	+	–	A	A & B	3 & 7[2]
			–	–	–	–	+	–	+	–	B & C	C & D[1]	4 & 8[2]
+	–	–	+	–	–	–	–	–	+	–	-	-	5 & 9[2]
			–	–	–	–	+	–	+	–	-	-	6 & 10[2]
–	–	+	+	–	–	–	–	–	+	–	D	E & F	-
			–	+	–	–	–	–	+	–	E	G	-
Cell lysate loaded on the column									+	–	HEK293	N2a	N2a
Sample ID											Lysate	H	1[2]

Table 17 b: Samples Collected from a Low Density FKBP51FK1 Affinity Column (20 µM).

Affinity Matrix			Wash	Elution					Buffer		Sample ID		
Control Beads: – HsFKBP51FK1	20 μ HsFKBP51FK1	950 μM HsFKBP51FK1	+ Buffer	Mock Elution: + Buffer	+ 100 μM THE212P	+ 100 μM SAFit1	+ 5 mM SAFit1	+ 100 μM PPU339	c(NaCl) = 100 mM	c(NaCl) = 200 mM	1st Run (SMe289)	2nd Run (SMe305)	3rd Run (SMe382)
+	–	–	+	–	–	–	–	–	–	+	-	-	11
			–	–	+	–	–	–	–	+	-	-	12
–	+	–	+	–	–	–	–	–	–	+	-	-	13
			–	–	+	–	–	–	–	+	-	-	14
+	–	–	+	–	–	–	–	–	–	+	-	-	15
			–	–	–	–	–	+	–	+	-	-	16
–	+	–	+	–	–	–	–	–	–	+	-	-	17
			–	–	–	–	–	+	–	+	-	-	18
+	–	–	+	–	–	–	–	–	–	+	-	-	19
			–	–	–	+	–	–	–	+	-	-	20
–	+	–	+	–	–	–	–	–	–	+	-	-	21
			–	–	–	+	–	–	–	+	-	-	22
Cell lysate loaded on the column										+	-	-	N2a
Sample ID											-	-	2

The FKBP51FK1 pull-down assay is described in detail below.

Column Preparation and Equilibration

To enrich FKBP51FK1 interacting partners, two different affinity resins carrying either 20 μM (3rd MS run) or 950 μM HsFKBP51FK1 (C103A/C107I/E140C) (all three MS runs) were prepared (chapter 3.2.16, p. 44 ff.). Beads that were not coupled to FKBP51FK1, only carrying blocked active groups, were used as a control in the 3rd MS run. The FKBP51FK1 affinity and the control resin were transferred into an empty MoBiTEC column with an inserted filter. An upper filter pre-wetted with equilibration buffer was mounted. All empty columns were rinsed with desalted water and equilibration buffer before use. All columns were equilibrated with 10 CV up to 20 CV NETN cell lysis buffer (=equilibration buffer: 100 mM NaCl, 20 mM Tris, 0.5 mM EDTA, 0.5% (v/v) Nonidet P40-substitute, 1 mM DTT, 1 mM PMSF, protease inhibitor cocktail (cOmplete mini, Roche, 1 tablet per 10 mL), pH 8, cp. Table 18).

Table 18: FKBP51FK1 Pull-Down Assay – Column Equilibration.

Exp. No./MS Run	Affinity Matrix/ HsFKBP51FK1 Density	Settled Bead Volume	Equilibration Buffer Volume
SMe289: 1st Run	950 μM HsFKBP51FK1 (2x)	350 μL	20 CV
SMe305: 2nd Run	950 μM HsFKBP51FK1 (2x)	400 μL	10 CV
SMe382: 3rd Run	No HsFKBP51FK1 (3x)	300 μL	10 CV
	20 μM HsFKBP51FK1 (3x)		
	No HsFKBP51FK1 (2x)	400 μL	10 CV
	950 μM HsFKBP51FK1 (2x)		

Sample Load

HEK293 or N2a cell lysate was added to the equilibrated FKBP51FK1 affinity matrix or to the control beads. 4.7 mg up to 5 mg total protein dissolved in NETN cell lysis buffer were added per 100 μL resin (Table 19). The total protein amount of the cell lysate was determined by BCA assay (= Bicinchoninic acid assay, cp. 3.2.15, p. 43).

Table 19: FKBP51FK1 Pull-Down Assay – Sample Load.

Exp. No./ MS Run	Affinity Matrix			Sample Load				
	Control Beads: – HsFKBP51FK1	+ 20 μM HsFKBP51FK1	+ 950 μM HsFKBP51FK1	Cell Lysate	$V_{Cell\ Lysate}$	$c_{Total\ Protein}$	$m_{Total\ Protein}$ per Column	$m_{Total\ Protein}$ per 100 μL Resin
SMe289: 1st Run	–	–	2x 350 μL	HEK 293	1.20 mL	13.9 mg/mL	16.7 mg	4.8 mg
SMe305: 2nd Run	–	–	2x 400 μL	N2a	1.26 mL	15.9 mg/mL	20.0 mg	5.0 mg
SMe382: 3rd Run	3x 300 μL	3x 300 μL	–	N2a	1.25 mL	11.3 mg/mL	14.1 mg	4.7 mg
	2x 400 μL	–	2x 400 μL	N2a	1.60 mL	11.9 mg/mL	19.0 mg	4.8 mg

Column Wash

All columns were washed with 50 CV buffer (= 100 mM or 200 mM NaCl, 20 mM Tris, 0.5 mM EDTA, 1 mM DTT, 1 mM PMSF, protease inhibitor cocktail, pH 8) after loading the cell lysate. The assay buffer supplemented with 200 mM NaCl was used in the pull-down assay applying a low density FKBP51FK1 affinity column to decrease unspecific interactions of potential binding proteins with the agarose based affinity matrix. The assay buffer supplemented with 100 mM NaCl was used in the FKBP51FK1 pull-down assay applying a high density FKBP51FK1 affinity column.

Elution from a High Density (950 μM) FKBP51FK1 Affinity Column

In the elution step, 10 CV up to 20 CV 5 mM SAFit1 were added to an affinity matrix carrying about 950 μM HsFKBP51FK1. Based on the previous mass spectrometric results (HEK samples, Figure 13 a) the elution step was extended from 10 CV to 20 CV (Figure 13 b, Figure 14) to prepare N2a samples for the 2nd and 3rd MS run. The pull-down assay analyzed in the 3rd MS run was performed in duplicate.

The elution buffer (5 mM SAFit1, 20 mM Tris, 100 mM NaCl, 0.5 mM EDTA, 1 mM DTT, 1 mM PMSF, protease inhibitor cocktail, pH 8) was only supplemented with 100 mM NaCl since the SAFit1 solubility was negatively affected by a higher NaCl concentration.

Elution from a Low Density (20 μM) FKBP51FK1 column

Either 20 CV 100 μM SAFit1, 100 μM THE212P or 100 μM PPU339 were added to the resin carrying 20 μM HsFKBP51FK1 or to the control column for the elution step. The buffer system included 200 mM NaCl to decrease the background of unspecific bound proteins. Due to the solubility limit of THE212P and PPU339 in water based buffers, the compounds were not used for the elution from the high density (950 μM) FKBP51FK1 affinity column.

Concentration and Buffer Exchange

To prepare samples for proteomics, the last 20 CV of the wash step and the eluate were concentrated using 2 mL and 0.5 mL amicon ultra centrifugal filters (exclusion limit: 3 kDa, Merck Millipore). The buffer was exchanged with 100 mM NH_4HCO_3 including 1 mM PMSF and protease inhibitor cocktail (cOmplete mini, Roche, 1 tablet per 10 mL). To calculate the total protein concentration the absorption was measured at 280 nm using a DS11$^+$-spectrophotometer (DeNovix). The mean was calculated from 3 up to 6 measured values. The photometric determination of the total protein concentration in sample 4, 6, 8 and 10 was not possible due to the background caused by SAFit1. The protein concentration was estimated by SDS-PAGE and Coomassie staining. The samples 4, 6, 8 and 10 became a viscous gel at temperatures below 20°C. The samples were pre-warmed at 25°C for 5-10 min in a thermomixer for each pipetting step. Precipitation (sample 4, 6, 8 and 10) occurred during the sample concentration. The precipitates were dissolved by adding 100 mM NH_4HCO_3.

The total HEK293 cell lysate analyzed in the 1st MS run was shipped to Trondheim and a sample for proteomic analysis was prepared by Hanne Haslene-Hox.

3.2.19. MS-Based Proteomic Analysis of the FKBP51FK1 Pull-Down Assay

The procedure for the MS-based proteomic analysis is summarized in Figure 16.

Protein Ranking

Protein items identified exclusively in the SAFit1 dependent eluate or showing a higher abundance in the SAFit1 dependent eluate in comparison with the control samples were further analyzed by PANTHER [4, 16, 61, 89].

1.1) Protein Item Sub-Grouping

After selecting protein items from the "raw data excel sheet" protein subgroups shown in the result section were selected.

1.2) Assigning Identified Protein Items to Cellular Components & Protein Classes by PANTHER

The sub-grouped protein items were assigned to cellular components and protein classes by PANTHER [4, 16, 61, 89]. Proteins and protein subunits were related to the GO terms "Organelles" (PANTHER class information on organelles: "Organized structure of distinctive morphology and function. Includes the nucleus, mitochondria, plastids, vacuoles, vesicles, ribosomes and the cytoskeleton, and prokaryotic structures such as anammoxosomes and pirellulosomes. Excludes the plasma membrane." [67]), "Membrane" (PANTHER class information on membrane: "A lipid bilayer along with all the proteins and protein complexes embedded in it an attached to it." [65]) and "Cytosol" (PANTHR class information on cytosol: "The part of the cytoplasm that does not contain organelles but which does contain other particulate matter, such as protein complexes." [66]).

A Homo sapiens/mus musculus gene list included in the database was used as reference list. However, the reference list might not be representative for the proteome in HEK293/N2a cells. The aim of the analysis was to assign the pre-selected protein items to cellular components and protein classes. The enrichment of proteins located in a distinct cellular compartment or enrichment of protein classes was not focused in the analysis. Nevertheless, the test type "Fisher´s Exact" was selected and the FDR (false discovery rate) was calculated. However, results classified as "not significant" were included.

The following criteria were selected:

- Analysis type: PANTHER Overrepresentation Test (Released 2021-02-24)
- Annotation Version and Release Date: PANTHER version 16.0 Released 2020-12-01
- Analyzed List: Subgroups shown in the result section, December 2021
- Reference List: Homo sapiens (all genes in database)
- Annotation Data Set: PANTHER GO-Slim Cellular Component or PANTHER Protein Class
- Test Type: Fisher´s Exact
- Correction: Calculate False Discovery Rate (FDR).

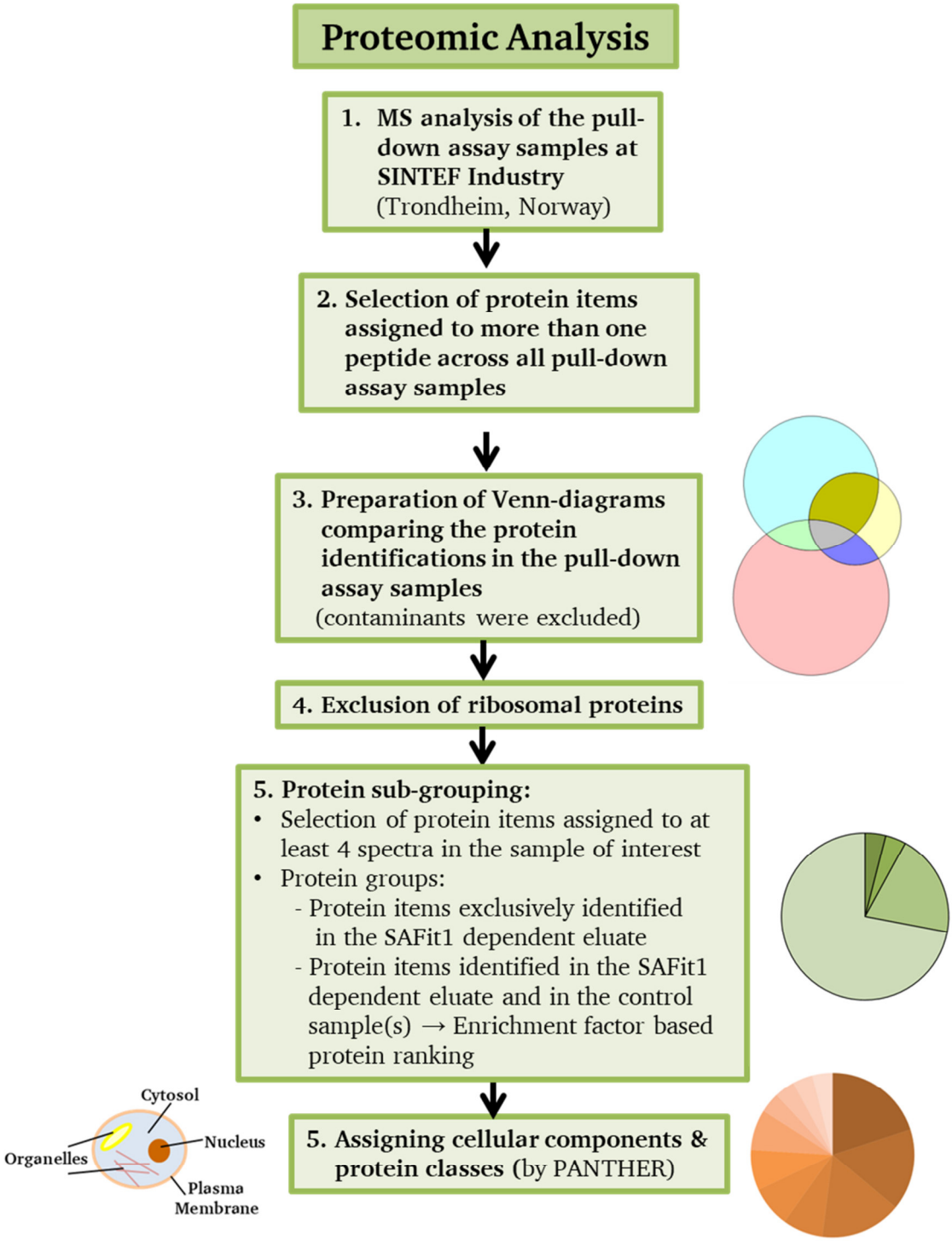

Figure 16: MS-Based Proteomic Analysis – Protein Selection Criteria and Procedure.

3.3. Cell Culture

All incubation steps were performed in cell incubator at 37°C and 5% CO_2.

3.3.1. Cell Cultivation and Passaging

Cells (HEK293 or N2a) were seeded in 10 cm TC-dishes and incubated for 2 up to 4 days in the cell incubator. The cells were passaged at a confluence of about 70% up to 80%. Therefore, cell media was removed and the cells were washed with 5 mL pre-warmed DPBS (-$CaCl_2$, -$MgCl_2$). 1 mL pre-warmed Trypsin-EDTA was added to detach the cells. The cells were incubated for 5 min at RT or at 37°C. The cells were resuspended in 5 mL cell culture media supplemented with FBS (10 % (v/v)) and centrifuged (Biofuge primoR, Heraeus: 1000 rpm, 3 min, RT). The supernatant was discarded and the cells were resuspended in cell culture media and seeded in a new TC-dish (Splitting ratio 1:20 at a confluence of about 70% up to 80%).

3.3.2. Coating of Tissue Culture Plates

TC-dishes were coated with poly-L-lysine (PLL) for N2a cell culturing. The PLL stock (0.002% (v/v)) was diluted in sterile water. Half of the recommended culture volume was added per TC-dish. The dishes were incubated with the PLL solution for 2 h up to 24 h at 37°C. The PLL solution was removed. The TC-dish was washed with sterile water (half of the recommended culture volume) and stored at 4°C.

3.3.3. Cell Counting

Cells were counted with a Neubauer counting chamber (Marienfeld) after resuspension. Therefore, 10 μL of the cell culture were mixed with 10 μL trypan blue. Thereof, 10 μL were transferred into the Neubauer counting chamber. All not blue colored cells in 4 large quadrants were counted. Each count was equal to 5,000 cells/1 mL cell suspension.

3.3.4. Preparation of Cell Lysates

TC-dishes coated with poly-L-lysine were used for N2a cell culturing. To prepare cell lysates for pull-down assays, 1x 10^6 HEK293 or N2a cells were seeded in a standard TC-dish 150 (Sarstedt, growth area: ~ 152 cm^2, V_{final}=36 mL, Media: DMEM +10% (v/v) FBS +1% (v/v) Pen/Strep) and incubated for 48 h (N2a cells) 72 h (HEK293 cells). After that, the media was removed and the cells were washed with 15 mL DPBS. To detach the adherent cells, 3 mL trypsin were added per TC-dish and the cells were incubated for 5 min at RT or at 37°C. To quench the enzymatic activity of trypsin and to harvest the cells, 15 mL media

(DMEM +10% (v/v) FBS -Pen/Strep) were added per TC-dish. The cell suspension was spun down (Biofuge primoR, Heraeus: 1000 rpm, 3 min, RT) and the supernatant discarded. The cell sediments were pooled by resuspension in 40 mL media (DMEM +10% (v/v) FBS -Pen/Strep). After an additional centrifugation step (120 g, 5 min, 4°C), the supernatant was discarded and the cell pellet was washed 5 times with 20 mL pre-cooled DPBS. Finally, the cell sediment was resuspended in NETN-Lysis buffer (100 mM NaCl, 20 mM Tris, 0.5 mM EDTA, 0.5% (v/v) Nonidet-P40 substitute, 1 mM DTT, 1 mM PMSF, protease inhibitor cocktail (cOmplete mini, Roche) pH 8). The suspension was transferred into a 5 mL protein LoBind tube (Eppendorf) and incubated at 4°C for 20 min on a rolling device. The suspension was spun down (13 000 g, 4°C, 20 min). The supernatant was transferred into a new 5 mL protein LoBind tube. Cell lysate aliquots were frozen in liquid nitrogen and stored at -80°C.

Cell culture media:
DMEM (500 mL) + 10% (v/v) FBS (50mL) (+1% (v/v) Pencillin/Streptomycin)

3.3.5. **Cryopreservation of Cell Lines**

To prepare cell stocks, the cells were resuspended in cell culture media supplemented with 10% (v/v) sterile filtered DMSO. The suspension was transferred into Cryo Pure tubes (Sarstedt, #72.379). The tubes were slowly frozen in a 1°C freezing container (Nalgene) at -80°C. The tube was stored in a liquid nitrogen tank after 24 h.

To start a new cell culture, media was added to a 10 cm TC-dish and a cell stock was thawed at 37°C in the water bath. The cell stock was resuspended in 5 mL fresh media and spun down (Biofuge primoR, Heraeus: 1000 rpm, 3 min, RT). The supernatant was discarded to remove the DMSO excess. The cells were seeded in the TC-dish and the cell culture media was changed after 24 h. The cells were cultured as described before.

4. Results

4.1. Expression and Purification of HsFKBP51FK1MonoCys

The expression and purification of HsFKBP51FK1MonoCys was analyzed by SDS-PAGE and Coomassie staining. A representative gel is shown (Figure 17). The expected molecular weight of HsFKBP51FK1MonoCys is about 18.5 kDa (cp. chapter 2.4, p. 27). A protein band in the designated range of 18 kDa up to 20 kDa appeared after inducing the protein expression (Figure 17, lane 2 and 3, red box). HsFKBP51FK1MonoCys was purified by Nickel affinity (Figure 17: lane 9) and size exclusion chromatography (SEC) (Figure 17: lane 10 - 12, Figure 18). SEC was applied as a polishing step, as quality control and for buffer exchange. No impurities were visible after SEC (Figure 17, Figure 18). The average yield of HsFKBP51FK1MonoCys from a 4 L bacterial culture is about 100 mg (Table 20).

Table 20: Summary Purification of HsFKBP51FK1MonoCys.

HsFKBP51FK1MonoCys was expressed in *E. coli* BL21(DE3)pLys. 1st column: Protein batch. 2nd column: Volume of the bacterial expression culture. 3rd column: Protein yield after size exclusion chromatography (SEC) calculated on the basis of the UV protein concentration. 4th column: UV-based (280 nm) protein concentration after SEC. 5th column: UV-based protein concentration after ultrafiltration. 6th column: Active-site-concentration using MTQ238 as tracer.

Protein Batch	V (Bacterial Culture)	m_{SEC}	c_{SEC} (UV) A280	c_{final} (UV) A280	c_{final} (AST)
SMe141	4 L	39 mg	90 μM	770 μM	930 μM
SMe142	4 L	80 mg	170 μM	700 μM	920 μM
SMe144	4 L	140 mg	190 μM	955 μM	1240 μM
SMe149	4 L	100 mg	160 μM	950 μM	1450 μM
SMe150	4 L	86 mg	140 μM	950 μM	1100 μM
SMe373	2 L	50 mg	100 μM	510 μM	670 μM

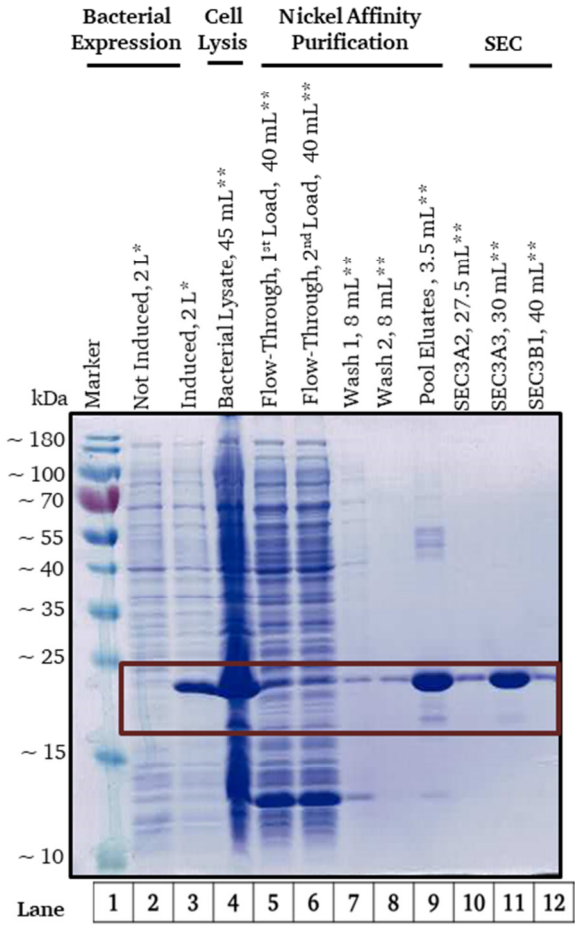

Figure 17: Expression and Purification of HsFKBP51FK1MonoCys.

Lane 1: Marker (PageRuler™ Prestained Protein Ladder, Thermo Scientific). Lane 2: Bacterial culture before inducing the protein expression. Lane 3: Bacterial culture induced with 0.6 mM IPTG at OD_{600} = 0.5 and incubated at 35°C for 4 h. *The sample volume of lane 2 and 3 was normalized to OD_{600}. Lane 4: Bacterial lysate after adding lysozyme for the enzymatic cell lysis. Lane 5: Flow-through after loading the sample to a Nickel column the 1st time. Lane 6: Flow-through after loading the flow-through shown in lane 5 a second time. Lane 7 & 8: 1st and 2nd wash of the Nickel column. Lane 9: Pooled eluates obtained from the Nickel column. The pool was loaded on a size exclusion column. Lane 10 - 12: Fractions (3A2, 3A3, 3B1) collected by size exclusion chromatography (SEC). HsFKBP51FK1MonoCys is marked by the red box.

To prepare the samples for SDS-PAGE, 3 parts of each sample were mixed with 1 part 4x laemmli buffer including 28 µL 2-mercaptoethanol per 1 mL. All samples were denatured for 10 min at 96°C. ** The sample volume per lane was normalized to the fraction volume. All samples were denatured for 10 min at 96°C.
Separation Gel: 14%. Coomassie staining.

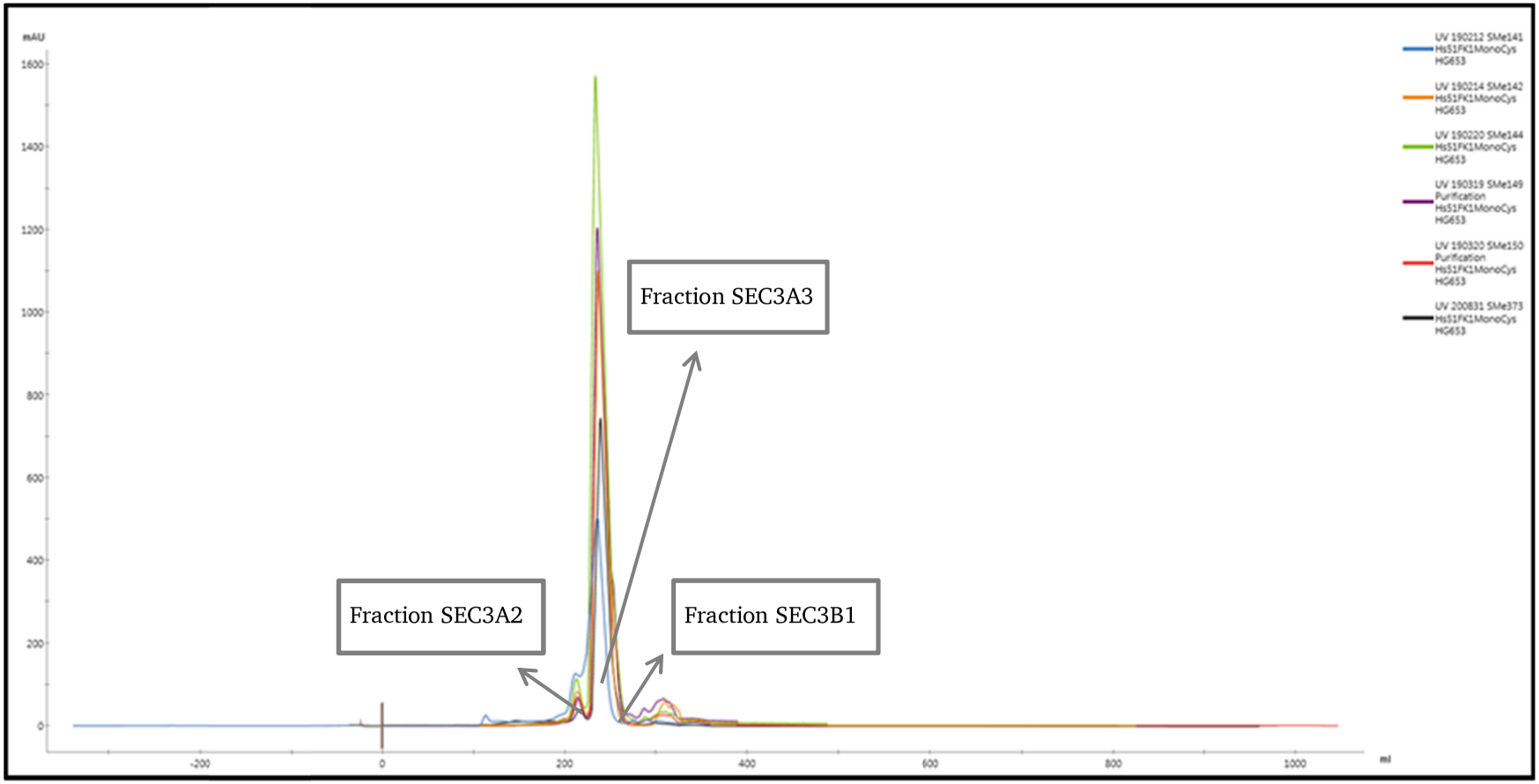

Figure 17: Overlay Size Exclusion Chromatogram HsFKBP51FK1MonoCys.
Size exclusion chromatography (ÄKTA pure, GE Healthcare, Column: HiLoad 26/600 Superdex 200 pg, flow rate: 1.3 mL/min, sample injection via superloop, UV trace: absorption at 280 nm) was performed after Nickel affinity purification. The purification of six HsFKBP51FK1MonoCys batches is shown. Running buffer, pH 8: 50 mM Tris, 5 mM EDTA, TCEP (510 µM: SMe373, 950 µM: SMe141, SMe142, SMe144, SMe149, SMe150). The small peak (Fraction SEC3A2), the main peak (Fraction SEC3A3) and the end of the main peak (Fraction SEC3B1) were analyzed by SDS-PAGE and Coomassie staining (Figure 17). The fraction numbering (grey arrows) of the run in SMe373 (black curve) is indicated.

4.2. Preparation of the FKBP51FK1 Affinity Matrix

Different FKBP51FK1 affinity resins exhibiting a final protein density in the range from 20 μM up to approximately 950 μM were prepared. The immobilization protocol was optimized with regard to the required incubation time to complete the coupling reaction and the concentration of the reducing agent TCEP in the coupling buffer. The volume ratio of the swollen settled beads and the dissolved protein was also considered (Table 21 a, Table 21 b).

The concentration of free (not coupled) HsFKBP51FK1MonoCys (~18.5 kDa) in the reaction mix was analyzed by SDS-PAGE and Coomassie staining to monitor the progress of the coupling reaction. The initial HsFKBP51FK1MonoCys stock concentration was determined spectrophotometrically (chapter 3.2.11, p. 40 f.) and by active-site titration (chapter 3.2.12, p. 41 f.). Representative Coomassie stained gels are shown below (Figure 19 a - c, Figure 20 a + b).

The protein band intensity of samples collected 20 min up to 90 min after starting the coupling reaction was reduced in comparison with the corresponding initial sample indicating a decrease of free HsFKBP51FK1MonoCys in the reaction mix (Figure 19 b: compare lane 4 with lane 5 & 6, lane 7 & 8, lane 9 & 10, Figure 19 c: compare lane 5 with lane 7, lane 9 & 10). No protein band was detected in the sample collected 1 h after mixing 20 μM HsFKBP51FK1MonoCys with an equal volume of equilibrated Sulfo Link® coupling resin (Figure 19 a: compare lane 6 with lane 8 & 9) suggesting the completeness of the coupling reaction or the achievement of the detection limit. Here, either no reducing agent (Figure 19 b) or an equimolar concentration of TCEP (Figure 19 a, Figure 19 c) in relation to the starting protein concentration was added to the coupling buffer.

The difference of the protein band intensities between the initial sample and the samples collected after incubating the reaction mix for 1 h up to 3 h seemed to be much higher by applying a coupling buffer supplemented with an equal amount of TCEP (Figure 19 b: compare lane 4 with lane 5 & 6, lane 7 & 8, lane 9 & 10, Figure 19 c: compare lane 5 with lane 7). No decrease of the protein band intensity was observed by extending the incubation time of the reaction mix up to 15 h 40 min applying a coupling buffer supplemented with an equimolar amount of TCEP (Figure 19 c: compare lane 7 with 9 and 10).

The doubling of the protein volume decelerated the coupling reaction (Table 21 b, compare experiment SMe79a and SMe79b).

In contrast to that, the protein band intensities of the starting sample and the samples collected after 45 min up to 3 h remained approximately on the same level (Figure 20 a: compare lane 7 & 8 with 9 & 10 and 11 & 12, Figure 20 b: compare lane 11 & 12 with lane 13 & 14, Table 21 a) using a coupling buffer supplemented with an excess of TCEP. A slight decrease of the protein band intensity was detected after extending the incubation time up to 23 h (Figure 20 a).

Taken together, the application of a coupling buffer supplemented with an equal amount of TCEP in relation to the protein stock concentration led to the largest difference of the protein band intensities between the initial or reference sample (purified HsFKBP51FK1MonoCys) and the samples collected after incubating the reaction mix for 1 h or 90 min (Table 21 b, Figure 19).

Figure 19: Coupling of HsFKBP51FK1MonoCys to SulfoLink® Coupling Resin.

Equal volumes (a: 1.5 mL, b: 150 µL, c: 3.5 mL) of HsFKBP51FK1MonoCys (a: 20 µM, b: 190 µM, c: 960 µM) and SulfoLink® coupling resin (Thermo Scientific) exhibiting reactive iodoacteyl groups (density: 19 mM) were mixed and incubated on a rolling device at RT for 1 h up to 3 h. The incubation step was continued overnight (ON) at 4°C. The bead volume was related to the settled beads. Purified HsFKBP51FK1MonoCys (18.5 kDa) is shown on all gels (Figure a: lane 2 - 4, Figure b: lane 2, Figure c: lane 3). Remaining active groups were blocked with 2-mercaptoethanol (= ß-Me). The affinity matrix was washed with buffer before (Figure c) and after the blocking step (Figure a & c).

The progress of the coupling reaction was analyzed by SDS-PAGE and Coomassie staining. Samples were collected after different time points (2 min up to 8 min, 21 min, 60 min, 90 min, 180 min and 15 h 40 min). The samples were collected by generating a flow (Figure a, b & c) or taken from the supernatant of the beads (Figure a & c).

Coupling reaction buffer: 50 mM Tris, 5 mM EDTA ± TCEP (pH 8) (Figure a: + 20 µM TCEP. Figure b: without TCEP, Figure c: + 950 µM TCEP). 3 parts of each sample were mixed with either 1 part (Figure a) or 3 parts (Figure b & c) 4x laemmli buffer + 14 µL 2-mercaptoethanol/mL. The samples were incubated at 96°C for 10 min and 5 µL (Figure c) up to 8 µL (Figure a & b) of each sample were loaded per lane. To assess the loading efficiency, some samples were loaded in duplicates (Figure b: 21 min, 1 h, 3 h, c: ON). Figure a: SMe378. Figure b: SMe79a. Figure c: SMe162. Separation gel: 14% (Figure a), 16% (Figure b & c). Marker: PageRuler™ Prestained Protein Ladder (Thermo Scientific), lane 1.

Figure a)

Density Hs51FK1: ~ 20 μM

Buffer, pH 8:

- 50 mM Tris
- 5 mM EDTA
- 20 μM TCEP

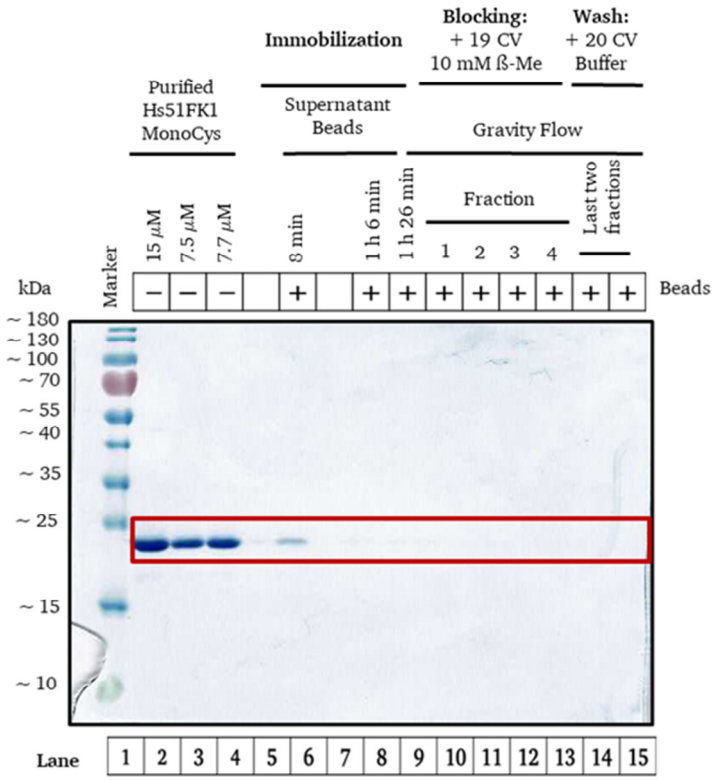

Figure b)

Density Hs51FK1: ~ 190 μM

Buffer, pH 8:

- 50 mM Tris
- 5 mM EDTA

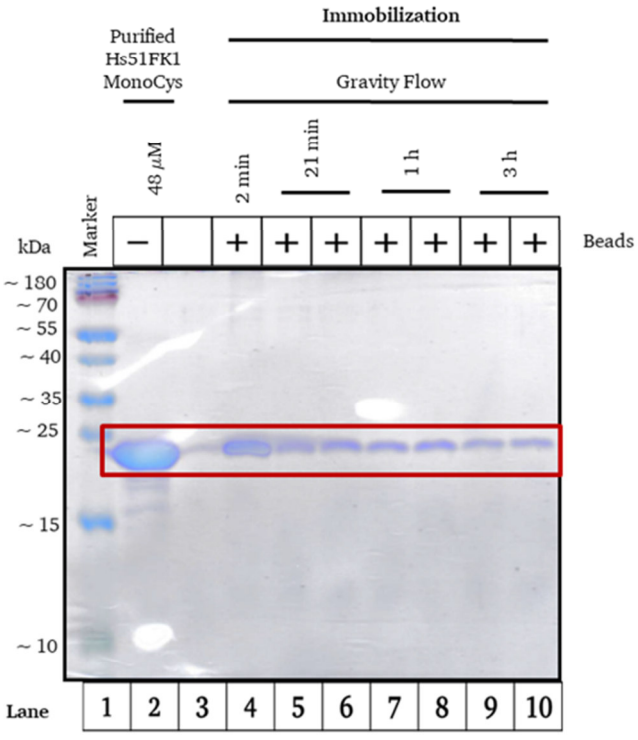

Figure 19: Coupling of HsFKBP51FK1MonoCys to SulfoLink® Coupling Resin.

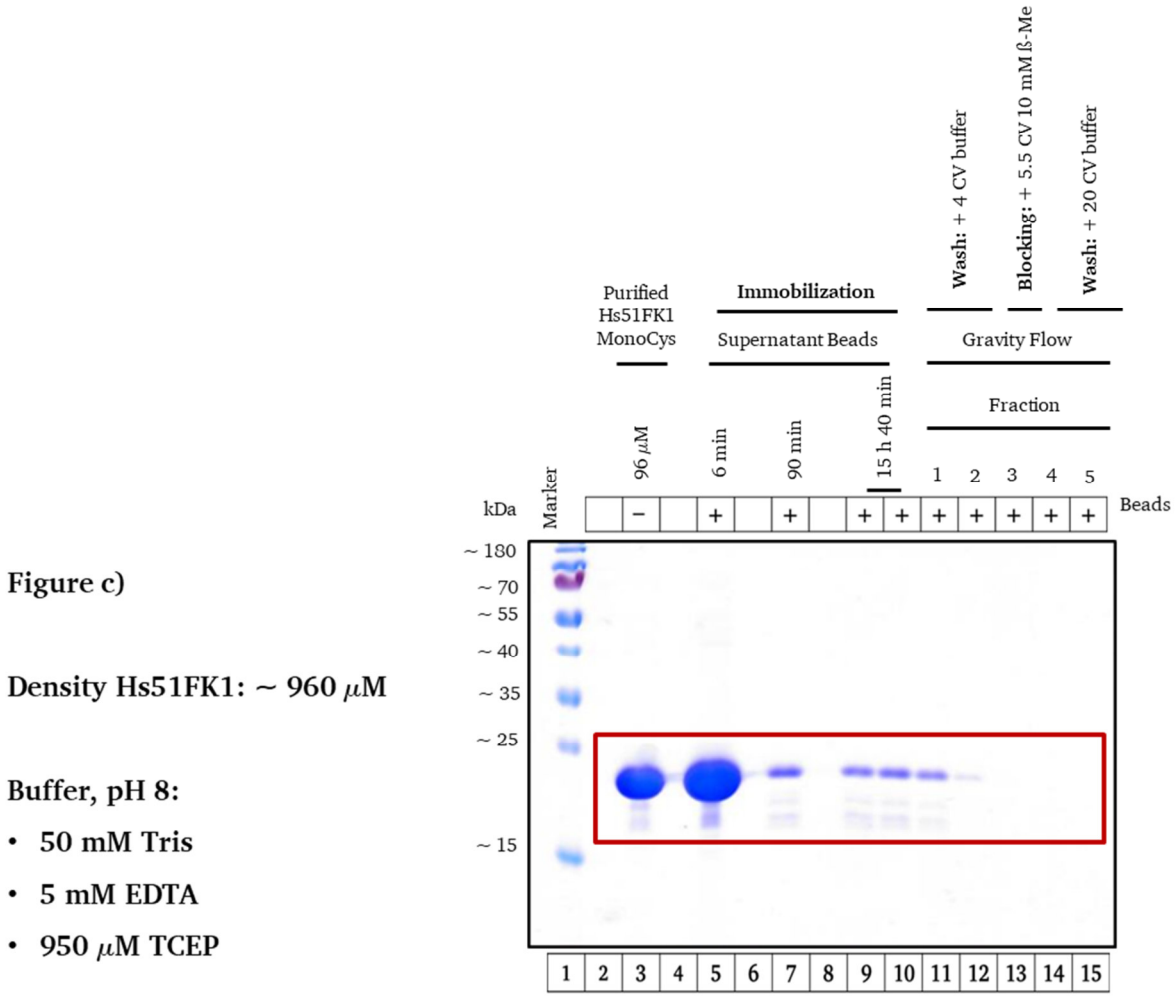

Figure 19: Coupling of HsFKBP51FK1MonoCys to SulfoLink® Coupling Resin.

Figure a)

Buffer, pH 8:

- 20 mM Hepes
- 20 mM NaCl
- 5% (v/v) Glycerol
- 10 mM TCEP

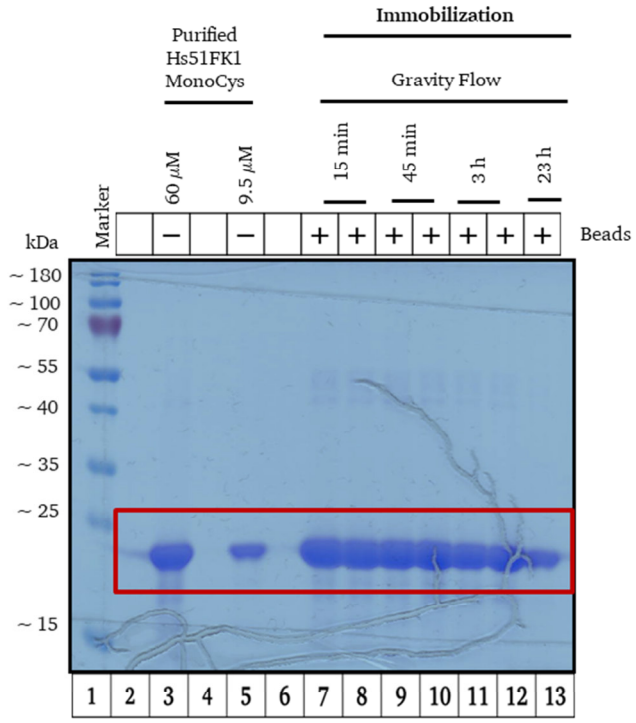

Figure b)

Buffer, pH 8:

- 50 mM Tris
- 5 mM EDTA
- 10 mM TCEP

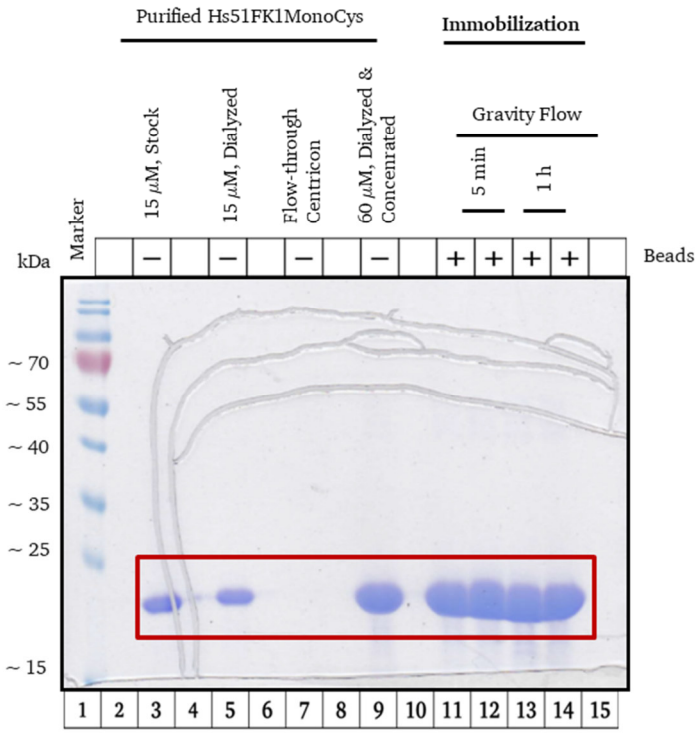

Figure 20: Excess of TCEP Inhibits the Immobilization of HsFKBP51FK1MonoCys.

Figure 20: Excess of TCEP Inhibits the Immobilization of HsFKBP51FK1MonoCys.

240 µL (Figure a) up to 250 µL (Figure b) 380 µM purified HsFKBP51FK1MonoCys (MW: 18.5 kDa, Figure a: lane 3 & 5, Figure b: lane 3, 5 & 9) were mixed with 250 µL (= settled bead volume) SulfoLink® coupling resin (Thermo Scientific) carrying 4.75 µmol iodoacteyl groups. The mix was incubated in an 800 µL column on a rolling device for 15 min (Figure a) up to 1 h (Figure b) at RT. Afterwards, the column was incubated at 4°C overnight standing upright (Figure a) or the experiment was stopped (Figure b).

To monitor the coupling efficiency one drop was collected after 5 min (b: lane 11 & 12), 15 min (a: lane 7 & 8), 45 min (a: lane 9 & 10), 1 h (b: lane 13 & 14), 3 h (a: lane 11 & 12) and 23 h (a: lane 13). The samples were analyzed by SDS-PAGE combined with Coomassie staining. Either 20 mM Hepes, 20 mM NaCl, 5% (v/v) glycerol, 10 mM TCEP, pH 8 (= protein purification buffer, Figure a) or 50 mM Tris, 5 mM EDTA, 10 mM TCEP, pH 8 (Figure b) were used for the coupling reaction.

HsFKBP51FK1MonoCys was dialyzed and concentrated (Figure b, lane 3: not dialyzed, not concentrated, lane 5: dialyzed, lane 9: dialyzed and concentrated) to exchange the protein purification buffer. The samples collected after 5 min, 15 min, 45 min, 1 h and 3 h were loaded on the gel as duplicates to verify the loading accuracy (Figure a & b).

To prepare samples for SDS-PAGE, 1 part of each sample was mixed with 1 part 4x laemmli buffer including 14 µL 2-mercaptoethanol per 1 mL. All samples were boiled at 96°C and subjected to SDS-PAGE (separation gel: 16%). Either 4 µL (Figure a) or 6 µL (Figure b) of each sample were loaded per lane. Not labeled lanes: no sample was loaded. Tears occurred during gel drying. Marker: PageRuler™ Prestained Protein Ladder (Thermo Scientific), lane 1.

Table 21: Immobilization of HsFKBP51FK1MonoCys on SulfoLink® Coupling Resin.

Different FKBP51FK1 affinity matrices exhibiting a protein density of 20 µM up to 950 µM were prepared. The UV based starting protein concentration and the density of the activated iodoacetyl groups are given (*c*). The volume of dissolved HsFKBP51FK1Monocys and the settled bead volume are indicated (*V*). Green colored entries belong to successful coupling reactions (Table 21 b). Light green indicates a low coupling efficiency and dark green suggests a high coupling efficiency. Conditions inhibiting the immobilization of HsFKBP51FK1MonoCys are red colored (Table 21 a). The indicated time is related to the duration of the coupling reaction or to the abortion of the experiment. The number of independent experiments is given by "#". Eg. = Equivalents.

Buffer 1: 50 mM Tris, 5 mM EDTA, pH 8. Buffer 2: Buffer 1 + 20 µM TCEP, pH 8. Buffer 3: Buffer 1 + 190 µM TCEP, pH 8. Buffer 4: Buffer 1 + 950 µM TCEP, pH 8. Buffer 5: Buffer 1 + 10 mM TCEP, pH 8. Buffer 6: 20 mM Hepes, 20 mM NaCl, 5% (v/v) Glycerol, 10 mM TCEP, pH 8.

Table 21 a: Immobilization of HsFKBP51FK1MonoCys on SulfoLink® Coupling Resin – Inhibition of the Coupling Reaction.

	Hs51FK1 MonoCys	SulfoLink® Coupling Resin	Density Hs51FK1	Time	#	Exp. No.
c	380 μM	19 mM	Coupling reaction failed	23 h	1	SMe49b
V	240 μL	250 μL				
Eq.	1	52				
Buffer	6	6				
c	380 μM	19 mM	Coupling reaction failed	1 h	1	SMe52b
V	250 μL	250 μL				
Eq.	1	50				
Buffer	5	5				

Table 21 b: Immobilization of HsFKBP51FK1MonoCys on SulfoLink® Coupling Resin - Successful Coupling Reactions.

	Hs51FK1 MonoCys	SulfoLink® Coupling Resin	Density Hs51FK1	Time	#	Exp. No.
c	700 μM	19 mM	< 700 μM	15 min	1	SMe56b
V	175 μL	175 μL				
Eq.	1	27				
Buffer	1	1				
c	350 μM - 380 μM	19 mM	< 350 μM/ 380 μM	15 min/ 20 min	3	SMe49a SMe52a SMe56a
V	175 μL - 250 μL	175 μL - 250 μL				
Eq.	1 eq.	50 - 55 eq.				
Buffer	1	1				
c	190 μM	19 mM	< 190 μM	20 min	1	SMe79a
V	150 μL	150 μL				
Eq.	1	100				
Buffer	1	1				
c	80 μM	19 mM	< 160 μM	1 h	1	SMe79b
V	300 μL	150 μL				
Eq.	1	120				
Buffer	1	1				
c	20 μM	19 mM	< 20 μM	1 h	2	SMe357 SMe378
V	400 μL	400 μL				
Eq.	1	950				
Buffer	2	1				
c	190 μM	19 mM	< 190 μM	1 h	1	SMe79c
V	150 μL	150 μL				
Eq.	1	100				
Buffer	3	3				
c	950 μM	19 mM	< 950 μM	90 min	4	SMe162
V	0.8 mL - 5 mL	0.8 mL - 5 mL		1 h		SMe182 SMe225 SMe303
Eq.	1	20				
Buffer	4	1				
c	700 μM/ 770 μM	19 mM	< 940 μM/ 810 μM	1 h	2	SMe249 SMe312/ JPK
V	5.1 mL/ 2.5 mL	3.8 mL/ 2.0 mL				
Eq.	1	20				
Buffer	4	1				

4.3. FKBP51FK1 Affinity Matrix Binding Assay

To assess the integrity of the FKBP51FK1 binding pocket after the protein immobilization a fluorescence-based binding assay was established. An excess of the fluorescent tracer CK182 interacting with the binding pocket was added to the FKBP51FK1 affinity matrix. A wash step was performed to remove not bound or unspecific bound CK182. CK182 interacting with the binding pocket was competitively eluted by adding FKBP ligands (Rapamycin, SAFit1, JK095). A column carrying naked beads not coupled to FKBP51FK1 was applied as a control to assess the unspecifc binding of the tracer to the agarose based beads.

The initial fluorescence intensity (FI) of the tracer CK182 loaded on the columns was compared with the fluorescence intensity of fractions carrying unbound or not specifically bound CK182 (= flow-through while adding CK182, wash fractions) as well as with the fluorescence intensity of fractions carrying the FKBP ligand dependent eluted tracer.

The initial fluorescence intensity of the diluted tracer loaded on the columns was set as 100 % for normalization (Equation 5).

$$Normalized\ FI(Sample) = \frac{FI(Sample) * V(Sample) * Dilution\ Factor(Sample)}{FI(CK182) * V(CK182) * Dilution\ Factor(CK182)}$$

Equation 5: Calculation of the Normalized Fluorescence Intensity.

The fluorescence intensity (FI) of a sample was related to the initial FI of the tracer CK182 added to the FKBP51FK1 affinity columns. *V*(Sample) = fraction volume. *V*(CK182) = tracer volume loaded on both columns. The dilution factor of the sample and the tracer CK182 was related to the sample dilution required for FI measurement. The normalized FI is given in % by multiplying the result with 100.

Representative results of one experiment are illustrated below (Figure 21). The normalized FI of the flow-through from the FKBP51FK1 affinity column (orange bar) was lower than the FI of the control column (blue bar). The FI decreased during the wash step. The wash step was stopped at a low FI level after adding 100 CV buffer. The FI of the wash fractions from the FKBP51FK1 affinity column declined faster than the FI of the wash fractions from the control column. The FI increased after adding the FKBP ligand SAFit1 to the FKBP51FK1 affinity column (orange bars, E1 - E5, red box) for competitive elution. No increase of the FI was observed after adding SAFit1 to the control beads (blue bars, E1 - E12). The elution was stopped at a low FI level above the background. As a validity check the FI sum of all fractions from both columns was built (bars at the right side).

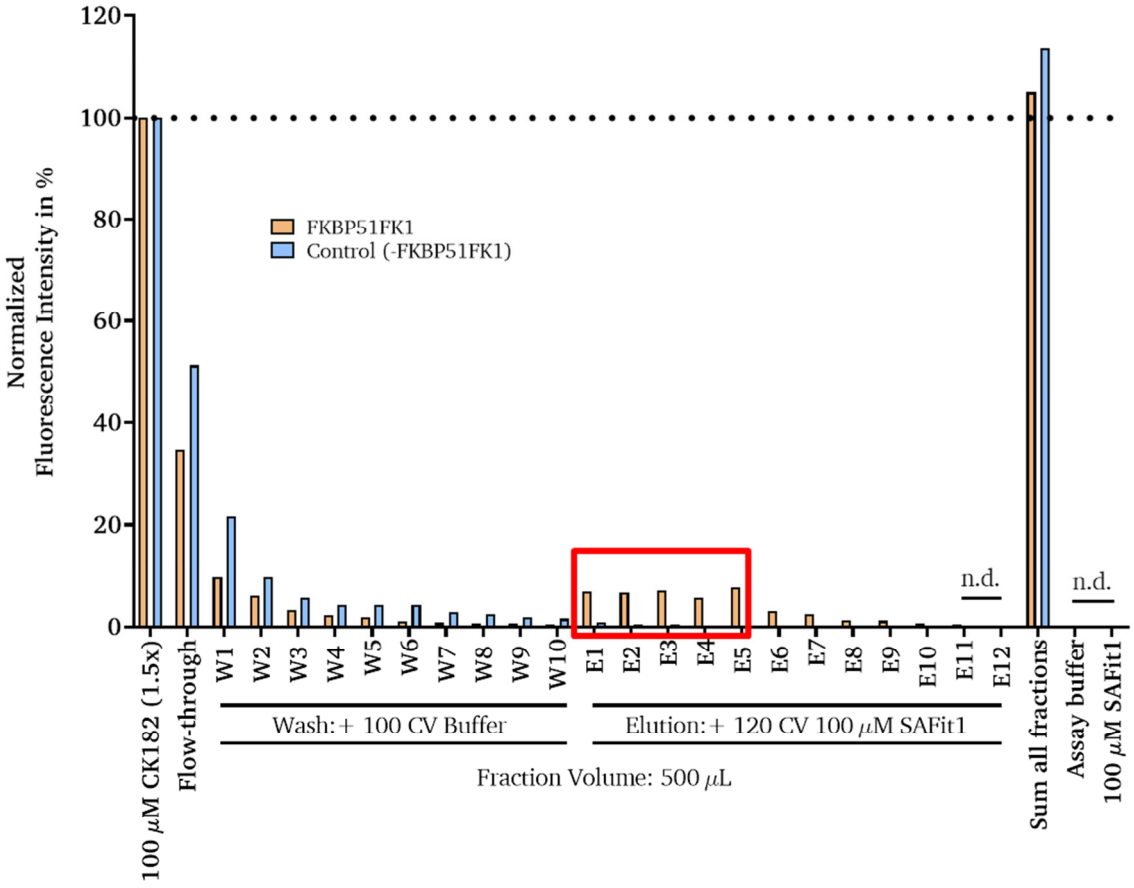

Figure 21: Binding of CK182 to the FKBP51FK1 Affinity Matrix.

710 µL CK182 (tracer) were loaded on a 50 µL (= 1 CV) column carrying 950 µM FKBP51FK1 (orange bar) and to a control column (- FKBP51FK1, blue bar). Both columns were washed with 100 CV assay buffer (W1 - W10). 120 CV 100 µM SAFit1 were added for elution (E1 - E12). The normalized fluorescence intensities (λ_{Ex} = 485 nm, λ_{EM} = 520 nm) of all fractions are indicated. n.d. = not detected. Experiment SMe456.

Assay buffer: 50 mM Tris, 0.02% (v/v) Triton X-100, 0.57 % (v/v) DMSO, pH 8.

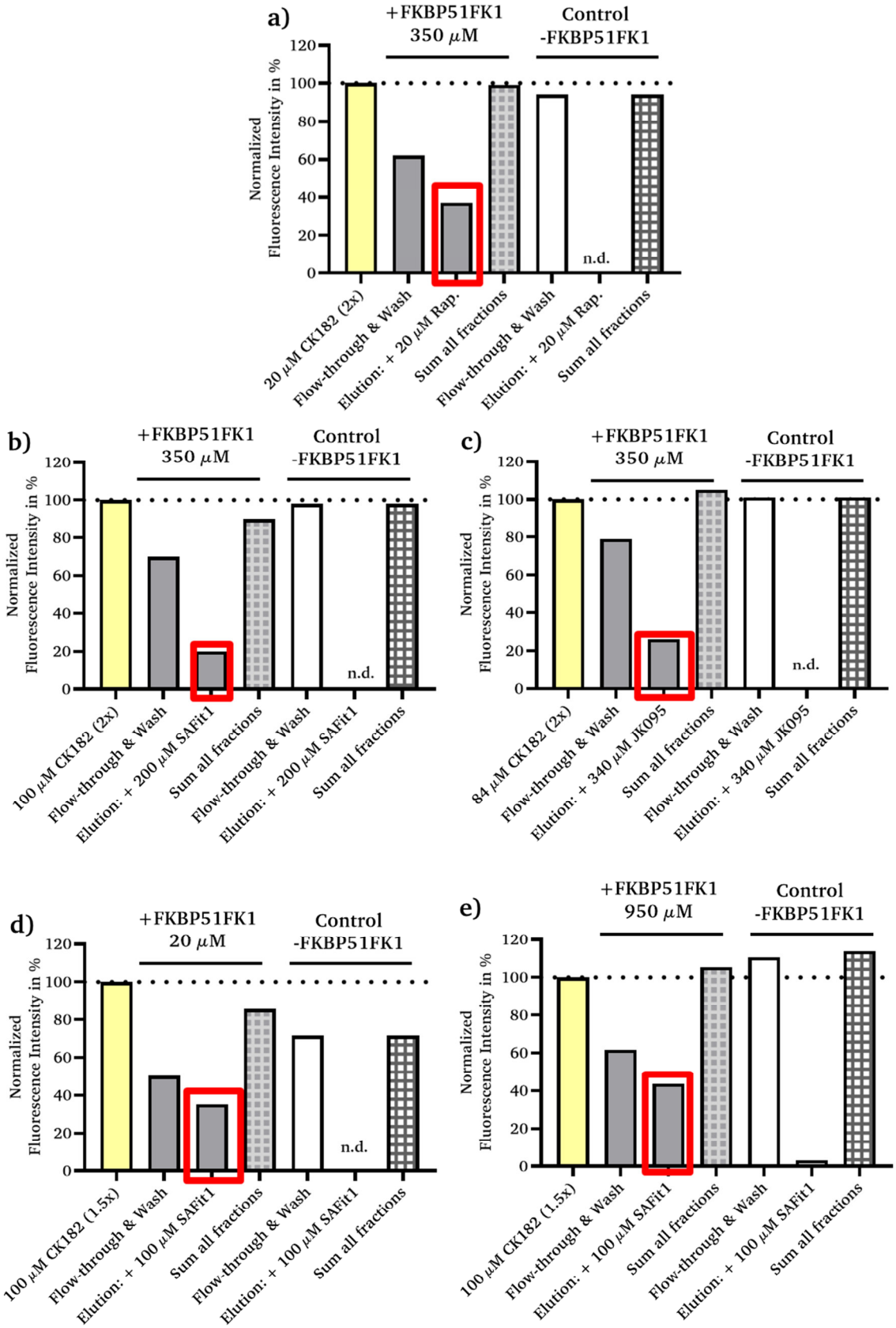

Figure 22: Competitive Elution of CK182 from a FKBP51FK1 Affinity Matrix by FKBP Ligands.

Figure 22: Competitive Elution of CK182 from a FKBP51FK1 Affinity Matrix by FKBP Ligands.

An excess of the tracer CK182 (a - c: 2x, d & e: 1.5x) was added to a column carrying a FKBP51FK1 affinity matrix. A column containing beads not coupled to FKBP51FK1 was applied as a control to analyze the unspecific interaction of CK182 with the resin. Not and unspecific bound CK182 was removed by washing the column. CK182 was eluted competitively by adding FKBP ligands (a: 20 µM Rapamycin (= Rap.), b: 200 µM SAFit1, c: 340 µM JK095, d & e: 100 µM SAFit1). Estimated density of immobilized FKBP51FK1: 350 µM (a - c), 20 µM (d), 950 µM (e).

Assay buffer, Figure a: 50 mM Tris, 5 mM EDTA, 0.002% (v/v) Triton X-100, 0.1% (v/v) DMSO, pH 8. Assay buffer, Figure b & c: 50 mM Tris, 5 mM EDTA, 0.02% (v/v) Triton X-100, 2% (v/v) DMSO, pH 8. Assay buffer, Figure d: 50 mM Tris, 5 mM EDTA, 0.002% (v/v) Triton X-100, 0.55% (v/v) DMSO, pH 8. Assay buffer, Figure e: 50 mM Tris, 0.02% (v/v) Triton X-100, 0.57% (v/v) DMSO, pH 8.

The initial fluorescence intensity (FI) of the tracer loaded on both columns and the FI of all fractions was determined. The wash and the elution step were completed after the FI baseline was reached. The FI of the fractions including unbound or unspecific bound CK182 (Flow-through & Wash) and of the eluates was normalized to the initial FI of CK182 that was set as 100% (yellow bar). The normalized FIs of fractions from the FKBP51FK1 affinity column are shown by grey bars. The normalized FIs of fractions from the control column are indicated by transparent bars. As an internal control the normalized FIs of all fractions from both columns were summed. The sum is indicated by bars showing a squared pattern. The 100% mark is given by a dotted line. n.d. = not detected.

The FI sum of the fractions carrying not or unspecific bound tracer (flow-through and wash fractions) and the FI sum of all eluates containing competitive eluted tracer was built (Figure 22). The corresponding FI sum was compared with the initial FI of the tracer. The experiment described before (Figure 21) is summarized in Figure 22 e.

The normalized fluorescence intensity (FI) of the flow-through and the wash fractions collected from a FKBP51FK1 affinity column (grey bar at the left side) was lower than the initial FI of the tracer (yellow bar) and lower than the normalized FI of the corresponding fractions obtained from a control column (transparent bar, Figure 22). The FKBP ligands – Rapamycin (Figure 22 a), SAFit1 (Figure 22 b, d, e) and JK095 (Figure 22 c) were added for elution. The normalized FI of the eluates from the FKBP51FK1 affinity column (red box, grey bar) was much higher than the corresponding FI from the control column (small transparent bar or no bar, Figure 22). The FI sum of all eluates (grey bar) was reduced in comparison with the FI sum of the flow-through and the wash fractions. Either no FI or FI at a low level (Figure 22 e) was detected in the eluates collected from the control column (Figure 22 a - d).

As an internal control the normalized fluorescence intensities of all fractions obtained from both columns were summed. The FI sum of all fractions from the FKBP51FK1 affinity column was approximately between 86% and 105% of the initial tracer FI. The FI sum of all fractions from the control column was in the range between 72% and 114%.

4.4. Binding Affinity of FKBP Ligands

Bicycles [51], macrocyclic FKBP ligands [11, 100] and "small-molecule degraders" [91] were characterized by competitive robot-based fluorescence polarization assays (FPAs). The binding constants of the FKBP ligands were determined for FKBP51FK1, FKBP52FK1, FKBP12 and FKBP12.6. The results are published somewhere else [11, 51, 91, 100].

The lacking binding of the SAFit1 analogue THE212P was confirmed by FP-assay (data not shown).

4.5. Pull-Down Assay Analysis by SDS-PAGE and Silver Staining

The pull-down assays aimed at enriching and identifying FKBP51 binding proteins exclusively interacting with the binding pocket of the FK1 domain. For that purpose, the FKBP ligand dependent eluate from either a low density (N2a samples: Figure 27) or a high density FKBP51FK1 affinity column (HEK293 samples: Figure 23, N2a samples: Figure 24, Figure 25) was compared with samples carrying unspecific eluting proteins. Samples from four different pull-down assays were analyzed by SDS-PAGE and silver staining. The 3rd pull-down assay comparing the SAFit1 dependent eluates from a high density FKBP51FK1 affinity column with the eluates from a mock column (- FKBP51FK1) was performed in a technical duplicate. Results from one experiment are shown (Figure 25).

The aim of the preliminary sample analysis by SDS-PAGE and silver staining was to verify the presence of proteins in the samples and to monitor the pull-down assay. The efficiency of each assay step was assessed: column equilibration, washing and elution. The background caused by unspecific eluting proteins was also analyzed. Another objective was to investigate the sample complexity and purity to develop a workflow for the subsequent MS-based proteomic analysis, especially for the 1st MS run. The assay steps were optimized based on the preliminary analysis by SDS-PAGE and silver staining as well as on the basis of the proteomic

analysis. The gels showing N2a samples from the 2nd pull-down assay (Figure 24) were stained together with Jan-Philip Kahl.

4.5.1. Pull-Down Assays Using a High Density FKBP51FK1 Affinity Matrix

Column Equilibration

All columns were equilibrated with 10 CV (SMe305: Figure 24 a + b, upper gel, lane 2; SMe382: Figure 25 a + b, upper gel, lane 3) up to 20 CV (SMe289: Figure 23, upper & lower gel, lane 3) cell lysis buffer before adding the total cell lysate. The flow-through during column equilibration was collected to assess the assay buffer, the FKBP51FK1 affinity matrix and the bead (- FKBP51FK1) purity. Either no protein bands (Figure 23: upper & lower gel, lane 3) or protein bands about 10 kDa (Figure 24 a + b: upper gel, lane 2; Figure 25 a + b: upper gel, lane 3), above 20 kDa (Figure 24 b: upper gel, lane 2), between 50 kDa and 70 kDa (Figure 25 a + b: upper gel, lane 3) were detected in the last part of the equilibration step.

Removing Unspecific Binding Proteins in the Wash Step

All columns were washed with 50 CV assay buffer to remove unspecific binding proteins. Comparing the wash fractions from a high density FKBP51FK1 affinity column or a mock column (- FKBP51FK1) the protein concentration and the number of protein bands decreased in the wash step (Figure 23, upper gel: lane 5 – 8; Figure 23, lower gel: lane 5 – 8: Figure 24 b, upper gel: lane 3 – 6; Figure 25 a, upper gel: lane 5 – 15; Figure 25 b, upper gel: lane 5 – 15). The wash fractions (Figure 24 b, upper gel: lane 3 – 6) and the mock eluates (= eluates collected after adding assay buffer instead of SAFit1; Figure 24 b, upper gel: lane 8 – 15, Figure 24 b, lower gel: lane 2 – 15) from a high density FKBP51FK1 affinity column displayed a similar protein pattern.

SAFit1 Dependent Elution

After adding 5 mM SAFit1 to a high density FKBP51FK1 affinity column various human or mouse proteins in the range between 15 kDa and above 250 kDa were eluted in contrast to the mock elution and the wash step. The results for the HEK293 samples are shown in Figure 23 (upper gel: last two wash fractions prior elution on lane 7 + 8, SAFit1 dependent eluates on lane 10 – 15; lower gel: mock eluates on lane 10 – 15). The findings for the N2a samples are illustrated in Figure 24 (Figure a, upper gel: last two wash fractions prior elution on lane

6 + 7, SAFit1 dependent eluates on 9 – 15; Figure a, lower gel: SAFit1 dependent eluates continued on lane 2 – 15; Figure b, upper gel: last wash fraction on lane 6, mock eluate on lane 8 – 15; Figure b, lower gel: mock eluates are continued on lane 2 – 15) and Figure 25 a (upper gel: wash fractions on lane 5 – 15; lower gel: wash fractions continued on lane 3 + 4, SAFit1 dependent eluates on lane 6 – 15).

Adding 20 CV 5 mM SAFit1 to a high density FKBP51FK1 affinity column seemed to be sufficient to complete the elution mostly as indicated by decreasing protein band intensities in the eluate (N2a samples; Figure 24 a: upper gel, lane 9 – 15 + lower gel, lane 2 – 15; Figure 25 a, lower gel: lane 6 – 15). By contrast, the elution of human proteins from a high density FKBP51FK1 affinity column did not seem to be completed after adding 10 CV 5 mM SAFit1 (HEK293 samples; Figure 23, upper gel, lane 10 – 15).

Various protein bands with a similar molecular weight were detected in the last wash fractions, the mock eluates and the SAFit1 dependent eluates from a high density FKBP51FK1 affinity column indicating the inclusion of unspecific eluting proteins in the samples of interest (Figure 23, upper + lower gel; Figure 24 a, upper + lower gel, Figure 24 b, upper gel; probably unspecific eluting proteins are indicated by white arrows). The protein band intensities of probably unspecific eluting proteins that were detected in the wash fractions and the SAFit1 dependent eluates from a high density FKBP51FK1 affinity column were relatively low in comparison with the protein band intensities of new proteins appearing in the SAFit1 dependent eluate (Figure 23, upper gel: last wash fractions on lane 7 + 8, eluates on lane 10 – 15; Figure 24 a, upper gel: last two wash fractions on lane 6 + 7, eluates on lane 9 – 15, Figure 24 a, lower gel: eluates were continued on lane 2 – 15; unspecific eluting proteins were indicated by white arrows, SAFit1 dependent eluting proteins were highlighted by green arrows).

Comparing the SAFit1 dependent eluate from a high density FKBP51FK1 affinity column (Figure 25 a, lower gel: lane 6 – 15) and a mock column (- FKBP51FK1; Figure 25 b, lower gel: lane 6 – 15) only slight differences in the elution profile were observed.

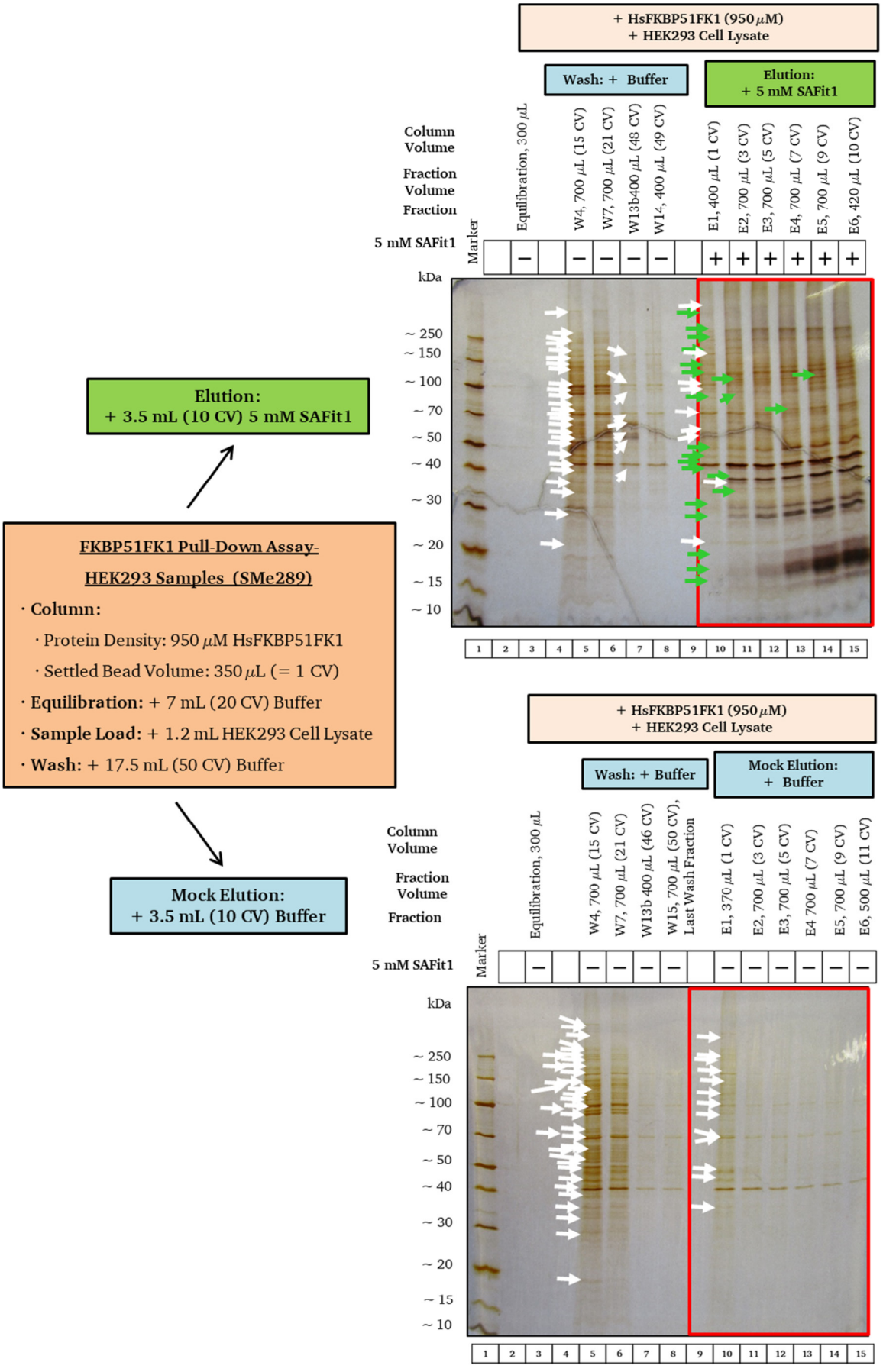

Figure 23: Comparing SAFit1 Dependent Elution of Human Proteins from a High Density FKBP51FK1 Affinity Column with Mock Elution.

Figure 23: Comparing SAFit1 Dependent Elution of Human Proteins from a High Density FKBP51FK1 Affinity Column with Mock Elution.

1.2 mL HEK293 Lysate containing about 16.7 mg total protein were loaded on two equilibrated columns (settled bead volume: 350 µL = 1 CV) carrying about 380 nmol covalently coupled HsFKBP51FK1 (C103A/C107I/E140C). 20 CV buffer were used for column equilibration (upper & lower gel, lane 3: last part of column equilibration). Both columns were washed with 50 CV assay buffer (upper & lower gel: lane 5 - 8). 20 CV 5 mM SAFit1 were added to one FKBP51FK1 affinity column for the FKBP ligand dependent protein elution (upper gel: lane 10 - 15, red box). 20 CV buffer were added to another FKBP51FK1 affinity column for mock elution to analyze unspecific eluting proteins (lower gel: lane 10 - 15, red box). SAFit1 dependent eluting proteins are marked by green arrows (upper gel). Unspecific eluting proteins are shown by white arrows (lower gel). The fraction and column volumes (CV) are indicated.

Equilibration and cell lysis buffer, pH 8: 20 mM Tris, 100 mM NaCl, 0.5 mM EDTA, 0.5% (v/v) Nonidet-P40 substitute, 1 mM PMSF, 1 mM DTT, Protease inhibitor cocktail (cOmplete mini, Roche, 1 tablet per 10 mL buffer).
Wash buffer, pH 8 = equilibration/cell lysis buffer not supplemented with Nonidet-P40 substitute. Elution buffer, pH 8 = wash buffer ± 5 mM SAFit1.
Pull-down assay: SMe289.

15 µL up to 30 µL of each sample were suspended with 5 µL or 10 µL 4x laemmli buffer supplemented with 28 µL 2-mercaptoethanol (ß-me) per 1 mL buffer. The mix was boiled at 95°C for 10 min. The samples were subjected to SDS-PAGE and silver staining. 10 µL of each sample were loaded per lane.

Lane 1, upper and lower gel: 5 µL Marker PageRuler™ Unstained Broad Range Protein Ladder (Thermo Scientific), pre-diluted 1:5 with 1x laemmli buffer including ß-Me. Gradient gel: 4% - 20%, 1.0 mm (Invitrogen). Tears occurred during gel drying (upper gel).

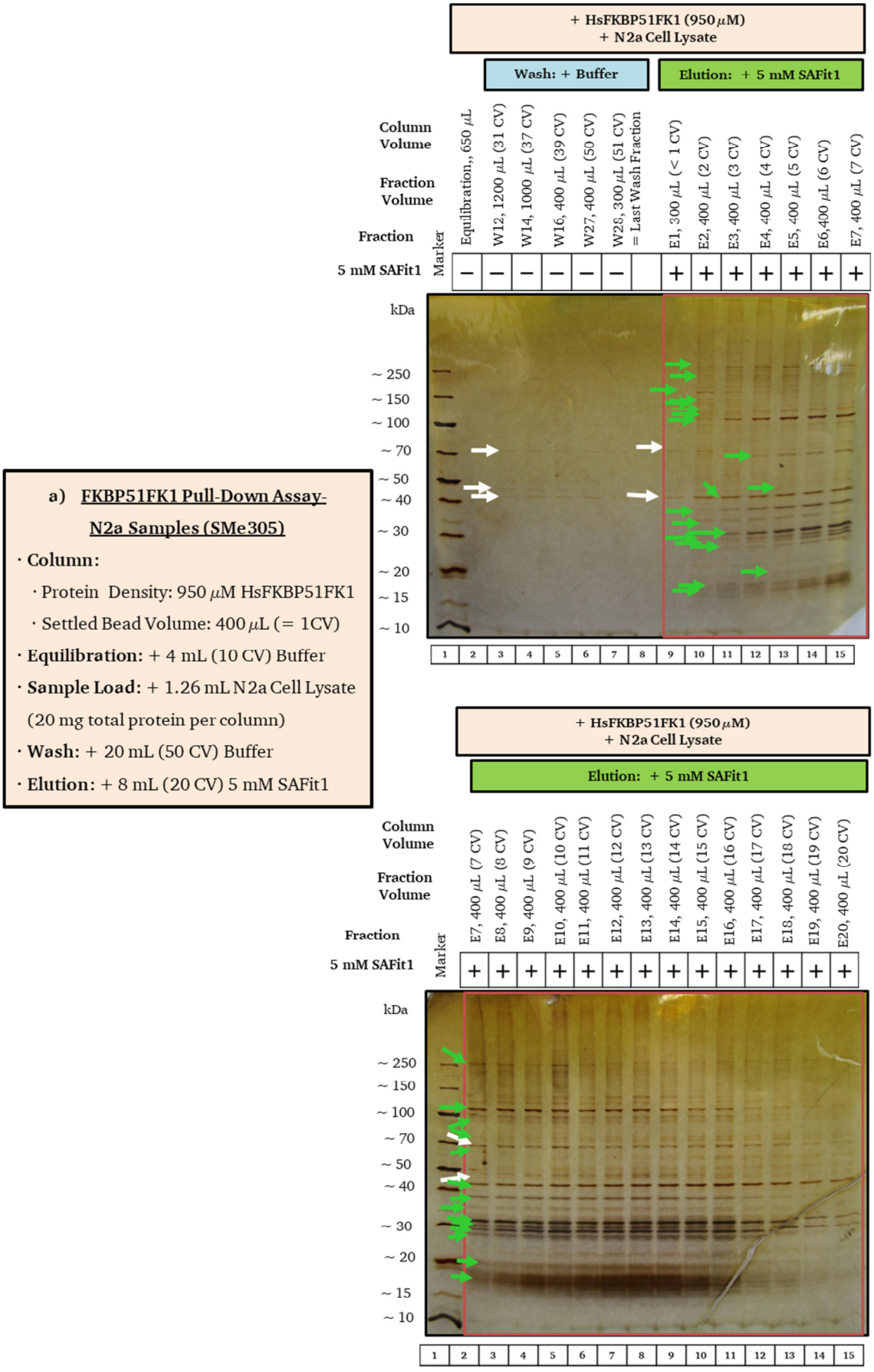

Figure 24 a: Comparing SAFit1 Dependent Elution of Mouse Proteins from a High Density FKBP51FK1 Column with Mock Elution – SAFit1 Dependent Elution Profile.

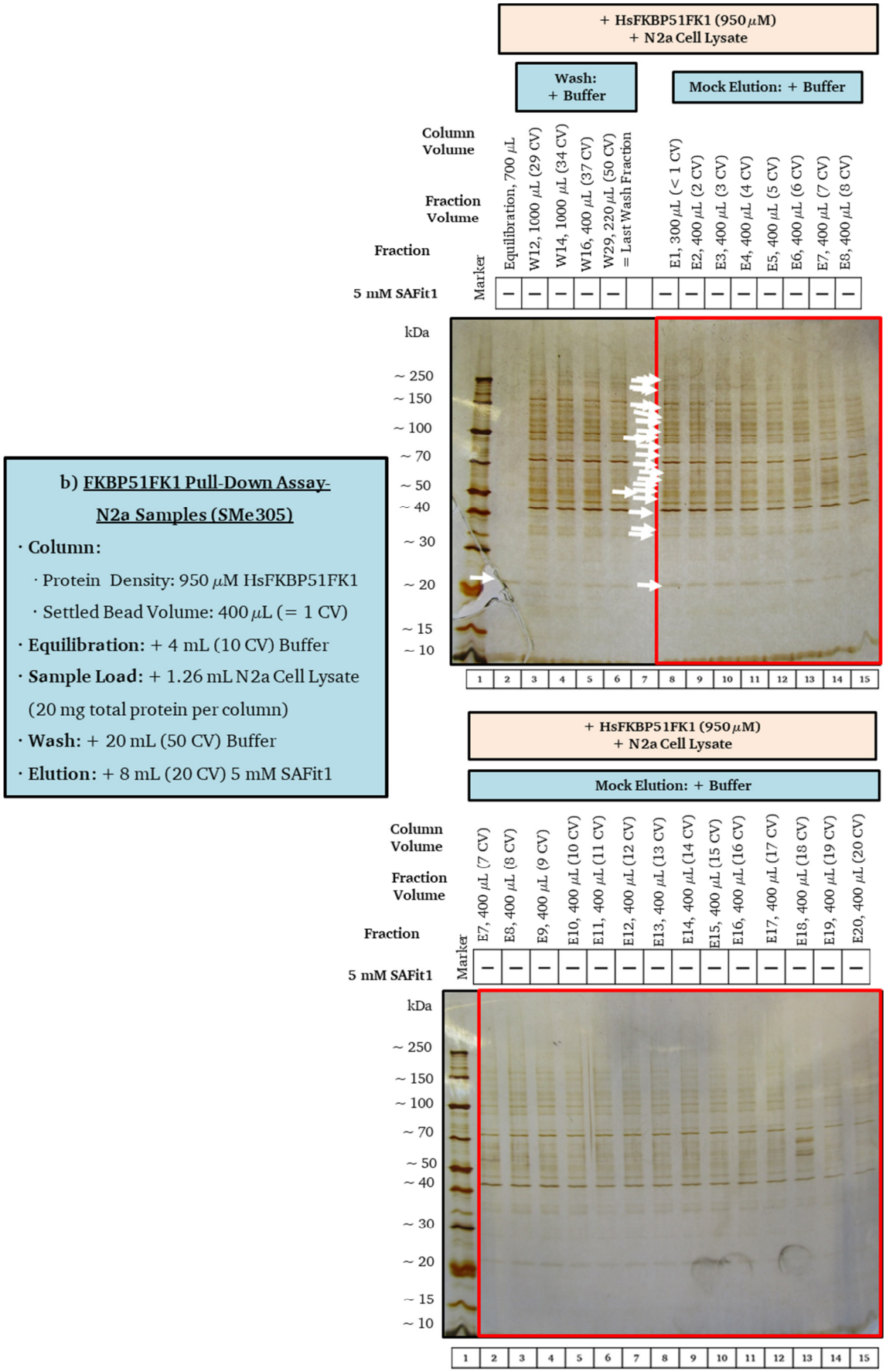

Figure 24 b: Comparing SAFit1 Dependent Elution of Mouse Proteins from a High Density FKBP51FK1 Column with Mock Elution – Mock Elution Profile.

Figure 24: Comparing SAFit1 Dependent Elution of Mouse Proteins from a High Density FKBP51FK1 Column with Mock Elution.

Figure a + b: 1.26 mL N2a cell lysate carrying about 20 mg total protein were added to two equilibrated affinity columns (settled bead volume: 400 µL) carrying about 380 nmol covalently coupled HsFKBP51FK1 (C103A/C107I/E140C). Both columns were washed with 50 CV buffer (Figure a: upper gel, lane 3 - 7; Figure b: upper gel, lane 3 - 6) to reduce the background caused by unspecific eluting proteins. 20 CV 5 mM SAFit1 (= FKBP ligand) were added for elution (Figure a: upper gel, lane 9 - 15; Figure a: lower gel, lane 2 - 15). 20 CV buffer were added for mock elution (Figure b: upper gel, lane 8 - 15; Figure b: lower gel, lane 2 - 15) to analyze the unspecific elution of proteins. SAFit1 dependent eluting proteins are indicated by green arrows (Figure a: upper gel, red box; Figure a: SAFit1 dependent protein elution is continued in the lower gel, red box). Unspecific eluting proteins are labeled by white arrows (Figure a + b: upper gel). Some samples (Figure a: upper gel, lane 15 & lower gel, lane 2; Figure b: upper gel, lane 14 - 15 & lower gel, lane 2 - 3) were loaded on two gels facilitating the comparison of both gels.
Figure a + b, upper gel, lane 2: last part of the flow-through collected during column equilibration with 10 CV buffer. CV = column volume.

Equilibration and cell lysis buffer, pH 8: 20 mM Tris, 100 mM NaCl, 0.5 mM EDTA, 0.5% (v/v) Nonidet-P40 substitute, 1 mM PMSF, 1 mM DTT, Protease inhibitor cocktail (cOmplete mini, Roche, 1 tablet per 10 mL buffer).

Wash buffer, pH 8 = equilibration/cell lysis buffer not supplemented with Nonidet-P40 substitute. Elution buffer, pH 8 = wash buffer ± 5 mM SAFit1.
Pull-down assay: SMe305.

15 µL (Figure a) or 22.5 µL (Figure b) of each sample were mixed with 5 µL (Figure a) or 7.5 µL (Figure b) 4x laemmli buffer supplemented with 28 µL 2-mercaptoethanol per 1 mL buffer. All samples were boiled at 95°C for 10 min and subjected to SDS-PAGE and silver staining. 8 µL (Figure a) up to 14 µL (Figure b) of each sample were loaded per lane.

Figure a + b: Lane 1, upper and lower gel: 5 µL Marker PageRuler™ Unstained Broad Range Protein Ladder (Thermo Scientific), pre-diluted 1:5 with 1x laemmli buffer including ß-Me. Gradient gel: 4% - 20%, 1.0 mm (Invitrogen). Tears occurred during gel drying (upper gel).

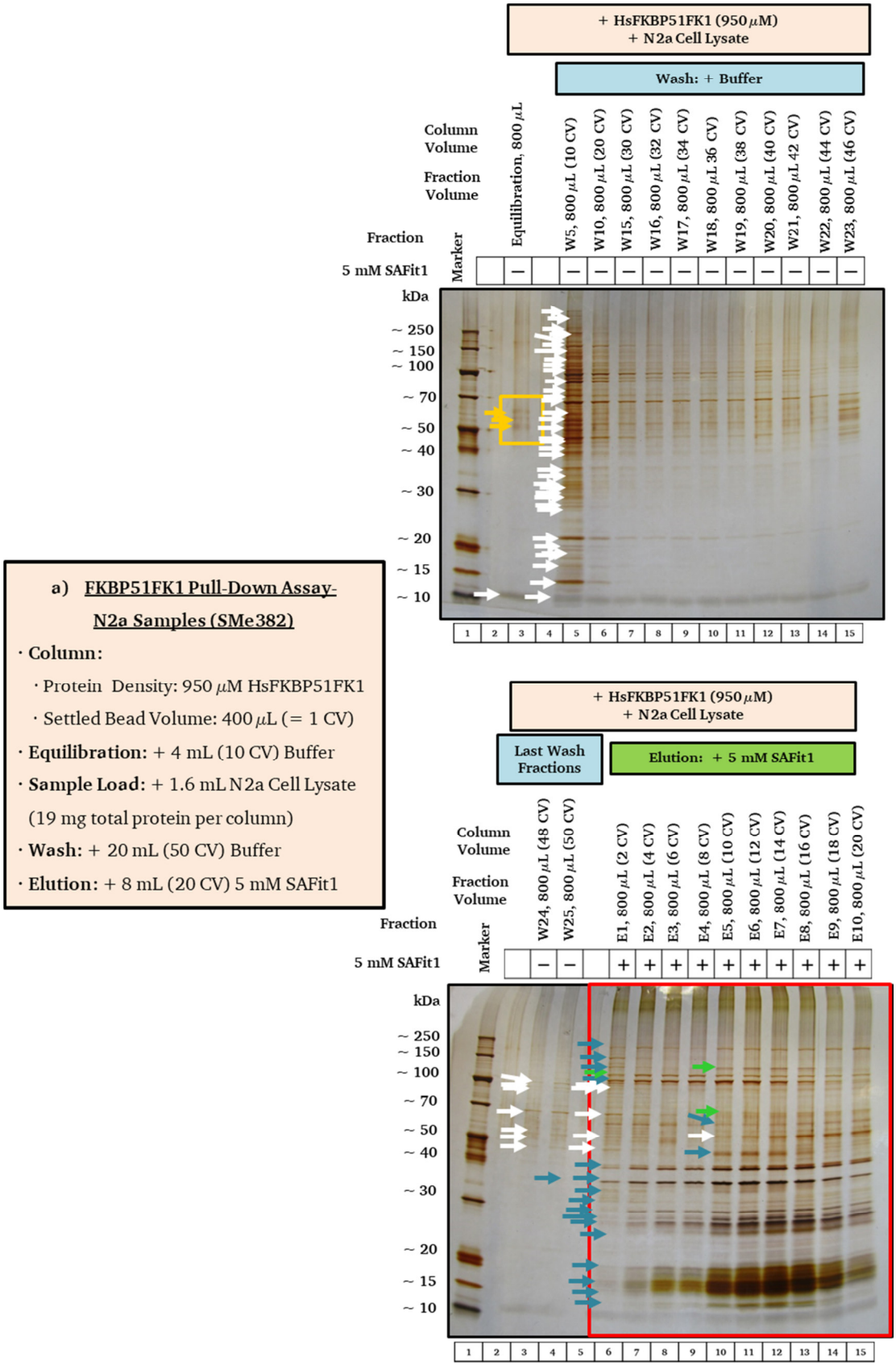

Figure 25 a: Comparing the SAFit1 Dependent Elution Profile of Mouse Proteins from a High Density FKBP51FK1 Affinity Column with the Elution Profile from a Mock Column – FKBP51FK1 Affinity Column.

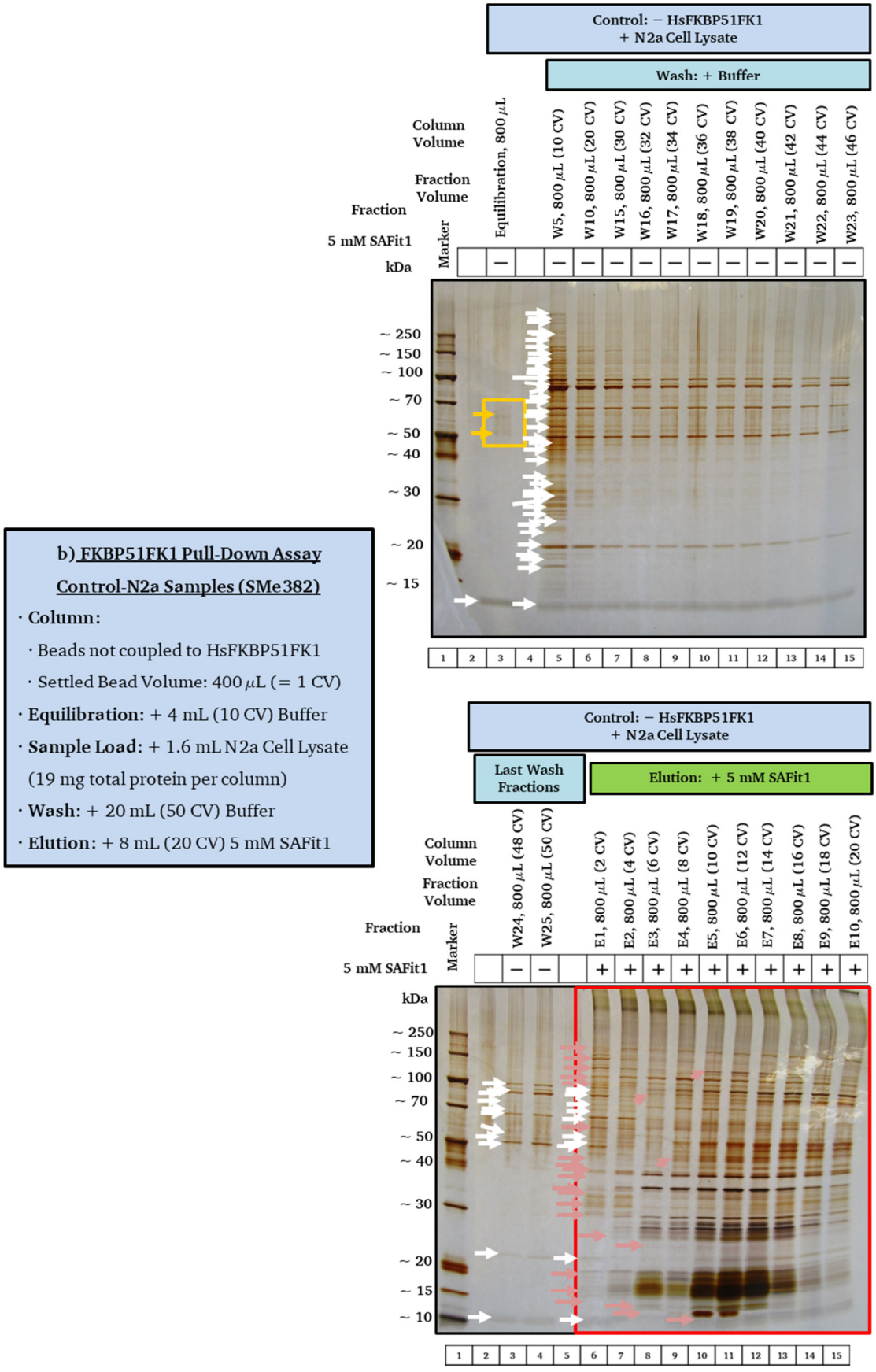

Figure 25 b: Comparing the SAFit1 Dependent Elution Profile of Mouse Proteins from a High Density FKBP51FK1 Affinity Column with the Elution Profile from a Mock Column – Mock Column.

Figure 25: Comparing the SAFit1 Dependent Elution Profile of Mouse Proteins from a High Density FKBP51FK1 Affinity Column with the Elution Profile from a Mock Column.

Figure 25 a + b: 1.6 mL N2a cell lysate containing about 19 mg total protein were added to an equilibrated 400 µL column carrying about 380 nmol covalently coupled HsFKBP51FK1 (C103A/C107I/E140C)(Figure a). A mock column filled with the blocked, "naked" beads was used as a control to analyze the unspecific elution from proteins (Figure b). Both columns were washed with 50 CV buffer (Figure a + b: upper gel, lane 5 - 15; the last two wash fractions are shown on the lower gel on lane 3 & 4). 20 CV 5 mM SAFit1 were added for elution (Figure a + b: lower gel lane 6 - 15). Figure a + b, upper gel, lane 3: Last two column volumes of the flow-through collected during column equilibration with 10 CV buffer. The fraction volume and numbers are indicated. CV = column volume.

Equilibration and cell lysis buffer, pH 8: 20 mM Tris, 100 mM NaCl, 0.5 mM EDTA, 0.5% (v/v) Nonidet-P40 substitute, 1 mM PMSF, 1 mM DTT, Protease inhibitor cocktail (cOmplete mini, Roche, 1 tablet per 10 mL buffer).

Wash buffer, pH 8 = equilibration/cell lysis buffer not supplemented with Nonidet-P40 substitute. Elution buffer, pH 8 = wash buffer ± 5 mM SAFit1.
Pull-down assay: SMe382.

15 µL of each sample were suspended with 5 µL 4x laemmli buffer supplemented with 28 µL 2-mercaptoethanol per 1 mL buffer. The mix was boiled at 95°C for 10 min and subjected to SDS-PAGE and silver staining. 15 µL of each sample were loaded per lane. Lane 1, all gels: 5 µL Marker PageRuler™ Unstained Broad Range Protein Ladder (Thermo Scientific), pre-diluted 1:5 with 1x laemmli buffer including ß-Me. Gradient gel: 4% - 20%, 1.0 mm (Invitrogen).

4.5.2. **Sample Processing Prior Protein Digestion**

The wash and elution fractions were pooled to reach the protein amount required for the subsequent MS analysis. The samples were desalted and concentrated and the sample buffer was exchanged with ammonium bicarbonate prior protein digestion. The sample processing was analyzed by SDS-PAGE and silver staining (Figure 26). A similar protein pattern was displayed by the samples prior and after processing. The protein band intensities of the processed samples (lane 4, 7, 10 and 13) are lowered in comparison with the corresponding initial samples (lane 3, 6, 9 and 12). Some protein bands were not detected in the processed samples (lane: 4, 7, 10 and 13: lacking protein bands are indicated by red arrows). A 100 kDa protein seemed to be enriched in the SAFit1 dependent eluate from a high density FKBP51FK1 affinity column (lane 6 & 7: protein band indicated by a green arrow).

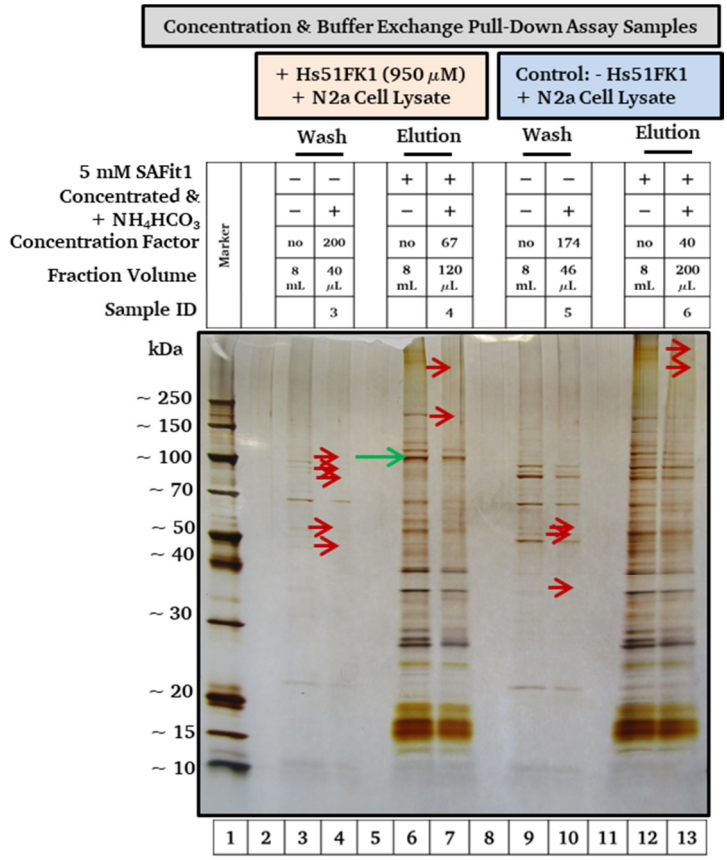

Figure 26: Desalting, Buffer Exchange and Protein Concentration – N2a Samples.

N2a cell lysate was loaded on an equilibrated high density FKBP51FK1 affinity column. After washing with 50 CV buffer, 20 CV 5 mM SAFit1 were added for elution. A mock column (- FKBP51FK1) was applied as a control (Pull-down assay: SMe382). The wash fractions and the eluates were pooled. The samples were concentrated and desalted and the buffer was exchanged with ammonium bicarbonate prior digestion. A concentration factor based on the sample volume prior and after sample concentration was calculated. The samples were analyzed by SDS-PAGE and silver staining (SMe389). Lane 3 & 4: Wash fraction pool from a high density FKBP51FK1 affinity column before (lane 3) and after (lane 4) sample processing. Lane 6 & 7: Pooled SAFit1 dependent eluates from a high density FKBP51FK1 affinity column before (lane 6) and after (lane 7) sample processing. Lane 9 & 10: Wash fraction pool from a mock column before (lane 9) and after (lane 10) sample processing. Lane 12 & 13: Pooled SAFit1 dependent eluates from a mock column before (lane 12) and after (lane 13) sample processing. A 100 kDa protein potentially enriched in the SAFit1 dependent eluate from a high density FKBP51FK1 affinity column is indicated by a green arrow. Protein bands that were not detected in the processed samples are highlighted by red arrows. 4 parts of each sample were mixed with 1 part 4x laemmli buffer supplemented with 2-mercaptoethanol (28 µL 2-mercaptoethanol per 1 mL buffer). The mix was boiled at 95°C for 10 min. Lane 3, 6, 9 & 12: 10 µL sample were loaded. Lane 4, 7, 10, 13: The sample volume per lane was normalized to the concentration factor in relation to the corresponding not concentrated, not desalted sample. Gradient gel: 4% - 20% (Invitrogen).

4.5.3. Pull-Down Assay Applying a Low Density FKBP51FK1 Affinity Column

Comparing the SAFit1 and the PPU339 dependent eluates from a low density FKBP51FK1 affinity column (Figure 27) with all control samples no additional protein bands were detected.

Figure 27: Pull-Down Assay Applying a Low Density FKBP51FK1 Affinity Column.

Figure a): Overview of the FKBP51FK1 pull-down-assay.
Figure b): Sample analysis by SDS-PAGE and silver staining.

a) & b): 1.25 mL N2a cell lysate (about 14 mg total protein) were loaded on three 300 µL columns carrying a low density FKBP51FK1 affinity matrix. All columns were washed with 50 CV buffer (lane 4, 9 and 14). 20 CV of a 100 µM FKBP ligand (SAFit1: lane 10 or PPU339: lane 15) were added for elution. A control experiment was performed with a non-binding SAFit1 analogue (Wash: lane 4, Elution with 20 CV 100 µM THE212P: lane 5). Three columns filled with blocked beads (- FKBP51FK1) were applied as a control (Wash: lane 2, 7 and 12, Elution with THE212P: lane 3, Elution with SAFit1: lane 8, Elution with PPU339: lane 13; pull-down assay: SMe382/383).

Equilibration and cell lysis buffer, pH 8: 100 mM NaCl, 20 mM Tris, 0.5 mM EDTA, 0.5% (v/v) Nonidet-P40 substitute, 1 mM PMSF, 1 mM DTT, Protease inhibitor cocktail (cOmplete mini, Roche, 1 tablet per 10 mL buffer).
Wash buffer, pH 8 = 200 mM NaCl, 20 mM Tris, 0.5 mM EDTA, 1 mM PMSF, 1 mM DTT, Protease inhibitor cocktail (cOmplete mini, Roche, 1 tablet per 10 mL buffer).
Elution buffer, pH 8 = wash buffer + 100 µM SAFit1/100 µM PPU339/100 µM THE212P.

The last 25 CV of the wash step and all eluates were pooled. The samples were concentrated and the buffer was exchanged with 100 mM NH_4HCO_3 by ultrafiltration. The UV based protein concentration of each sample is given.

6 µL of each sample were suspended with 2 µL 4x laemmli buffer supplemented with 2-mercaptoethanol (28 µL ß-Me per 1 mL buffer). The samples were incubated for 10 min at 95°C and subjected to SDS-PAGE and silver staining (SMe389). About 5 µg total protein were loaded per lane. Marker (lane 1): 5 µL PageRuler™ Unstained Broad Range Protein Ladder (Thermo Scientific), pre-diluted 1:5 in 1x laemmli buffer + ß-Me. Gradient gel: 4% - 20%, 1.0 mm (Invitrogen).

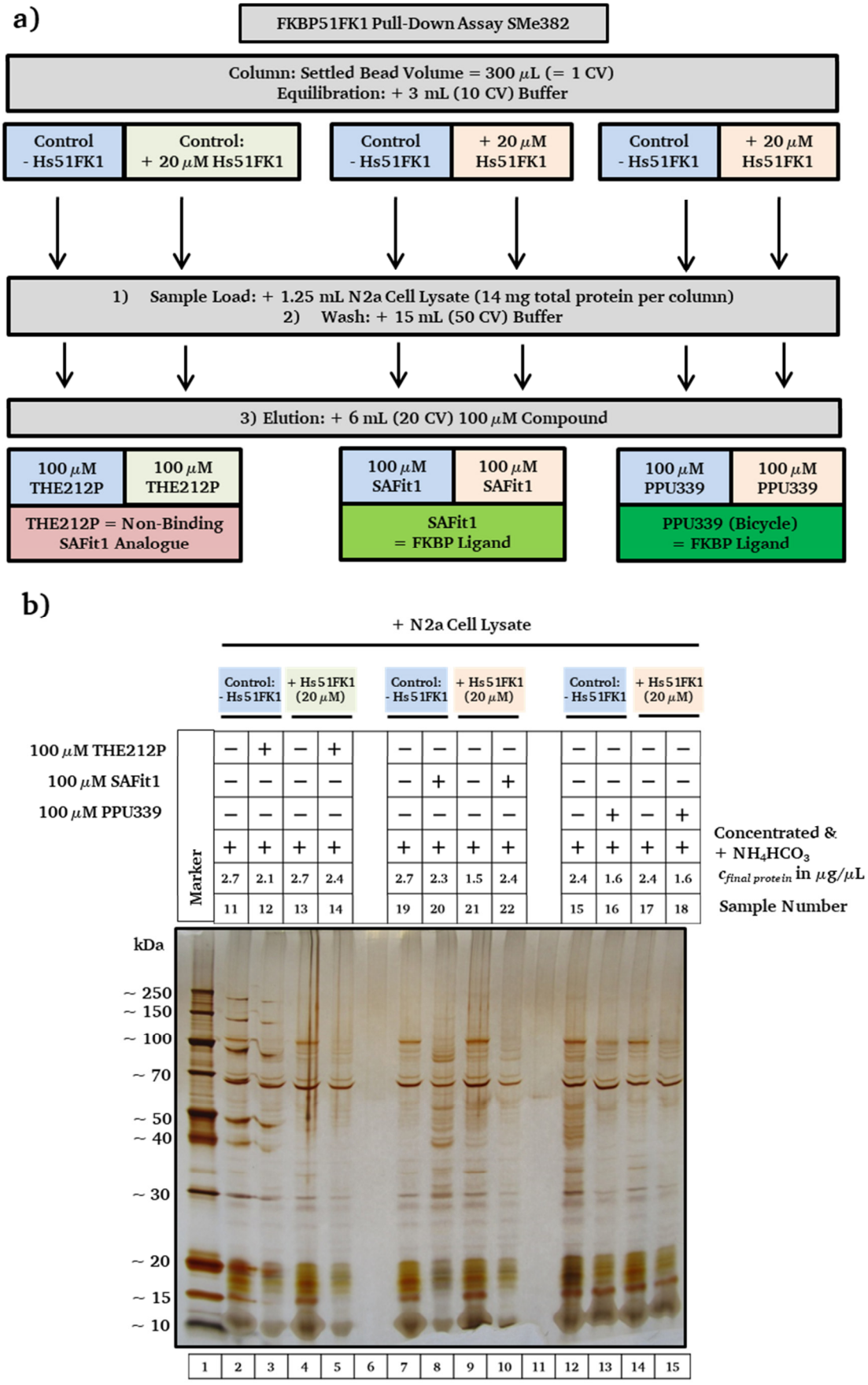

Figure 27: Pull-Down Assay Applying a Low Density FKBP51FK1 Affinity Column.

4.6. Proteomic Pull-Down Assay Analysis

The pull-down assay samples (Table 17, p. 63) were analyzed by a label-free bottom-up proteomic approach to identify possible FKBP51 binding proteins enriched in the FKBP ligand dependent eluate from either a low or high density FKBP51FK1 affinity column. The protein abundance in the FKBP ligand (SAFit1 or PPU339) dependent eluates was compared with the protein abundance in samples carrying unspecific eluting proteins and in the complete cell lysate. For that purpose, proteins were relatively quantified by spectral counting [23, 69] to estimate the protein abundance in each sample. In total, three MS runs (Table 17) were executed to analyze one HEK293 sample set (1st MS run) and two N2a sample sets (2nd MS and 3rd MS run).

The pull-down assay samples of each MS run (Table 17) were analyzed as a group. The complete HEK293 cell lysate was analyzed separately from the pull-down assay samples in the 1st MS run. For that reason, the protein abundance in the SAFit1 dependent eluates was not compared with the complete HEK293 cell lysate. In the 2nd MS run, the pull-down assay samples and the total N2a cell lysate were analyzed together. To decrease the number of false-positive results, the pull-down assay samples were re-analyzed excluding the total N2a cell lysate. The subsequent proteomic analysis of the N2a samples is based on the re-analyzed data. In contrast to the data analysis in the 2nd MS run, all pull-down assay samples from either a low or a high density FKBP51FK1 affinity column as well as two batches of the complete N2a cell lysate were analyzed together as one group in the 3rd MS run to save time. Therefore, the protein abundance in the SAFit1 dependent eluate from a high density FKBP51FK1 affinity column could be compared with the protein abundance in the total cell lysate as a control.

Various excel files including all proteins that were identified in each sample were received from Hanne Haslene-Hox. All identified single proteins and protein subunits included in the UniProtKB database were counted as one protein item. Single proteins were not differentiated from protein subunits in the early data analysis. The total number of identified spectra and peptides assigned to all protein identifications were given for each sample. All different peptides related to a distinct protein in a sample were counted to calculate the number of identified peptides. A unique single peptide that appeared several times in a distinct sample was counted as one peptide. The multiple appearance of a distinct peptide was considered by counting peptide-spectra matches (PSMs) assigned to a protein item in a distinct sample. The number of identified spectra is related to all peptides identified uniquely or multiple times in

one sample. For example, the identification of four identical peptides in one sample resulted in a spectral count of four and a peptide count of one. Only proteins identified on the basis of more than one unique peptide across all samples in one sample group were selected for further analysis to decrease the number of false positive results.

The proteomic analysis described below was supervised by Hanne Haslene-Hox. The following proteomic analysis of the HEK293 and the N2a samples is partially in correspondence with a report draft prepared by Hanne Haslene-Hox, Anna Nordborg, Geir Klinkenberg, Susana Belen Bravo Lopez and Eduardo Medina Dominguez summarizing the proteomic results [41]. The proteomic analysis of the HEK293 samples is also in accordance with another report draft written by Hanne Haslene-Hox, Anna Nordborg and Geir Klingenberg focusing on the HEK293 sample analysis in the 1st MS run [40]. Both reports were prepared in the context of the EU-OPENSCREEN-DRIVE transnational chemoproteomic access project.

4.6.1. Determination of the Protein and Peptide Amount

The total protein concentration in the pull-down assay samples was estimated after sample pooling, buffer exchange, desalting and sample concentration prior digestion to adjust the digestion protocol. The protein concentration of all HEK293 samples, all N2a samples from a pull-down assay using a low density FKBP51FK1 affinity column and all N2a samples without SAFit1 from a high density FKBP51FK1 affinity column (Table 17 a + b: sample overview) was determined spectrophotometrically (A280).

The protein concentration in eluates including a high SAFit1 concentration (N2a samples: elution with 5 mM SAFit1 from either a high density FKBP51FK1 affinity or a mock column) was estimated by SDS-PAGE and Coomassie staining (Figure 28). The high SAFit1 concentration caused a high background in the absorption spectrum at 280 nm (data not shown) and disturbed the protein quantitation by Bradford and BCA assay (data not shown).

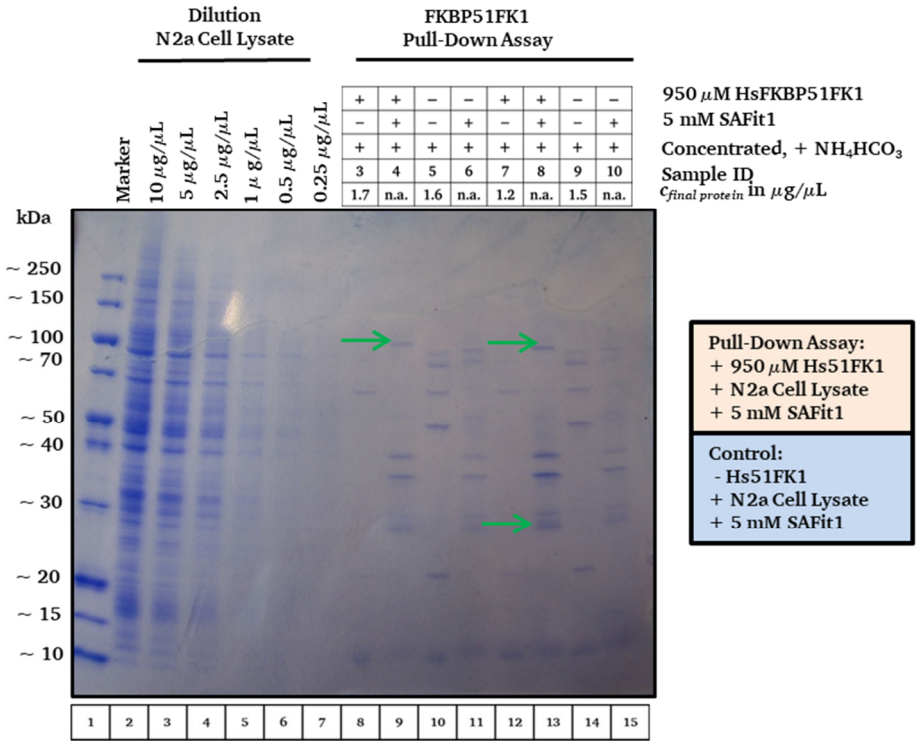

Figure 28: Estimating the Protein Concentration of 5 mM SAFit1 Dependent Eluates by SDS-PAGE and Coomassie Staining.

The SAFit1 dependent elution profile from a high density FKBP51FK1 column (density of immobilized FKBP51FK1: 950 µM) was compared with the elution profile from a mock column (- FKBP51). The pattern generated by unspecific eluting proteins from both columns (± FKBP51FK1) in the wash step was also analyzed. The proteins in the samples were originated from N2a cell lysate. The FKBP51 pull-down assay was performed in duplicate (SMe370/SMe382). The wash fractions and the SAFit1 dependent eluates from both columns (± FKBP51FK1) were pooled, desalted and concentrated. The sample buffer was exchanged. The prepared samples were analyzed by SDS-PAGE and Coomassie staining (SMe393). A serial dilution of complete N2a cell lysate is shown in lane 2-7 to estimate the protein concentration of the SAFit1 dependent eluates. The protein concentration of the complete N2a cell lysate determined by BCA assay is indicated (lane 2 - 7). Lane 1: 5 µL Marker (Page Ruler Broad Range Unstained Protein Ladder, Thermo Scientific). Lane 8 & 12: Wash fraction pool from a high density FKBP51FK1 affinity column. Lane 9 & 13: Pooled SAFit1 dependent eluates from a high density FKBP51FK1 affinity column. Lane 10 & 14: Wash fraction pool from a mock column (- FKBP51FK1). Lane 11 & 15: SAFit1 dependent eluate from a mock column (- FKBP51FK1). The UV absorption (A280) based estimation of the protein concentration in the prepared wash fraction pools is given (lane 8, lane 10, lane 12, lane 14). n.a. = not available. Protein bands that might be exclusively identified in the SAFit1 dependent eluates from a high density FKBP51FK1 affinity column are highlighted by green arrows (lane 9: ~100 kDa protein band; lane 13: protein band above 30 kDa and ~100 kDa). 3 parts of each sample were resuspended with 1 part 4x laemmli buffer supplemented with 28 µL 2-mercaptoethanol per 1 mL buffer. The mix was boiled at 95°C for 10 min. 1.5 µL of each sample were loaded per lane. Gradient gel: 4% - 20% (Invitrogen).

After protein digestion the peptides were quantified with a "Pierce™ Quantitative Fluorometric Peptide Assay" by Hanne Haslene-Hox. The protein and peptide yields for the HEK293 samples (Table 22), the N2a samples of the 2nd MS run (Table 23) and the N2a samples of the 3rd MS run (Table 24) are given below.

Peptide yields between 0.4 μg and 0.9 μg were received for the HEK293 samples (Table 22) and the N2a samples of the 2nd MS run (Table 23). Peptides yields between 2 μg and 13 μg were reached for N2a samples in the 3rd MS run (Table 24).

Table 22: Protein and Peptide Yield – HEK293 Samples (1st MS Run).

HEK293 samples from a pull-down assay applying two high density FKBP51FK1 affinity columns (protein density about 950 µM immobilized FKBP51FK1) were processed (fraction pooling, buffer exchange, desalting and sample concentration). The protein concentration determined by a spectrophotometer at 280 nm is given as mean of 3 up to 6 measured values (6th column). The protein concentration of the complete HEK293 cell lysate was determined before sample processing by BCA-assay. The proteins were denatured, reduced, alkylated and digested with trypsin. The peptide yield (8th column) was determined by "Pierce™ Quantitative Fluorometric Peptide Assay" in duplicates.

Sample ID	Sample Description			V_{Sample} (μL)	$c_{total\ protein}$ (mg/mL)	m (μg)	Peptide Yield (μg)
	± FKBP 51FK1	Wash	Eluting Agent				
A	+ 950 μM	Wash	–	235	0.17	40	0.86
B		–	5 mM SAFit1	200	0.13	26	0.60
C		–	5 mM SAFit1	25	4.2	105	0.67
D		Wash	–	156	0.18	28	0.65
E		–	Buffer	138	0.21	29	0.71
Complete HEK293 Cell Lysate				2	13.9	30	3.69

Table 23: Protein and Peptide Yield – N2a Samples (2nd MS Run).

N2a samples from a pull-down assay using two high density FKBP51FK1 affinity columns were processed (fraction pooling, buffer exchange, desalting and sample concentration). The protein concentration was determined (6th column) either: (1) spectrophotometrically at 280 nm (mean of 3 up to 5 measurements), (2) by SDS-PAGE and Coomassie staining or (3) by BCA-assay (mean of technical duplicates). The proteins were denatured, reduced, alkylated and digested with trypsin. The peptide yield (8th column) was determined by "Pierce™ Quantitative Fluorometric Peptide Assay" in duplicates.

Sample ID	**Sample Description**			V_{Sample} (μL)	$c_{total\ protein}$ (mg/mL)	**m** (μg)	**Peptide Yield** (μg)
	±FKBP 51FK1	**Wash**	**Eluting Agent**				
A	+ 950 μM	Wash 1	–	150	0.16 (1)	24	0.45
B		Wash 2	–	130	0.17 (1)	22	0.53
C		–	5 mM SAFit1	260	0.15 (2)	39	0.77
D				270	0.03 (2)	8	0.44
E		Wash 1	–	110	0.25 (1)	27.5	0.39
F		Wash 2	–	100	0.15 (1)	15	0.41
G		–	Buffer	90	0.25 (1)	22.5	0.44
H	Complete N2a Cell Lysate Batch 1			30	1.0 (3)	30	1.91

Table 24: Protein and Peptide Yield – N2a Samples (3rd MS Run).

N2a samples from pull-down assays comparing either a high (sample 4 - 10) or a low (sample 11 - 22) density FKBP51FK1 affinity column with a mock column (- FKBP51FK1) were processed (fraction pooling, buffer exchange, desalting and sample concentration). The protein concentration was determined (6th column) either: (1) spectrophotometrically at 280nm (mean of 3 up to 6 measurements), (2) by SDS-PAGE and Coomassie staining or (3) by BCA-assay (mean of technical duplicates). The proteins were denatured, reduced, alkylated and digested with trypsin. The peptide yield (8th column) was determined by Pierce™ Quantitative Fluorometric Peptide Assay in duplicates.

Sample ID	Sample Description			V_{Sample} (μL)	$c_{total\ protein}$ (mg/mL)	m (μg)	Peptide Yield (μg)
	±FKBP 51FK1	Wash	Eluting Agent				
1	Complete N2a Cell Lysate Batch 2			30	7 (3)	213	6.78
2	Complete N2a Cell Lysate Batch 3			25	8 (3)	205	7.33
3	+ 950 μM	Wash		14	1.7 (1)	24	6.06
4		–	5 mM SAFit1	35	1-2 (2)	35-70	6.99
5	–	Wash		16	1.6 (1)	26	3.04
6		–	5 mM SAFit1	70	1-2 (2)	70-140	12.9
7	+ 950 μM	Wash		16	1.2 (1)	19	3.90
8		–	5 mM SAFit1	25	1-2 (2)	25-50	4.77
9	–	Wash		18	1.5 (1)	27	6.16
10		–	5 mM SAFit1	25	1-2 (2)	25-50	5.35
11	–	Wash		17	2.7 (1)	46	5.85
12		–	100 μM THE212P	13	2.1 (1)	27	8.21
13	+ 20 μM	Wash		15	2.7 (1)	41	5.88
14		–	100 μM THE212P	12	2.4 (1)	29	6.24
15	–	Wash		16	2.4 (1)	38	3.55
16		–	100 μM PPU339	17	1.6 (1)	27	7.35
17	+ 20 μM	Wash		18	2.4 (1)	43	2.41
18		–	100 μM PPU339	18	1.6 (1)	29	3.94
19	–	Wash		18	2.7 (1)	49	4.19
20		–	100 μM SAFit1	14	2.3 (1)	32	5.93
21	+ 20 μM	Wash		21	1.5 (1)	32	7.79
22		–	100 μM SAFit1	13	2.4 (1)	31	4.81

4.6.2. **Total Number of Identified Spectra**

Human and mouse proteins identified in the pull-down assay samples and the total cell lysate were relatively quantified by spectral counting. The protein items were identified on the basis of at least two assigned peptides across all samples in the sample analysis group (Table 17, p. 63).

About 15,000 up to 25,000 validated spectra were counted for the complete HEK293 and N2a cell lysate (Figure 29, Figure 30). Comparing the HEK293 and N2a samples across the analysis group, the number of identified spectra fluctuated. About 350 up to approximately 15,000 validated spectra were counted for the pull-down assay samples (Figure 29, Figure 30). The pull-down assay using a low density FKBP51FK1 affinity matrix and an assay buffer supplemented with a higher salt concentration (200 mM NaCl instead of 100 mM NaCl) led to a lower number of identified spectra (Figure 30: 1,000 up to 1,500 validated spectra for samples 11 - 22). An assay buffer supplemented with 100 mM NaCl was used for the pull-down assays with a high density FKBP51FK1 affinity matrix (samples shown in Figure 29). 2,500 up to 9,000 spectra were identified in the HEK samples from a high density FKBP51FK1 affinity column (Figure 29). 350 up to 15,000 spectra were identified in the N2a samples from a high density FKBP51FK1 affinity column in the 2nd MS run. In the 3rd MS run, 3,000 up to 10,000 spectra were identified in the N2a samples from either a high density FKBP51FK1 affinity or a mock column (- FKBP51) (Figure 29). The total number of validated spectra in the SAFit1 dependent eluates carrying a high SAFit1 concentration from either a high density FKBP51FK1 affinity column or a mock column was higher than the total number of validated spectra in the corresponding wash fraction pools (Figure 29; exception: early SAFit1 dependent eluate in the 1st MS run = HEK293 sample B, dissolved pellet of the SAFit1 dependent eluate in the 2nd MS run = N2a sample D). 85 up to 450 of the validated spectra in each sample were assigned to common contaminants such as trypsin, human/mouse/sheep keratin and keratin associated proteins, human/bovine albumin, human serotransferrin and hemoglobin (Figure 29, Figure 30: red bars). The ratio of the contaminants was higher than 20% in sample F and G (Figure 29: 2nd MS run, N2 samples) and in sample 12, 14, 18 and 22 (Figure 30, 3rd MS run, N2a samples).

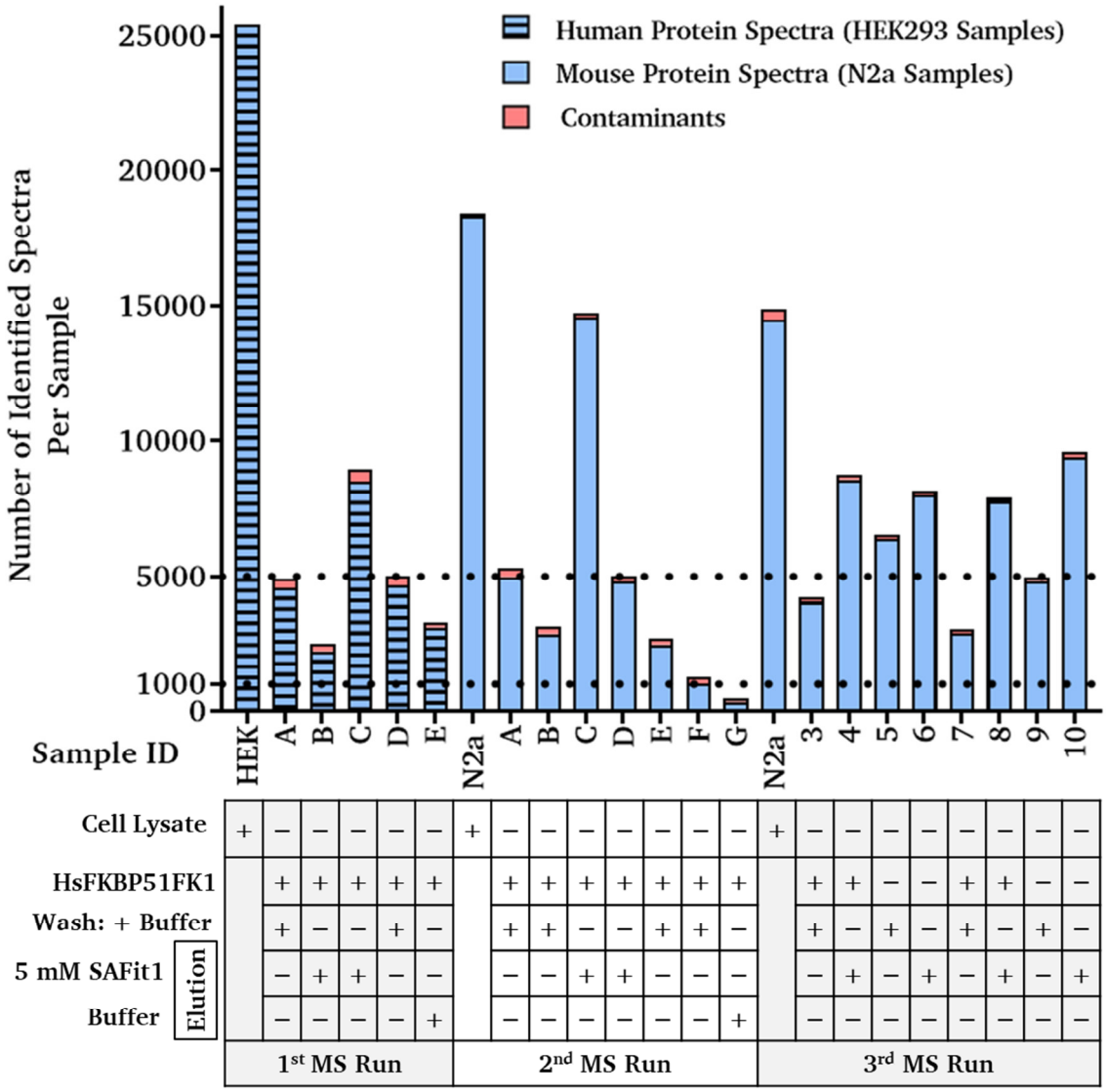

Figure 29: Total Number of Identified Spectra in the Pull-Down Assay Samples Using a "Low" Salt Buffer.

Figure 29: Total Number of Identified Spectra in the Pull-Down Assay Samples Using a "Low" Salt Buffer.

Either HEK293 (1st MS run) or N2a cell lysate (2nd and 3rd MS run) was added to a 350 µL (1st MS run) or a 400 µL (2nd and 3rd MS run) column carrying a FKBP51FK1 affinity matrix with a protein density of approximately 950 µM. A column filled with the blocked, naked beads (- FKBP51FK1) was applied as a control in the 3rd run. All columns were washed with 50 CV buffer. 10 CV (1st MS run) up to 20 CV 5 mM SAFit1 were added for elution. The 1st and the 2nd run included samples from a mock elution as a control.

Equilibration and cell lysis buffer, pH 8: 20 mM Tris, 100 mM NaCl, 0.5 mM EDTA, 0.5% (v/v) Nonidet-P40 substitute, 1 mM PMSF, 1 mM DTT, Protease inhibitor cocktail (cOmplete mini, Roche, 1 tablet per 10 mL).
Wash buffer, pH 8 = Equilibration/lysis buffer not supplemented with Nonidet-P40 substitute. Elution buffer, pH 8 = Wash buffer ± 5 mM SAFit1.

The pull-down assay samples and the complete cell lysates were analyzed by MS. Sample B of the 1st MS run included the early SAFit1 dependent eluate. Sample C carried the 2nd part of the SAFit1 dependent eluate. Sample precipitation occurred in the SAFit1 dependent eluate during the sample preparation for the 2nd MS run. The precipitate was separated and dissolved (= sample D, 2nd MS run). Sample C of the 2nd MS run included the not precipitated part of the SAFit1 dependent eluate. The pull-down assay samples of the 1st MS run (sample A - E, left side) were analyzed as a group. Two samples of the complete HEK293 cell lysate were analyzed together as a separate group. In the 2nd and the 3rd MS run, the pull-down assay samples were analyzed together with the total cell lysate in one group.

The proteins in all samples were relatively quantified by spectral counting. The protein items were identified on the basis of at least two different peptides across all samples. The total number of the corresponding spectra assigned to human proteins (HEK293 samples, 1st MS run) is given by stripped blue bars. The total number of identified spectra related to mouse proteins (N2a samples, 2nd MS run and 3rd MS run) is given by blue bars. The total number of spectra assigned to sample contaminants is shown by red bars.

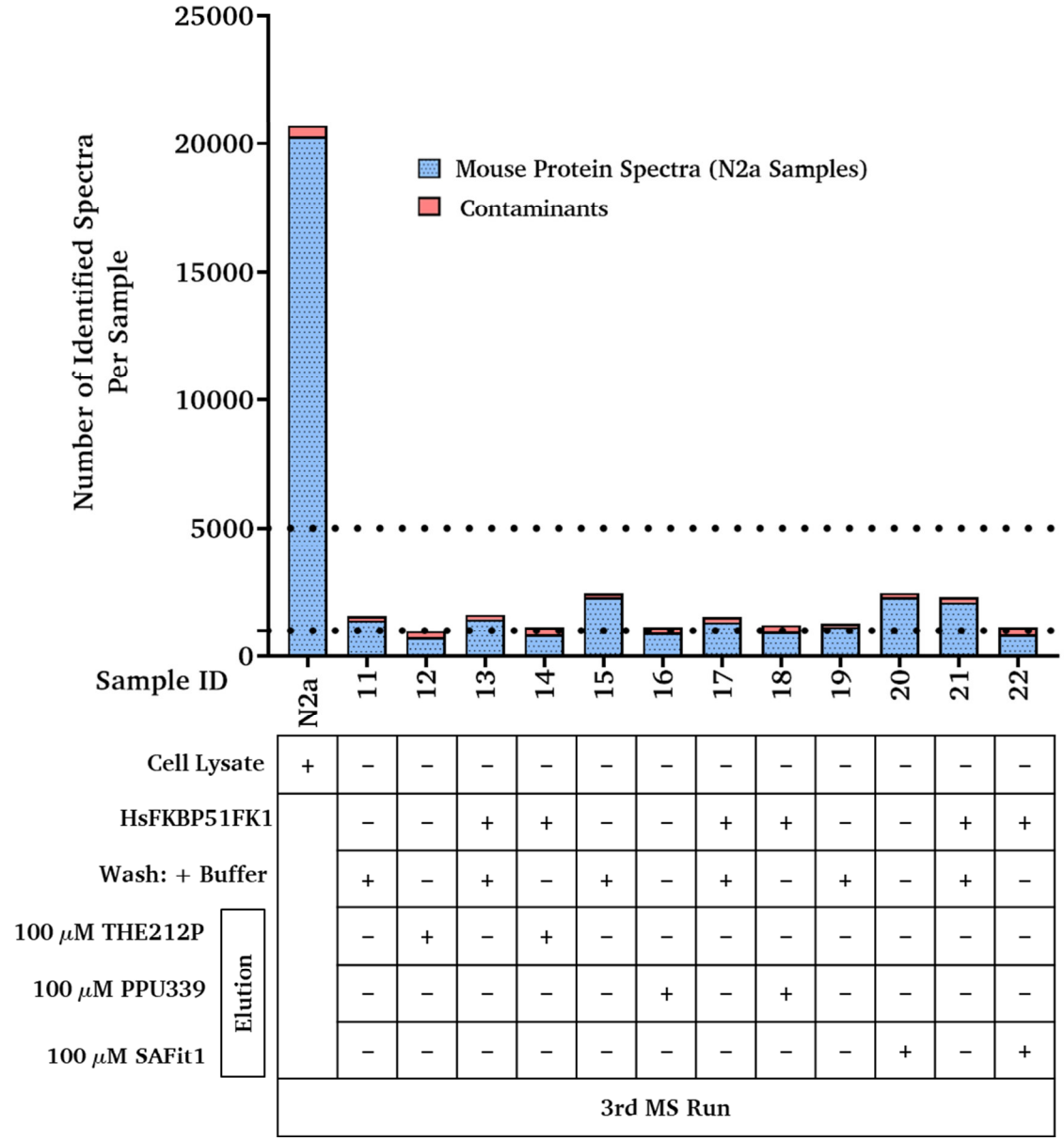

Figure 30: Number of Identified Spectra in the Pull-Down Assay Samples Applying a "High" Salt Buffer.

Figure 30: Number of Identified Spectra in the Pull-Down Assay Samples Applying a "High" Salt Buffer.

N2a cell lysate was loaded on three 300 µL FKBP51FK1 affinity columns exhibiting a protein density of about 20 µM. After washing the columns with 50 CV buffer either 20 CV of a 100 µM FKBP ligand (SAFit1 or PPU339) or 20 CV of a 100 µM non-binding SAFit1 analogue (THE212P) were added for elution. The columns filled with the blocked, naked beads (- FKBP51FK1) were applied as a control.

Equilibration and cell lysis buffer, pH 8: 20 mM Tris, 100 mM NaCl, 0.5 mM EDTA, 0.5% (v/v) Nonidet-P40 substitute, 1 mM PMSF, 1 mM DTT, Protease inhibitor cocktail (cOmplete mini, Roche, 1 tablet per 10 mL).
Wash buffer, pH 8: 20 mM Tris, 200 mM NaCl, 0.5 mM EDTA, 1 mM PMSF, 1 mM DTT, Protease inhibitor cocktail (cOmplete mini, Roche, 1 tablet per 10 mL).
Elution buffer, pH 8: 20 mM Tris, 200 mM NaCl, 0.5 mM EDTA, 1 mM PMSF, 1 mM DTT, Protease inhibitor cocktail (cOmplete mini, Roche, 1 tablet per 10 mL) ± 100 µM SAFit1/100 µM PPU339/100 µM THE212P.

After processing, all shown samples (11 - 22) including the complete N2a cell lysate were analyzed together with samples 3 - 10 (shown in Figure 29) by MS (3rd run). Only protein items assigned to at least two different peptides across all samples in the sample group were considered. The total number of the corresponding spectra related to mouse proteins is given by blue dotted bars. The number of spectra related to sample contaminants is shown by red bars.

The total number of validated spectra assigned to a distinct protein item was related to all validated spectra in the sample to enable the comparison of different samples (Equation 6). Spectra assigned to contaminants were also included because of the fluctuating sample contamination ratio (Figure 29, Figure 30).

$$\text{Relative number of spectra (RNS)} = \frac{\text{Number of spectra related to a distinct protein item in a sample}}{\text{Total number of spectra in a sample}}$$

Equation 6: Calculation of the Relative Number of Spectra.

All validated spectra related to a distinct protein item in a sample were divided by the total number of identified spectra in the sample to calculate the relative number of spectra (= RNS).

4.6.3. Comparing SAFit1 Dependent Elution with Mock Elution from a High Density FKBP51FK1 Affinity Column

HEK293 Samples – 1st MS Run

The SAFit1 dependent eluate from a high density FKBP51FK1 affinity column carrying human proteins originated from HEK293 cell lysate was compared with samples carrying unspecific eluting proteins (= mock eluate pool from another high density FKBP51FK1 affinity column and wash fraction pools from both columns, pull-down assay SMe289, Figure 13 a, p. 57). The pull-down assay aimed at differentiating between early (= first two eluates, 3 CV) and late SAFit1 (= subsequent eluting fractions, 7 CV) dependent eluting proteins. This approach was not pursued in the 2nd and 3rd MS run.

More than 2,400 human protein subunits or single proteins were identified in the complete HEK293 cell lysate on the basis of at least two assigned peptides across all pull-down assay samples and both samples of the complete cell lysate. 2,376 protein items were identified in both samples of the total HEK293 cell lysate differing in the LC injection volume (1.5 μL and 3 μL) (Figure 31: intermediate grey and orange area). 880 protein items excluding sample contaminants were identified in the pull-down assay samples comprising the SAFit1 dependent eluate and the mock eluate from a high density FKBP51FK1 affinity column as well as the corresponding wash fraction pools. Thereof, 131 protein items were exclusively identified in the HEK293 samples (Figure 31: light orange area). 731 protein items were also identified in the complete HEK293 cell lysate (Figure 31: intermediate orange area).

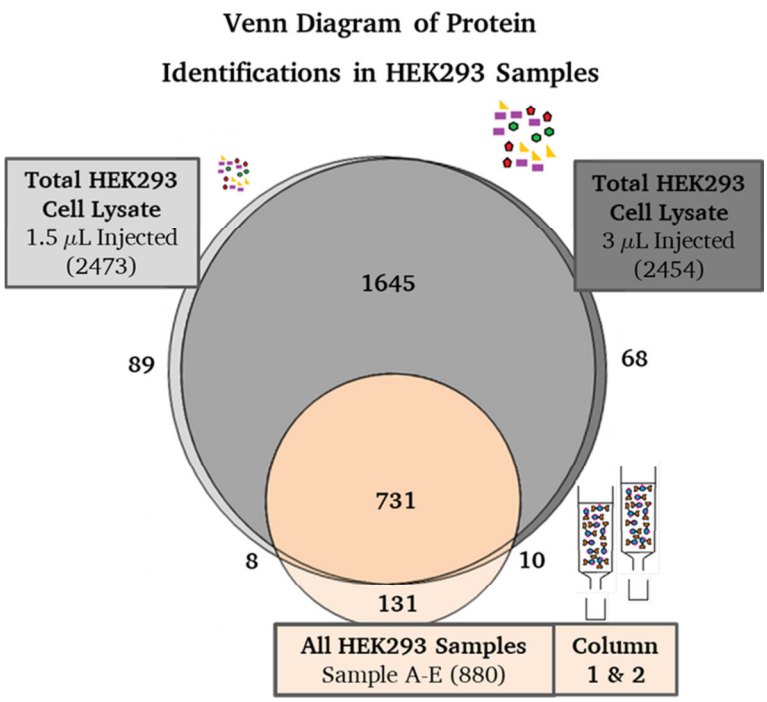

Figure 31: Protein Identifications in the Complete HEK293 Cell Lysate and the Pull-Down Assay Samples.

The number of protein identifications in the complete HEK293 cell lysate (grey) and all pull-down assay samples (orange) from two high density FKBP51FK1 affinity columns carrying human proteins is shown. The complete cell lysate was analyzed twice varying the LC sample injection volume (light grey: 1.5 µL were injected, dark grey: 3 µL were injected). Protein identifications in various samples are illustrated by overlapping areas: identified in both samples of the total cell lysate (intermediate grey), identified in one sample of the complete cell lysate and in the pull-down assay samples (intermediate orange), identified in both samples of the complete HEK293 cell lysate and in the pull-down assay samples (intermediate orange). The numbers given in the Venn diagram comprise single proteins and protein subunits identified either in various samples (overlapping areas), exclusively in the HEK293 samples (outer part of the orange circle) or exclusively in one sample of the complete cell lysate (outer part of the grey circles). The total number of all counted protein items in both samples of the complete HEK293 cell lysate (light and dark grey box) and in all HEK293 samples (orange box) is given. Contaminants such as bovine albumin, human and sheep keratin as well as pig and bovine trypsin were excluded.

674 protein items were identified in the samples carrying unspecific eluting proteins, namely the wash fraction pools from both high density FKBP51FK1 affinity columns and the mock eluate. Thereof, 379 protein items were identified in all three samples, 45 in the wash fraction pool from column 1, 69 in the wash fraction pool from column 2 and 11 in the mock eluate (Figure 32 a). Comparing the SAFit1 dependent eluate with the samples carrying unspecific eluting proteins, 6 protein items were exclusively identified in the early (light green) SAFit1 dependent eluate, 167 exclusively in the late (dark green) SAFit1 dependent eluate and 33 in both (intermediate green) eluates (Figure 32 b). 295 protein items were identified in both SAFit1 dependent eluates and at least in one sample carrying unspecific eluting proteins (Figure 32 b: orange area). 59 protein items were identified in the early SAFit1 dependent eluate (light yellow), respectively 183 in the late SAFit1 dependent eluate (yellow) and at least in one sample carrying unspecific eluting proteins (Figure 32 b).

Figure 32: Protein Identifications in HEK293 Samples (1st MS Run) – Comparing SAFit1 Dependent and Mock Elution from a High Density FKBP51FK1 Affinity Column.

The numbers shown in the Venn diagrams are related to all human single proteins and protein subunits identified in the HEK293 samples.

Figure a): Protein identifications in the HEK293 samples carrying unspecific eluting proteins from two high density FKBP51FK1 affinity columns: wash fraction pool from column 1 and 2, mock eluate.

Figure b): The protein identifications in the early and the late SAFit1 dependent eluate (green) from a high density FKBP51FK1 affinity column were compared with the protein identifications in the samples carrying unspecific eluting proteins (blue).

The number of protein items exclusively identified in one sample (figure a + b) or in at least one sample carrying unspecific eluting proteins (figure b: blue) are displayed in the outer part of the circles. The number of protein items identified in various samples is shown in overlapping areas. The total number of identified protein items in each sample (figure a: blue boxes, figure b: light and dark green box) or in a sample subset (figure b: blue box) is given. Contaminants such as bovine albumin, human and sheep keratin as well as pig and bovine trypsin were excluded.

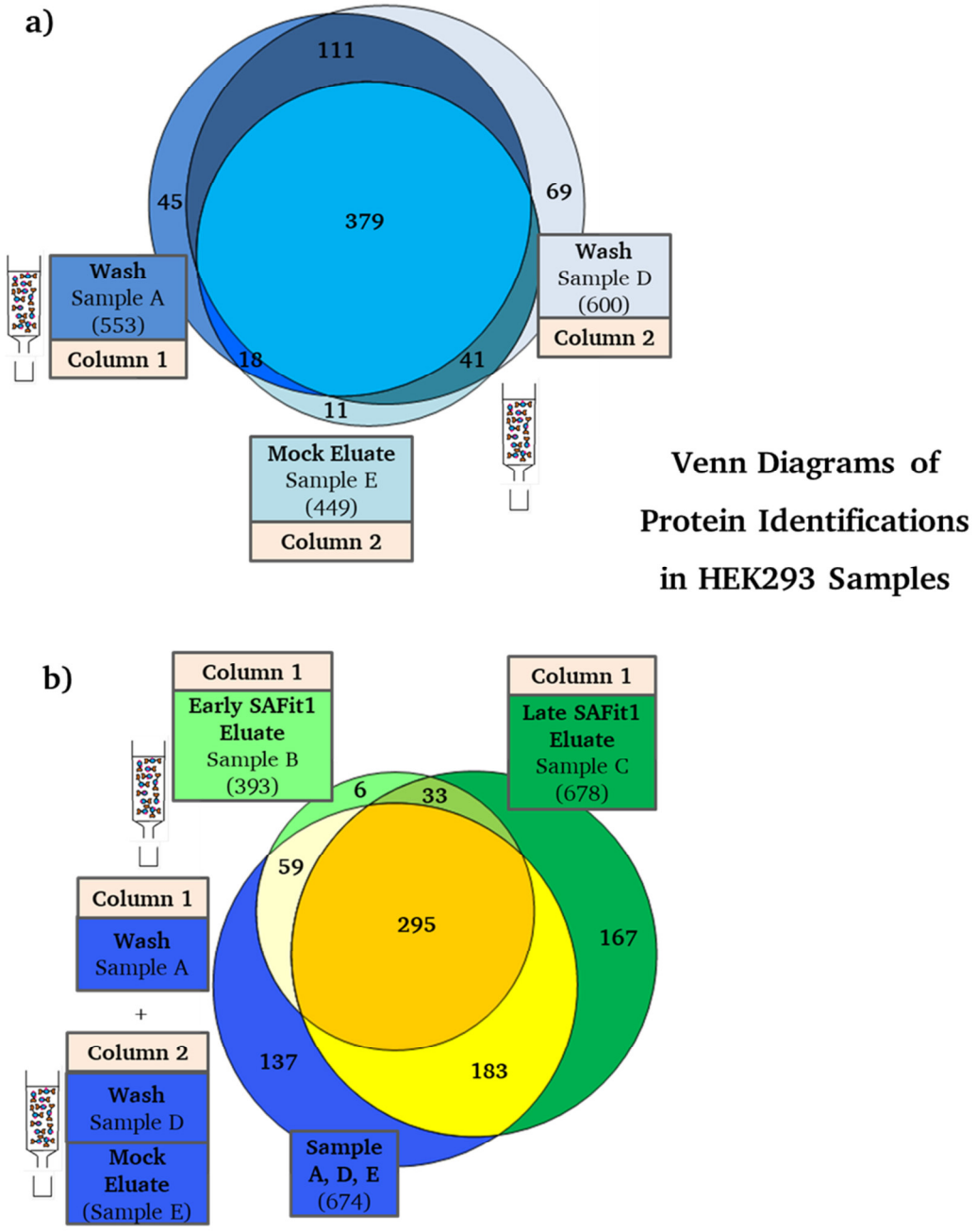

Figure 32: Protein Identifications in HEK293 Samples (1st MS Run) – Comparing SAFit1 Dependent and Mock Elution from a High Density FKBP51FK1 Affinity Column.

A protein enrichment factor (EF) was calculated to assess the enrichment of proteins identified in the early and/or late SAFit1 dependent eluate and at least in one of the samples carrying unspecific eluting proteins. The relative protein abundance in the early (Equation 7) and the late (Equation 8) SAFit1 dependent eluate was compared with the average relative protein abundance in the wash fraction pools from both high density FKBP51FK1 affinity columns and the mock eluate.

$$\mathrm{EF(Early\ SAFit1\ Eluate)} = \frac{\mathrm{RNS\ Sample\ B}}{(\mathrm{RNS\ Sample\ A} + \mathrm{RNS\ Sample\ D} + \mathrm{RNS\ Sample\ E})/3}$$

Equation 7: Relative Protein Abundance in the Early SAFit1 Dependent Eluate.

Sample B = Early SAFit1 dependent eluate from a high density FKBP51FK1 affinity column (final protein density about 950 µM). Sample A = Corresponding wash fraction pool. Sample E = Mock eluate from another high density FKBP51FK1 affinity column. Sample D = Corresponding wash fraction pool. Sample A and B were collected from one FKBP51FK1 affinity column. Sample D and E were collected from another FKBP51FK1 affinity column. EF = Enrichment Factor. RNS = Relative number of identified spectra.

$$\mathrm{EF(Late\ SAFit1\ Eluate)} = \frac{\mathrm{RNS\ Sample\ C}}{(\mathrm{RNS\ Sample\ A} + \mathrm{RNS\ Sample\ D} + \mathrm{RNS\ Sample\ E})/3}$$

Equation 8: Relative Protein Abundance in the Late SAFit1 Dependent Eluate.

Sample C = Late SAFit1 dependent eluate from a high density FKBP51FK1 affinity column (final protein density about 950 µM).
Sample A = Corresponding wash fraction pool. Sample E = Mock eluate from another high density FKBP51FK1 affinity column. Sample D = Corresponding wash fraction pool. Sample A and B were collected from one FKBP51FK1 affinity column. Sample D and E were collected from another FKBP51FK1 affinity column. EF = Enrichment Factor. RNS = Relative number of identified spectra.

As a control, the relative protein abundance in the mock eluate was compared with the relative protein abundance in the wash fraction pool from the corresponding high density FKBP51FK1 affinity column to detect late unspecific eluting proteins (Equation 9, Suppl. Table 31 b, p. 177 ff.).

$$\mathrm{EF(Mock\ Eluate)} = \frac{\mathrm{RNS\ Mock\ Eluate}}{\mathrm{RNS\ Wash\ Fraction\ Pool}}$$

Equation 9: Relative Protein Abundance in the Mock Eluate in Relation to the Wash Step.

The wash fraction pool and the mock eluate were collected from a high density FKBP51FK1 affinity column. EF = Enrichment factor. RNS = Relative number of identified spectra.

All protein items identified on the basis of at least two assigned peptides across all pull-down assay samples were sub-grouped: (i) protein items exclusively identified in either the early or/and SAFit1 dependent eluate(s), (ii) protein items identified in at least one control sample

and in either the early, late or in both SAFit1 dependent eluate(s) with an enrichment factor higher than 2, (iii) ribosomal proteins, (iv) contaminants, (v) background proteins (Figure 33). 2% of all identified protein items were contaminants (bovine albumin, human and sheep keratin, bovine and pig trypsin). The ribosomal proteins made 8% of all identified protein items and were excluded from the subsequent analysis due to lacking biological interest (Figure 33). Only protein items related to at least 4 spectra in either the early or late SAFit1 dependent eluate were selected for subsequent analysis to decrease the number of false positive results and to increase the confidence in the preliminary findings. Only 70 of 167 protein items exclusively identified in the late SAFit1 dependent eluate, one protein item of 6 exclusively identified in the early SAFit1 dependent eluate and 9 of 33 protein items exclusively identified in both eluates were assigned to at least 4 validated spectra (Figure 32 b, Figure 33). 162 of 537 protein items fulfilled the following selection criteria: (i) protein identification in the early or/and late SAFit1 dependent eluate(s), (ii) relation to at least 4 spectra in one of the SAFit1 dependent eluates, (iii) enrichment factor higher than 2. Thereof, 25 (3% of all) protein items showed a higher abundance in the early SAFit1 dependent eluate (EF > 2) in comparison with the control samples. 90 (10% of all) protein items showed a higher abundance in the late SAFit1 dependent eluate (EF > 2). 47 (5% of all) protein items had an enrichment factor higher than 2 in both SAFit1 dependent eluates (Figure 33). Protein lists including the ranking with regard to the described selection criteria are given in the supplement (Table 31 a + b, p. 173 ff.). Protein items excluded on the basis of the described criteria were assigned to the background comprising 63% of all preliminary identified protein items (Figure 32 b, Figure 33).

Protein items showing a higher abundance in the early or/and late SAFit1 dependent eluate in comparison with the control samples were sub-grouped in relation to the enrichment factor (Figure 34). One protein item in the early SAFit1 dependent eluate (Figure 34 a) and 5 protein items in the late SAFit1 dependent eluate (Figure 34 b) had an enrichment factor higher than 20. 6 protein items showed an enrichment factor higher than 20 in both, the early and late SAFit1 dependent eluate (Figure 34 c). The majority of the pre-selected protein items showed an enrichment factor at a low level between 2 and 10 (Figure 34 a: 92% of the pre-selected protein items in the early SAFit1 dependent eluate, Figure 34 b: 79% of the pre-selected protein items in the late SAFit1 dependent eluate, Figure 34 c: 70% of the pre-selected protein items in both, the early and late SAFit1 dependent eluate).

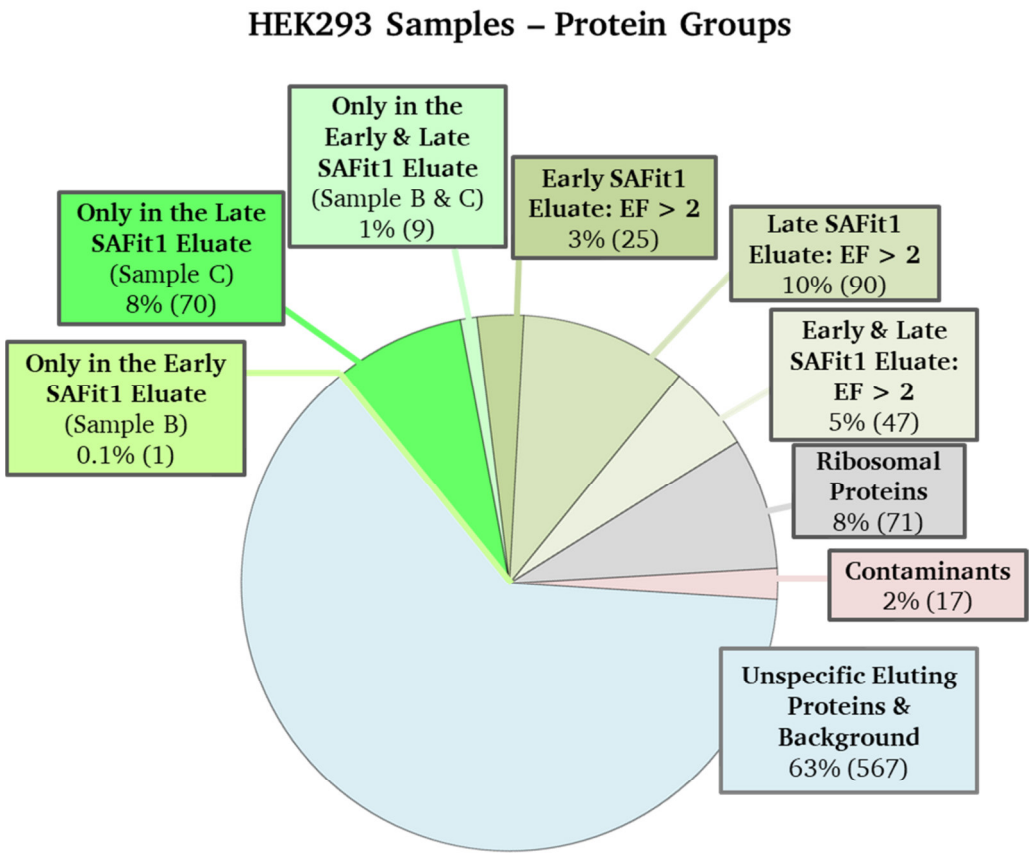

Figure 33: Protein Enrichment Analysis in HEK293 Samples.

All human protein items (in total 897) identified on the basis of at least two different assigned peptides across all HEK293 pull-down assay samples from a high density FKBP51FK1 affinity column were grouped into the following categories: (i) protein items exclusively identified in the early and/or late SAFit1 dependent eluate but not in the samples carrying unspecific eluting proteins (green; sample B, C and B & C), (ii) protein items showing a higher protein abundance in the early and/or late SAFit1 dependent eluate in comparison with samples carrying unspecific eluting proteins (olive green, EF > 2), (iii) ribosomal proteins (grey), (iv) contaminants (red; bovine albumin, human and sheep keratin, pig and bovine trypsin),(v) unspecific eluting proteins and background (blue). All protein items in group (i) and (ii) were related to at least 4 spectra in at least one of both SAFit1 dependent eluates. The relation between the protein identifications in each group and the total protein identifications is given in %. The total protein count in each group is given by the numbers in brackets. EF = enrichment factor.

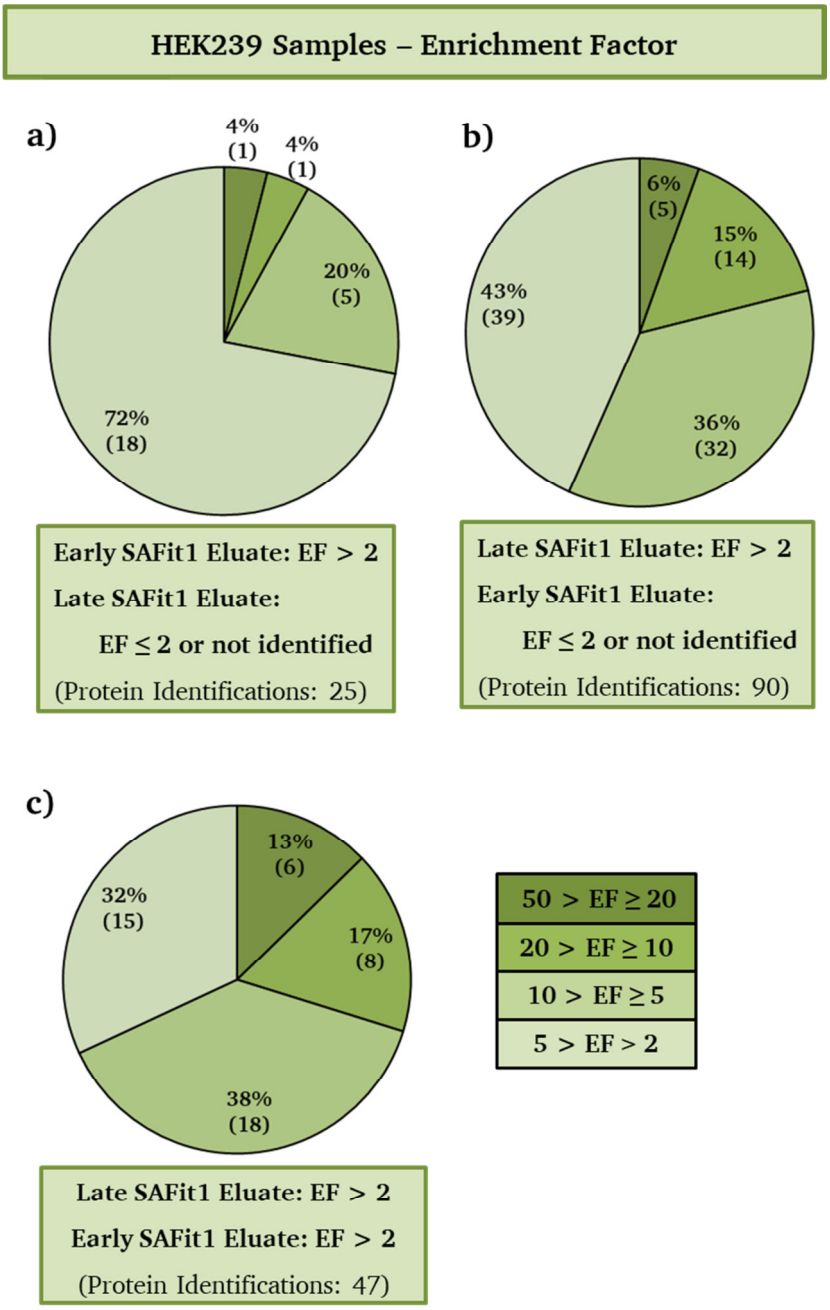

Figure 34: Enrichment Factor Distribution – HEK293 Samples.

Figure a - c: Protein items identified in the SAFit1 dependent eluate and at least in one control sample were sub-grouped in relation to the relative protein abundance given by the enrichment factor (EF). The wash fraction pools from two high density FKBP51FK1 affinity columns and the mock eluate were applied as controls. Protein items were identified in at least one control sample and (i) either in the early SAFit1 dependent eluate (EF > 2) or in both SAFit1 dependent eluates [EF(early SAFit1 eluate) > 2, EF (late SAFit1 eluate) ≤ 2; Figure a], (ii) either in the late SAFit1 dependent eluate (EF > 2) or in both SAFit1 dependent eluates [EF(late SAFit1 eluate) > 2, EF(early SAFit1 eluate) ≤ 2; Figure b], (iii) in both SAFit1 dependent eluates with EF > 2 (Figure c). The EF distribution is given in %. The total number of identified proteins in each subgroup is given by the numbers in brackets.

The members of the selected protein subgroups (Figure 33, Figure 34) were assigned to cellular components and protein classes by PANTHER [4, 16, 61, 89]. The results for the protein items exclusively identified (Figure 35) or showing the highest enrichment factors in the early (Figure 36) or/and late (Figure 37, Figure 38) SAFit1 dependent eluate(s) are shown below. The analysis of protein items associated with low enrichment factors is shown in the supplement (Figure 52 - Figure 54, p. 183 - 185).

Most of the protein items exclusively identified or showing a higher protein abundance in the early and/or late SAFit1 dependent eluate in comparison with the control samples were related to the GO term [6] “cell organelles” (43% up to 58%) or were not classified (21% up to 29%) by PANTHER (Figure 35 a, Figure 37 a, Figure 38 a) [4, 16, 61, 89]. Most of the protein items related to the GO term “cell organelles” were found in the nucleus (61% up to 90%; Figure 35 a, Figure 36 a, Figure 37 a, Figure 38 a). Cytosolic proteins made up to 14% of the identified protein items (Figure 35 a, Figure 38 a). The most common identified protein classes were “nucleic acid or RNA metabolism proteins” or “cytoskeletal proteins” (Figure 35 b, Figure 36 b, Figure 37 b, Figure 38 b).

Figure 35: Assigning Human Protein Items Exclusively Identified in the SAFit1 Dependent Eluate to Cellular Components and Protein Classes.

Human protein items exclusively identified in the SAFit1 dependent eluate (either in the early, the late or in both SAFit1 dependent eluate(s); 80 protein items in total) were assigned to cellular components (Figure a) and protein classes (Figure b) by PANTHER [4, 16, 61, 89]. The protein item distribution is given in %.

Figure a: The Venn diagram shows the cellular component affiliation. Overlapping areas are related to protein items assigned to several cellular components. 29% of the analyzed protein items were not assigned (grey circle). Protein items localized in cellular organelles were sub-grouped into the following categories: nucleus, cytoskeleton, mitochondrium and others. There was no overlap between these groups.

Figure b: The ratio of the identified protein classes is shown in %. Protein items can be assigned either to one or different protein classes.

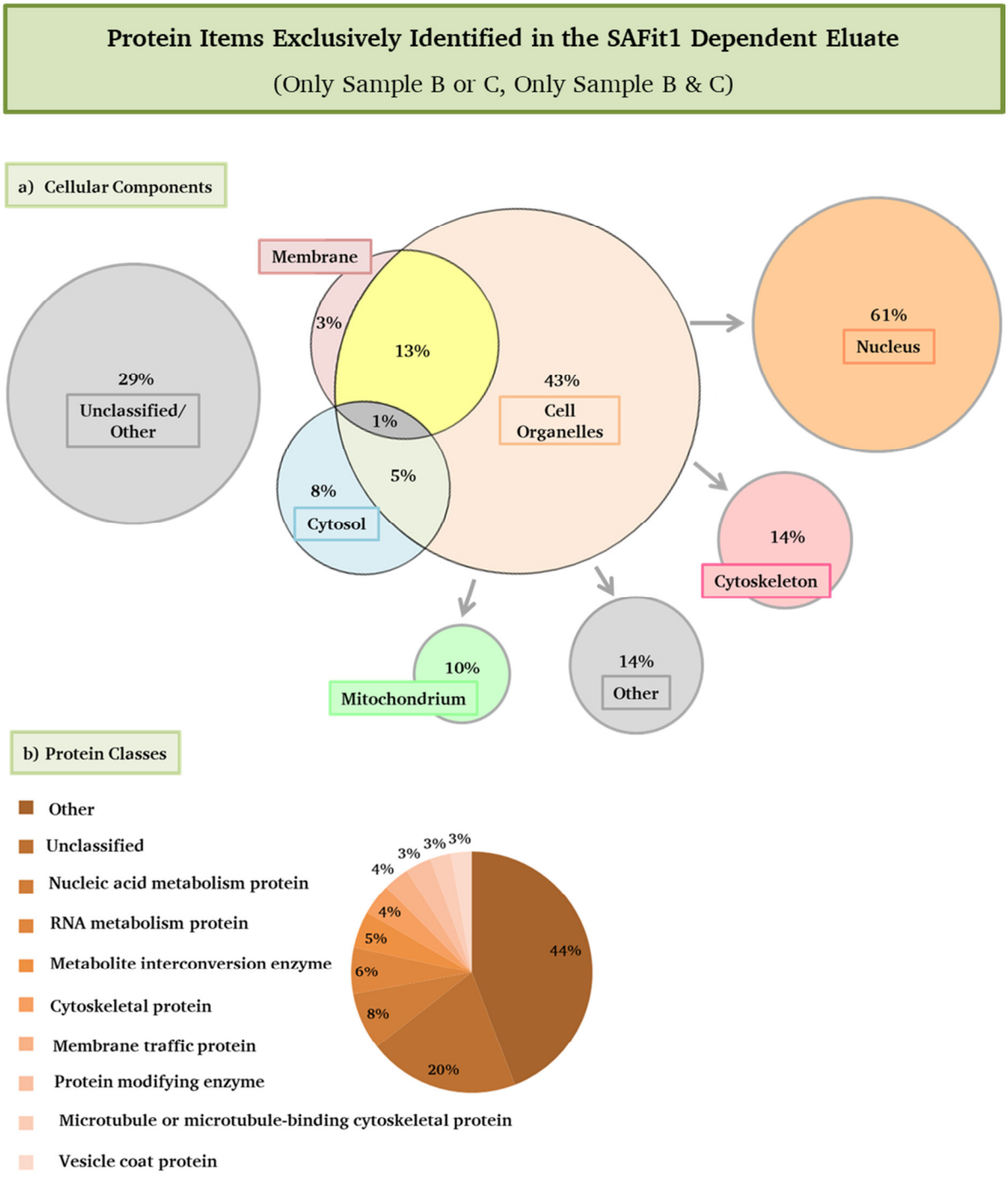

Figure 35: Assigning Human Protein Items Exclusively Identified in the SAFit1 Dependent Eluate to Cellular Components and Protein Classes.

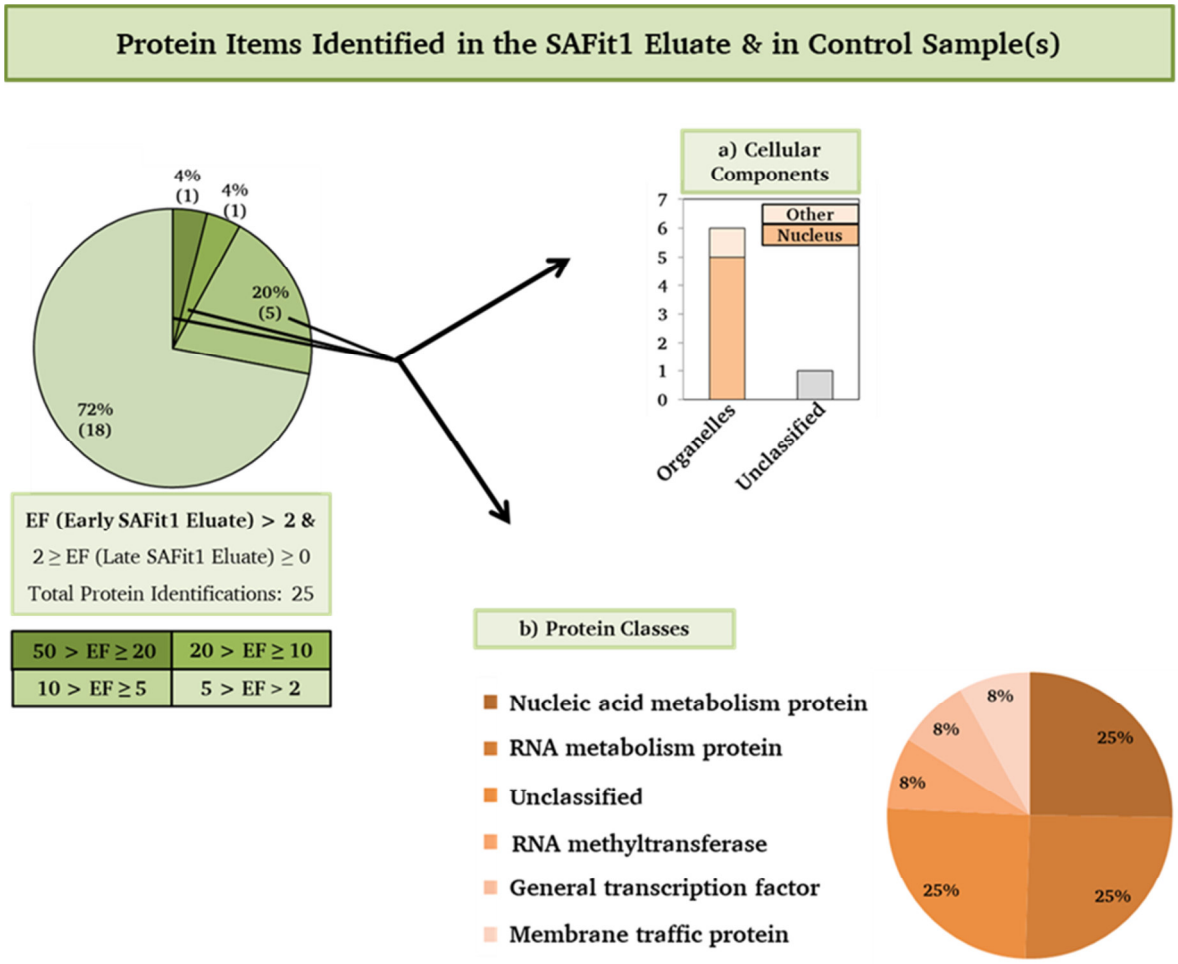

Figure 36: Assigning Protein Items identified in the Early SAFit1 Dependent Eluate to Cellular Components and Protein Classes – "Intermediate/Low" Enrichment Factor.

Human protein items identified in the early SAFit1 dependent eluate with an enrichment factor (EF) higher than 5 and lower than 50 (7 protein items in total) were assigned to cellular components (Figure a) and protein classes (Figure b) by PANTHER [4, 16, 61, 89].

Figure a: The total number of protein items related to cell organelles, especially to the nucleus and of unclassified protein items is given.

Figure b: The distribution of the identified protein classes is given in %. Protein items can be assigned to one or several protein classes.

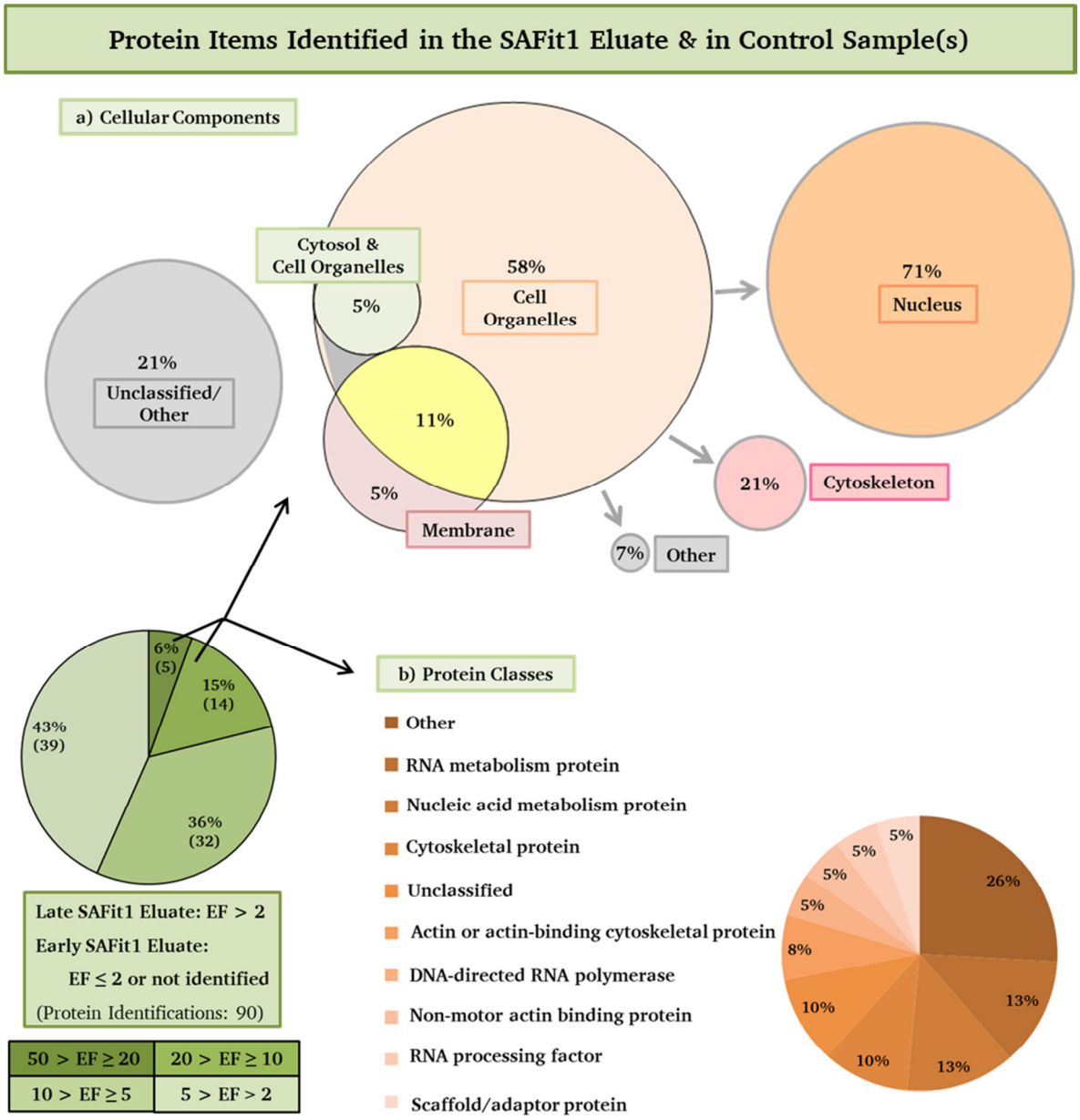

Figure 37: Assigning Human Protein Items Identified in the Late SAFit1 Dependent Eluate to Cellular Components and Protein Classes – "High" Enrichment Factor.

Human protein items identified in the late SAFit1 dependent eluate with an enrichment factor (EF) higher than 10 and lower than 50 (19 protein identifications in total) were assigned to cellular components (Figure a) and protein classes (Figure b) by PANTHER [4, 16, 61, 89].

Figure a: The Venn diagram shows the protein item assignment to cellular components (cell organelles and membrane). The ratio is given in %. The protein items related to "cell organelles" were assigned to the subgroups "nucleus" (orange circle) and "cytoskeleton (red circle). 21% of the protein items were not classified (grey circle).

Figure b: The distribution of the identified protein classes is given in %. Protein items can be assigned to one or several protein classes.

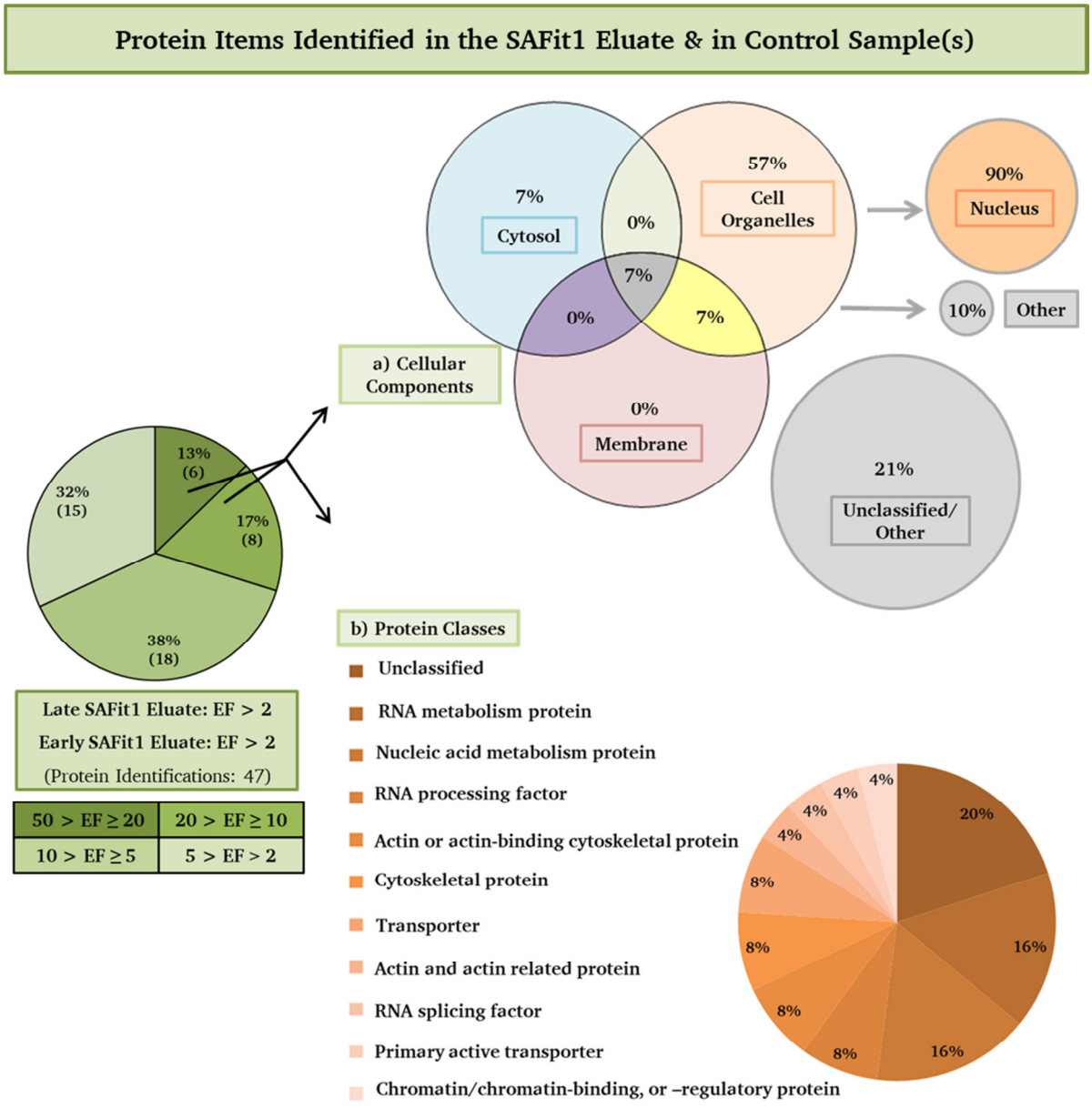

Figure 38: Assigning Human Protein Items Identified in the Early and Late SAFit1 Dependent Eluate to Cellular Components and Protein Classes – "High" Enrichment Factor.

Human protein items identified in the early and late SAFit1 dependent eluate with an enrichment factor (EF) higher than 10 and lower than 50 (14 protein identifications in total) were assigned to cellular components (Figure a) and protein classes (Figure b) by PANTHER [4, 16, 61, 89].

Figure a: The distribution of the protein items assigned to cellular components (cell organelles, cytosol and membrane) is given in %. Protein assignments to different cellular components are indicated by overlapping areas. 90% of the protein items related to "cell organelles" were assigned to the subgroup "nucleus" (orange circle). 21% of the protein items were not classified (grey circle).

Figure b: The distribution of the identified protein classes is given in %. Protein items can be assigned to one or several protein classes.

N2a Samples – 2nd MS Run

The SAFit1 dependent eluate from a high density FKBP51FK1 affinity column was compared with the mock eluate from another high density FKBP51FK1 affinity column and the wash fraction pools (Wash 2 = last 10 wash fractions, Wash 1 = previous 10 wash fractions) from both columns (Figure 13 b, p. 58). The SAFit1 dependent eluate precipitated partially in the sample concentration step required for the subsequent MS analysis. The precipitate was dissolved with ammonium bicarbonate and both samples of the SAFit1 dependent eluate, the supernatant and the dissolved pellet were analyzed.

1298 mouse protein items were identified across all pull-down assay samples (Figure 39: orange circle) and 1525 protein items in the complete N2a cell lysate (Figure 39: grey circle). Thereof, 485 protein items were exclusively identified in the supernatant (Figure 40 b: light green), 21 in the dissolved precipitate (dark green) and 313 in both samples (intermediate green) of the SAFit1 dependent eluate. 224 mouse protein items were identified in both samples (Figure 40 b: orange), 195 in the supernatant (light yellow) and 9 in the dissolved precipitate (yellow box) of the SAFit1 dependent eluate and at least in one of the control samples. 479 mouse protein items were identified in the control samples (Figure 40 a, Figure 40 b: blue box). Almost all (477 of 479) of these protein items were found in the wash fraction pools from one high density FKBP51FK1 affinity column (Figure 40 a: outer circle, light blue, column 1). Only 273 of these protein items were also identified in the wash fraction pools from another high density FKBP51FK1 affinity column (Figure 40 b: intermediate blue colored circle). Comparing the wash fraction pools (sample E & F) and the mock eluate (sample G) from a high density FKBP51FK1 affinity column, no additional protein items were identified in the mock eluate (Figure 40 b: small “dark” blue colored circle).

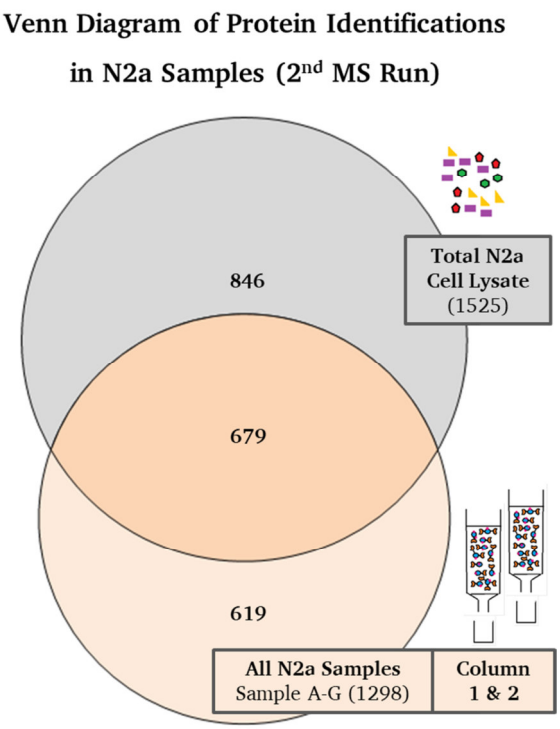

Figure 39: Protein Identifications in the Complete N2a Cell Lysate and the Pull-Down Assay Samples.

All N2a samples (pull-down assay samples A - G: orange circle) were analyzed in one group. The complete N2a cell lysate was analyzed separately (grey circle). Protein identifications in the N2a samples and in the complete N2a cell lysate are indicated by the overlapping area (dark orange). Common contaminants such as human keratin, pig trypsin, human and bovine albumin were excluded.

Figure 40: Protein Identifications in N2a Samples (2nd MS Run) – Comparing SAFit1 Dependent and Mock Elution from a High Density FKBP51FK1 Affinity Column.

Figure a: Venn diagram showing the mouse protein identifications in the control samples. The inner circle (dark blue) shows the protein identifications in all control samples, the intermediate blue colored circle the protein identifications in the wash fraction pools from two high density FKBP51FK1 affinity columns and the outer circle (light blue) the protein identifications in the wash fraction pools from column 1.

Figure b: Venn diagram comparing the mouse protein identifications in the SAFit1 dependent eluate and the control samples. Mouse protein items exclusively identified in either the supernatant (light green), the dissolved precipitate (dark green) or in both samples of the SAFit1 dependent eluate are displayed. Protein identifications in both, the SAFit1 dependent eluate and at least in one of the control samples are indicated by overlapping areas (orange, yellow). Protein items identified in the control samples but not in the SAFit1 dependent eluate are shown by the blue area of the lower circle. The total numbers of protein identifications are given. Common contaminants were excluded.

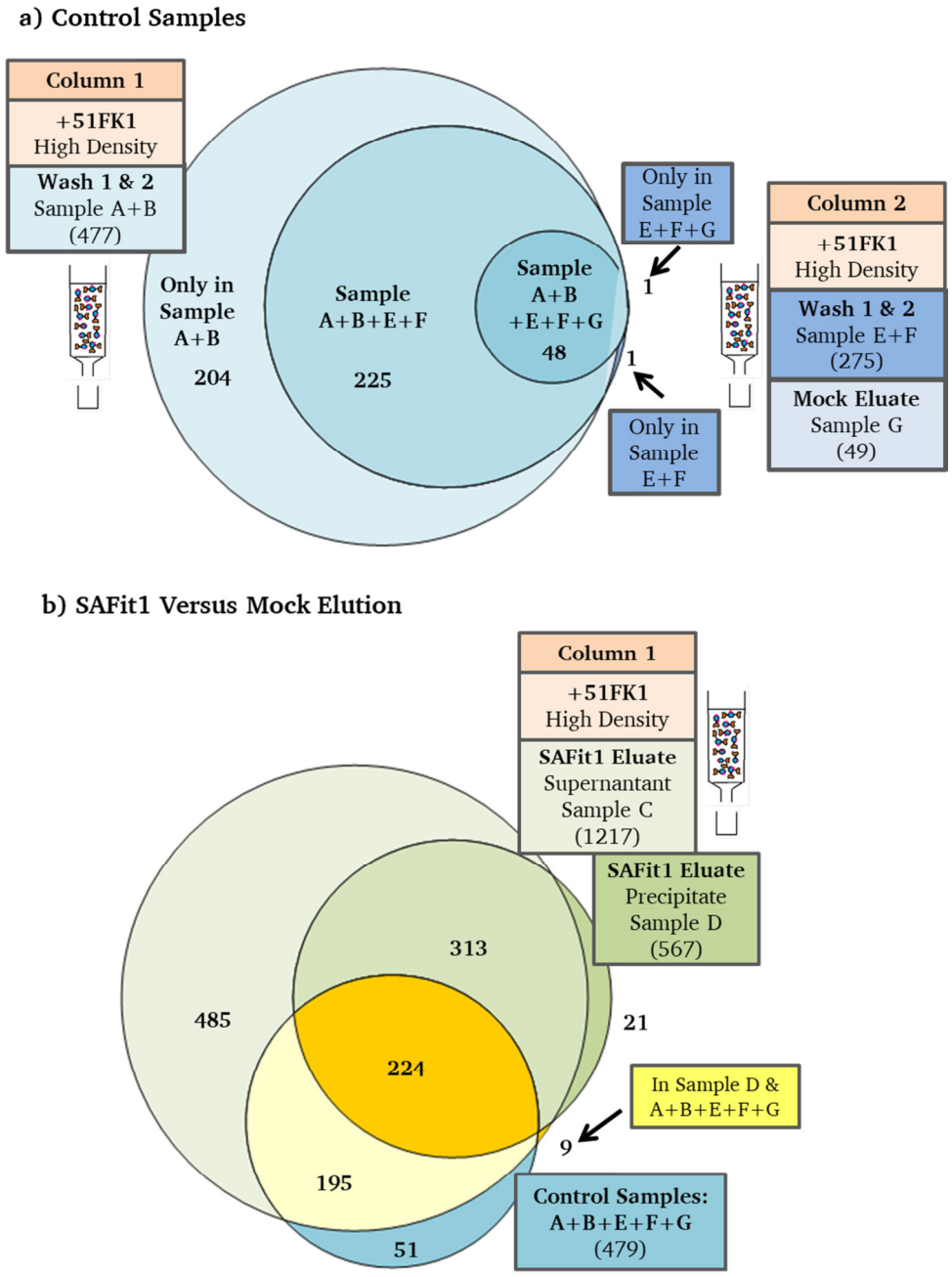

Figure 40: Protein Identifications in N2a Samples (2nd MS Run) – Comparing SAFit1 Dependent and Mock Elution from a High Density FKBP51FK1 Affinity Column.

An enrichment factor was calculated to compare the relative protein abundance in the SAFit1 dependent eluate from a high density FKBP51FK1 affinity column with the relative protein abundance in the control samples (Equation 10).

$$\mathrm{EF(SAFit1\ Eluate)} = \frac{\mathrm{RNS\ Sample\ C\ or\ D}}{(\mathrm{RNS\ Sample\ A + B + E + F + G})/5}$$

Equation 10: Relative Protein Abundance in the SAFit1 Dependent Eluate.

Each sample set (samples A – D and samples E – G) was collected from one high density FKBP51FK1 affinity column (final protein density: 950 µM). Sample A & E: Pool of the 10 penultimate wash fractions. Sample B & F: Pool of the last 10 wash fractions. Sample C: Supernatant of the SAFit1 dependent eluate. Sample D: Dissolved precipitate of the SAFit1 dependent eluate. G: Mock eluate.
EF = Enrichment factor. RNS = Relative number of identified spectra.

As a control, the relative protein abundance in the mock eluate was compared with the mean relative abundance in the other samples carrying unspecific eluting proteins (Equation 11).

$$\mathrm{EF(Mock\ Eluate)} = \frac{\mathrm{RNS\ Sample\ G}}{(\mathrm{RNS\ Sample\ A + B + E + F})/4}$$

Equation 11: Relative Protein Abundance in the Mock Eluate.

Each sample set (sample A & B and samples E – G) including unspecific eluting proteins was collected from one high density FKBP51FK1 affinity column. Sample A & E: Pool of the 10 penultimate wash fractions. Sample B & F: Pool of the last 10 wash fractions. G: Mock eluate. EF = Enrichment factor. RNS = Relative number of identified spectra.

The mouse protein items identified on the basis of at least two different assigned peptides across all N2a samples (Figure 39, Figure 40) were sub-grouped and ranked with regard to the following criteria: (1) exclusion of contaminants (red), (2) exclusion of ribosomal proteins (grey), (3) selection of all protein items assigned to at least 4 spectra in one of the SAFit1 dependent eluates, (4) selection of all protein items exclusively identified in the SAFit1 dependent eluate or showing an enrichment factor higher than 2 (Figure 41). Only 234 of the 485 protein items exclusively identified in the supernatant, 12 of the 21 protein items exclusively identified in the re-dissolved precipitate and 190 of the 224 protein items exclusively identified in both samples of the SAFit1 dependent eluate fulfilled the described criteria. 4 mouse protein items with an enrichment factor (EF) between 70 and 100 or 50 and 70 as well as 13 protein items with an EF between 20 and 50 were identified. 21 protein items showed an EF between 10 and 20, 27 protein items an EF between 5 and 10 and 40 protein items an EF between 2 and 5 (Figure 41). The contaminants made about 1% (18 protein items in total) and the ribosomal proteins about 10% (129 protein items in total) of all protein identifications. 46% (600 protein items in total) were related to the background

and unspecific eluting proteins. Complete lists of all pre-selected protein items with regard to the described criteria are given in the supplement (Table 32 a & b, p. 186 ff.).

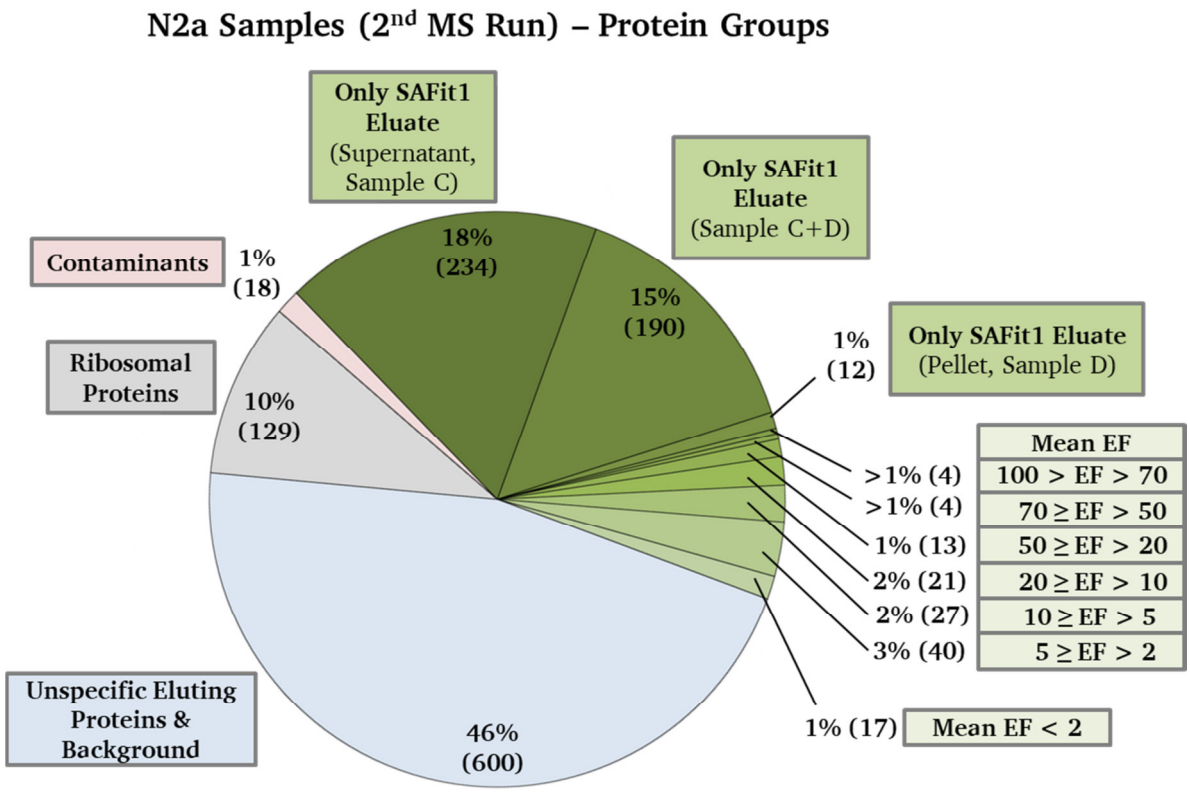

Figure 41: Subgrouping N2a Samples (2nd MS Run).

All mouse protein items identified on the basis of at least two peptides across all pull-down assay samples were assigned to the following groups: (1) protein items exclusively identified in the supernatant or/and the dissolved precipitate of the SAFit1 dependent eluate (olive green boxes), (2) protein items identified in the SAFit1 dependent eluate and at least in one control sample with an enrichment factor (EF) higher than 2 (light green), (3) background and unspecific eluting proteins (blue) including protein items with an enrichment factor lower than 2 and either not identified or related to less than 4 spectra in both samples of the SAFit1 dependent eluate,(4) ribosomal proteins (grey), (5) contaminants (red) such as human and mouse keratins or keratin associated proteins, human and bovine albumin and pig trypsin.

Protein items exclusively identified in the SAFit1 dependent eluate but not in the samples carrying unspecific eluting proteins (Figure 42) as well as protein items showing an intermediate up to a high enrichment factor (Figure 43, Figure 44) were assigned to cellular components and protein classes by PANTHER [4, 16, 61, 89].

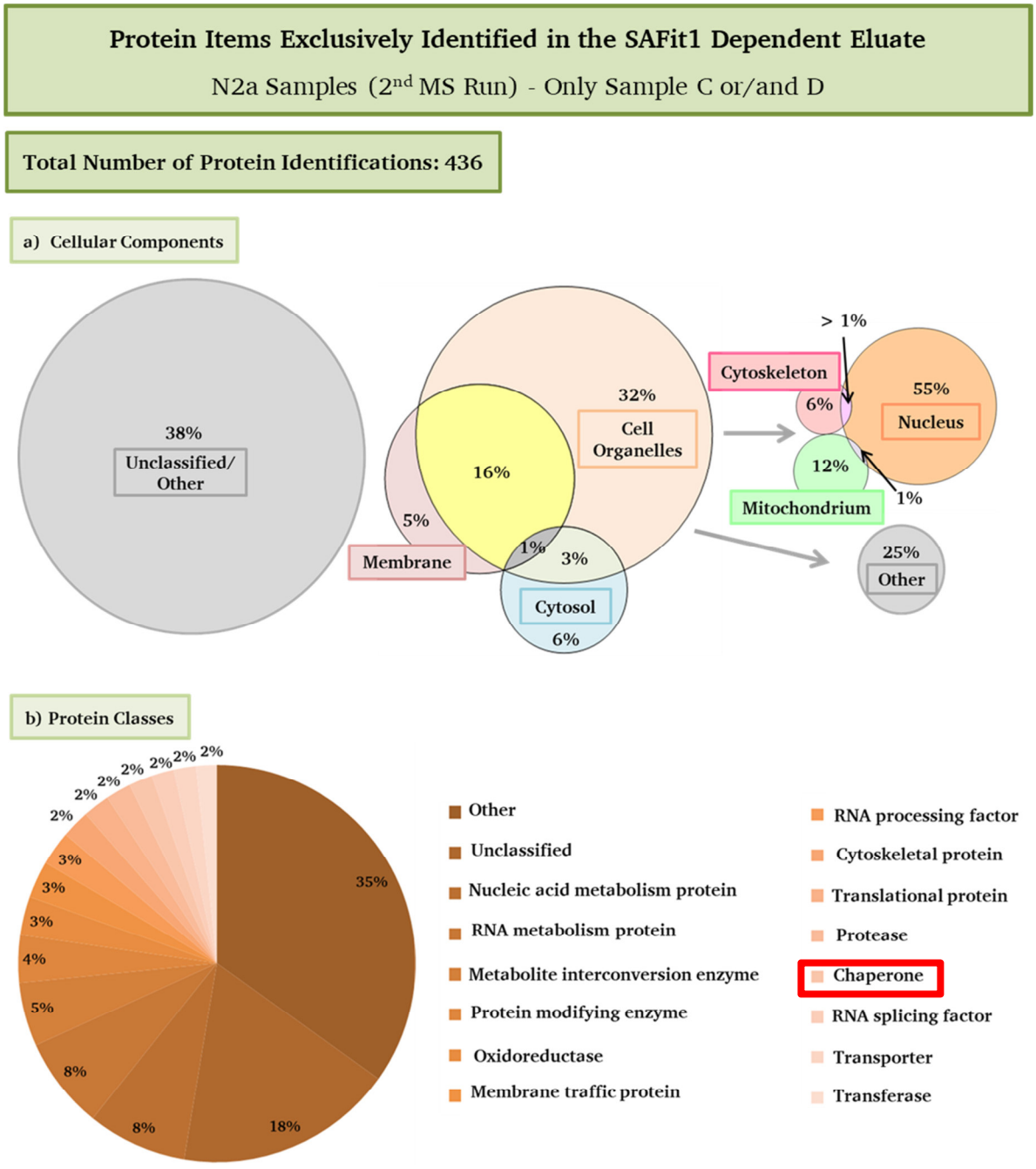

Figure 42: Assigning Cellular Components and Protein Classes to Mouse Protein Items Exclusively Identified in the SAFit1 Dependent Eluate.

Figure 42: Assigning Cellular Components and Protein Classes to Mouse Protein Items Exclusively Identified in the SAFit1 Dependent Eluate.

Mouse protein items exclusively identified in the SAFit1 dependent eluate (sample C or/and D) from a high density FKBP51FK1 affinity column were assigned to cellular components (Figure a) and protein classes (Figure b) by PANTHER [4, 16, 61, 89]. Mouse protein items assigned to at least 4 spectra in at least one of the SAFit1 dependent eluates were selected for the analysis (436 mouse protein items).

Figure a: Venn diagram showing the assignment of cellular components (cell organelles: orange circle, cytosol: blue circle, membrane: red circle). Protein identifications in different cellular components are indicated by overlapping areas. Protein items related to cell organelles were sub-grouped into "nucleus" (dark orange circle), "cytoskeleton" (red circle) and "mitochondrium" (green circle). The protein distribution is given in %.

Figure b: Assigned protein classes. The ratio of the protein classes is given in %. One protein item can be related to different protein classes.

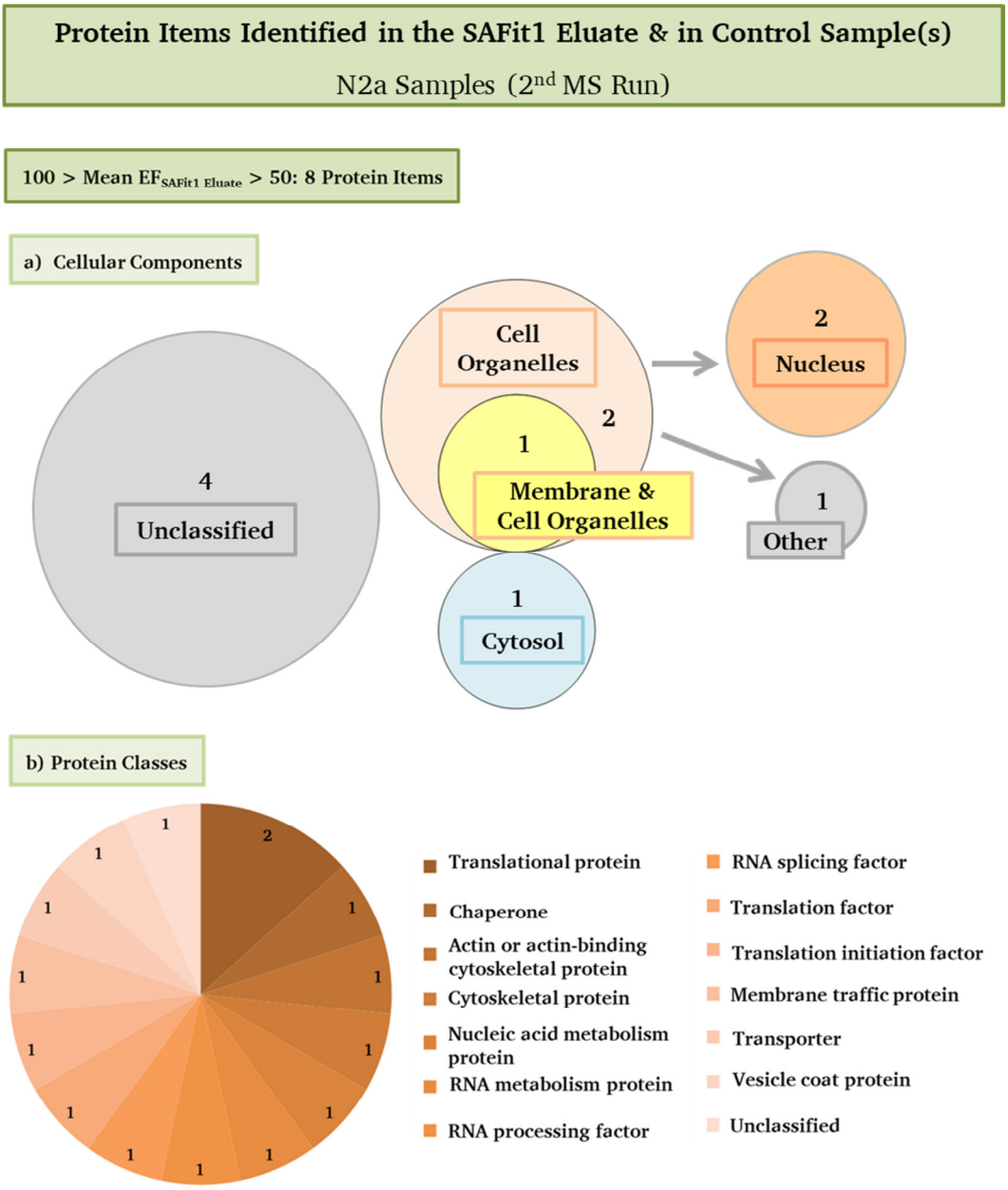

Figure 43: Assigning Mouse Protein Items Identified in the SAFit1 Dependent Eluate to Cellular Components and Protein Classes – "High" Enrichment Factor.

Mouse protein items identified in the SAFit1 dependent eluate (sample C or/and sample D) and at least in one of the control samples showing an enrichment factor (EF) between 50 and 100 were assigned to cellular components (Figure a) and protein classes (Figure b) by PANTHER [4, 16, 61, 89]. 8 protein items were identified in the "high" enrichment factor group.

Figure a: The number of protein items in each group is given. One protein item was assigned to two cellular components ("membrane" and "cell organelles") as indicated by the overlapping area in the Venn diagram (yellow). Two of the protein items assigned to "cell organelles" were related to the subgroup "nucleus" (dark orange).

Figure b: The number of protein items related to each protein class is given. One protein item can be assigned to different protein classes.

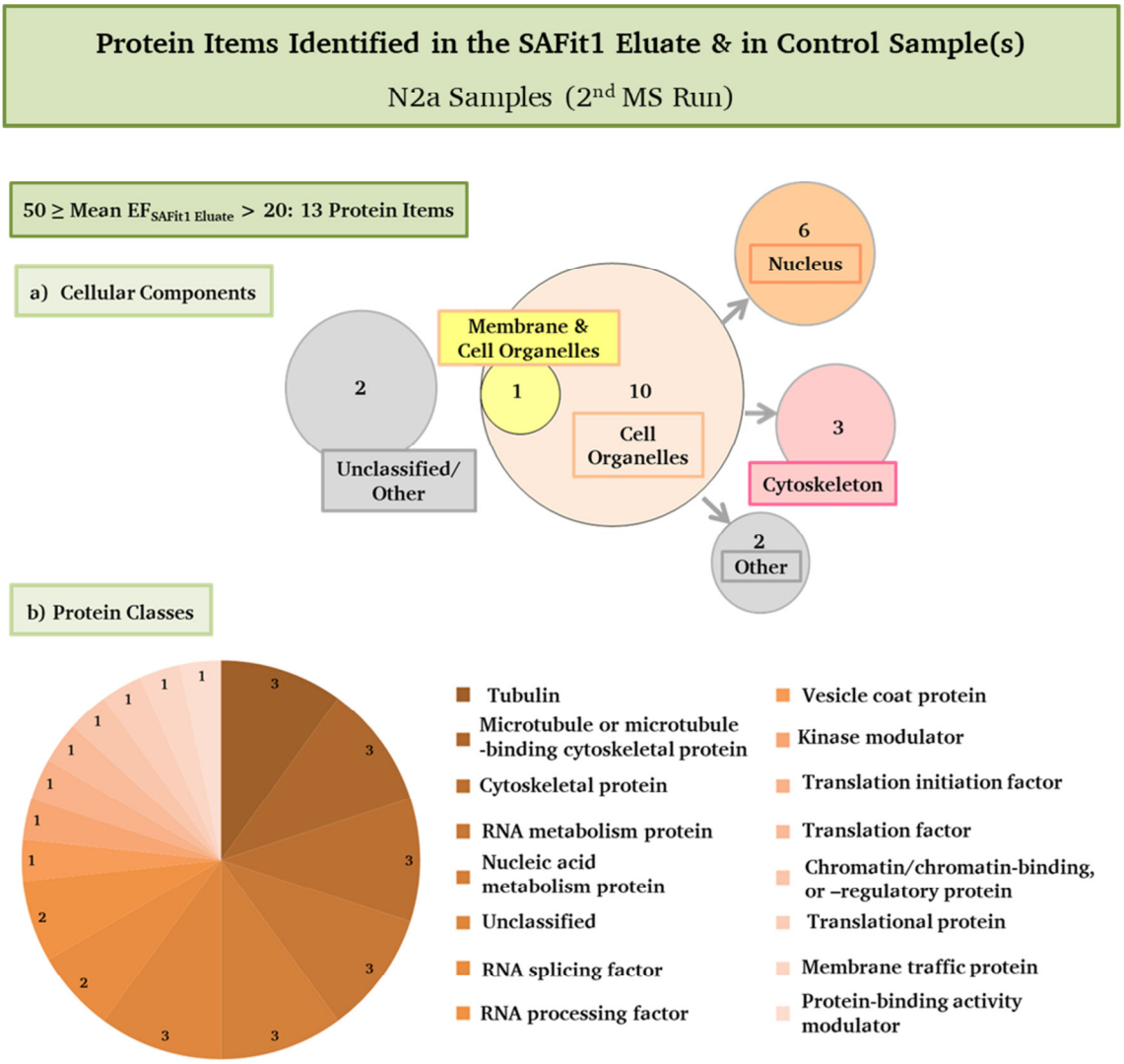

Figure 44: Assigning Mouse Protein Items Identified in the SAFit1 Dependent Eluate to Cellular Components and Protein Classes – Intermediate Enrichment Factor.

13 mouse protein items with an enrichment factor (EF) between 20 and 50 were identified. The protein items were assigned to cellular components and protein classes by PANTHER [4, 16, 61, 89].

Figure a: The total number of mouse protein items related to cell organelles (light orange circle), the nucleus (dark orange circle) and the cytoskeleton (red circle) is given. One protein item was related to "membrane" and "cell organelles". Unclassified protein items and additional protein groups are shown by grey circles.

Figure b: The assigned protein classes are shown. The total number of all protein items related to one protein class is given. One protein item can be assigned to different protein groups.

The majority of the analyzed mouse protein items was either related to "cell organelles" (light orange circle) or related to other groups (not shown, grey circle) or not assigned (grey circle) by PANTHER (Figure 42 a, Figure 43 a, Figure 44 a). More than half of the protein items

assigned to “cell organelles” were found in the nucleus (dark orange circle). Only few protein items were found in the cytosol (10% of the protein items exclusively identified in the SAFit1 dependent eluate, Figure 42 a: lower, blue circle) or related to the “cytoskeleton” (about 2% of all protein items exclusively identified in the SAFit1 dependent eluate and pre-selected, Figure 42 a: red circle) or the “mitochondrium” (about 4% of all mouse protein items identified exclusively in the SAFit1 dependent eluate and pre-selected, Figure 42 a: green circle). A minor part of the analyzed protein items was associated with “cell organelles” and “membrane” (16 % of the protein items exclusively identified in the SAFit1 dependent eluate: Figure 42 a: yellow area). In accordance with the HEK samples “nucleic acid/RNA metabolism proteins” and “cytoskeletal proteins” made a large part of all identified protein classes (Figure 42 b, Figure 43 b, Figure 44 b). In contrast to the HEK samples, few numbers of chaperones (2% of all selected protein items) were identified exclusively in the SAFit1 dependent eluates carrying mouse proteins (Figure 42 b, red box).

4.6.4. Comparing a High Density FKBP51FK1 Affinity Column with a Mock Column

All N2a samples from a pull-down assay using either a high density (sample 3 - 10) or a low density (sample 11 - 22) FKBP51FK1 affinity column and 2 batches of the complete N2a cell lysate (sample 1 & 2) were analyzed in one sample group by MS-based proteomics (Table 17, p. 63). The results of the pull-down assay using a high density FKBP51FK1 affinity column are shown below. The results of the pull-down assay applying a low density FKBP51FK1 affinity column are shown in chapter 4.6.5 (p. 142 ff.).

In contrast to the 1st and 2nd MS run, the SAFit1 dependent protein elution profile from a high density FKBP51FK1 affinity and a mock column (- FKBP51FK1) were compared with each other in the 3rd MS run to differentiate specific eluting proteins from the background. The wash fraction pools from both, a high density FKBP51FK1 affinity and a mock column served as additional controls. The pull-down assay was performed in duplicate. 1259 mouse protein items were identified in all N2a samples from a pull-down assay using a high density FKBP51FK1 affinity column (Figure 45: red box, red circle). Thereof, 270 protein items were identified in the N2a samples but not in the complete N2a cell lysate (Figure 45: light red part of the circle). 1579 mouse protein items were identified in batch 2 and 1919 mouse protein items in batch 3 of the complete N2a cell lysate.

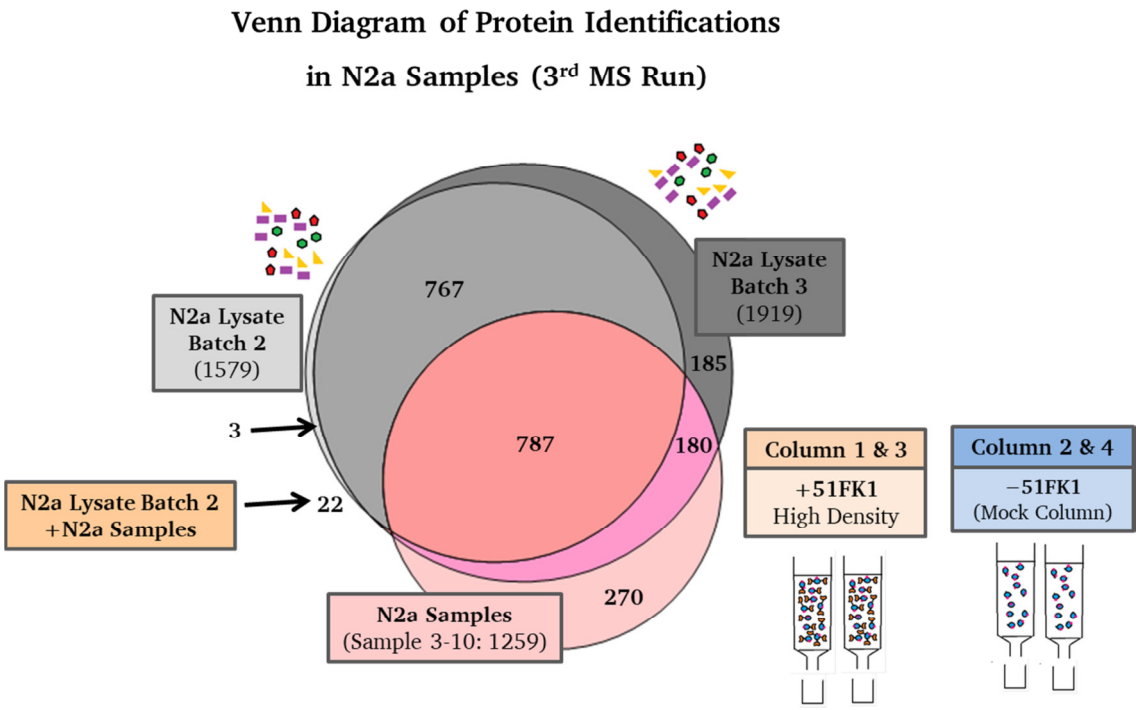

Figure 45: Protein Identifications in N2a Samples (3rd MS Run) – Applying a High Density FKBP51FK1 Affinity Matrix.

The Venn diagram shows the protein identifications in the N2a samples (red circle) from a pull-down assay using a high density FKBP51FK1 affinity column and the complete N2a cell lysate (batch 2: light grey circle, batch 3: dark grey circle). The protein items were identified on the basis of at least two peptides across all samples in the analysis group. Overlapping areas indicate the protein identification in different samples: (i) identification in both N2a cell lysate batches but not in the N2a samples (intermediate grey), (ii) identification in the N2a samples and in the N2a cell lysate (dark red: in both N2a cell lysate batches, pink: only in the 3rd batch, orange box: only in the 2nd batch). Common contaminants were excluded.

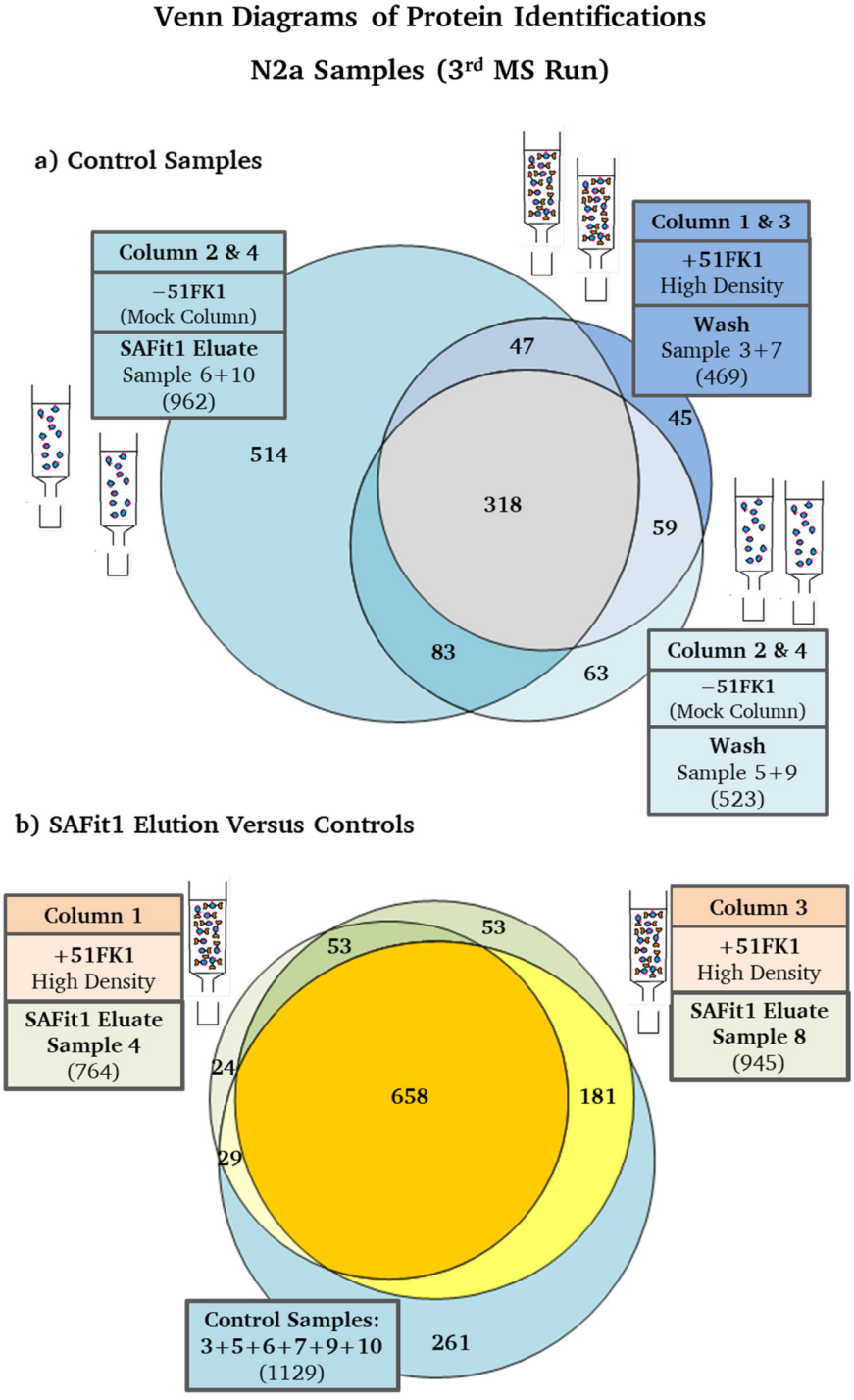

Figure 46: Protein Identifications N2a Samples (3rd MS Run) – Comparing SAFit1 Dependent Elution from a High Density FKBP51FK1 Affinity and a Mock Column.

The protein identifications in the N2a samples from a pull-down assay using a high density FKBP51FK1 affinity column are illustrated by Venn diagrams. Protein identifications in different samples are indicated by overlapping areas. The mouse protein items were identified on the basis of at least two peptides across all samples in the analysis group. The total number of protein identification is given for each group (boxes: number in brackets). Common contaminants were excluded.

Figure 46: Protein Identifications N2a Samples (3rd MS Run) – Comparing SAFit1 Dependent Elution from a High Density FKBP51FK1 Affinity and a Mock Column

Figure a: The protein identifications in the control samples are displayed. Sample 3 + 7: Wash fraction pools from two high density FKBP51FK1 affinity columns (upper circle, intermediate blue). Sample 5 + 9: Wash fraction pools from two mock columns (- FKBP51FK1)(lower circle, light blue). Sample 6 + 10: SAFit1 dependent eluates from two mock columns (- FKBP51FK1) (left circle).

Figure b: The protein identifications in the SAFit1 dependent eluate (light and dark green circle) were compared with the protein identifications in the control samples (blue circle). Protein identifications in different samples are indicated by overlapping areas (green: exclusive identification in both SAFit1 dependent eluates, orange: identification in both SAFit1 dependent eluates and at least in one of the control samples, light and dark yellow: identification in one SAFit1 dependent eluate and at least in one of the control samples).

130 mouse protein items were identified exclusively in the SAFit1 dependent eluates (Figure 46 b: green areas). Thereof, only 53 mouse protein items (Figure 46 b: dark green area) were identified in both SAFit1 dependent eluates. 658 mouse protein items were identified in both SAFit1 dependent eluates and at least in one control sample (Figure 46 b: orange area). 210 mouse protein items were identified in one of the SAFit1 dependent eluates and at least in one control sample (Figure 46 b: light yellow and yellow part of the circle). 1129 mouse protein items were identified across all control samples (Figure 46 a & b). 514 mouse protein items were identified in the SAFit1 dependent eluates from both mock columns (- FKBP51FK1) but neither in the corresponding wash fraction pools nor in the wash fraction pools from both high density FKBP51FK1 affinity columns (Figure 46 a).

To assess the enrichment of protein items identified in the SAFit1 dependent eluates and in the control samples as well, enrichment factors comparing the relative protein abundance in the samples of interest with the relative protein abundance in the samples carrying unspecific eluting proteins were calculated.

Firstly, the SAFit1 dependent eluate from a high density FKBP51FK1 affinity and a mock column were compared with each other (Equation 12).

$$\mathrm{EF}\begin{pmatrix}+\,\mathrm{SAFit1}\\ +\,\mathrm{51FK1}\\ \mathrm{Versus}\\ +\,\mathrm{SAFit1}\\ -\,\mathrm{51FK1}\end{pmatrix}=\frac{(\mathrm{RNS\ Eluate\ I}\,(+\,\mathrm{51FK1}+\mathrm{SAFit1})+\mathrm{RNS\ Eluate\ II}\,(+\,\mathrm{51FK1}+\mathrm{SAFit1}))/2}{((\mathrm{RNS\ Eluate\ III}\,(-\,\mathrm{51FK1}+\mathrm{SAFit1})+\mathrm{RNS\ Eluate\ IV}\,(-\,\mathrm{51FK1}+\mathrm{SAFit1}))/2}$$

Equation 12: Comparing the Relative Protein Abundance in the SAFit1 Dependent Eluate from a High Density FKBP51FK1 Affinity and a Mock Column.

The relative protein abundance in the SAFit1 dependent eluates (eluate I and II) from two high density FKBP51FK1 affinity columns was compared with the relative protein abundance in the SAFit1 dependent eluates from two mock columns (- FKBP51FK1) (eluate III and IV). EF = Enrichment factor. RNS = Relative number of identified spectra.

Secondly, the relative protein abundance in the SAFit1 dependent eluate from a high density FKBP51FK1 affinity column was compared with the relative protein abundance in the wash fraction pools from either a high density FKBP51FK1 affinity column or a mock column (Equation 13).

$$\mathrm{EF}\begin{pmatrix}+\,\mathrm{SAFit1}\\ +\,\mathrm{51FK1}\\ \mathrm{Versus}\\ \mathrm{Wash}\\ \pm\,\mathrm{51FK1}\end{pmatrix}=\frac{(\mathrm{RNS\ Eluate\ I}\,(+\,\mathrm{51FK1}+\mathrm{SAFit1})+\mathrm{RNS\ Eluate\ II}\,(+\,\mathrm{51FK1}+\mathrm{SAFit1}))/2}{(\mathrm{RNS\ Wash\ I}\,(\pm\,\mathrm{51FK1})+\mathrm{RNS\ Wash\ II}(\pm\,\mathrm{51FK1}))/2}$$

Equation 13: Relative Protein Abundance in the SAFit1 Dependent Eluate from a Mock Column in Comparison with the Wash Fraction Pool.

The relative protein abundance in the SAFit1 dependent eluate (I & II) from two high density FKBP51FK1 affinity columns was compared with the protein abundance in either the corresponding wash fraction pools or in the wash fractions pools (I & II) from two mock columns (- FKBP51FK1). The average relative number of identified spectra (RNS) was calculated for each protein item. EF = Enrichment factor.

The relative protein abundance in the SAFit1 dependent eluate from a high density FKBP51FK1 affinity column was also related to the complete N2a cell lysate (Equation 14).

$$EF\begin{pmatrix} +\,SAFit1 \\ +\,51FK1 \\ Versus \\ Lysate \end{pmatrix} = \frac{(RNS\ Eluate\ I\ (+\,51FK1 + SAFit1) + RNS\ Eluate\ II\ (+\,51FK1 + SAFit1))/2}{(RNS\ (Cell\ Lysate\ Sample\ I) + RNS\ (Cell\ Lysate\ Sample\ II))/2}$$

Equation 14: Comparing the Relative Protein Abundance in the SAFit1 Dependent Eluate from a High Density FKBP51FK1 Affinity Column with the Relative Protein Abundance in the Complete Cell Lysate.

The relative protein abundance in the SAFit1 dependent eluate from a high density FKBP51FK1 affinity column (mean of an assay replicate) was compared with the relative abundance in the complete N2a cell lysate (mean of two different batches). EF = Enrichment factor. RNS = Relative number of spectra.

The identified mouse protein items (Figure 45, Figure 46) were selected and ranked regarding the criteria described in chapter 3.2.19 (p. 67 ff.). The identified protein groups are shown below (Figure 47). Unspecific eluting proteins made 51% (blue part of the circle), ribosomal proteins 6% (light grey part of the circle) and common sample contaminants (red part of the circle) 1% of all protein identifications. 36% of all identified protein items were only identified in the complete N2a cell lysate but not in the pull-down assay samples (dark grey part of the circle). 110 mouse protein items eluted from a high density FKBP51FK1 affinity column had an enrichment factor (EF) between 2 and 30 and were in accordance with the selection criteria (Suppl. Table 34, p. 209 ff.: list including all identified mouse protein items with an EF between 2 and 30). Only 22 of the mouse protein items identified exclusively in the SAFit1 dependent eluate from a high density FKBP51FK1 affinity column fulfilled the selection criteria (dark green part of the circle). These protein items were assigned to cell organelles and protein classes by PANTHER [4, 16, 61, 89] (Figure 48). Only 13 of these mouse protein items were related to 4 or more spectra on average (mean of a technical duplicate, cp. Suppl. Table 33, p. 207 f.).

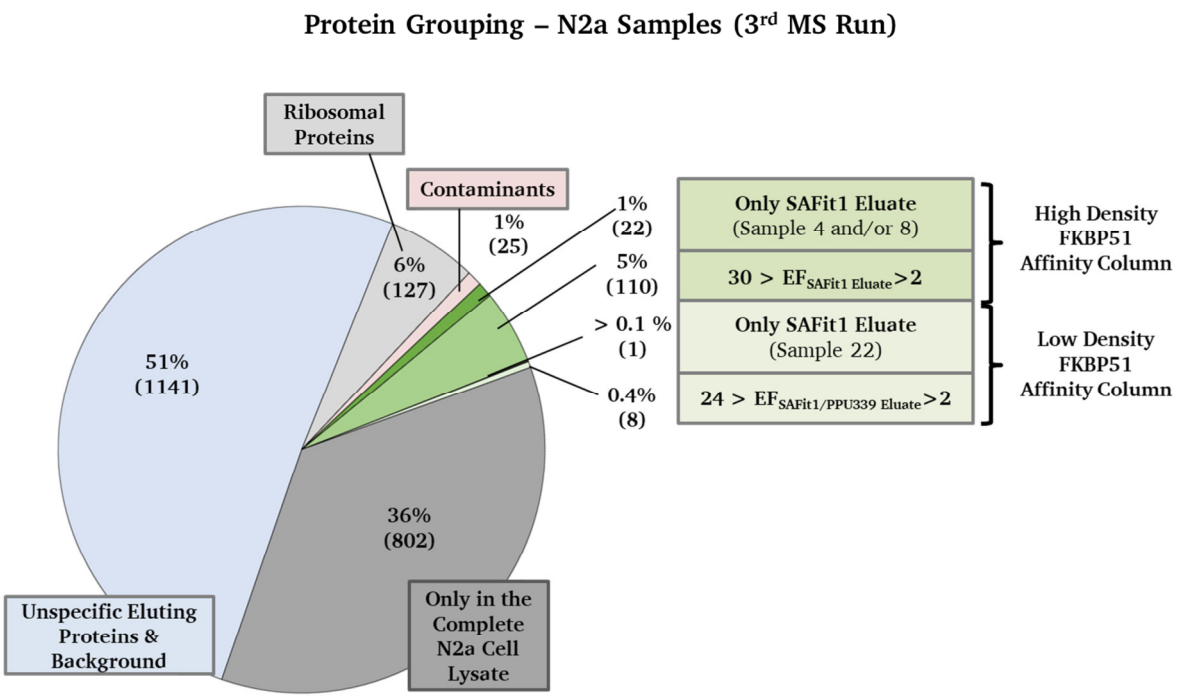

Figure 47: Protein Enrichment Analysis – N2a Samples (3rd MS Run).

The protein items identified on the basis of at least two peptides across all samples in the analysis group (sample 1 - 22) were further sub-grouped. The analysis group included two batches of the complete N2a cell lysate and N2a samples from pull-down assays using either a low or a high density FKBP51FK1 affinity matrix. The following criteria were applied: (i) exclusion of contaminants from other species and mouse keratins (red box), (ii) exclusion of ribosomal proteins (light grey box), (iii) selection of protein items identified in the N2a cell lysate but not in the N2a pull-down assay samples (dark grey box), (iv) selection of mouse protein items exclusively identified in the SAFit1 dependent eluate from a FKBP51FK1 affinity column (high density FKBP51FK1 affinity column: sample 4 & 8, dark green; low density FKBP51FK1 affinity column: sample 22, light green), (v) selection of mouse protein items identified in the FKBP ligand dependent eluate (SAFit1 or PPU339) from a FKBP51FK1 affinity column and in at least one control sample having an enrichment factor (EF) higher than 2 (intermediate and light green). The protein group ratio was related to the absolute protein count in each group and is given in %. The total number of protein identifications in each group is also given (number in brackets).

Most of the protein items exclusively identified in the SAFit1 dependent eluate from a high density FKBP51FK1 affinity column and assigned to at least 4 spectra in at least one of the SAFit1 dependent eluates were either related to “cell organelles” (Figure 48 a: light orange circle), other cell components or not classified by PANTHER (grey circle). In accordance with the previous findings some of the identified protein items belonged to “nucleid acid/RNA metabolism proteins” (Figure 48 b).

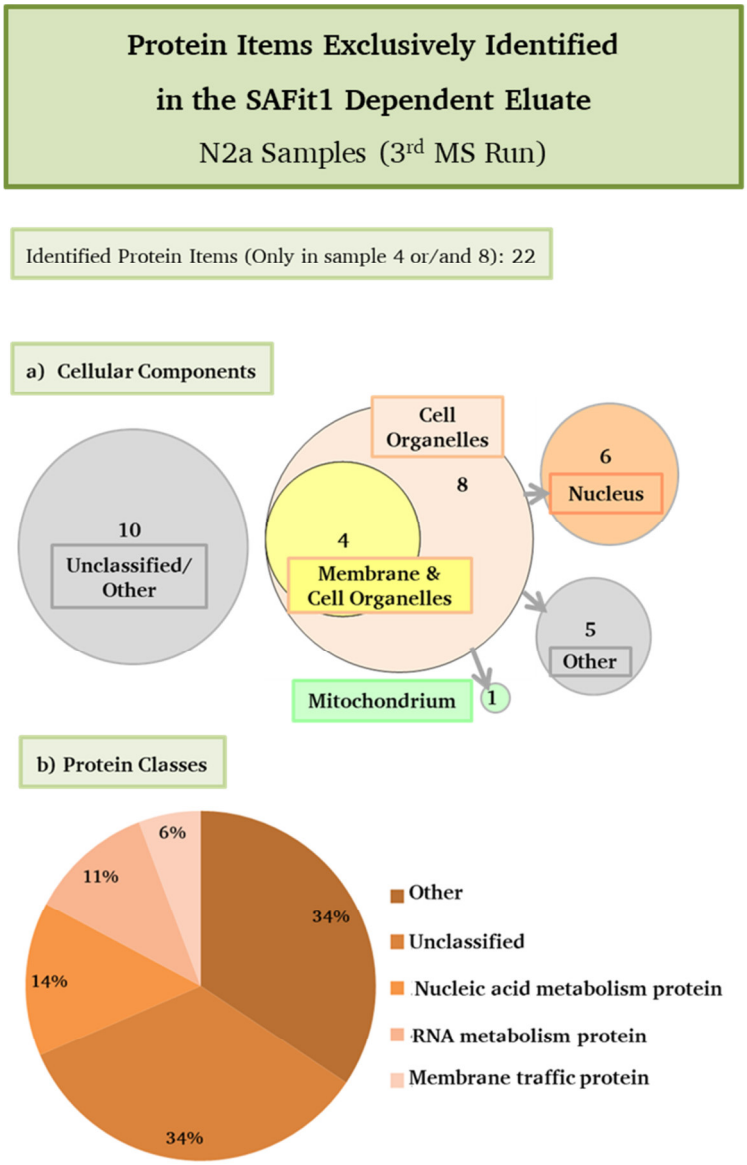

Figure 48: Assigning Mouse Protein Items Exclusively Identified in the SAFit1 Dependent Eluate to Cellular Components and Protein Classes.

22 mouse protein items were exclusively identified in the SAFit1 dependent eluate from a high density FKBP51FK1 affinity column on the basis of at least 4 assigned spectra. The mouse protein items were related to cellular components (Figure a) and protein classes (Figure b) by PANTHER [4, 16, 61, 89].

Figure a: The number of mouse protein items assigned to different cellular components is given (light orange: "cell organelles", yellow: "membrane and cell organelles"). 6 protein items were assigned to the subgroup "nucleus" and 1 protein item was assigned to the "mitochondrium".

Figure b: The relative ratio of the assigned protein classes is given in %. One protein item can be assigned to various protein classes.

4.6.5. Elution from a Low Density FKBP51FK1 Affinity Column

The FKBP ligand (SAFit1, PPU339) dependent protein elution profile from a low density FKBP51FK1 affinity matrix was compared with the proteins identified in samples carrying unspecific eluting proteins. A non-binding SAFit1-analogue, THE212P, was applied as a control to distinguish SAFit1 specific from unspecific eluting proteins. In addition to that, the samples of interest were compared with the compound dependent eluates (SAFit1, THE212P, PPU339) from a mock column (- FKBP51FK1) as well as with the wash fraction pools from three low density FKBP51FK1 affinity and three mock (- FKBP51FK1) columns.

493 mouse protein items originating from N2a cell lysate were identified in the pull-down assay samples (Figure 49: red circle) on the basis of at least two identified peptides across all analyzed samples (sample 1 - 22, sample overview is given in chapter 3.2.18, Table 17, p. 63 f.). Thereof, 22 protein items were not identified in the complete cell lysate (neither in batch 2 nor in batch 3, light red part of the lower circle). 471 protein items were also identified in the complete N2a cell lysate (cell lysate batch 2 + 3: 451, only cell lysate batch 3: 19, only cell lysate batch 2: 1).

15 mouse protein items were exclusively identified in the SAFit1 dependent eluate (Figure 50 b: olive green area) and two mouse protein items in the PPU339 dependent eluate (dark green area). However, 14 of the protein items identified in the SAFit1 dependent eluate and both protein items in the PPU339 dependent eluate did not fulfill the following selection criteria: (i) no ribosomal protein, (ii) protein identification on the basis of more than 4 spectra in the sample of interest, (iii) enrichment factor higher than 2 (Figure 47, p. 140). Only one of the protein items exclusively identified in the SAFit1 dependent eluate fulfilled the selection criteria, namely tubulin alpha-chain (P05214 or P68369). 80 mouse protein items were identified in the SAFit1 and the PPU339 dependent eluate and at least in one of the control samples as well (orange area). 46 mouse protein items were identified in the SAFit1 dependent eluate and in at least one of the control samples (light yellow area). 59 mouse protein items were identified in the PPU339 dependent eluate and in the control samples (yellow area).

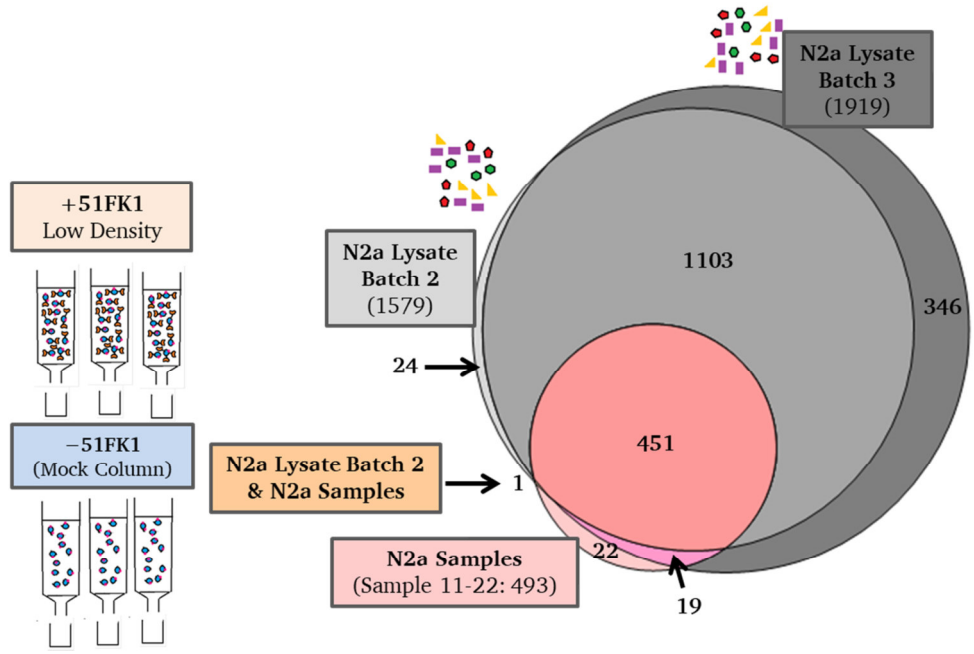

Figure 49: Protein Identifications in the Complete N2a Cell Lysate and in the N2a Samples (3rd MS Run) – Applying a Low Density FKBP51FK1 Affinity Matrix.

The Venn diagram shows the mouse protein identifications in the N2a samples from a pull-down assay using a low density FKBP51FK1 affinity matrix and in the complete N2a cell lysate (light grey: batch 2, dark grey: batch 3). Overlapping areas indicate the protein identification in several samples (red: N2a samples + N2a cell lysate batch 2 + N2a cell lysate batch 3, pink: N2a samples + N2a cell lysate batch 3, orange box: N2a samples + N2a cell lysate batch 2). The number of all identified mouse protein items on the basis of at least two identified peptides across all samples in the analysis group (both N2a cell lysate batches, N2a samples from pull-down assays using a low and a high density FKBP51FK1 affinity matrix: sample 3 - 22) is given. Common contaminants were excluded.

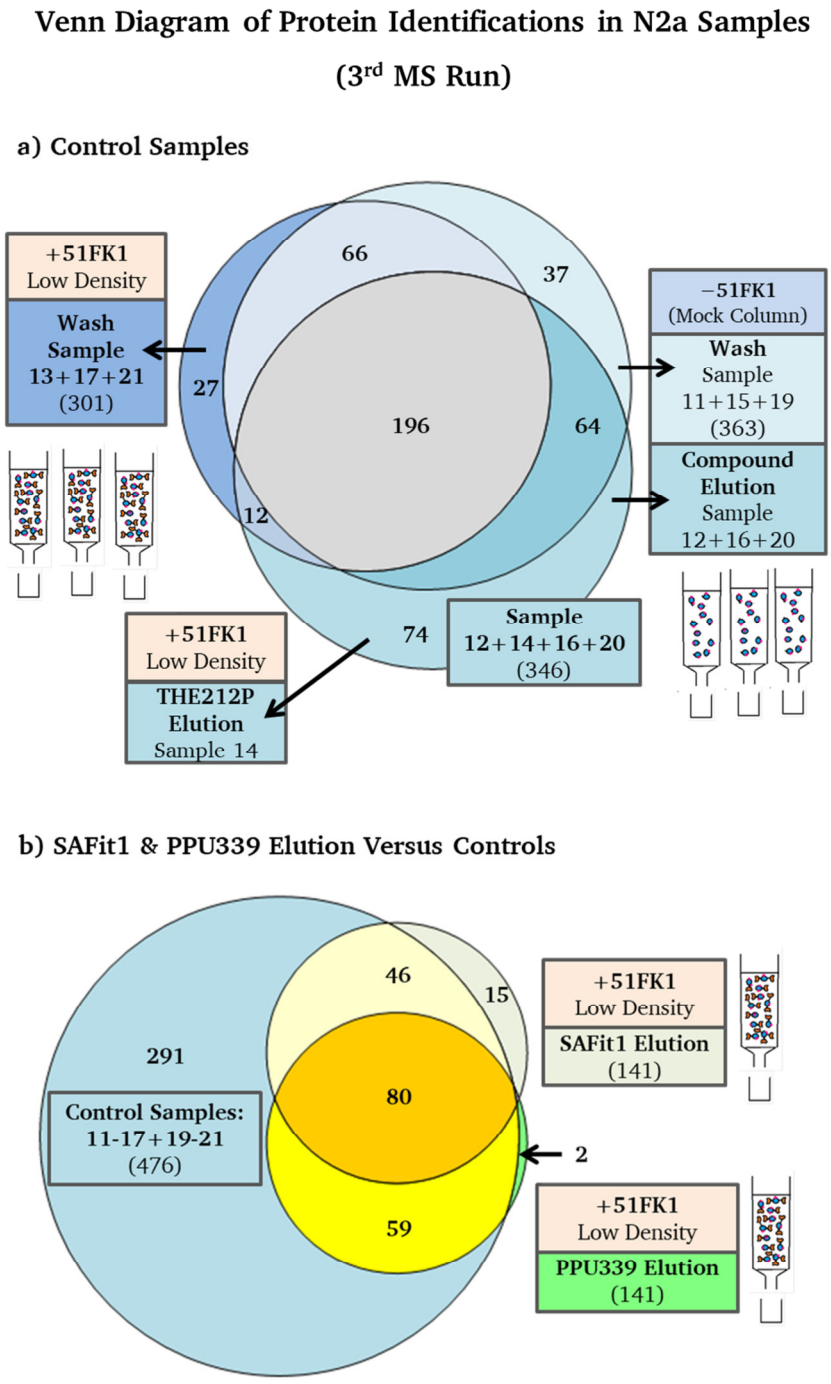

Figure 50: Protein Identifications in N2a Samples (3rd MS Run) – Applying a Low Density FKBP51FK1 Affinity Matrix.

The protein identifications in N2a samples from a pull-down assay using a low density FKBP51FK1 affinity matrix are displayed. The mouse protein items were identified on the basis of at least two peptides in the analysis group (sample 1 - 22). Common contaminants were excluded. Overlapping areas indicate protein identifications in several samples.

Figure 50: Protein Identifications in N2a Samples (3rd MS Run) – Applying a Low Density FKBP51FK1 Affinity Matrix.

Figure a: The protein identifications in the control samples (left circle: wash fraction pool from three low density FKBP51FK1 affinity columns, right circle: wash fraction pools from three mock columns (- FKBP51FK1), lower circle: SAFit1/PPU339/THE212P dependent eluates from three mock columns + THE212P dependent eluate from a low density FKBP51FK1 affinity column) are given.

Figure b: The protein identifications in the SAFit1 (light olive green circle) and the PPU339 (light green circle) dependent eluate were compared with the protein identifications in the control samples (blue circle). Protein items identified in at least one FKBP ligand dependent eluate and at least in one of the control samples as well are indicated by overlapping areas (yellow and orange).

The relative protein abundance in the SAFit1 and PPU339 dependent eluates from a low density FKBP51FK1 affinity column was also compared with the relative protein abundance in the corresponding eluates from a mock column carrying naked, blocked beads (- FKBP51FK1) (Equation 15).

$$\mathrm{EF}\left(\begin{array}{c}+\ \mathrm{FKBP\ Ligand}\\ +\ 51\mathrm{FK1}\\ \mathrm{Versus}\\ +\ \mathrm{FKBP\ Ligand}\\ -\ 51\mathrm{FK1}\end{array}\right)=\frac{\mathrm{RNS\ Eluate}\ (+\ 51\mathrm{FK1}+\mathrm{FKBP\ Ligand})}{\mathrm{RNS\ Eluate}\ (-\ 51\mathrm{FK1}+\mathrm{FKBP\ Ligand})}$$

Equation 15: Comparing the Relative Protein Abundance in the FKBP Ligand Dependent Eluate from a Low Density FKBP51FK1 Affinity and a Mock column.

The relative number of spectra related to a distinct protein item in the FKBP ligand (SAFit1 or PPU339) dependent eluate from a low density FKBP51FK1 affinity column was divided by the relative number of spectra identified in the FKBP ligand dependent eluate from a mock column (- FKBP51FK1) to calculate an enrichment factor (EF).

In addition to that, the protein elution profile of SAFit1 was compared with the elution profile of the non-binding SAFit1 analogue, THE212P (Equation 16).

$$EF\begin{pmatrix} +\,SAFit1 \\ +\,51FK1 \\ Versus \\ +\,THE212P \\ +\,51FK1 \end{pmatrix} = \frac{RNS\ Eluate\ (+\,51FK1 + SAFit1)}{RNS\ Eluate\ (+\,51FK1 + THE212P)}$$

Equation 16: Relative Protein Abundance in the SAFit1 Dependent Eluate in Comparison with the THE212P Dependent Eluate.

The relative number of identified spectra (RNS) in the SAFit1 dependent eluate from a low density FKBP51FK1 affinity column was divided by the relative number of identified spectra in the THE212P (non-binding SAFit1 analogue) dependent eluate from a low density FKBP51FK1 affinity column to calculate the enrichment factor (EF).

The relative protein abundance in the SAFit1 or PPU339 dependent eluate from a low density FKBP51FK1 affinity column was also compared with the relative abundance in the wash fraction pools from three low density FKBP51FK1 affinity and three mock columns (Equation 17).

$$EF\begin{pmatrix} +\,FKBP\ Ligand \\ +\,51FK1 \\ Versus \\ -\,FKBP\ Ligand \\ \pm\,51FK1 \end{pmatrix} = \frac{RNS\ Eluate\ (+\,51FK1 + FKBP\ Ligand)}{(RNS\ WashI + RNS\ WashII + RNS\ WashIII)/3}$$

Equation 17: Relative Protein Abundance in the SAFit1 and PPU339 Dependent Eluate in Relation to the Wash Step.

The relative number of spectra (RNS) related to a distinct protein item in the SAFit1 and PPU339 dependent eluate from a low density FKBP51FK1 affinity column was related to the wash fraction pools from three low density FKBP51FK1 affinity and three mock (- FKBP51FK1) columns. EF = Enrichment factor. FKBP ligand: SAFit1, PPU339.

Only 8 mouse protein items showed an enrichment factor higher than 2 at a very low level comparing the SAFit1 and PPU339 dependent eluate with samples carrying unspecific eluting proteins (Figure 47, p. 140, Suppl. Table 36, p. 216).

5. Discussion

5.1. Development of a FKBP51FK1 Affinity Matrix

HsFKBP51FK1MonoCys was successfully purified and immobilized on SulfoLink® coupling resin (Thermo Scientific). Affinity matrices exhibiting a protein density of 20 μM up to 950 μM were prepared. The concentration of free HsFKBP51FK1MonoCys in the reaction mix was used as an indicator for the progress of the coupling reaction (Figure 19, p. 76 ff.; Table 21 b, p. 82). The concentration of unbound HsFKBP51FK1MonoCys was analyzed by SDS-PAGE and Coomassie staining (Figure 19). This approach does not distinguish between covalently coupled and unspecific bound HsFKBP51FK1MonoCys.

The highest coupling efficiency was reached by applying an equimolar amount of HsFKBP51FK1MonoCys and the reducing agent TCEP (Figure 19, Table 21 b). The immobilization of HsFKBP51FK1 seemed to be completed after 1 h by applying a coupling buffer supplemented with an equimolar amount of TCEP (Figure 19, Table 21 b). The extension of the incubation time up to 15 h 40 min did not improve the coupling efficiency (Figure 19 c: compare lane 7 with lane 9 & 10). A small amount of residual HsFKBP51FK1MonoCys was detected after extending the incubation time although a twentyfold excess of iodoacteyl groups was applied (Figure 19 c: lane 9 & 10). This fact indicates the partial oxidation of the mono cysteine residue that was not prevented by adding an equimolar amount of the reducing agent TCEP. The limited stability of TCEP in water based buffers might have also played a role. An incubation time less than 1 h might be sufficient but was not tested under optimized conditions.

The use of a coupling buffer (50 mM Tris, 5 mM EDTA, pH 8) not supplemented with TCEP lowered the coupling efficiency (Figure 19, Table 21 b). This fact can be explained by the oxidation of the mono cysteine residue and the reduced availability of thiol groups for the coupling reaction. The coupling reaction was inhibited by using a buffer supplemented with 10 mM TCEP (Figure 20, p. 79 f.).

Equal volumes of settled, swollen beads and HsFKBP51FK1MonoCys up to the double protein volume were applied. The effect of the volume ratio on the coupling progress was hardly investigated (Table 21 b). The deceleration of the coupling reaction by doubling the protein volume underlined the relevance of the reaction volume.

5.2. Fluorescence-Based FKBP51FK1 Affinity Matrix Binding Assay

A fluorescence based binding test was developed and applied to analyze the integrity of the FKBP51FK1 affinity matrix binding pocket (chapter 3.2.17, p. 47 ff.). Affinity matrices with an estimated FKBP51FK1 density of 20 μM and 950 μM were analyzed.

An excess of the fluorescent tracer CK182 (Figure 5, p. 23: chemical structure) was added to the FKBP51FK1 affinity matrix to saturate all binding sites (Figure 10, p. 49; Figure 21, p. 84). The fluorescence intensity (FI) sum of the fractions from the FKBP51FK1 affinity column carrying unbound or unspecific bound CK182 (= flow-through and wash fractions) was between 50% and 80% of the initial tracer FI indicating the binding of CK182 (Figure 22, p. 85). In contrast, the normalized FI sum of the flow-through and the wash fractions from the control column (- FKBP51FK1) was as high as the initial tracer FI in principle.

To distinguish between an unspecific wash effect and an interaction of the tracer with the FK1 binding pocket the wash step was only stopped after reaching a low FI level or the background level (Figure 21). The tracer was eluted from the FKBP51FK1 affinity column by adding the ligands – Rapamycin (Figure 22 a), SAFit1 (Figure 21, Figure 22 b, d, e) and JK095 (Figure 22 c) as indicated by detecting fluorescence in the eluates. Whereas, no tracer or (Figure 22 a - d) only a few amount of CK182 (Figure 21, Figure 22 e) was detected in the eluates collected from the control column (- FKBP51FK1). These results suggest the competitive elution of CK182 from the FKBP51FK1 affinity column.

In contrast to the expectations, the normalized FI of the flow-through and the wash fractions from the FKBP51FK1 affinity column was higher than 50% of the initial FI after adding a twofold amount of CK182 and higher than 33% of the initial FI after adding one and a half time amount of the tracer. This issue might be explained by the following reasons. The assay buffer, especially the supplement of DMSO (c_{final} = 0.55% up to 2% (v/v)) might have disturbed the interaction of the tracer with the FKBP51FK1 binding pocket. Another reason could be the partial degradation of the immobilized protein. The structure of the SulfoLink® coupling beads and the distribution as well as the orientation of immobilized FKBP51FK1 on the beads is unknown. It should be noted that the availability of the binding pocket could have been limited.

The fluorescence based measurement itself and the assay protocol are error-prone. Samples with a high tracer concentration were diluted to exploit the proportional relation between the FI and the tracer concentration. A large buffer volume was required for the wash step to reach the baseline (Figure 21). This fact can be explained by the unspecific binding of the tracer to the agarose based beads and by the unspecific interaction of the fluorophore fluorescein with immobilized FKBP51FK1.

The application of the tracer MTQ238 (= FTSP11, Figure 5, p. 23: chemical structure) was tested (data not shown). The tracer was not suitable due to the limited solubility in water based buffers and the unspecific binding of the fluorophore 5-TAMRA to the agarose based beads and to plastic surfaces.

Taken together, the tracer CK182 bound to the FKBP51FK1 affinity column was competitively eluted by adding the FKBP ligands SAFit1, JK095 and Rapamycin. The integrity of the FKBP51FK1 binding pocket seemed to be maintained by the protein immobilization.

The efforts required for the tracer synthesis and the long duration of the wash as well as of the elution step are disadvantages of the assay. A mass spectrometric based assay could offer another possibility to characterize FKBP affinity matrices. An excess of a (commercially available) FKBP ligand could be added to the FKBP affinity matrix. The average density of immobilized FK506 binding proteins on the beads exhibiting an intact binding pocket could be calculated by analyzing the ligand amount in the flow-through. The ligand concentration could be determined by HPLC and/or mass spectrometry.

5.3. Development of a FKBP51FK1 Pull-Down Assay

The identification of a protein-interaction network provides a technical challenge. The FKBP51FK1 pull-down assay was developed to identify FKBP51 binding proteins interacting exclusively with the binding pocket of the FK1 domain. The mapping of potential binding proteins should be a starting point to gain insights into the signal transduction and cellular functions of FKBP51. Especially, the cellular functions and signaling points affected by the binding of the FKBP ligand SAFit1 should be addressed. Another objective was to develop an assay for protein binding-partner enrichment showing a low background in comparison with co-immunoprecipitation assays.

The FKBP51FK1 pull-down assay as *in vitro* model has some drawbacks. Technical issues such as the properties of the applied beads, cell lysing methods, the assay buffer and the solubility of the chemical FKBP ligands are discussed below. The compatibility of detergents with a downstream mass spectrometric based analysis is also discussed.

Evaluation of the FKBP51FK1 Pull-Down Assay by SDS-PAGE and Silver Staining

The preliminary sample analysis by SDS-PAGE and silver staining indicated a very high sample complexity. No single unique protein bands with high intensities were detected in the samples of interest. For that reason, the complete samples instead of single protein bands were analyzed by MS. These findings are in line with the MS results discussed below.

5.4. MS-Based Proteomic Pull-Down Assay Analysis

5.4.1. Evaluation of the Proteomic Results

The aim of the MS-based proteomic analysis was to identify potential FKBP51FK1 interacting proteins enriched by the FKBP51FK1 affinity matrix. For that purpose, the proteins and protein subunits identified in the samples of interest and the control samples were relatively quantified by spectral counting. In the best case, FKBP51 interacting proteins would have been only present and exclusively identified in the FKBP ligand (SAFit1, PPU339) dependent eluate from a FKBP51FK1 affinity column but not in the samples carrying unspecific eluting proteins.

5.4.2. Spectral Counting

Spectral counting is a fast, cost-efficient label-free method that enabled the relative quantitation of more than 1,900 proteins across all samples (Figure 31, p. 113; Figure 39, p. 126; Figure 45, p. 135; Figure 49, p. 143). The spectral counting strategy assumes that high abundant proteins are accompanied with an increased peptide count and thus a high spectral count [23, 24]. The fact that unique peptides can appear several times and lead to an increased number of spectra is considered by this approach. However, spectral counting is an idealized concept that does not meet the high sample complexity of all analyzed samples as indicated by SDS-PAGE and silver staining (Figure 23 - Figure 26). Peptides co-eluting from the LC column might cause MS signal overlap, reduction or depletion. Therefore, the relative protein abundance in very complex samples might be underestimated and dependent on the

sample composition. Nevertheless, spectral counting is a less elaborating approach suitable for assay establishment.

Spectra Validation

The total number of all validated spectra for each sample fluctuated across the analyzed sample groups (Figure 29 p. 108, Figure 30, p. 110) impeding the relative protein quantitation. For that reason, the number of identified spectra assigned to a distinct protein (subunit) in the sample was normalized to the total number of validated spectra in the sample. As expected the highest number of validated spectra was identified in the complete HEK293 and N2a cell lysates. However, samples with similar peptide yields (Table 22 - Table 24, p. 104 ff.) led to different numbers of validated spectra. This issue might be explained by the high sample complexity or the less robust sample preparation protocol comprising several steps and requiring extensive sample handling. The protein concentration step prior digestion was extended in the 3rd MS run resulting in an overall higher peptide yield (5 up to 10-fold). Nevertheless, higher numbers of validated spectra in the SAFit1 dependent eluates from a high density FKBP51FK1 affinity column were not reached (Figure 29, p. 108: compare samples 4 and 8 of the N2a samples in the 3rd MS run with sample C of the HEK293 samples and sample C of the N2a samples in the 2nd MS run).

The overall spectral count was reduced in the N2a samples from a pull-down assay applying a low density FKBP51FK1 affinity column and a “high” salt buffer (supplemented with 200 mM NaCl instead of 100 mM NaCl) (Figure 30, p. 110). This finding is in accordance with the preliminary sample analysis by SDS-PAGE and silver staining indicating a lowered protein amount (Figure 26, p. 98) but in contrast to the determined peptide yield (Table 24, p. 106).

Samples that should be similar in theory such as N2a sample A & E and N2a sample B & F (2nd MS run) as well as N2a sample 4 & 8, N2a sample 3 & 7, N2a sample 5 & 9 and N2a sample 6 & 10 (3rd MS run) showed differences in the number of validated spectra (Figure 29, p. 108). These sample pairs were received from different FKBP51FK1 affinity or control columns but prepared in the same pull-down assay and analyzed in the same MS run.

Sample Contamination

The number of validated spectra related to common contaminants such as keratin or keratin associated proteins, trypsin and albumin varied between 85 and 421 validated spectra per sample. In most of the samples, the contamination ratio was between 2% up to 13% at an

acceptable level. More than 20% up to 35% of the validated spectra were related to contaminants in samples with a low spectral count (2nd MS run: sample F & G, 3rd MS run: sample 12, 14, 16, 18 and 22). The higher sample contamination ratio might have caused signal suppression. Unfortunately, human and mouse keratins belong to the proteome of HEK293 and N2a cells. The sample contamination might be reduced by restricting the sample handling to a clean bench or by optimizing the sample preparation protocol requiring less extensive sample handling but the selected methods are dependent on the cost-benefit ratio and the access to required instruments.

5.4.3. **Protein Identifications**

Firstly, the protein identifications in the FKBP ligand dependent eluates from a FKBP51FK1 affinity column were compared with the protein identifications in the control samples (Figure 32 p. 115, Figure 40 p. 127, Figure 46 p. 136, Figure 50 p. 144). The protein identifications are related to UniProtKB accession numbers. This means that each protein subunit was counted as one item. Therefore, proteins consisting of different subunits such as protein-phosphatase 6 [62] might lead to a higher number of protein identifications. The following sample groups were illustrated by Venn diagrams: (i) protein items exclusively identified in the sample(s) of interest, (ii) proteins identified in the sample(s) of interest and in the control samples, (iii) protein items only identified in the control samples. All protein items identified on the basis of at least two unique assigned peptides across all samples in the analysis group were counted. There is a common agreement in the community to exclude proteins identified by one peptide to decrease the number of false positive results [24].

Comparing the results from all four pull-down assays the number of protein identifications varied. This might be in accordance with the different assay setups. In HEK293 samples, the majority of the identified human protein items (537) were found in the samples of interest and in the control samples as well. Only 6 protein items were exclusively identified in the early and 167 protein items in the late SAFit1 dependent eluate. 33 protein items were identified in both samples of the SAFit1 dependent eluate (Figure 32 b, p. 115). Whereas 819 mouse protein items were exclusively identified in the N2a samples of interest in the 2nd MS run. Here, 428 mouse protein items were identified in the samples of interest and the control samples (Figure 40 b, p. 127). This might be explained by extending the elution step (elution with 20 CV instead of 10 CV 5 mM SAFit1) in the pull-down assay analyzed in the 2nd MS run. The comparability between HEK293 and N2a samples is limited since the peptide and protein identifications are dependent on the peptide and protein references included in the applied

databases differing for mouse and human proteins. In the 3rd MS run, only 130 mouse protein items were exclusively identified in the SAFit1 dependent eluate from a high density FKBP51FK1 affinity column but not in the control samples (Figure 46 b, p. 136). In contrast to the 1st and 2nd MS run, a mock column carrying blocked naked beads was included as a control to assess unspecific protein interactions with the agarose-based beads resulting in a higher number of protein items identified in both, the samples of interest and the control samples (868 protein identifications in total). The N2a samples from the pull-down assay using a low density FKBP51FK1 affinity column and a "high" salt assay buffer showed the lowest number of protein identifications (493) across all N2a samples (Figure 49, p. 143). In comparison, 880 human protein items were identified across all HEK293 samples (Figure 31, p. 113), 1298 mouse protein items across all N2a sample in the 2nd MS run (Figure 39, p. 126) and 1259 mouse protein items across all N2a samples from a pull-down assay applying a high density FKBP51FK1 affinity column in the 3rd MS run (Figure 45, p. 135).

5.4.4. Protein Subgrouping

Ribosomal proteins were excluded from further analysis due to lacking biological interest. Ribosomal proteins made about 6% up to 10% of all human and mouse protein identifications contributing to the background (Figure 33 p. 118, Figure 41 p. 129, Figure 47, p. 140). To increase the confidence in the proteomic results only protein items related to at least four validated spectra in the sample(s) of interest were selected for further analysis. This approach takes the possibility of false negative results into account.

Only a part of the proteins and protein subunits identified in the samples of interest on the basis of at least two unique peptides across all samples in the analysis group was related to at least four spectra in the sample(s) of interest. Applying this selection criterion only one human protein was exclusively found in the early SAFit1 dependent eluate from a high density FKBP51FK1 affinity column. 8% (70) of all human protein identifications were related exclusively to the late SAFit1 dependent eluate and 1% (9) to both, the early and the late SAFit1 dependent eluate (Figure 33). In contrast to that, 436 (34%) of the mouse protein items exclusively identified in the SAFit1 dependent eluate from a high density FKBP51FK1 affinity column were assigned to at least four spectra (Figure 41, p. 129). Applying a mock column (- FKBP51FK1) as a control lowered the number of mouse protein items exclusively identified in the SAFit1 dependent eluate from a high density FKBP51FK1 affinity column in the N2a samples (3rd MS run). 22 (1%) mouse protein items were identified in this subgroup. 13 of these mouse protein items were identified on the basis of at least 4 spectra on average

(mean of an assay duplicate). Whereas, only one mouse protein subunit was identified exclusively in the SAFit1 dependent eluate from a low density FKBP51FK1 affinity column and none protein was exclusively identified in the PPU339 dependent eluate (Figure 47, p. 140).

Comparing the relative protein abundance in the sample(s) of interest with the controls, 18% (162) of all human protein identifications showed increased protein abundance in the sample(s) of interest, at least at a low level (Figure 33, p. 118, enrichment factor > 2). About 9% (109) of all mouse proteins identified in the N2a samples that were analyzed in the 2nd MS run exhibited higher protein abundance in the samples of interest in relation to the controls (Figure 41, p. 129). In the 3rd MS run, about 5% (110) of the identified mouse proteins showed elevated protein abundance in the SAFit1 dependent eluate from a high density FKBP51FK1 affinity column and less than 1% (8) in the FKBP ligand dependent eluate from a low density FKBP51FK1 affinity column in comparison with the controls (Figure 47, p. 140). However, the enrichment factors calculated for the proteins and protein subunits identified in the FKBP ligand dependent eluates from a low density FKBP51FK1 affinity column were at a very low level (Suppl. Table 36, p. 216). These proteins and protein subunits were hardly distinguishable from background proteins and not of biological interest. A subunit of Tubulin (P05214 or P68369), a high abundant protein and the major part of the microtubules [98], was the only protein subunit exclusively identified in the SAFit1 dependent eluate from a low density FKBP51FK1 affinity column. Taken together, no potential FKBP51FK1 interacting proteins could be identified in this sample set.

In the HEK293 samples 12 human protein items had an enrichment factor higher than 20 but lower than 50 (Figure 34, p. 119). In the 2nd MS run, 4 mouse protein items were identified with an enrichment factor higher than 70 but below 100 or between 50 and 70 (Figure 41, p. 129). The calculated enrichment factors in the 3rd MS run were below 30 (Figure 47, p. 140). The background was very high in all sample groups and made about 46% up to 63% of all selected protein items (Figure 33 p. 118, Figure 41 p. 129, Figure 47 p. 140). The background could be lowered by adding detergents such as SDS, Triton (SDS-PAGE and silver staining not shown) or Tween to the sample buffer but these detergents were not compatible with the applied MS method. Different sample preparation methods such as S-Trap (suspension trapping), FASP (filter aided sample preparation) or the use of MS compatible detergents could be tested.

It should be noted that a protein exclusively identified in the sample of interest does not have to be truly absent in the control samples. Underlying reasons can be found at the peptide or

protein level. The following reasons might impede the detection of distinct peptides: (i) the protein digest was not completed or miscleavage occurred, (ii) the corresponding spectrum was not matched with the peptide due to algorithm failure, (iii) post-translational (e.g. phosphorylation, acetylation, farnesylation) or artificial (e.g. methionine, tryptophan or cysteine oxidation, iodoacetamide-based cysteine modification to carbamydomethyl cysteine) peptide modifications were not included in the database search, (iv) the peptide was missing in the applied database, (v) the peptide could not be ionized, (vi) the detection limit of the mass spectrometer was not reached, (vii) the spectra quality was poor, (viii) spectra from different fragment ions overlapped [23, 24]. Furthermore, PTMs (e.g. glycosylation, disulfide bridges) can have a negative effect on protein digestion and thus leading to false negative results [24]. In addition to that, heterogeneous glycosylation leads to a wide distribution of the total ion current [23]. It should be noted that especially proteins carrying modifications might be underrepresented in the MS findings or not been identified [23, 24]. Low abundant peptides can be obscured by high abundant peptides co-eluting from the LC column [23]. The protein identification can be hampered by the following facts: (i) the protein was lost during sample preparation, (ii) the protein coverage was low, (iii) the protein was not assigned to the identified peptides by the applied algorithm, (iv) the protein was not included in the applied database [23, 24]. This issue is addressed by the false discovery rate.

Setting the cut-off at four validated spectra seems to be random. Unfortunately, there is no common guideline for proteomic data analysis to my knowledge. Comparing the number of validated spectra in both samples of the SAFit1 dependent eluate from a high density FKBP51FK1 affinity column (N2a samples, 3rd MS) the relative number of validated spectra related to a distinct protein item was varied. The average absolute error of the relative number of validated spectra was increased at a low spectra count and higher than 50% if less than four spectra were counted (data not shown).

Proteins or protein subunits that were identified in the samples of interests and the controls as well were ranked regarding to their relative abundance in the sample(s) of interest. Proteins or protein subunits exclusively identified in the sample(s) of interest were also grouped and sorted in relation to the total number of validated spectra. This approach does not reflect necessarily the protein enrichment degree comparing different proteins in one group. Comparing the relative abundance of a unique protein in different samples such as the eluate and the wash fractions is possible by spectral counting with all limitations as described. However, the amino acid sequence, the molecular weight and the sample composition can have a high impact on the number of validated peptide-spectra-matches. The digestion of

larger proteins might lead to a higher number of peptides and thus validated spectra. Furthermore, the basic protein expression level and the protein abundance in the complete cell lysate should be considered. Hydrophobic proteins might also be underrepresented or not detected due to poor peptide ionization [24]. “Missing value imputation methods” would have been required to calculate enrichment factors for proteins exclusively identified in the sample of interest [48]. The confidence in this method is dependent on the analyzed sample number. In this study, different pull-down assay setups were tested to optimize the method impeding the assay comparability. Protein ranking within one sample is very complex, would require an extended data set (at least three independent experiments in duplicates) and was not the aim of this study.

5.4.5. Cellular Component Distribution

The proteins and protein subunits identified in the HEK293 and N2a samples from pull-down assays using a high density FKBP51FK1 affinity column were assigned to cellular components (annotation data set: PANTHER GO-Slim Cellular Component) and protein classes (annotation data set: PANTHER Protein Class) by PANTHER [4, 16, 61, 89] (Figure 35 a - Figure 38 a, p. 121 ff.; Figure 42 a - Figure 44 a, p. 130 ff.; Figure 48 a, p. 141). The identified human and mouse proteins and protein subunits were related to the GO terms “Organelles” [67], “Membrane” [65] and “Cytosol” [66]. The ratio of protein items that were either not classified by PANTHER or not related to one of these categories was between 15% and 50%. The number of unclassified protein items could be reduced by applying the GO data annotation set “GO cellular component complete” including automated not reviewed annotations by algorithms but these results would provide less confidence [30].

The majority of proteins and protein subunits exclusively identified in the samples of interest or showing the highest enrichment factor within the HEK293 samples or the N2a sample sets were either not assigned to one of the three GO terms (14% up to 50%) or related to cell organelles (38% up to 86%). Thereof, most of the proteins were related to the nucleus (50% up to 90%). The ratio of proteins assigned to the GO term “membrane” was about 8% up to 22%. The ratio of proteins assigned only to the cytosol or to the cytosol and other cellular compartments was between 0% up to 14%. Human and mouse proteins with lower enrichment factors across the analyzed sample sets showed a similar cellular distribution (Suppl. Figure 52 a - Figure 58 a, p. 183 ff.). By contrast, the well described protein interaction complex of FKBP51/Hsp90/GR [37] was found in the cytosol. The localization of FKBP51 in the nucleus was discussed in the context of the NFκB pathway but there is no

evidence for FKBP51/drug interactions in the nucleus. Especially, potential FKBP51FK1 binding proteins interacting with the binding pocket of the FK1 domain were addressed by the described study to gain insights into the cellular and molecular effects of FKBP ligands. More recently, the intracellular binding of FKBP ligands including SAFit1 and bicyclic compounds to overexpressed FKBPs (FKBP51, FKBP52, FKBP12 and FKBP12.6) in the cytosol was shown by a NanoBret binding assay [34]. Therefore, the cytosolic location of the target proteins is expected. The preparation of cytosolic cell extracts might be beneficial but the lowered protein yield in comparison with the complete cell lysate might be a drawback [71].

5.4.6. Protein Classes

The PANTHER classification system includes parent classes. “Nucleic acid metabolism protein” is the parent class of “RNA metabolism protein”, for example. Proteins that are classified as RNA metabolism protein are also found in the group “nucleic acid metabolism protein”, but not all “nucleic acid metabolism proteins” have to be “RNA metabolism proteins”. Unique proteins or protein subunits can be assigned to different protein classes.

A large part of the analyzed human and mouse proteins as well as protein subunits was not classified by PANTHER [4, 16, 61, 89]. The main protein classes that were identified in the analyzed protein subgroups are: nucleic acid/RNA metabolism protein, metabolite interconversion enzyme, cytoskeletal protein, membrane traffic protein, RNA processing factor (Figure 35 b - Figure 38 b, p. 121 ff; Figure 42 b - Figure 44 b, p. 130 ff.; Figure 48 b, p. 141). Similar results were found for the HEK293 and the N2a subgroups with lower enrichment factors (Suppl. Figure 52 b - Figure 58 b, p. 183 ff.). A “higher” number of mouse chaperones was only identified in the SAFit1 dependent eluate from a high density FKBP51FK1 affinity column (Figure 42 b, red box, p. 130) but not in other sample sets in contrast to the expectations.

5.4.7. FKBP51FK1 Pull-Down Assay - Summary & Troubleshooting

In the 1st and 2nd MS run, several human (Figure 32 b, p. 115) and mouse (Figure 40 b, p. 127) proteins and protein subunits were found exclusively in the SAFit1 dependent eluate from a high density FKBP51FK1 affinity matrix but the highest spectra count was related to high abundant proteins such as Actin [32] and Tubulin [98] (Suppl. Table 32, p. 186).

The proteomic results for the N2a samples from a pull-down assay using a high density FKBP51FK1 affinity and a mock column (- FKBP51FK1) provide the highest confidence

(3rd MS run). Among the proteins and protein subunits exclusively identified in the SAFit1 dependent eluate from a high density FKBP51FK1 affinity column (Suppl. Table 33, p. 207 f.) a member of the DnaJ family (Q9QYI4), a co-chaperone [31], showed the highest average number of validated spectra (8) but the spectra count was still at a low level. Comparing the relative protein abundance in the SAFit1 dependent eluate from a high density FKBP51FK1 affinity column and a mock column (- FKBP51FK1) all calculated enrichment factors were below 30 (Suppl. Table 34, p. 209 ff.; Table 35, p. 213). Among the proteins and protein subunits identified in the sample(s) of interest and the control sample(s) as well IKKγ (Suppl. Table 34, p. 209 ff.: O88522 NF-kappa-B essential modulator, NEMO) was the most prominent protein described in the context of FKBP51 biology [37] but the enrichment factor of 6 does not indicate affinity enrichment. The protein-protein interaction between Hsp90, the glucocorticoid receptor and FKBP51 is very well described [12, 25, 36, 54, 72, 73, 83, 99]. Additional potential FKBP51 interaction partners have been reported on the basis of more (AKT, Glomulin [36], PHLPP, progesterone receptor) or less (estrogen receptor, mineralcorticoid receptor, androgen receptor, IKKα, IKKβ, IKKε, TBK1, ReIA, Cdc37, MAVS, GSK3β, cyclin-dependent kinases, Tau, Ago2, DNA methyltransferase 1, TRAF2/3/6, IRF3/7, AS160, hTERT [46, 55], PPARγ [84, 85], p23 [25]) experimental evidence, often in a controversial context [37]. The described protein interactions are not necessarily based on direct FKBP51-protein interactions and might require client proteins. In contrast to the developed FKBP51FK1 pull-down assay, the intracellular formation of protein-protein complexes is enabled by co-immunoprecipitation assays. None of the (potential) FKBP51 interacting proteins was clearly identified by the FKBP51FK1 pull-down assay and the proteomic approach. This could be explained by several reasons: (i) the potential target protein was absent in the prepared cell lysate or the protein concentration was at a very low level, (ii) the target protein was not captured by the FKBP51FK1 affinity matrix, (iii) the target protein was not eluted by SAFit1, (iv) the high background impeded the identification of FKBP51FK1 interaction partners, (v) the peptide and protein identification failed by mass spectrometry. The first three issues are discussed in more detail:

1. Protein Abundance in the Cell Lysate

The expression level of target proteins is tissue and cell specific [12]. Jurkat cells are used very often to study the NFκB pathway [37] and A375 or SAN cells are applied in the context of melanoma [74, 75], for example. Low abundant proteins might not have been reached the detection limit overall pull-down assay steps and might have been covered by high abundant proteins. In contrast to the described FKBP51FK1 pull-down assay, several

co-immunoprecipitation assays are based on the overexpression of a tagged bait-protein and a target protein [13, 26, 50] leading to higher target protein concentrations. It might be necessary to stimulate cells to induce a pathway to address proteins in a specific context such as the NFκB pathway. The target protein might have been lost in the protein extraction step. The expression level of known target proteins can be analyzed by Western blotting.

2. Effects Hampering FKBP51FK1 Affinity Matrix-Target Protein Interactions

The protein integrity and solubility is dependent on the assay buffer and protein environment. The salt concentration and the non-ionic detergent Nonidet P-40 substitute required for cell lysis might have had a negative effect on the integrity of the target proteins impeding the protein interaction with the FKBP51FK1 affinity matrix. The total protein concentration in the complete cell lysate in the range between 11 mg/mL up to 16 mg/mL might have led to protein precipitation hampering target protein-FKBP51FK1 affinity matrix interactions. The integrity of the binding pocket of the FKBP51FK1 affinity matrix was shown by the fluorescence based binding assay (Figure 22, p. 85). However, the integrity of the complete FK1 domain cannot be assessed by this assay. The properties of the SulfoLink® coupling resin (Thermo Scientific) used for the preparation of the FKBP51FK1 affinity matrix, especially the distance and orientation of the activated iodoacetyl groups and thus the orientation of immobilized FKBP51FK1 were unknown. The availability of the FK1 domain binding pocket might have been limited. In addition to that, the cysteine mutation sites might have inhibited potential FKBP51FK1-protein interactions. To address these issues, different beads and immobilization strategies could be tested. However, testing different beads would not be beneficial in my opinion since the high background caused by the agarose based beads was one of the major problems. To my knowledge, there are no other beads that are suitable for protein immobilization and exhibiting a low assay background available on the market.

Additional proteins might be involved in or required for the target protein-FKBP51FK1 affinity matrix interaction. Thus, the application of intracellular assays such as proximity based crosslinking [20] or photo-crosslinking [19, 44, 106] enabling the intracellular protein-protein complex formation might be beneficial. Furthermore, the FKBP51 TPR or/and FK2 domain might be essential for the formation of the FKBP51-target protein complex [37]. However, the development and application of a FKBP51FK1 affinity matrix seemed to provide the following advantages. In my experience, the expression and purification of smaller proteins such as the 18.5 kDa FK1 domain construct gives higher protein yields than the purification of large full-length proteins. The project aimed at identifying protein-FKBP51FK1 interactions located at

the binding pocket and inhibited by FKBP ligands. Therefore, limiting the possible protein-FKBP51 binding sites beyond the binding pocket seemed to be reasonable to reduce the expected background related to other FKBP51 interaction proteins. The reduction of the sample complexity before MS analysis is very important to prevent MS signal depletion, suppression and overlap.

3. Insufficient Elution

A high SAFit1 excess (at least 100-fold in theory) was required to finish the elution step (Figure 23 a, p. 91; Figure 24 a, p. 94; Figure 25 a+b, p. 97). A relatively high SAFit1 concentration (5 mM) was applied for protein elution to reach the highest protein concentrations as possible in the eluates. Unfortunately, the water solubility of all developed and commercially available FKBP ligands (e.g. Rapamycin, FK506) is relatively poor. SAFit1 might build micelles at high concentration levels removing SAFit1 molecules available for competitive protein elution. In addition to that, micelles can also cause unspecific protein elution. Various FKBP ligands were characterized by competitive fluorescence polarization assays (FPAs) to determine binding affinities for different FKBPs [11, 51, 53, 70, 91, 100]. Based on these results compound precipitation or micelle building is not expected for compound concentrations between 100 μM and 200 μM. For that reason, a pull-down assay using a low density FKBP51FK1 affinity column was performed but no enriched protein was identified.

The proteomic data indicated the elution of several protein complexes (data analysis by STRING [87], not shown). Bulky protein complexes might lower the “flow rate” in the elution step, interact with SAFit1 in an unspecific manner or impede the interaction with the FK1 binding pocket.

The SAFit1 dependent elution of various proteins from the mock column (- FKBP51FK1) demonstrated unspecific protein interactions with the agarose based beads impeding the differentiation between potential FKBP51FK1 binding proteins and unspecific eluting proteins (Figure 25 b, p. 97; Figure 46 a, p. 136). Protein fractionation by SDS-PAGE or SEC and peptide fractionation could be beneficial to reduce the sample complexity facilitating the MS analysis.

In my opinion, there is no clear evidence for the identification of a FKBP51 binding partner exclusively interacting with the binding pocket of the FK1 domain neither by SDS-PAGE and silver staining nor by MS-based proteomics due to the high protein background. FKBP51FK1

binding proteins might have bound to the FKBP51FK1 affinity matrix and the agarose based beads as well impeding the clear identification of possible FKBP51 interaction partners. However, proteins either exclusively identified (Suppl. Table 33, p. 207 f.) or showing a higher relative protein abundance (Suppl. Table 34, p. 209 ff.) in the SAFit1 dependent eluate from a high density FKBP51FK1 affinity column might pop up as FKBP51 binding partners in future studies.

5.5. Summary

Firstly, a FKBP51FK1 affinity matrix was developed to catch FKBP51 binding proteins. The protein immobilization protocol was optimized enabling fast and easy affinity matrix preparation. The immobilization protocol can be applied for other members of the FKBP family such as FKBP52 and FKBP12. In addition to that, a fluorescence-based binding assay was developed to characterize the FKBP51FK1 affinity matrix. Here, the binding pocket integrity was shown by the binding and competitive elution of a tracer. Applications of the FKBP51FK1 affinity matrix comprise the confirmation of known protein-protein interactions by pull-down assays and western blotting or the affinity enrichment of isotopic labeled FKBP ligands in the context of binding isotope effect studies.

Secondly, a FKBP51FK1 pull-down assay was developed to enrich FKBP51 binding proteins from cell lysates. Especially FKBP51 binding partners interacting with the binding pocket of the FK1 domain were addressed by SAFit1 dependent elution. The protein enrichment was analyzed by a bottom-up proteomic approach. Therefore, a sample preparation protocol was established. Finally, 13 mouse protein items were exclusively identified in the sample of interest comparing the SAFit dependent elution from a high density FKBP51FK1 affinity and a mock column. Various mouse protein items with increased protein abundance in the SAFit1 dependent eluate were also identified. These proteins might pop up as FKBP51 interaction partners in future studies. However, the proteomic analysis emphasizes the challenge to differentiate between potential FKBP51 binding proteins and the assay background. The proteomic data indicate the need for other biological methods to identify and to study FKBP51/protein interactions inhibited by FKBP ligands.

Thirdly, various new FKBP ligands were characterized by robot-based fluorescence polarization assays contributing to the development of new drug candidates with increased binding affinity and selectivity within the FKBP protein family [11, 51, 91, 100].

6. Supplement

6.1. Methods

6.1.1. FKBP51FK1 Affinity Matrix Development

The FKBP51FK1 affinity matrix preparation protocol was optimized with regard to the assay buffer and the incubation time. The test experiments are summarized in Table 25 and the differences between the experiments are described below.

Table 25: Experimental Setup Coupling Reaction.

Purified HsFKBP51FK1MonoCys was mixed with equilibrated SulfoLink© coupling resin (Thermo Scientific). The volume *V* and the concentration *c* of the dissolved protein are indicated. The resin volume is related to the swollen settled bead volume and the concentration to the density of the reactive iodoacetyl groups as indicated by the manufacturer. Eq. = Equivalents.

Buffer 1: 50 mM Tris, 5 mM EDTA, pH 8. Buffer 2: Buffer 1 + 20 µM TCEP, pH 8. Buffer 3: Buffer 1 + 190 µM TCEP, pH 8. Buffer 4: Buffer 1 + 950 µM TCEP, pH 8. Buffer 5: Buffer 1 + 10 mM TCEP, pH 8. Buffer 6: 20 mM Hepes, 20 mM NaCl, 5% (v/v) Glycerol, 10 mM TCEP, pH 8. The same buffer was used to dissolve HsFKBP51FK1MonoCys and to equilibrate the beads.

	HsFKBP51FK1 MonoCys	SulfoLink® Coupling Resin	Number *N* of Independent Experiments	Exp. No.
c	700 μM	19 mM	*N*=1	SMe56b
V	175 μL	175 μL		
Eq.	1	27		
Buffer	1	1		
c	350 μM - 380 μM	19 mM	Buffer 1: *N*=3	SMe49a SMe52a SMe56a
V	175 μL - 250 μL	175 μL - 250 μL		
Eq.	1	50-55	Buffer 5: *N*=1	SMe52b
Buffer	1, 5, 6	1, 5, 6	Buffer 6: *N*=1	SMe49b
c	190 μM	19 mM	Buffer 1: *N*=1	SMe79a
V	150 μL	150 μL		
Eq.	1	100	Buffer 3: *N*=1	SMe79c
Buffer	1, 3	1, 3		
c	80 μM	19 mM	*N*=1	SMe79b
V	300 μL	150 μL		
Eq.	1	120		
Buffer	1	1		

1. Equilibration of SulfoLink® Coupling Resin

SulfoLink® coupling resin was transferred into an appropriate empty column (rinsed with VE-H_2O and equilibration buffer). A filter (10 μm, #2110 or 35 μm, small, MoBiTec, #M513515) was pre-wetted with equilibration buffer and mounted if columns without an inserted filter were applied. The storage solution (10 mM EDTA-Na, 0.05% (w/v) NaN_3, 50% (v/v) glycerol) of the beads was drained and discarded. The resin was washed with 7 CV up to 27 CV equilibration buffer (Table 26). The coupling reaction was performed in a column or in a tube depending on the sample size.

Table 26: Equilibration of SulfoLink® Coupling Resin.

Buffer 1: 50 mM Tris, 5 mM EDTA, pH 8. Buffer 2: Buffer 1 + 20 µM TCEP, pH 8. Buffer 3: Buffer 1 + 190 µM TCEP, pH 8. Buffer 4: Buffer 1 + 950 µM TCEP, pH 8. Buffer 5: Buffer 1 + 10 mM TCEP, pH 8. Buffer 6: 20 mM Hepes, 20 mM NaCl, 5% (v/v) Glycerol, 10 mM TCEP, pH 8. 1 CV = 1 column volume = settled bead volume.

Equilibration Buffer	Equilibration Volume	Settled Bead Volume	Experiment
Buffer 1	8 CV	250 μL	SMe49a, SMe49b
Buffer 1	16 CV	250 μL	SMe52a
Buffer 5	16 CV	250 μL	SMe52b
Buffer 1	23 CV	175 μL	SMe56a, SMe56b
Buffer 1	27 CV	150 μL	SMe79a, SMe79b
Buffer 3	27 CV	150 μL	SMe79c
Buffer 1	10 CV	3.6 mL	SMe162
Buffer 1	10 CV	0.8 mL	SMe182
Buffer 1	10 CV	1.9 mL	SMe225
Buffer 1	10 CV	3.8 mL	SMe249
Buffer 1	7 CV	5 mL	SMe303 (Column 1 & 2)
Buffer 1	10 CV	1.9 mL	SMe312/JPK
Buffer 1	10 CV	400 μL	SMe357
Buffer 1	10 CV	1.5 mL	SMe378

2. Coupling of FKBP51FK1MonoCys

HsFKBP51FK1MonoCys stocks were stored in either buffer 4 (50 mM Tris, 5 mM EDTA, 950 μM TCEP, pH 8), buffer 5 (50 mM Tris, 5 mM EDTA, 10 mM TCEP, pH 8) or buffer 6 (20 mM Hepes, 20 mM NaCl, 5% (v/v) glycerol, 10 mM TCEP, pH 8, Table 25).

HsFKBP51FK1MonoCys was dialyzed (Slide-A-Lyzer mini dialysis devices, 3.5K MWCO, Thermo Scientific, # 88403) to exchange the storage buffer with the buffer applied for the coupling reaction (Table 25). Centricon-10 centrifugal filters (Ultracel YM-10, Amicon® Bioseparations, # 4205) and Amicon® Ultra-2 mL centrifugal filters (Ultracel®-3 K, Merck Millipore, UFC 200324) were applied if a protein concentration step was required.

HsFKBP51FK1MonoCys was added to the equilibrated resin. The column/reaction tube was carefully inverted to suspend the beads. The mix was incubated for up to 24 h. Incubation steps at 4°C and RT were combined. The incubation in a column standing upright and on a rolling device was tested (Table 27). The volume ratio of HsFKBP51FK1MonoCys and the settled beads was between 1:1 and 2:1 (Table 25). 20 μM up to 950 μM protein stocks were used depending on the desired final protein density of the affinity matrix. Protein stocks were pre-diluted with buffer if required.

To monitor the efficiency and the progress of the coupling reaction, the concentration of unbound HsFKBP51FK1MonoCys in the reaction mix was analyzed by SDS-PAGE and Coomassie staining at different time points (Table 27). Samples were collected either by gravity flow or taken from the supernatant of the beads. A “flow” was initiated by gravity, by screwing the lid of small columns (1 mL column) or by exerting pressure with a connected syringe (2.5 mL and 10 mL columns). Before taking a sample from the supernatant, the column was incubated for 5 min up to 10 min at RT standing upright to avoid bead aspiration (Table 27). The HsFKBP51FK1MonoCys stock was initially diluted by mixing the protein with swollen equilibrated beads. The initial dilution factor was unknown and could only be estimated. Therefore, a sample was taken from the reaction mix immediately after starting the coupling reaction. The liquid part of the swollen settled beads delivered as 50% (v/v) slurry was estimated based on the manufacturer´s specification (cp. instructions 0527.3 SulfoLink® Coupling Resin, Thermo Scientific, USA). The estimated liquid part of the resin is about 75% of the settled bead volume. The estimated dilution factor is about 1.75 after mixing a distinct volume of the protein stock with an equal volume of settled beads.

Table 27: Optimization of the FKBP51FK1 Affinity Matrix Preparation Protocol – Determination of the Incubation Time.

Equal volumes of HsFKBP51FK1MonoCys and equilibrated SulfoLink® coupling beads were mixed. The double volume of HsFKBP51FK1MonoCys was tested in SMe79b. [1)]The column was incubated on a rolling device at RT for 15 min up to 90 min. Afterwards, the column was incubated standing upright[2)] or on a rolling device[3)] at 4°C. Samples were collected from the supernatant of the mix or/and by gravity flow at several time points (sample 1 to sample 5). Temp. = Temperature.

Sample	1st Sample	2nd Sample	3rd Sample	4th Sample	5th Sample	Exp. No.
Time	15 - 20 min	45 min	3 h	22.5 - 23 h	—	SMe49 a & b
Temp.	RT[1)]	4°C[2)]	4°C[2)]	4°C[2)]		
Collected by/from	Gravity Flow	Gravity Flow	Gravity Flow	Gravity Flow		
Time	5 min	17 min	90 min	3 h	5 h	SMe52a
Temp.	RT	RT[1)]	RT[1)]	4°C[2)]	4°C[2)]	
Collected by/from	Gravity Flow	Gravity Flow	Gravity Flow	Gravity Flow	Gravity Flow	
Time	5 min	1 h	Experiment SMe52b was aborted after 1h because the lower column filter was lost and the resuspension of the resin was not possible.			SMe52b
Temp.	RT	RT[1)]				
Collected by/from	Gravity Flow	Gravity Flow				
Time	2 min	18 - 19 min	45 - 48 min	3 h	23 h	SMe56a
Temp.	RT	RT[1)]	RT[1)]	4°C[2)]	4°C[2)]	
Collected by/from	Gravity Flow	Supernatant	Supernatant	Supernatant	Supernatant	
Time	2 min	18 - 19 min	45 - 48 min	3 h	24 h	SMe56b
Temp.	RT	RT[1)]	RT[1)]	4°C[2)]	4°C[2)]	
Collected by/from	Supernatant	Supernatant	Supernatant	Supernatant	Supernatant	
Time	5 min	19 - 26 min	1 h	3 h	—	SMe79 a, b & c
Temp.	RT	RT[2)]	RT[2)]	RT[2)]		
Collected by/from	Gravity Flow	Gravity Flow	Gravity Flow	Gravity Flow		
Time	6 min	90 min	15 h 40 min	—	—	SMe162
Temp.	RT	RT[1)]	4°C[3)]			
Collected by/from	Supernatant	Supernatant	Gravity Flow & Supernatant			
Time	8 min	66 min	86 min	—	—	SMe378
Temp.	RT	RT[1)]	RT			
Collected by/from	Supernatant	Supernatant	Gravity Flow			

3. Bead Wash

The beads were transferred into a column if the coupling reaction was run in a tube. The column was washed with 3 CV up to 6.5 CV buffer to remove unbound HsFKBP51FK1MonoCys (Table 28). This wash step was skipped in SMe303, SMe312/JPK, SMe357 and SMe378.

Table 28: Bead Wash after Coupling HsFKBP51FK1MonoCys.

Buffer 1: 50 mM Tris, 5 mM EDTA, pH 8. Buffer 2: Buffer 1 + 20 µM TCEP, pH 8. Buffer 3: Buffer 1 + 190 µM TCEP, pH 8. 1 CV = 1 column volume = settled bead volume.

Wash Buffer	Volume Wash Buffer	Settled Bead Volume	Experiment
Buffer 1	3 CV	250 µL	SMe49a, SMe49b
Buffer 1	3 CV	250 µL	SMe52a
Buffer 1	5.3 CV	175 µL	SMe56a
Buffer 1	6.5 CV	175 µL	SMe56b
Buffer 1	3 CV	150 µL	SMe79a, SMe79b
Buffer 3	3 CV	150 µL	SMe79c
Buffer 1	4 CV	3.6 mL	SMe162
Buffer 1	4 CV	0.8 mL	SMe182
Buffer 1	4 CV	1.9 mL	SMe225
Buffer 1	4.4 CV	3.8 mL	SMe249

4. Blocking of Residual Active Iodoacetyl Groups With 2-Mercaptoethanol

To block residual active iodoacetyl groups of the beads, 5.5 CV up to 19 CV blocking buffer I (50 mM Tris, 5 mM EDTA, 10 mM 2-mercaptoethanol, pH 8) or 4.4 CV blocking buffer II (50 mM Tris, 5 mM EDTA, 50 mM 2-mercaptoethanol, pH 8) were added to the column. Different incubation steps were run to ensure the “blocking” of free iodoacetyl groups by 2-mercaptoethanol (Table 29). 2-mercaptoethanol was added daily to a premix of 50 mM Tris (pH 8)/5 mM EDTA to prevent oxidation.

Table 29: Blocking Residual Active Groups with 2-Mercaptoethanol.

After the coupling reaction was completed, free iodoacetly groups were blocked with 10 mM[1)] or 50 mM[2)] 2-mercaptoethanol (ß-Me). SulfoLink® coupling resin exhibited a 19 mM density of free iodoacetyl groups according to the manufacturer´s specification (lowest estimated density of active groups after the protein immobilization: 18 mM). Eq. = equivalents.
Blocking buffer: 50 mM Tris, 5 mM EDTA,[1)]10 mM or [2)]50 mM 2-mercaptoethanol, pH 8.

Conditions		Experimental Procedure	Exp. No.
Settled Bead Volume	0.17 mL	2 CV blocking buffer (50 mM ß-me) were added to the column standing upright at RT. The column was closed, 1.2 CV blocking buffer were added and the column was incubated for 15 min at RT. The buffer was drained by gravity flow. 1.2 CV blocking buffer were added and the column was incubated for 15 min at RT for a second time. The buffer was drained by gravity flow.	SMe52a, 56a & b
V (Blocking Buffer) [2)]	4.4 CV		
Eq. 2-Mercaptoethanol	11.6		
Total Incubation Time	-		
Settled Bead Volume	3.6 mL	5.5 CV blocking buffer were added to the column standing upright at RT. The gravity flow was interrupted for 15 min after the 1st and the 2nd CV. The remaining buffer passed the column by gravity flow.	SMe162
V (Blocking Buffer) [1)]	5.5 CV		
Eq. 2-Mercaptoethanol	3		
Total Incubation Time	40 min		
Settled Bead Volume	0.8 mL	18.1 CV blocking buffer were added to the column standing upright at RT. The column was closed for 15 min after 1.3 CV. The incubation step was repeated 5 times.	SMe182
V (Blocking Buffer) [1)]	18.1 CV		
Eq. 2-Mercaptoethanol	9.5		
Total Incubation Time	2 h		
Settled Bead Volume	1.9 mL	2 CV blocking buffer were added and the beads were suspended by inverting the column. The mix was incubated for 15 min at RT on a rolling device. The flow-through was discarded. This step was repeated 8 times. 4 CV blocking buffer were used in the last step.	SMe225
V (Blocking Buffer) [1)]	19 CV		
Eq. 2-Mercaptoethanol	10		
Total Incubation Time	3.5 h		
Settled Bead Volume	3.8 mL	2 CV blocking buffer were added and the beads were suspended by inverting the column. The flow-through was discarded after incubating the column for 15 min at RT on a rolling device. This incubation step was repeated two times. 12.6 CV blocking buffer were added to the column standing upright.	SMe249
V (Blocking Buffer) [1)]	18.6 CV		
Eq. 2-Mercaptoethanol	9.8		
Total Incubation Time	1 h 45 min		
Settled Bead Volume	5 mL	The beads were suspended with 1 CV blocking buffer and incubated on a rolling device for 15 min at RT. The flow-through was discarded. This step was repeated 5 times. Subsequently, 12 CV blocking buffer were added to the column standing upright at RT. The flow was stopped for 10 – 15 min all the time 1 CV passed the column.	SMe303
V (Blocking Buffer) [1)]	18 CV		
Eq. 2-Mercaptoethanol	9.5		
Total Incubation Time	6 h		

Table 29 Continued: Blocking Residual Active Groups with 2-Mercaptoethanol.

Conditions		Experimental Procedure	Exp. No.
Settled Bead Volume	1.9 mL	1 CV blocking buffer was added to the column and the beads were suspended by inverting. The column was incubated for 15 min at RT on a rolling device. This step was repeated 5 times. 1 CV blocking buffer was added and the column was incubated for 15 min at RT standing upright. This step was repeated 11 times.	SMe312/JPK
V (Blocking Buffer) [1)]	18 CV		
Eq. 2-Mercaptoethanol	9.5		
Total Incubation Time	-		
Settled Bead Volume	0.4 mL	The beads were suspended with 1 CV blocking buffer and incubated for 5 – 10 min at RT on a rolling device. The supernatant was discarded after the resin was settled down. This step was repeated two times. The beads were suspended with 1 CV blocking buffer and transferred into a column. 12 CV blocking buffer were added by gravity flow.	SMe357
V (Blocking Buffer) [1)]	16 CV		
Eq. 2-Mercaptoethanol	8.4		
Total Incubation Time	1 h 43 min		
Settled Bead Volume	1.5 mL	1 CV blocking buffer was added and the beads were suspended by inverting the tube. The mix was incubated for 15 min at RT on a rolling device. After incubating the tube for 10 min at RT in an upright direction to settle the beads, the supernatant was discarded. This step was repeated two times. The beads were transferred into a column and 16 CV blocking buffer were added by gravity flow.	SMe378
V (Blocking Buffer) [1)]	19 CV		
Eq. 2-Mercaptoethanol	10		
Total Incubation Time	2 h 20 min		

5. Column Wash and Storage

The column was washed with 5 CV up to 20 CV storage buffer (50 mM Tris, 5 mM EDTA, pH 8, Table 30). Aliquots were prepared (protein low binding tubes, Sarstedt) and the affinity matrices were stored at 4°C.

Table 30: Bead Wash After Blocking.

Buffer 1: 50 mM Tris, 5 mM EDTA, pH 8.

1 CV = 1 column volume = settled bead volume.

Wash Buffer	Volume Wash Buffer	Settled Bead Volume	Experiment
Buffer 1	5 CV	0.17 mL	SMe52a, SMe56a & b
Buffer 1	20 CV	3.6 mL	SMe162
Buffer 1	21 CV	0.8 mL	SMe182
Buffer 1	20 CV	1.9 mL	SMe225
Buffer 1	20 CV	3.8 mL	SMe249
Buffer 1	19 CV	5 mL	SMe303
Buffer 1	20 CV	1.9 mL	SMe312/JPK
Buffer 1	20 CV	0.4 mL	SMe357
Buffer 1	20 CV	1.5 mL	SMe378

6.1.2. Proteomics

The following section describing the sample preparation and the MS-based proteomic analysis was written by Hanne Haslene-Hox and copied from the resport draft with her permission [40, 41]. Table affiliations were adjusted.

N2a Samples

"Samples were frozen immediately at arrival at SINTEF. Sample set 1 is denoted with letters A - H and was received on the 27th of April 2020 (Table 17 a, p. 63). These samples where thawed at arrival at SINTEF. Sample set 2 is denoted with numbers 1-22, and was received at 8th of October 2020 (Table 17 b, p. 63). […] Peptide quantity was determined after trypsin digest and clean-up. Samples were stored at -20 °C until analysis and processed for proteomics within two weeks."

Trypsin Digestion

"Part of lysate (1,2) or whole samples (A - G, 3 - 22) were diluted to appropriate volumes in ammonium bicarbonate buffer (100 mM), denatured and reduced in 2,2,2-trifluoroethanol (1:1 TFE:sample volume-ratio) with 1,4-dithiotreitol (DTT, 200 mM, 1:10 DTT:sample volume-ratio) at 90° C for 20 minutes. To alkylate cysteine residues, iodoacetamide (IAM, 200 mM, 1:2.5 IAM:sample volume-ratio) was added and incubated in the dark at room temperature for 1 hour. DTT was added to inactivate surplus IAM (200 mM, 1:10 DTT:sample volume-ratio) and incubated in the dark at room temperature for 1 hour. Ammonium bicarbonate (25mM) was added 16:1 Ambic:sample volume ratio before samples were digested by trypsin (1:35 enzyme:protein weight-ratio) and desalted by Pierce C18 spin columns (Cat. No. 89870, Thermo Scientific), following instructions from manufacturer, using

50% Acetonitrile (ACN) for column activation, 5% ACN with 0.5% Trifluoroacetic acid (TFA) for column equilibration and wash, and 70% ACN with 0.1% Formic acid (FA) for elution. For samples with large volumes, the samples were split in 2 - 3 C18 spin columns. The desalted samples from sample set 1 (total elution volume 40 μL) were split in two aliquots, 5 μL for peptide quantity determination and 35 μL for proteomic analysis and dried after C18 clean-up. For sample set 2, the entire eluted peptide volume was dried and submitted to proteomic analysis. For peptide quantification, 5 μL of each sample were rehydrated in 25 μL 0.1% formic acid (FA) and peptide quantification was done with Pierce Quantitative Fluorometric Peptide Assay (Cat. No. 23290) in duplicates."

MS Analysis

"For mass spectrometry, dried peptides were reconstituted in 11.5 μL (set 1) or 10 μL (set 2) 2% ACN, 0.5% FA. Samples were injected (4 μL for N2a samples A - H, 1 μL for N2a samples 1 - 22) into an Ultimate 3000 RSLC system (Thermo Scientific, Sunnyvale, California, USA) connected online to a Q-Exactive HF mass spectrometer (Thermo Scientific, Bremen, Germany) equipped with EASY-spray nano-electrospray ion source (Thermo Scientific) for a 120 min ACN gradient 5 - 90% ACN […]. The raw data was converted to Mascot Generic Format (mgf) peak lists with MS convert with peak picking of MS2 to convert to centroid data. Peak lists obtained from MS/MS spectra were identified using SearchGUI (version 3.3.18, X!Tandem and Omssa search engines) and PeptideShaker (version 1.16.45). Protein identification was conducted against a concatenated target/decoy database of Mus Musculus (uniprot.org, 2020-06, 17 038 sequences) or UniProt database for *Homo sapiens* (uniprot.org, 2020-04; 20 365 sequences). Interferences from common contaminants (cRAP database, version 2012.01.01) were included to rule out confounding protein identities. The decoy sequences were created by reversing the target sequences in SearchGUI. The identification settings were as follows: specific trypsin digest with a maximum of 2 missed cleavages; 10 ppm as MS1 and 0.02 Da as MS2 tolerances; fixed modifications: Carbamidomethylation of C (+57.021464 Da); variable modifications: Oxidation of M (+15.994915 Da); fixed modifications during refinement procedure: Carbamidomethylation of C (+57.021464 Da). Peptides and proteins were inferred from the spectrum identification results using PeptideShaker (v1.16.38). Peptide-spectrum matches (PSMs), peptides and proteins were validated at a 1.0% False Discovery Rate (FDR) estimated using the decoy hit distribution. All samples were processed in parallel in PeptideShaker to provide data for all identified proteins across all samples, with individual quantitative measures for each sample. The number of

peptide-spectra matches allocated to a given protein in a given sample, was used for label-free quantitative evaluation."

6.2. Results

6.2.1. Fluorescence-Based FKBP51FK1 Binding Assay

The fluorescence signal of a fluorophore is proportional to the compound concentration within a specified range. This range is dependent on the properties of the applied plate reader, the measurement conditions (e.g. Gain) and the assay buffer. A serial dilution of the tracer CK182 was performed to estimate the range showing a linear relation of the compound concentration and the measured fluorescence intensity (e.g. SMe449, SMe450). Therefore, a 50 μM CK182 DMSO stock was diluted in assay buffer (50 mM Tris, 5 mM EDTA, 0.002% (v/v) Triton X-100, pH 8) to prepare 1 μM CK182. A serial dilution was performed in duplicate (2x 11 measurement values). 20 μL assay buffer were transferred into a 384-well assay plate (# 3575, Corning) and 40 μL 1 μM CK182 were transferred into the 1st wells (2x). 20 μL of one well were transferred into the next well and mixed with the buffer. The background fluorescence intensity of the buffer was measured.

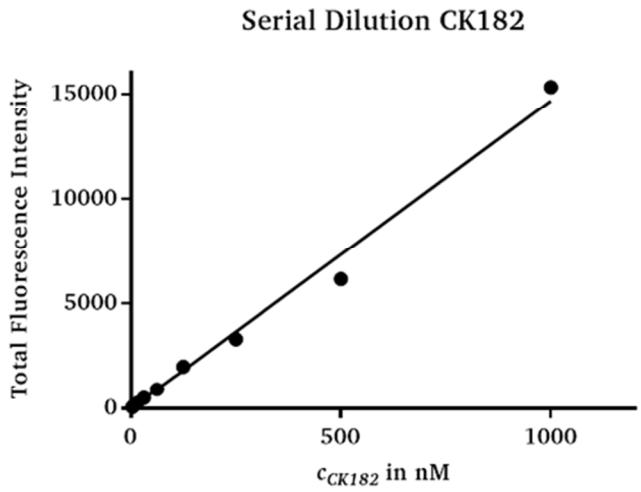

Figure 51: Serial Dilution of the Tracer CK182.

A 1:1 serial dilution (20 µL + 20 µL) of the tracer CK182 was performed in assay buffer in duplicate. Final volume per well: 20 µL. 1st well: 1 µM CK182, last well: approximately 1 nM CK182. The fluorescence intensity was measured by a plate reader (TECAN Spark, Excitation: 485 ± 20 nm, Emission: 535 nm ± 25 nm, Gain: 37, 29 °C). The absolute error of both measured values was at a low level that cannot be illustrated. Assay buffer: 50 mM Tris, 5 mM EDTA, 0.002% (v/v) Triton X-100, pH 8.

Samples with mean fluorescence intensities in the range between 70 and 16,000 were in the linear range (Figure 51).

6.2.2. Comparing SAFit1 Dependent Elution with Mock Elution from a High Density FKBP51FK1 Affinity Column

HEK293 Samples – 1st MS Run

Human protein items that were identified exclusively either in the early or in the late SAFit1 dependent eluate or in both but not in the control samples (wash fraction pools, mock eluate) from a high density FKBP51FK1 affinity column are listed in Table 31 a. Table 31 b includes a list of human protein items identified in at least one control sample and in at least one SAFit1 dependent eluate with an enrichment factor higher than 2. The identified proteins were sub-grouped regarding the calculated enrichment factor and assigned to cellular components and protein classes by PANTHER [4, 16, 61, 89] (Figure 52 - Figure 54).

Table 31: Comparing SAFit1 Dependent Elution with Mock Elution from a High Density FKBP51FK1 Affinity Column – HEK293 Samples.

HEK293 cell lysate was added to two equilibrated high density FKBP51FK1 affinity columns (final protein density about 950 µM). Both columns were washed with 50 CV assay buffer. Either 10 CV 5 mM SAFit1 or 10 CV buffer (mock elution) were added for elution. Pools of the last wash fractions (10 CV) prior elution, the complete mock eluate (10 CV) as well as the early (3 CV) and late (7 CV) SAFit1 dependent eluate were analyzed by a bottom-up proteomic approach.

Pull-down assay buffer, pH 8: 20 mM Tris, 100 mM NaCl, 0.5 mM EDTA, 1 mM PMSF, 1 mM DTT, Protease inhibitor cocktail (cOmplete mini, Roche, 1 tablet per 10 mL buffer).
Equilibration and cell lysis buffer, pH 8 = assay buffer + 0.5% (v/v) Nonidet-P40 substitute. Elution buffer, pH 8 = ± 5 mM SAFit1. 1 CV = 1 column volume.

Table 31 a: Human Protein Items Exclusively Identified in the SAFit1 Dependent Eluate.

The protein items (1st column: UniProtKB database accession number) were identified neither in a wash fraction pool nor in the mock eluate but in the SAFit1 dependent eluate. The total number of identified spectra (3rd column) related to a distinct protein item in the early (4th column) and/or late (5th column) SAFit1 dependent eluate is given.

Accession Number (UniProtKB)	Description	Number of Identified Spectra	Early Eluate	Late Eluate
P60709	Actin, cytoplasmic 1 (ACTB_HUMAN)	271		x
P68371	Tubulin beta-4B chain (TBB4B_HUMAN)	46		x
P68363	Tubulin alpha-1B chain (TBA1B_HUMAN)	24		x
P35606	Coatomer subunit beta' (COPB2_HUMAN)	32		x
Q5H9R7	Serine/threonine-protein phosphatase 6 regulatory subunit 3 (PP6R3_HUMAN)	32		x
P67809	Y-box-binding protein 1 (YBOX1_HUMAN)	22		x
P09874	Poly [ADP-ribose] polymerase 1 (PARP1_HUMAN)	26	x	x
P50542	Peroxisomal targeting signal 1 receptor (PEX5_HUMAN)	24		x
Q9HD40	O-phosphoseryl-tRNA(Sec) selenium transferase (SPCS_HUMAN)	20	x	x
P11387	DNA topoisomerase 1 (TOP1_HUMAN)	19	x	x
P52294	Importin subunit alpha-5 (IMA5_HUMAN)	15		x
Q9UHB9	Signal recognition particle subunit SRP68 (SRP68_HUMAN)	18		x
P40939	Trifunctional enzyme subunit alpha, mitochondrial (ECHA_HUMAN)	18		x
P61326	Protein mago nashi homolog (MGN_HUMAN)	5	x	
Q6IA86	Elongator complex protein 2 (ELP2_HUMAN)	17		x
P26368	Splicing factor U2AF 65 kDa subunit (U2AF2_HUMAN)	16	x	x
P17844	Probable ATP-dependent RNA helicase DDX5 (DDX5_HUMAN)	15	x	x
Q14974	Importin subunit beta-1 (IMB1_HUMAN)	16		x
P16403	Histone H1,2 (H12_HUMAN)	15		x
Q9Y3C6	Peptidyl-prolyl cis-trans isomerase-like 1 (PPIL1_HUMAN)	14		x
O60814	Histone H2B type 1-K (H2B1K_HUMAN)	8		x
P61923	Coatomer subunit zeta-1 (COPZ1_HUMAN)	13		x
P31930	Cytochrome b-c1 complex subunit 1, mitochondrial (QCR1_HUMAN)	13		x
P10412	Histone H1,4 (H14_HUMAN)	13		x
P36954	DNA-directed RNA polymerase II subunit RPB9 (RPB9_HUMAN)	12		x
O60907	F-box-like/WD repeat-containing protein TBL1X (TBL1X_HUMAN)	12		x

Q8N7H5	RNA polymerase II-associated factor 1 homolog (PAF1_HUMAN)	12		x
O14744	Protein arginine N-methyltransferase 5 (ANM5_HUMAN)	11		x
Q9UPN7	Serine/threonine-protein phosphatase 6 regulatory subunit 1 (PP6R1_HUMAN)	11		x
P55084	Trifunctional enzyme subunit beta, mitochondrial (ECHB_HUMAN)	11		x
Q96B54	Zinc finger protein 428 (ZN428_HUMAN)	11		x
Q16698	2,4-dienoyl-CoA reductase, mitochondrial (DECR_HUMAN)	10		x
Q15046	Lysine--tRNA ligase (SYK_HUMAN)	10		x
Q9UL42	Paraneoplastic antigen Ma2 (PNMA2_HUMAN)	10		x
O75381	Peroxisomal membrane protein PEX14 (PEX14_HUMAN)	10		x
Q99460	26S proteasome non-ATPase regulatory subunit 1 (PSMD1_HUMAN)	9		x
P11586	C-1-tetrahydrofolate synthase, cytoplasmic (C1TC_HUMAN)	7		x
Q96C19	EF-hand domain-containing protein D2 (EFHD2_HUMAN)	7		x
P46976	Glycogenin-1 (GLYG_HUMAN)	7		x
P07195	L-lactate dehydrogenase B chain (LDHB_HUMAN)	7		x
Q9Y265	RuvB-like 1 (RUVB1_HUMAN)	7		x
Q9Y230	RuvB-like 2 (RUVB2_HUMAN)	7		x
Q9NQ92	Coordinator of PRMT5 and differentiation stimulator (COPRS_HUMAN)	6	x	x
Q9BRJ6	Uncharacterized protein C7orf50 (CG050_HUMAN)	6	x	x
P52272	Heterogeneous nuclear ribonucleoprotein M (HNRPM_HUMAN)	6	x	x
Q96A33	Coiled-coil domain-containing protein 47 (CCD47_HUMAN)	6		x
O15173	Membrane-associated progesterone receptor component 2 (PGRC2_HUMAN)	6		x
Q9NQC3	Reticulon-4 (RTN4_HUMAN)	6		x
P41091	Eukaryotic translation initiation factor 2 subunit 3 (IF2G_HUMAN)	5	x	x
P08195	4F2 cell-surface antigen heavy chain (4F2_HUMAN)	5		x
P00167	Cytochrome b5 (CYB5_HUMAN)	5		x
Q07065	Cytoskeleton-associated protein 4 (CKAP4_HUMAN)	5		x
Q5TAQ9	DDB1- and CUL4-associated factor 8 (DCAF8_HUMAN)	5		x
O75935	Dynactin subunit 3 (DCTN3_HUMAN)	5		x
Q5RKV6	Exosome complex component MTR3 (EXOS6_HUMAN)	5		x
Q96B26	Exosome complex component RRP43 (EXOS8_HUMAN)	5		x
Q9Y664	KICSTOR complex protein kaptin (KPTN_HUMAN)	5		x
P78406	mRNA export factor (RAE1L_HUMAN)	5		x
Q9BQG2	Peroxisomal NADH pyrophosphatase NUDT12 (NUD12_HUMAN)	5		x
Q15366	Poly(rC)-binding protein 2 (PCBP2_HUMAN)	5		x
P50990	T-complex protein 1 subunit theta (TCPQ_HUMAN)	5		x
O43818	U3 small nucleolar RNA-interacting protein 2 (U3IP2_HUMAN)	5		x
Q9H7D7	WD repeat-containing protein 26 (WDR26_HUMAN)	5		x
P43686	26S proteasome regulatory subunit 6B (PRS6B_HUMAN)	4		x

Q92572	AP-3 complex subunit sigma-1 (AP3S1_HUMAN)	4		x
Q9NW68	BSD domain-containing protein 1 (BSDC1_HUMAN)	4		x
P41208	Centrin-2 (CETN2_HUMAN)	4		x
P63172	Dynein light chain Tctex-type 1 (DYLT1_HUMAN)	4		x
Q86YZ3	Hornerin (HORN_HUMAN)	4		x
Q969R8	KICSTOR complex protein ITFG2 (ITFG2_HUMAN)	4		x
Q14165	Malectin (MLEC_HUMAN)	4		x
O43684	Mitotic checkpoint protein BUB3 (BUB3_HUMAN)	4		x
Q08AG7	Mitotic-spindle organizing protein 1 (MZT1_HUMAN)	4		x
P29966	Myristoylated alanine-rich C-kinase substrate (MARCS_HUMAN)	4		x
Q9BU61	NADH dehydrogenase [ubiquinone] 1 alpha subcomplex assembly factor 3 (NDUF3_HUMAN)	4		x
Q9Y3B4	Splicing factor 3B subunit 6 (SF3B6_HUMAN)	4		x
Q14232	Translation initiation factor eIF-2B subunit alpha (EI2BA_HUMAN)	4		x
Q8WW01	tRNA-splicing endonuclease subunit Sen15 (SEN15_HUMAN)	4		x
Q9UBQ0	Vacuolar protein sorting-associated protein 29 (VPS29_HUMAN)	4		x
Q6UXN9	WD repeat-containing protein 82 (WDR82_HUMAN)	4		x

Table 31 b: Human Protein Items Identified in the SAFit1 Dependent Eluate and in Samples Carrying Unspecific Eluting Proteins.

The relative abundance of protein items identified in the early (4th column) or late (3rd column) SAFit1 dependent eluate in comparison with samples carrying unspecific eluting proteins is given. The relative protein abundance in the mock eluate was compared with the relative abundance in the corresponding wash fraction pool (5th column). The total number of identified spectra assigned to the corresponding protein item in the mock eluate is given in brackets (5th column). EF = Enrichment factor.

Accession Number (UniProtKB)	Description	EF (Late SAFit1 Dependent Eluate)	EF (Early SAFit1 Dependent Eluate)	EF (Mock Eluate)
Q9BZK7	F-box-like/WD repeat-containing protein TBL1XR1 (TBL1R_HUMAN)	48.9	0.0	0.0
O43719	HIV Tat-specific factor 1 (HTSF1_HUMAN)	33.9	2.4	1.5
O14579	Coatomer subunit epsilon (COPE_HUMAN)	24.8	0.0	0.8
Q13200	26S proteasome non-ATPase regulatory subunit 2 (PSMD2_HUMAN)	23.3	0.0	0.0
Q9NWU2	Glucose-induced degradation protein 8 homolog (GID8_HUMAN)	21.9	0.0	0.0
Q01105	Protein SET (SET_HUMAN)	21.0	19.5	3.1
Q9Y535	DNA-directed RNA polymerase III subunit RPC8 (RPC8_HUMAN)	20.2	0.0	0.0
Q9BW83	Intraflagellar transport protein 27 homolog (IFT27_HUMAN)	20.2	30.2	0.0
Q9UMS4	Pre-mRNA-processing factor 19 (PRP19_HUMAN)	18.5	12.1	0.0
Q9UN86	Ras GTPase-activating protein-binding protein 2 (G3BP2_HUMAN)	18.0	29.3	n.a. (0)
Q12874	Splicing factor 3A subunit 3 (SF3A3_HUMAN)	17.4	0.0	0.0
P60660	Myosin light polypeptide 6 (MYL6_HUMAN)	16.3	2.6	0.8
P35613	Basigin (BASI_HUMAN)	15.2	0.0	0.0
Q9BRP8	Partner of Y14 and mago (PYM1_HUMAN)	15.2	6.0	0.0
Q13185	Chromobox protein homolog 3 (CBX3_HUMAN)	14.7	0.0	n.a. (0)
O43504	Ragulator complex protein LAMTOR5 (LTOR5_HUMAN)	14.7	5.9	n.a. (0)
P09132	Signal recognition particle 19 kDa protein (SRP19_HUMAN)	13.7	22.5	0.8
Q8IWZ3	Ankyrin repeat and KH domain-containing protein 1 (ANKH1_HUMAN)	13.5	0.0	0.0
Q9NYL9	Tropomodulin-3 (TMOD3_HUMAN)	13.4	0.0	0.0
Q9BQE3	Tubulin alpha-1C chain (TBA1C_HUMAN)	13.2	0.0	n.a. (2)

O96019	Actin-like protein 6A (ACL6A_HUMAN)	13.2	7.1	n.a. (1)
P16989	Y-box-binding protein 3 (YBOX3_HUMAN)	12.3	11.7	n.a. (0)
Q15417	Calponin-3 (CNN3_HUMAN)	11.8	0.0	0.0
Q9H1D9	DNA-directed RNA polymerase III subunit RPC6 (RPC6_HUMAN)	11.8	0.0	0.0
P26599	Polypyrimidine tract-binding protein 1 (PTBP1_HUMAN)	11.8	0.0	0.0
Q7KZ85	Transcription elongation factor SPT6 (SPT6H_HUMAN)	11.8	0.0	0.0
Q16643	Drebrin (DREB_HUMAN)	11.2	1.1	0.5
P55735	Protein SEC13 homolog (SEC13_HUMAN)	10.7	2.0	0.0
O60684	Importin subunit alpha-7 (IMA7_HUMAN)	10.6	0.0	n.a. (0)
Q15393	Splicing factor 3B subunit 3 (SF3B3_HUMAN)	10.5	0.3	0.4
Q96AY3	Peptidyl-prolyl cis-trans isomerase FKBP10 (FKB10_HUMAN)	10.1	0.0	0.0
Q96EY4	Translation machinery-associated protein 16 (TMA16_HUMAN)	10.1	36.2	0.0
Q15369	Elongin-C (ELOC_HUMAN)	9.9	5.3	1.5
P08579	U2 small nuclear ribonucleoprotein B" (RU2B_HUMAN)	9.8	0.0	n.a. (0)
O00743	Serine/threonine-protein phosphatase 6 catalytic subunit (PPP6_HUMAN)	9.2	2.6	1.5
O00303	Eukaryotic translation initiation factor 3 subunit F (EIF3F_HUMAN)	9.1	0.0	0.0
P55769	NHP2-like protein 1 (NH2L1_HUMAN)	9.1	0.0	0.0
P10155	60 kDa SS-A/Ro ribonucleoprotein (RO60_HUMAN)	8.8	2.0	0.0
P47224	Guanine nucleotide exchange factor MSS4 (MSS4_HUMAN)	8.8	0.0	n.a. (1)
P30049	ATP synthase subunit delta, mitochondrial (ATPD_HUMAN)	8.4	0.0	0.0
P23246	Splicing factor, proline- and glutamine-rich (SFPQ_HUMAN)	8.4	18.1	0.0
Q15029	116 kDa U5 small nuclear ribonucleoprotein component (U5S1_HUMAN)	8.2	0.0	0.0
P23526	Adenosylhomocysteinase (SAHH_HUMAN)	8.2	0.0	n.a. (0)
Q92688	Acidic leucine-rich nuclear phosphoprotein 32 family member B (AN32B_HUMAN)	8.1	4.4	2.5
Q9UNP9	Peptidyl-prolyl cis-trans isomerase E (PPIE_HUMAN)	8.0	1.7	1.5
P47756	F-actin-capping protein subunit beta (CAPZB_HUMAN)	7.6	0.9	1.5
Q8NFH3	Nucleoporin Nup43 (NUP43_HUMAN)	7.5	0.0	0.0
O14561	Acyl carrier protein, mitochondrial (ACPM_HUMAN)	7.4	0.0	n.a. (0)
P09661	U2 small nuclear ribonucleoprotein A' (RU2A_HUMAN)	7.2	0.0	n.a. (1)
Q9UNS2	COP9 signalosome complex subunit 3 (CSN3_HUMAN)	7.0	0.0	0.0
O00264	Membrane-associated progesterone receptor component 1 (PGRC1_HUMAN)	6.9	2.0	3.1

O00233	26S proteasome non-ATPase regulatory subunit 9 (PSMD9_HUMAN)	6.7	0.0	0.0
O75575	DNA-directed RNA polymerase III subunit RPC9 (RPC9_HUMAN)	6.7	0.0	0.0
Q9C005	Protein dpy-30 homolog (DPY30_HUMAN)	6.7	0.0	0.0
Q13247	Serine/arginine-rich splicing factor 6 (SRSF6_HUMAN)	6.7	6.0	0.0
P48643	T-complex protein 1 subunit epsilon (TCPE_HUMAN)	6.7	0.0	0.0
O15355	Protein phosphatase 1G (PPM1G_HUMAN)	6.7	0.3	1.3
P10809	60 kDa heat shock protein, mitochondrial (CH60_HUMAN)	6.7	0.0	0.8
P39687	Acidic leucine-rich nuclear phosphoprotein 32 family member A (AN32A_HUMAN)	6.7	5.7	1.5
Q13428	Treacle protein (TCOF_HUMAN)	6.6	5.9	0.0
Q9BTT0	Acidic leucine-rich nuclear phosphoprotein 32 family member E (AN32E_HUMAN)	6.4	6.1	1.3
P47755	F-actin-capping protein subunit alpha-2 (CAZA2_HUMAN)	6.1	0.0	0.0
Q9NZI8	Insulin-like growth factor 2 mRNA-binding protein 1 (IF2B1_HUMAN)	6.0	7.1	1.5
P27694	Replication protein A 70 kDa DNA-binding subunit (RFA1_HUMAN)	5.9	0.0	0.0
P62312	U6 snRNA-associated Sm-like protein LSm6 (LSM6_HUMAN)	5.8	0.0	0.0
P15927	Replication protein A 32 kDa subunit (RFA2_HUMAN)	5.7	0.0	0.8
Q9BQA1	Methylosome protein 50 (MEP50_HUMAN)	5.5	0.0	0.0
Q96BR5	Cytochrome c oxidase assembly factor 7 (COA7_HUMAN)	5.5	0.0	n.a. (0)
P02794	Ferritin heavy chain (FRIH_HUMAN)	5.3	0.0	n.a. (1)
Q9UBQ5	Eukaryotic translation initiation factor 3 subunit K (EIF3K_HUMAN)	5.3	0.0	0.0
O14950	Myosin regulatory light chain 12B (ML12B_HUMAN)	5.2	0.0	1.5
P07437	Tubulin beta chain (TBB5_HUMAN)	5.1	0.0	0.5
O60841	Eukaryotic translation initiation factor 5B (IF2P_HUMAN)	5.1	8.0	0.0
Q9NR28	Diablo homolog, mitochondrial (DBLOH_HUMAN)	5.0	0.0	0.0
Q9BY44	Eukaryotic translation initiation factor 2A (EIF2A_HUMAN)	5.0	3.6	0.0
P61962	DDB1- and CUL4-associated factor 7 (DCAF7_HUMAN)	5.0	0.0	0.0
P12956	X-ray repair cross-complementing protein 6 (XRCC6_HUMAN)	5.0	5.9	0.0
P49458	Signal recognition particle 9 kDa protein (SRP09_HUMAN)	4.7	8.5	1.5
Q15370	Elongin-B (ELOB_HUMAN)	4.7	5.9	2.0
Q9NXG2	THUMP domain-containing protein 1 (THUM1_HUMAN)	4.7	2.8	0.8
P46060	Ran GTPase-activating protein 1 (RAGP1_HUMAN)	4.6	0.0	0.0
Q99627	COP9 signalosome complex subunit 8 (CSN8_HUMAN)	4.6	0.0	0.0
Q9BVG4	Protein PBDC1 (PBDC1_HUMAN)	4.4	0.7	0.8

Q9UIL1	Short coiled-coil protein (SCOC_HUMAN)	4.4	0.0	n.a. (1)
Q9UK45	U6 snRNA-associated Sm-like protein LSm7 (LSM7_HUMAN)	4.4	0.0	n.a. (1)
Q9Y224	RNA transcription, translation and transport factor protein (RTRAF_HUMAN)	4.3	0.0	0.8
P54105	Methylosome subunit pICln (ICLN_HUMAN)	4.3	0.2	0.7
O75534	Cold shock domain-containing protein E1 (CSDE1_HUMAN)	4.3	0.0	1.5
Q9BWJ5	Splicing factor 3B subunit 5 (SF3B5_HUMAN)	4.2	0.0	0.0
P56537	Eukaryotic translation initiation factor 6 (IF6_HUMAN)	4.1	8.8	n.a. (0)
Q13283	Ras GTPase-activating protein-binding protein 1 (G3BP1_HUMAN)	3.9	8.1	0.0
P63151	Serine/threonine-protein phosphatase 2A 55 kDa regulatory subunit B alpha isoform (2ABA_HUMAN)	3.8	0.0	n.a. (0)
P14735	Insulin-degrading enzyme (IDE_HUMAN)	3.8	6.6	0.4
P63261	Actin, cytoplasmic 2 (ACTG_HUMAN)	3.7	0.0	n.a. (81)
P13010	X-ray repair cross-complementing protein 5 (XRCC5_HUMAN)	3.4	3.0	0.0
Q16531	DNA damage-binding protein 1 (DDB1_HUMAN)	3.4	2.2	0.9
O43809	Cleavage and polyadenylation specificity factor subunit 5 (CPSF5_HUMAN)	3.3	2.0	0.0
Q9BSL1	Ubiquitin-associated domain-containing protein 1 (UBAC1_HUMAN)	3.3	0.0	0.9
P61769	Beta-2-microglobulin (B2MG_HUMAN)	3.3	0.0	1.5
Q9BRP4	Proteasomal ATPase-associated factor 1 (PAAF1_HUMAN)	3.3	0.0	1.5
P06576	ATP synthase subunit beta, mitochondrial (ATPB_HUMAN)	3.3	1.9	0.0
P20674	Cytochrome c oxidase subunit 5A, mitochondrial (COX5A_HUMAN)	3.3	0.0	1.5
Q8TBZ6	tRNA methyltransferase 10 homolog A (TM10A_HUMAN)	3.3	0.0	0.0
P09497	Clathrin light chain B (CLCB_HUMAN)	3.3	2.9	n.a. (0)
P60228	Eukaryotic translation initiation factor 3 subunit E (EIF3E_HUMAN)	3.3	0.0	n.a. (0)
Q00059	Transcription factor A, mitochondrial (TFAM_HUMAN)	3.3	8.8	n.a. (0)
Q8NFH4	Nucleoporin Nup37 (NUP37_HUMAN)	3.2	2.7	0.8
P63208	S-phase kinase-associated protein 1 (SKP1_HUMAN)	3.0	1.8	0.9
Q12906	Interleukin enhancer-binding factor 3 (ILF3_HUMAN)	2.9	7.1	0.5
P0DP23	Calmodulin-1 (CALM1_HUMAN)	2.9	0.8	0.8
P18859	ATP synthase-coupling factor 6, mitochondrial (ATP5J_HUMAN)	2.9	0.0	0.8
P27824	Calnexin (CALX_HUMAN)	2.8	0.6	0.0
P37108	Signal recognition particle 14 kDa protein (SRP14_HUMAN)	2.8	4.5	1.5

Q92841	Probable ATP-dependent RNA helicase DDX17 (DDX17_HUMAN)	2.8	8.0	0.0
Q8NC51	Plasminogen activator inhibitor 1 RNA-binding protein (PAIRB_HUMAN)	2.8	4.0	0.7
P53999	Activated RNA polymerase II transcriptional coactivator p15 (TCP4_HUMAN)	2.8	3.1	0.9
Q13547	Histone deacetylase 1 (HDAC1_HUMAN)	2.7	0.0	n.a. (0)
Q9BXR0	Queuine tRNA-ribosyltransferase catalytic subunit 1 (TGT_HUMAN)	2.7	0.0	0.8
P34897	Serine hydroxymethyltransferase, mitochondrial (GLYM_HUMAN)	2.7	1.2	0.0
P12004	Proliferating cell nuclear antigen (PCNA_HUMAN)	2.6	0.0	0.0
Q8N4Q1	Mitochondrial intermembrane space import and assembly protein 40 (MIA40_HUMAN)	2.6	1.9	2.3
P55786	Puromycin-sensitive aminopeptidase (PSA_HUMAN)	2.6	3.0	0.0
P84090	Enhancer of rudimentary homolog (ERH_HUMAN)	2.6	3.1	1.1
O60506	Heterogeneous nuclear ribonucleoprotein Q (HNRPQ_HUMAN)	2.5	4.0	0.9
P14314	Glucosidase 2 subunit beta (GLU2B_HUMAN)	2.4	0.3	0.2
P62306	Small nuclear ribonucleoprotein F (RUXF_HUMAN)	2.4	0.0	0.8
P83876	Thioredoxin-like protein 4A (TXN4A_HUMAN)	2.3	0.0	1.5
P60604	Ubiquitin-conjugating enzyme E2 G2 (UB2G2_HUMAN)	2.3	0.6	0.8
Q7L5N1	COP9 signalosome complex subunit 6 (CSN6_HUMAN)	2.3	0.0	0.0
Q9Y3D0	Cytosolic iron-sulfur assembly component 2B (CIA2B_HUMAN)	2.2	0.0	0.0
Q9GZS3	WD repeat-containing protein 61 (WDR61_HUMAN)	2.2	3.4	1.5
Q9BT78	COP9 signalosome complex subunit 4 (CSN4_HUMAN)	2.2	0.0	0.0
P61978	Heterogeneous nuclear ribonucleoprotein K (HNRPK_HUMAN)	2.1	0.7	1.0
Q8N108	Mesoderm induction early response protein 1 (MIER1_HUMAN)	2.1	0.0	0.0
Q12905	Interleukin enhancer-binding factor 2 (ILF2_HUMAN)	2.1	4.5	0.8
O43390	Heterogeneous nuclear ribonucleoprotein R (HNRPR_HUMAN)	2.1	4.3	n.a. (3)
Q9UBP6	tRNA (guanine-N(7)-)-methyltransferase (TRMB_HUMAN)	2.1	1.5	0.0
Q07955	Serine/arginine-rich splicing factor 1 (SRSF1_HUMAN)	1.8	2.3	0.9
A5A3E0	POTE ankyrin domain family member F (POTEF_HUMAN)	1.7	2.0	1.3
Q01130	Serine/arginine-rich splicing factor 2 (SRSF2_HUMAN)	1.7	2.1	1.5
Q9NXH9	tRNA (guanine(26)-N(2))-dimethyltransferase (TRM1_HUMAN)	1.7	6.0	0.0
Q16630	Cleavage and polyadenylation specificity factor subunit 6 (CPSF6_HUMAN)	1.5	4.3	0.5
P68104	Elongation factor 1-alpha 1 (EF1A1_HUMAN)	1.5	2.6	0.8
Q13151	Heterogeneous nuclear ribonucleoprotein A0 (ROA0_HUMAN)	1.4	8.5	1.5
P29401	Transketolase (TKT_HUMAN)	1.4	2.5	3.1
P35637	RNA-binding protein FUS (FUS_HUMAN)	1.4	4.6	0.6

Q96A72	Protein mago nashi homolog 2 (MGN2_HUMAN)	1.3	5.9	n.a. (0)
Q9P258	Protein RCC2 (RCC2_HUMAN)	1.3	2.3	1.8
P09651	Heterogeneous nuclear ribonucleoprotein A1 (ROA1_HUMAN)	1.3	2.4	0.9
P51991	Heterogeneous nuclear ribonucleoprotein A3 (ROA3_HUMAN)	1.2	3.0	0.9
Q13867	Bleomycin hydrolase (BLMH_HUMAN)	0.9	2.3	1.3
Q86V81	THO complex subunit 4 (THOC4_HUMAN)	0.9	2.6	2.2
P11940	Polyadenylate-binding protein 1 (PABP1_HUMAN)	0.8	5.9	0.0
Q14444	Caprin-1 (CAPR1_HUMAN)	0.8	2.4	0.9
P81605	Dermcidin (DCD_HUMAN)	0.7	4.7	0.0
Q00839	Heterogeneous nuclear ribonucleoprotein U (HNRPU_HUMAN)	0.6	2.9	1.1
P19338	Nucleolin (NUCL_HUMAN)	0.6	2.6	1.4
P07910	Heterogeneous nuclear ribonucleoproteins C1/C2 (HNRPC_HUMAN)	0.2	3.4	1.1
P36957	Dihydrolipoyllysine-residue succinyltransferase component of 2-oxoglutarate dehydrogenase complex, mitochondrial (ODO2_HUMAN)	0.1	2.0	1.1
P35269	General transcription factor IIF subunit 1 (T2FA_HUMAN)	0.0	11.9	0.0
P0CG39	POTE ankyrin domain family member J (POTEJ_HUMAN)	0.0	5.2	n.a. (0)
Q01844	RNA-binding protein EWS (EWS_HUMAN)	0.0	23.4	n.a. (0)

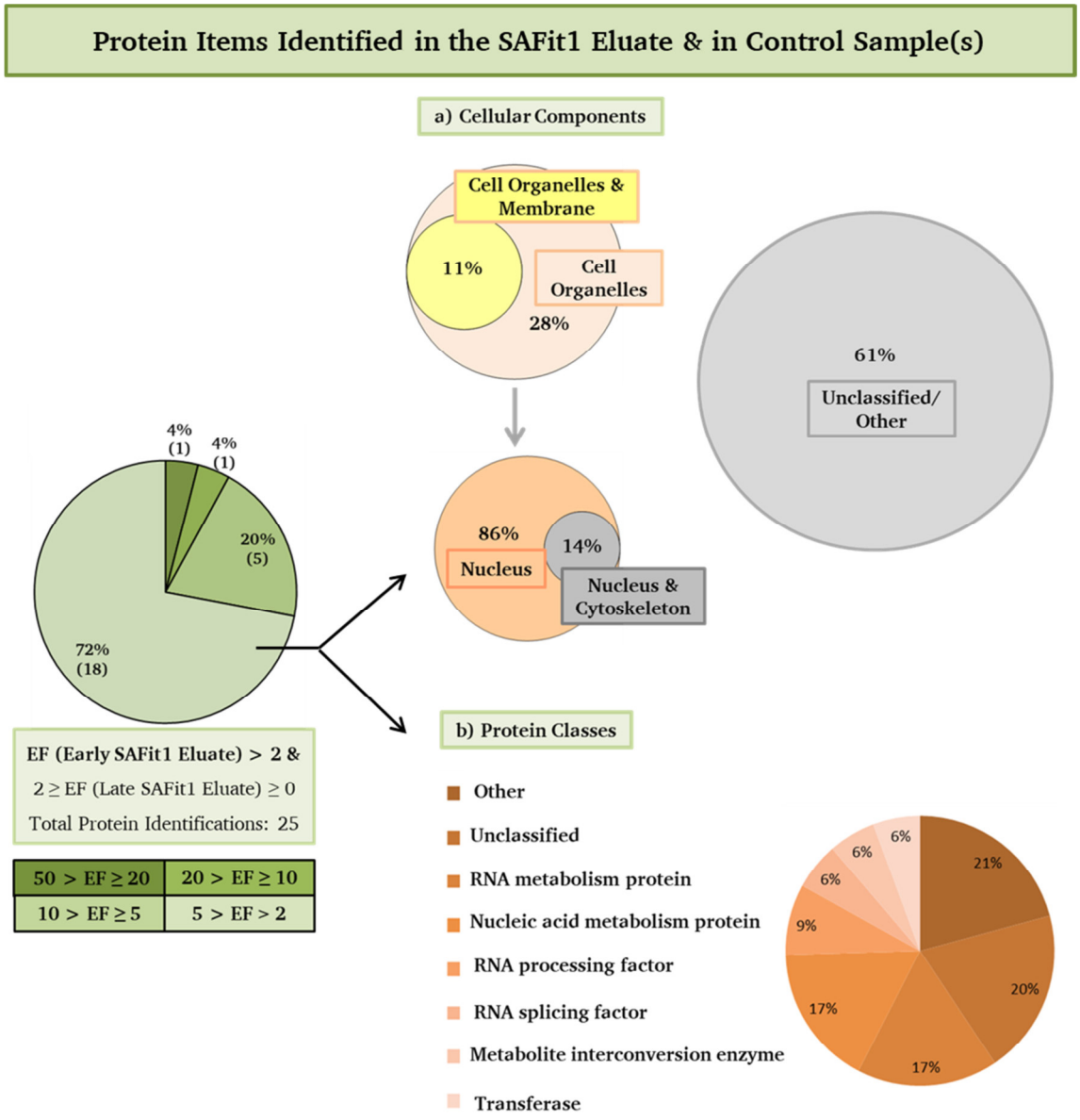

Figure 52: Assigning Human Protein Items Identified in the Early SAFit1 Dependent Eluate to Cellular Components and Protein Classes – Low Enrichment Factor.

Human protein items identified in the early SAFit1 dependent eluate with an enrichment factor (EF) between 2 and 5 (18 protein items in total) were assigned to cellular components (Figure a) and protein classes (Figure b) by PANTHER [4, 16, 61, 89].

Figure a: The relative distribution of the assigned protein items is given in %.

Figure b: The distribution of the identified protein classes is given in %. Protein items can be related to one or several protein classes.

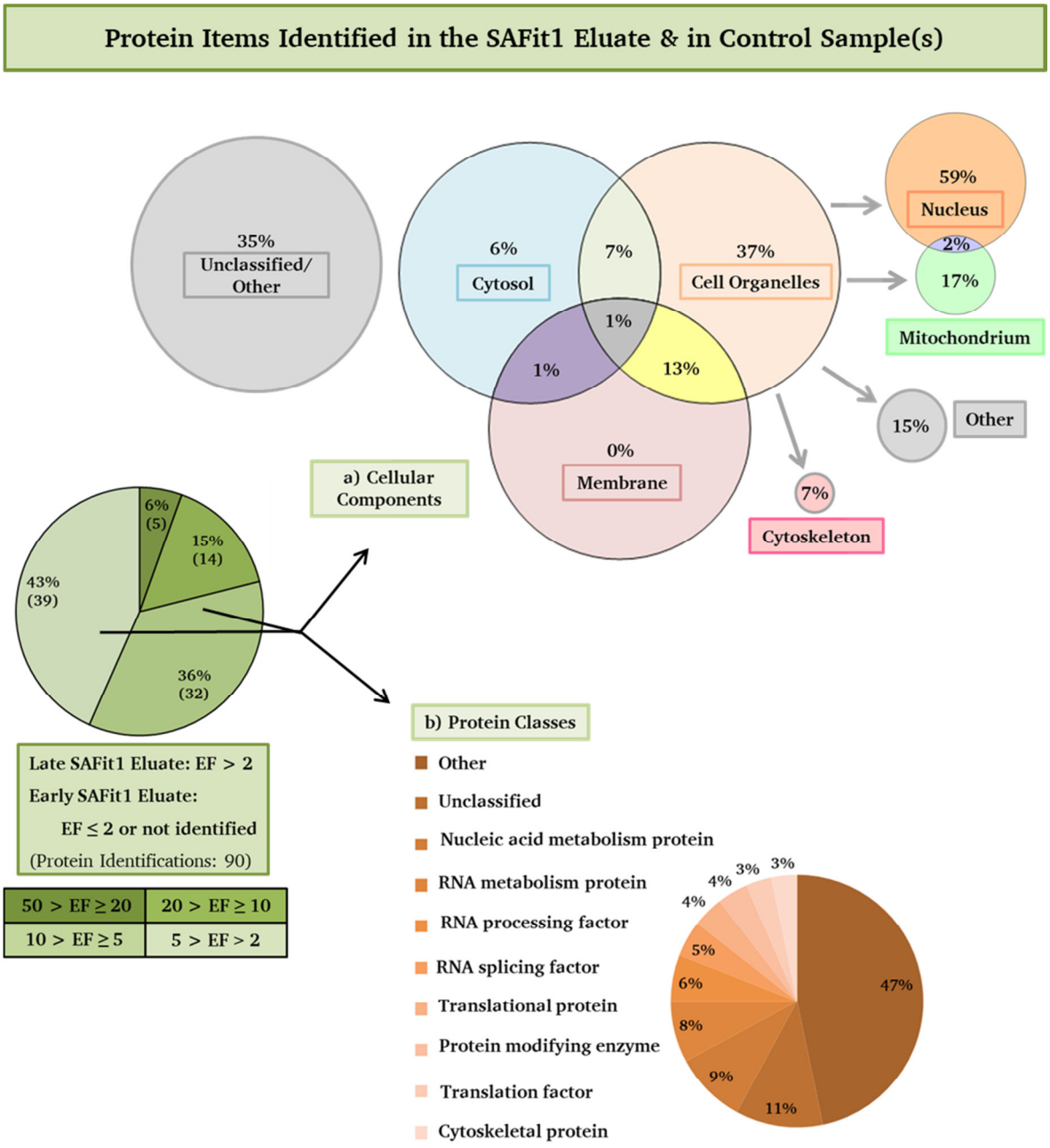

Figure 53: Assigning Human Protein Items Identified in the Late SAFit1 Dependent Eluate to Cellular Components and Protein Classes – Low Enrichment Factor.

Human protein items identified in the late SAFit1 dependent eluate with an enrichment factor (EF) higher than 2 and lower than 10 (71 protein identifications in total) were assigned to cellular components (Figure a) and protein classes (Figure b) by PANTHER [4, 16, 61, 89].

Figure a: The relative cellular compartment distribution is given in %.

Figure b: The distribution of the identified protein classes is given in %. Protein items can be assigned to one or several protein classes.

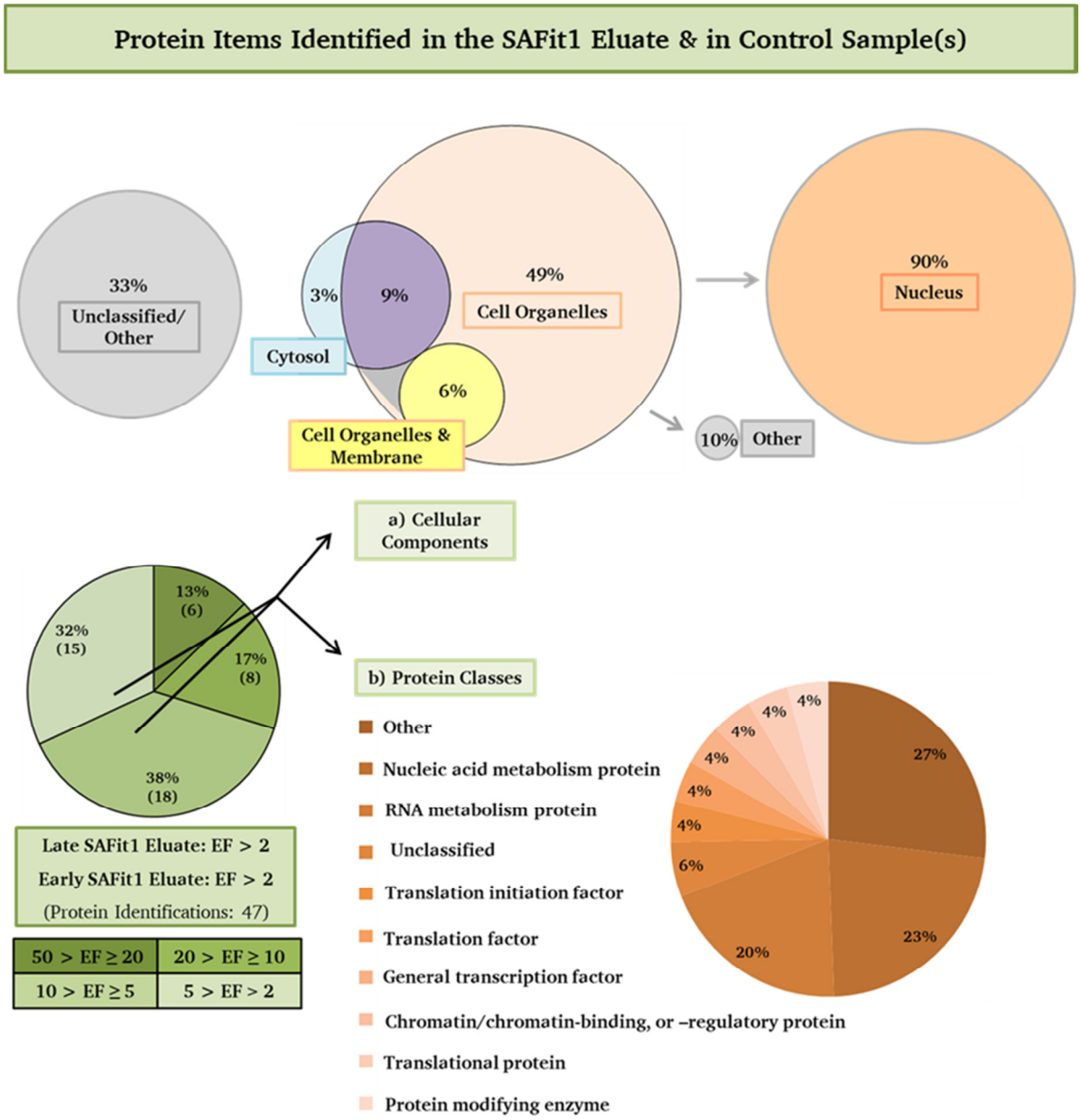

Figure 54: Assigning Human Protein Items Identified in the Early and Late SAFit1 Dependent Eluate to Cellular Components and Protein Classes – Low Enrichment Factor.

Human protein items identified in the early and late SAFit1 dependent eluate with an enrichment factor (EF) higher than 2 and lower than 10 (33 protein identifications in total) were assigned to cellular components (Figure a) and protein classes (Figure b) by PANTHER [4, 16, 61, 89].

Figure a: The distribution of the protein items assigned to cellular components is given in %.

Figure b: The distribution of the identified protein classes is given in %. Protein items can be assigned to one or several protein classes.

N2a Samples – 2nd MS Run

Mouse proteins not identified in samples carrying unspecific eluting proteins (= wash fraction pools, mock eluate) but in the SAFit1 dependent eluate were ranked according to the total number of identified spectra (Table 32 a). Precipitation occurred in the SAFit1 dependent eluate in the required sample concentration step. For that reason, the supernatant and the dissolved pellet of the SAFit1 dependent eluate were analyzed separately. Mouse protein items identified in the SAFit1 dependent eluate and at least in one sample carrying unspecific eluting proteins were ranked according to the calculated enrichment factor (Table 32 b). The identified mouse proteins and protein subunits ware assigned to cellular components and protein classes by PANTHER [4, 16, 61, 89] (Figure 55, Figure 56).

Table 32: Comparing SAFit1 Dependent Elution from a High Density FKBP51FK1 Affinity Column with Mock Elution – N2a Samples.

N2a cell lysate was loaded on two equilibrated high density FKBP51FK1 affinity columns (final protein density: about 950 µM). Both columns were washed with 50 CV buffer. Either 20 CV buffer (= mock elution) or 20 CV 5 mM SAFit1 were added for elution. The following sample pools were analyzed by MS: (i) the 10 second to last wash fractions from both columns, (ii) the last 10 wash fractions from both columns, (iii) the SAFit1 dependent eluates (supernatant and dissolved pellet), (iv) the mock eluate.

Pull-down assay buffer, pH 8: 20 mM Tris, 100 mM NaCl, 0.5 mM EDTA, 1 mM PMSF, 1 mM DTT, Protease inhibitor cocktail (cOmplete mini, Roche, 1 tablet per 10 mL buffer).
Equilibration and cell lysis buffer, pH 8 = assay buffer + 0.5% (v/v) Nonidet-P40 substitute. Elution buffer, pH 8 = assay buffer ± 5 mM SAFit1.

Table 32 a: Mouse Proteins Exclusively detected in the SAFit1 Dependent Eluate.

The mouse proteins were not detected in the samples carrying unspecific eluting proteins but in the SAFit1 dependent eluate. The total number of identified spectra in both samples of the SAFit1 dependent eluate, the supernatant (4th column) and the dissolved pellet (5th column), is given. The proteins were ranked according to the spectra sum (3rd column).

SAFit1 Dependent Eluate		Number of Identified Spectra		
Accession Number (UniProtKB)	Description	Sum	Supernatant	Pellet
P60710	Actin, cytoplasmic 1 (ACTB_MOUSE)	366	283	83
P63260	Actin, cytoplasmic 2 (ACTG_MOUSE)	280	280	0
Q8VDD5	Myosin-9 (MYH9_MOUSE)	209	108	101
Q7TMM9	Tubulin beta-2A chain (TBB2A_MOUSE)	198	152	46
Q61879	Myosin-10 (MYH10_MOUSE)	164	76	88
Q9JLI8	Squamous cell carcinoma antigen recognized by T-cells 3 (SART3_MOUSE)	145	111	34
Q8BMA6	Signal recognition particle subunit SRP68 (SRP68_MOUSE)	119	91	28
Q921M3	Splicing factor 3B subunit 3 (SF3B3_MOUSE)	87	74	13
P97855	Ras GTPase-activating protein-binding protein 1 (G3BP1_MOUSE)	71	42	29
P05214	Tubulin alpha-3 chain (TBA3_MOUSE)	68	49	19
Q8VDM4	26S proteasome non-ATPase regulatory subunit 2 (PSMD2_MOUSE)	67	61	6
Q8VEK3	Heterogeneous nuclear ribonucleoprotein U (HNRPU_MOUSE)	66	30	36
Q922F4	Tubulin beta-6 chain (TBB6_MOUSE)	62	62	0
O08810	116 kDa U5 small nuclear ribonucleoprotein component (U5S1_MOUSE)	58	52	6
P35564	Calnexin (CALX_MOUSE)	53	50	3
Q91WM3	U3 small nucleolar RNA-interacting protein 2 (U3IP2_MOUSE)	53	26	27
O88545	COP9 signalosome complex subunit 6 (CSN6_MOUSE)	52	44	8
P05213	Tubulin alpha-1B chain (TBA1B_MOUSE)	51	51	0
P25976	Nucleolar transcription factor 1 (UBF1_MOUSE)	49	46	3
Q61656	Probable ATP-dependent RNA helicase DDX5 (DDX5_MOUSE)	48	34	14
Q8BGC0	HIV Tat-specific factor 1 homolog (HTSF1_MOUSE)	46	43	3
Q9D024	Coiled-coil domain-containing protein 47 (CCD47_MOUSE)	46	42	4
Q922D4	Serine/threonine-protein phosphatase 6 regulatory subunit 3 (PP6R3_MOUSE)	45	42	3

Q99KK9	Histidine--tRNA ligase, mitochondrial (SYHM_MOUSE)	45	36	9
P03975	IgE-binding protein (IGEB_MOUSE)	43	28	15
Q8BQM4	HEAT repeat-containing protein 3 (HEAT3_MOUSE)	43	34	9
Q9D0I8	mRNA turnover protein 4 homolog (MRT4_MOUSE)	43	37	6
Q9QYJ0	DnaJ homolog subfamily A member 2 (DNJA2_MOUSE)	43	32	11
P46061	Ran GTPase-activating protein 1 (RAGP1_MOUSE)	41	30	11
Q8R1Q8	Cytoplasmic dynein 1 light intermediate chain 1 (DC1L1_MOUSE)	40	37	3
Q91ZV0	Melanoma inhibitory activity protein 2 (MIA2_MOUSE)	40	39	1
Q99LD4	COP9 signalosome complex subunit 1 (CSN1_MOUSE)	40	36	4
Q3TXS7	26S proteasome non-ATPase regulatory subunit 1 (PSMD1_MOUSE)	38	36	2
Q6P6M7	O-phosphoseryl-tRNA(Sec) selenium transferase (SPCS_MOUSE)	37	32	5
P10852	4F2 cell-surface antigen heavy chain (4F2_MOUSE)	36	28	8
P37040	NADPH--cytochrome P450 reductase (NCPR_MOUSE)	36	33	3
Q9WTM5	RuvB-like 2 (RUVB2_MOUSE)	36	30	6
Q9CZ13	Cytochrome b-c1 complex subunit 1, mitochondrial (QCR1_MOUSE)	35	27	8
O08583	THO complex subunit 4 (THOC4_MOUSE)	34	17	17
Q62318	Transcription intermediary factor 1-beta (TIF1B_MOUSE)	34	32	2
Q9CZ04	COP9 signalosome complex subunit 7a (CSN7A_MOUSE)	34	23	11
O88543	COP9 signalosome complex subunit 3 (CSN3_MOUSE)	33	29	4
P63038	60 kDa heat shock protein, mitochondrial (CH60_MOUSE)	33	28	5
Q8CHP5	Partner of Y14 and mago (PYM1_MOUSE)	33	12	21
Q8CI75	DIS3-like exonuclease 2 (DI3L2_MOUSE)	33	32	1
P54775	26S proteasome regulatory subunit 6B (PRS6B_MOUSE)	32	29	3
Q60960	Importin subunit alpha-5 (IMA5_MOUSE)	32	21	11
Q7TNC4	Putative RNA-binding protein Luc7-like 2 (LC7L2_MOUSE)	32	5	27
Q7TT37	Elongator complex protein 1 (ELP1_MOUSE)	32	29	3
Q91WK2	Eukaryotic translation initiation factor 3 subunit H (EIF3H_MOUSE)	32	27	5
Q05CL8	La-related protein 7 (LARP7_MOUSE)	31	8	23
Q99KP6	Pre-mRNA-processing factor 19 (PRP19_MOUSE)	31	30	1
Q8BHJ5	F-box-like/WD repeat-containing protein TBL1XR1 (TBL1R_MOUSE)	30	28	2
P80314	T-complex protein 1 subunit beta (TCPB_MOUSE)	29	26	3
P80318	T-complex protein 1 subunit gamma (TCPG_MOUSE)	29	25	4
Q7TSI3	Serine/threonine-protein phosphatase 6 regulatory subunit 1 (PP6R1_MOUSE)	29	28	1
Q9WV55	Vesicle-associated membrane protein-associated protein A (VAPA_MOUSE)	29	26	3
Q6ZQ58	La-related protein 1 (LARP1_MOUSE)	28	10	18
Q9JJF3	Ribosomal oxygenase 1 (RIOX1_MOUSE)	28	23	5

P15331	Peripherin (PERI_MOUSE)	27	13	14
P42932	T-complex protein 1 subunit theta (TCPQ_MOUSE)	27	22	5
Q9D554	Splicing factor 3A subunit 3 (SF3A3_MOUSE)	27	25	2
Q9QY76	Vesicle-associated membrane protein-associated protein B (VAPB_MOUSE)	27	26	1
Q9CZT6	Protein CMSS1 (CMS1_MOUSE)	26	19	7
Q9DCX2	ATP synthase subunit d, mitochondrial (ATP5H_MOUSE)	26	22	4
P60898	DNA-directed RNA polymerase II subunit RPB9 (RPB9_MOUSE)	25	23	2
Q61753	D-3-phosphoglycerate dehydrogenase (SERA_MOUSE)	25	21	4
Q9QXE7	F-box-like/WD repeat-containing protein TBL1X (TBL1X_MOUSE)	25	25	0
P97379	Ras GTPase-activating protein-binding protein 2 (G3BP2_MOUSE)	24	14	10
Q60715	Prolyl 4-hydroxylase subunit alpha-1 (P4HA1_MOUSE)	24	19	5
Q91VM5	RNA binding motif protein, X-linked-like-1 (RMXL1_MOUSE)	24	13	11
Q91YQ5	Dolichyl-diphosphooligosaccharide--protein glycosyltransferase subunit 1 (RPN1_MOUSE)	24	20	4
Q3U487	E3 ubiquitin-protein ligase HECTD3 (HECD3_MOUSE)	23	22	1
Q6P5E4	UDP-glucose:glycoprotein glucosyltransferase 1 (UGGG1_MOUSE)	23	19	4
Q9CXY6	Interleukin enhancer-binding factor 2 (ILF2_MOUSE)	23	22	1
O88685	26S proteasome regulatory subunit 6A (PRS6A_MOUSE)	22	20	2
P62334	26S proteasome regulatory subunit 10B (PRS10_MOUSE)	22	21	1
Q9CYI4	Putative RNA-binding protein Luc7-like 1 (LUC7L_MOUSE)	22	4	18
Q9D1D4	Transmembrane emp24 domain-containing protein 10 (TMEDA_MOUSE)	22	18	4
Q9JIG7	Coiled-coil domain-containing protein 22 (CCD22_MOUSE)	22	22	0
P80317	T-complex protein 1 subunit zeta (TCPZ_MOUSE)	21	17	4
Q91WG4	Elongator complex protein 2 (ELP2_MOUSE)	21	18	3
Q922Q8	Leucine-rich repeat-containing protein 59 (LRC59_MOUSE)	21	10	11
Q99104	Unconventional myosin-Va (MYO5A_MOUSE)	21	9	12
B8ZXI1	Queuine tRNA-ribosyltransferase accessory subunit 2 (QTRT2_MOUSE)	20	17	3
O08579	Emerin (EMD_MOUSE)	20	18	2
P10853	Histone H2B type 1-F/J/L (H2B1F_MOUSE)	20	7	13
P80316	T-complex protein 1 subunit epsilon (TCPE_MOUSE)	20	18	2
Q8JZN5	Complex I assembly factor ACAD9, mitochondrial (ACAD9_MOUSE)	20	18	2
Q8K3A9	7SK snRNA methylphosphate capping enzyme (MEPCE_MOUSE)	20	10	10
Q9D0I9	Arginine--tRNA ligase, cytoplasmic (SYRC_MOUSE)	20	18	2

O55022	Membrane-associated progesterone receptor component 1 (PGRC1_MOUSE)	19	17	2
P15864	Histone H1,2 (H12_MOUSE)	19	0	19
Q60716	Prolyl 4-hydroxylase subunit alpha-2 (P4HA2_MOUSE)	19	16	3
Q9WU20	Methylenetetrahydrofolate reductase (MTHR_MOUSE)	19	17	2
O08638	Myosin-11 (MYH11_MOUSE)	18	7	11
P43274	Histone H1,4 (H14_MOUSE)	18	0	18
P59708	Splicing factor 3B subunit 6 (SF3B6_MOUSE)	18	14	4
P60122	RuvB-like 1 (RUVB1_MOUSE)	18	14	4
Q99P72	Reticulon-4 (RTN4_MOUSE)	18	17	1
Q9CXL3	Uncharacterized protein C7orf50 homolog (CG050_MOUSE)	18	5	13
Q62186	Translocon-associated protein subunit delta (SSRD_MOUSE)	17	16	1
Q8R3Q2	Serine/threonine-protein phosphatase 6 regulatory subunit 2 (PP6R2_MOUSE)	17	17	0
Q6NZL0	Protein SOGA3 (SOGA3_MOUSE)	16	16	0
Q9CQX2	Cytochrome b5 type B (CYB5B_MOUSE)	16	15	1
Q9D7M1	Glucose-induced degradation protein 8 homolog (GID8_MOUSE)	16	16	0
Q9Z0Y1	Dynactin subunit 3 (DCTN3_MOUSE)	16	13	3
P18572	Basigin (BASI_MOUSE)	15	13	2
P61290	Proteasome activator complex subunit 3 (PSME3_MOUSE)	15	15	0
P67778	Prohibitin (PHB_MOUSE)	15	13	2
Q8BMK4	Cytoskeleton-associated protein 4 (CKAP4_MOUSE)	15	15	0
Q8C6G8	WD repeat-containing protein 26 (WDR26_MOUSE)	15	14	1
Q9CR59	Growth arrest and DNA damage-inducible proteins-interacting protein 1 (G45IP_MOUSE)	15	12	3
Q9DBR1	5'-3' exoribonuclease 2 (XRN2_MOUSE)	15	15	0
Q9QYI4	DnaJ homolog subfamily B member 12 (DJB12_MOUSE)	15	15	0
P56873	Protein ZNRD2 (ZNRD2_MOUSE)	14	12	2
Q3TVI4	Protein HEXIM2 (HEXI2_MOUSE)	14	12	2
Q61029	Lamina-associated polypeptide 2, isoforms beta/delta/epsilon/gamma (LAP2B_MOUSE)	14	12	2
Q80WJ7	Protein LYRIC (LYRIC_MOUSE)	14	1	13
Q8BX10	Serine/threonine-protein phosphatase PGAM5, mitochondrial (PGAM5_MOUSE)	14	11	3
Q8R5C5	Beta-centractin (ACTY_MOUSE)	14	14	0
Q91XD7	Protein disulfide isomerase Creld1 (CREL1_MOUSE)	14	13	1
Q9D287	Pre-mRNA-splicing factor SPF27 (SPF27_MOUSE)	14	14	0
Q9WUB0	RanBP-type and C3HC4-type zinc finger-containing protein 1 (HOIL1_MOUSE)	14	14	0
O88522	NF-kappa-B essential modulator (NEMO_MOUSE)	13	13	0
P21995	Embigin (EMB_MOUSE)	13	11	2
P43276	Histone H1,5 (H15_MOUSE)	13	0	13
P70168	Importin subunit beta-1 (IMB1_MOUSE)	13	12	1

Q501J6	Probable ATP-dependent RNA helicase DDX17 (DDX17_MOUSE)	13	13	0
Q62383	Transcription elongation factor SPT6 (SPT6H_MOUSE)	13	12	1
Q923D4	Splicing factor 3B subunit 5 (SF3B5_MOUSE)	13	10	3
Q99J62	Replication factor C subunit 4 (RFC4_MOUSE)	13	12	1
Q9CQE8	RNA transcription, translation and transport factor protein (RTRAF_MOUSE)	13	13	0
Q9D0E1	Heterogeneous nuclear ribonucleoprotein M (HNRPM_MOUSE)	13	10	3
Q9D0M3	Cytochrome c1, heme protein, mitochondrial (CY1_MOUSE)	13	13	0
Q9DB42	Zinc finger protein 593 (ZN593_MOUSE)	13	8	5
P19783	Cytochrome c oxidase subunit 4 isoform 1, mitochondrial (COX41_MOUSE)	12	12	0
P46638	Ras-related protein Rab-11B (RB11B_MOUSE)	12	8	4
P63087	Serine/threonine-protein phosphatase PP1-gamma catalytic subunit (PP1G_MOUSE)	12	11	1
Q8R010	Aminoacyl tRNA synthase complex-interacting multifunctional protein 2 (AIMP2_MOUSE)	12	7	5
Q91WE3	Ribonuclease P protein subunit p25 (RPP25_MOUSE)	12	9	3
Q9DBG3	AP-2 complex subunit beta (AP2B1_MOUSE)	12	12	0
Q9DCW4	Electron transfer flavoprotein subunit beta (ETFB_MOUSE)	12	12	0
O08848	60 kDa SS-A/Ro ribonucleoprotein (RO60_MOUSE)	11	11	0
O89050	Muskelin (MKLN1_MOUSE)	11	11	0
P62996	Transformer-2 protein homolog beta (TRA2B_MOUSE)	11	0	11
Q03958	Prefoldin subunit 6 (PFD6_MOUSE)	11	11	0
Q06335	Amyloid-like protein 2 (APLP2_MOUSE)	11	11	0
Q5XJE5	RNA polymerase-associated protein LEO1 (LEO1_MOUSE)	11	9	2
Q61249	Immunoglobulin-binding protein 1 (IGBP1_MOUSE)	11	9	2
Q6P2L7	Protein GOLM2 (GOLM2_MOUSE)	11	11	0
Q7TMF2	3'-5' exoribonuclease 1 (ERI1_MOUSE)	11	10	1
Q80UU9	Membrane-associated progesterone receptor component 2 (PGRC2_MOUSE)	11	10	1
Q8BG32	26S proteasome non-ATPase regulatory subunit 11 (PSD11_MOUSE)	11	11	0
Q8BJH1	Zinc finger C2HC domain-containing protein 1A (ZC21A_MOUSE)	11	4	7
Q8BP47	Asparagine--tRNA ligase, cytoplasmic (SYNC_MOUSE)	11	11	0
Q8BTI8	Serine/arginine repetitive matrix protein 2 (SRRM2_MOUSE)	11	6	5
Q8BXZ1	Protein disulfide-isomerase TMX3 (TMX3_MOUSE)	11	11	0
Q8CI43	Myosin light chain 6B (MYL6B_MOUSE)	11	8	3
Q8K019	Bcl-2-associated transcription factor 1 (BCLF1_MOUSE)	11	0	11
Q8VHK9	ATP-dependent DNA/RNA helicase DHX36 (DHX36_MOUSE)	11	10	1
Q91VN6	Probable ATP-dependent RNA helicase DDX41 (DDX41_MOUSE)	11	11	0

Q91W96	Anaphase-promoting complex subunit 4 (APC4_MOUSE)	11	11	0
Q9CZW5	Mitochondrial import receptor subunit TOM70 (TOM70_MOUSE)	11	10	1
Q9CZX0	Elongator complex protein 3 (ELP3_MOUSE)	11	11	0
Q9DB05	Alpha-soluble NSF attachment protein (SNAA_MOUSE)	11	11	0
Q9DBD5	Proline-, glutamic acid- and leucine-rich protein 1 (PELP1_MOUSE)	11	11	0
Q9QZH6	Evolutionarily conserved signaling intermediate in Toll pathway, mitochondrial (ECSIT_MOUSE)	11	11	0
Q9Z1X4	Interleukin enhancer-binding factor 3 (ILF3_MOUSE)	11	9	2
O70252	Heme oxygenase 2 (HMOX2_MOUSE)	10	10	0
P11438	Lysosome-associated membrane glycoprotein 1 (LAMP1_MOUSE)	10	8	2
P43275	Histone H1,1 (H11_MOUSE)	10	2	8
P63330	Serine/threonine-protein phosphatase 2A catalytic subunit alpha isoform (PP2AA_MOUSE)	10	10	0
P97452	Ribosome biogenesis protein BOP1 (BOP1_MOUSE)	10	10	0
Q14C51	Pentatricopeptide repeat domain-containing protein 3, mitochondrial (PTCD3_MOUSE)	10	10	0
Q62465	Synaptic vesicle membrane protein VAT-1 homolog (VAT1_MOUSE)	10	9	1
Q8BJY1	26S proteasome non-ATPase regulatory subunit 5 (PSMD5_MOUSE)	10	10	0
Q8K1H7	T-complex protein 11-like protein 2 (T11L2_MOUSE)	10	10	0
Q8VDL4	ADP-dependent glucokinase (ADPGK_MOUSE)	10	9	1
Q91WN1	DnaJ homolog subfamily C member 9 (DNJC9_MOUSE)	10	9	1
Q921X6	DNA-directed RNA polymerase III subunit RPC6 (RPC6_MOUSE)	10	9	1
Q99JP7	Glutathione hydrolase 7 (GGT7_MOUSE)	10	10	0
Q99LF4	RNA-splicing ligase RtcB homolog (RTCB_MOUSE)	10	9	1
Q9CYH6	Ribosome biogenesis regulatory protein homolog (RRS1_MOUSE)	10	0	10
Q9CZG3	COMM domain-containing protein 8 (COMD8_MOUSE)	10	10	0
Q9D0B0	Serine/arginine-rich splicing factor 9 (SRSF9_MOUSE)	10	10	0
Q9WVJ2	26S proteasome non-ATPase regulatory subunit 13 (PSD13_MOUSE)	10	10	0
P12787	Cytochrome c oxidase subunit 5A, mitochondrial (COX5A_MOUSE)	9	8	1
P28658	Ataxin-10 (ATX10_MOUSE)	9	9	0
P53564	Homeobox protein cut-like 1 (CUX1_MOUSE)	9	9	0
P97450	ATP synthase-coupling factor 6, mitochondrial (ATP5J_MOUSE)	9	9	0
Q4VBE8	WD repeat-containing protein 18 (WDR18_MOUSE)	9	7	2
Q63829	COMM domain-containing protein 3 (COMD3_MOUSE)	9	9	0
Q6ZQI3	Malectin (MLEC_MOUSE)	9	9	0
Q80TR8	DDB1- and CUL4-associated factor 1 (DCAF1_MOUSE)	9	9	0
Q80UW8	DNA-directed RNA polymerases I, II, and III subunit RPABC1 (RPAB1_MOUSE)	9	7	2

Q8BWM0	Prostaglandin E synthase 2 (PGES2_MOUSE)	9	9	0
Q8BWW4	La-related protein 4 (LARP4_MOUSE)	9	5	4
Q8BXC6	COMM domain-containing protein 2 (COMD2_MOUSE)	9	9	0
Q8C0L0	Thioredoxin-related transmembrane protein 4 (TMX4_MOUSE)	9	9	0
Q8K370	Acyl-CoA dehydrogenase family member 10 (ACD10_MOUSE)	9	9	0
Q8QZY9	Splicing factor 3B subunit 4 (SF3B4_MOUSE)	9	6	3
Q8R2Y8	Peptidyl-tRNA hydrolase 2, mitochondrial (PTH2_MOUSE)	9	7	2
Q8R3F9	Speckle targeted PIP5K1A-regulated poly(A) polymerase (STPAP_MOUSE)	9	9	0
Q91W59	RNA-binding motif, single-stranded-interacting protein 1 (RBMS1_MOUSE)	9	9	0
Q99J95	Cyclin-dependent kinase 9 (CDK9_MOUSE)	9	7	2
Q99NB9	Splicing factor 3B subunit 1 (SF3B1_MOUSE)	9	9	0
Q9CQQ7	ATP synthase F(0) complex subunit B1, mitochondrial (AT5F1_MOUSE)	9	8	1
Q9D1M4	Eukaryotic translation elongation factor 1 epsilon-1 (MCA3_MOUSE)	9	9	0
Q9D2N9	Vacuolar protein sorting-associated protein 33A (VP33A_MOUSE)	9	9	0
Q9D855	Cytochrome b-c1 complex subunit 7 (QCR7_MOUSE)	9	9	0
Q9D903	Probable rRNA-processing protein EBP2 (EBP2_MOUSE)	9	1	8
Q9DBZ1	Inhibitor of nuclear factor kappa-B kinase-interacting protein (IKIP_MOUSE)	9	9	0
Q9DCS9	NADH dehydrogenase [ubiquinone] 1 beta subcomplex subunit 10 (NDUBA_MOUSE)	9	9	0
P0C0S6	Histone H2A,Z (H2AZ_MOUSE)	8	5	3
P18872	Guanine nucleotide-binding protein G(o) subunit alpha (GNAO_MOUSE)	8	6	2
P21126	Ubiquitin-like protein 4A (UBL4A_MOUSE)	8	8	0
P35700	Peroxiredoxin-1 (PRDX1_MOUSE)	8	8	0
P46735	Unconventional myosin-Ib (MYO1B_MOUSE)	8	6	2
P51863	V-type proton ATPase subunit d 1 (VA0D1_MOUSE)	8	8	0
P52651	Homeobox protein Rhox5 (RHOX5_MOUSE)	8	7	1
P60879	Synaptosomal-associated protein 25 (SNP25_MOUSE)	8	7	1
P62192	26S proteasome regulatory subunit 4 (PRS4_MOUSE)	8	7	1
P80315	T-complex protein 1 subunit delta (TCPD_MOUSE)	8	7	1
P97434	Myosin phosphatase Rho-interacting protein (MPRIP_MOUSE)	8	8	0
Q3TX08	tRNA (guanine(26)-N(2))-dimethyltransferase (TRM1_MOUSE)	8	8	0
Q505D1	Serine/threonine-protein phosphatase 6 regulatory ankyrin repeat subunit A (ANR28_MOUSE)	8	8	0
Q6NVF9	Cleavage and polyadenylation specificity factor subunit 6 (CPSF6_MOUSE)	8	3	5
Q8BGA5	KRR1 small subunit processome component homolog (KRR1_MOUSE)	8	4	4

Q8BUR9	Mitotic-spindle organizing protein 1 (MZT1_MOUSE)	8	7	1
Q8JZY2	COMM domain-containing protein 10 (COMDA_MOUSE)	8	8	0
Q8JZZ7	Adhesion G protein-coupled receptor L2 (AGRL2_MOUSE)	8	8	0
Q8K2C7	Protein OS-9 (OS9_MOUSE)	8	7	1
Q8VDD8	WASH complex subunit 1 (WASH1_MOUSE)	8	8	0
Q91VD9	NADH-ubiquinone oxidoreductase 75 kDa subunit, mitochondrial (NDUS1_MOUSE)	8	8	0
Q91WS0	CDGSH iron-sulfur domain-containing protein 1 (CISD1_MOUSE)	8	8	0
Q99KV1	DnaJ homolog subfamily B member 11 (DJB11_MOUSE)	8	7	1
Q9CRB9	MICOS complex subunit Mic19 (MIC19_MOUSE)	8	8	0
Q9D8Y0	EF-hand domain-containing protein D2 (EFHD2_MOUSE)	8	8	0
Q9JKY0	CCR4-NOT transcription complex subunit 9 (CNOT9_MOUSE)	8	8	0
Q9Z0N1	Eukaryotic translation initiation factor 2 subunit 3, X-linked (IF2G_MOUSE)	8	6	2
Q9Z1Z0	General vesicular transport factor p115 (USO1_MOUSE)	8	8	0
O35114	Lysosome membrane protein 2 (SCRB2_MOUSE)	7	7	0
P13595	Neural cell adhesion molecule 1 (NCAM1_MOUSE)	7	7	0
P42669	Transcriptional activator protein Pur-alpha (PURA_MOUSE)	7	6	1
P58404	Striatin-4 (STRN4_MOUSE)	7	7	0
P60335	Poly(rC)-binding protein 1 (PCBP1_MOUSE)	7	5	2
Q08288	Cell growth-regulating nucleolar protein (LYAR_MOUSE)	7	0	7
Q60749	KH domain-containing, RNA-binding, signal transduction-associated protein 1 (KHDR1_MOUSE)	7	4	3
Q61739	Integrin alpha-6 (ITA6_MOUSE)	7	7	0
Q6P4S6	Serine/threonine-protein kinase SIK3 (SIK3_MOUSE)	7	7	0
Q6P6I6	DNA-directed RNA polymerase II subunit GRINL1A (GRL1A_MOUSE)	7	7	0
Q6PD26	GPI transamidase component PIG-S (PIGS_MOUSE)	7	6	1
Q7TQ95	Endoplasmic reticulum junction formation protein lunapark (LNP_MOUSE)	7	6	1
Q8BFX1	E3 ubiquitin-protein ligase RNF187 (RN187_MOUSE)	7	7	0
Q8BXA1	Golgi integral membrane protein 4 (GOLI4_MOUSE)	7	7	0
Q8CCF0	U4/U6 small nuclear ribonucleoprotein Prp31 (PRP31_MOUSE)	7	7	0
Q8CGC7	Bifunctional glutamate/proline--tRNA ligase (SYEP_MOUSE)	7	3	4
Q8K2Q0	COMM domain-containing protein 9 (COMD9_MOUSE)	7	6	1
Q8R1V4	Transmembrane emp24 domain-containing protein 4 (TMED4_MOUSE)	7	6	1
Q920E5	Farnesyl pyrophosphate synthase (FPPS_MOUSE)	7	7	0
Q922B2	Aspartate--tRNA ligase, cytoplasmic (SYDC_MOUSE)	7	5	2

Q923D5	WW domain-binding protein 11 (WBP11_MOUSE)	7	3	4
Q923E4	NAD-dependent protein deacetylase sirtuin-1 (SIR1_MOUSE)	7	7	0
Q99M08	Uncharacterized protein C4orf3 homolog (CD003_MOUSE)	7	6	1
Q9CQ22	Ragulator complex protein LAMTOR1 (LTOR1_MOUSE)	7	7	0
Q9CYX7	RRP15-like protein (RRP15_MOUSE)	7	2	5
Q9D1K2	V-type proton ATPase subunit F (VATF_MOUSE)	7	7	0
Q9D394	Protein RUFY3 (RUFY3_MOUSE)	7	7	0
Q9D824	Pre-mRNA 3'-end-processing factor FIP1 (FIP1_MOUSE)	7	5	2
Q9DCT2	NADH dehydrogenase [ubiquinone] iron-sulfur protein 3, mitochondrial (NDUS3_MOUSE)	7	7	0
Q9JKK7	Tropomodulin-2 (TMOD2_MOUSE)	7	6	1
Q9QYE6	Golgin subfamily A member 5 (GOGA5_MOUSE)	7	7	0
Q9WUP7	Ubiquitin carboxyl-terminal hydrolase isozyme L5 (UCHL5_MOUSE)	7	7	0
O35129	Prohibitin-2 (PHB2_MOUSE)	6	6	0
O54734	Dolichyl-diphosphooligosaccharide--protein glycosyltransferase 48 kDa subunit (OST48_MOUSE)	6	5	1
O54825	Bystin (BYST_MOUSE)	6	5	1
P18155	Bifunctional methylenetetrahydrofolate dehydrogenase/cyclohydrolase, mitochondrial (MTDC_MOUSE)	6	6	0
P18242	Cathepsin D (CATD_MOUSE)	6	6	0
P26369	Splicing factor U2AF 65 kDa subunit (U2AF2_MOUSE)	6	2	4
P55821	Stathmin-2 (STMN2_MOUSE)	6	6	0
P57776	Elongation factor 1-delta (EF1D_MOUSE)	6	4	2
P61965	WD repeat-containing protein 5 (WDR5_MOUSE)	6	2	4
P62196	26S proteasome regulatory subunit 8 (PRS8_MOUSE)	6	6	0
P62874	Guanine nucleotide-binding protein G(I)/G(S)/G(T) subunit beta-1 (GBB1_MOUSE)	6	4	2
P63024	Vesicle-associated membrane protein 3 (VAMP3_MOUSE)	6	6	0
P70279	Surfeit locus protein 6 (SURF6_MOUSE)	6	0	6
P83887	Tubulin gamma-1 chain (TBG1_MOUSE)	6	6	0
P99028	Cytochrome b-c1 complex subunit 6, mitochondrial (QCR6_MOUSE)	6	5	1
Q3TC46	Protein PAT1 homolog 1 (PATL1_MOUSE)	6	6	0
Q3THK3	General transcription factor IIF subunit 1 (T2FA_MOUSE)	6	4	2
Q3V4B5	COMM domain-containing protein 6 (COMD6_MOUSE)	6	6	0
Q60899	ELAV-like protein 2 (ELAV2_MOUSE)	6	6	0
Q64523	Histone H2A type 2-C (H2A2C_MOUSE)	6	6	0
Q68FL6	Methionine--tRNA ligase, cytoplasmic (SYMC_MOUSE)	6	6	0
Q6PEB6	MOB-like protein phocein (PHOCN_MOUSE)	6	5	1
Q7TMX5	Protein SHQ1 homolog (SHQ1_MOUSE)	6	6	0
Q7TN79	A-kinase anchor protein 7 isoform gamma (AKA7G_MOUSE)	6	6	0

Q8BHD8	Protein-L-isoaspartate O-methyltransferase domain-containing protein 2 (PCMD2_MOUSE)	6	6	0
Q8BLN5	Lanosterol synthase (LSS_MOUSE)	6	6	0
Q8K0V4	CCR4-NOT transcription complex subunit 3 (CNOT3_MOUSE)	6	6	0
Q8K2B0	Endoplasmic reticulum protein SC65 (SC65_MOUSE)	6	6	0
Q8K4M5	COMM domain-containing protein 1 (COMD1_MOUSE)	6	6	0
Q8R015	Biogenesis of lysosome-related organelles complex 1 subunit 5 (BL1S5_MOUSE)	6	6	0
Q8R035	Peptidyl-tRNA hydrolase ICT1, mitochondrial (ICT1_MOUSE)	6	5	1
Q8R323	Replication factor C subunit 3 (RFC3_MOUSE)	6	6	0
Q8R395	COMM domain-containing protein 5 (COMD5_MOUSE)	6	6	0
Q8VDJ3	Vigilin (VIGLN_MOUSE)	6	6	0
Q8VEH8	Endoplasmic reticulum lectin 1 (ERLEC_MOUSE)	6	6	0
Q8VEJ9	Vacuolar protein sorting-associated protein 4A (VPS4A_MOUSE)	6	6	0
Q91WA6	Sharpin (SHRPN_MOUSE)	6	6	0
Q99JI4	26S proteasome non-ATPase regulatory subunit 6 (PSMD6_MOUSE)	6	6	0
Q99LJ0	CTTNBP2 N-terminal-like protein (CT2NL_MOUSE)	6	6	0
Q9CPT5	Nucleolar protein 16 (NOP16_MOUSE)	6	6	0
Q9CRA8	Exosome complex component RRP46 (EXOS5_MOUSE)	6	6	0
Q9D187	Cytosolic iron-sulfur assembly component 2B (CIA2B_MOUSE)	6	5	1
Q9D1M0	Protein SEC13 homolog (SEC13_MOUSE)	6	6	0
Q9DB20	ATP synthase subunit O, mitochondrial (ATPO_MOUSE)	6	6	0
Q9DB77	Cytochrome b-c1 complex subunit 2, mitochondrial (QCR2_MOUSE)	6	6	0
Q9DBR7	Protein phosphatase 1 regulatory subunit 12A (MYPT1_MOUSE)	6	6	0
Q9DCN2	NADH-cytochrome b5 reductase 3 (NB5R3_MOUSE)	6	5	1
Q9EP72	ER membrane protein complex subunit 7 (EMC7_MOUSE)	6	6	0
Q9EPA7	Nicotinamide/nicotinic acid mononucleotide adenylyltransferase 1 (NMNA1_MOUSE)	6	4	2
Q9QZE5	Coatomer subunit gamma-1 (COPG1_MOUSE)	6	6	0
Q9R0A0	Peroxisomal membrane protein PEX14 (PEX14_MOUSE)	6	6	0
Q9WUK4	Replication factor C subunit 2 (RFC2_MOUSE)	6	6	0
C0HKE1	Histone H2A type 1-B (H2A1B_MOUSE)	5	5	0
O09012	Peroxisomal targeting signal 1 receptor (PEX5_MOUSE)	5	5	0
O35295	Transcriptional activator protein Pur-beta (PURB_MOUSE)	5	5	0
O35685	Nuclear migration protein nudC (NUDC_MOUSE)	5	5	0
P24668	Cation-dependent mannose-6-phosphate receptor (MPRD_MOUSE)	5	5	0
P26339	Chromogranin-A (CMGA_MOUSE)	5	5	0
P28663	Beta-soluble NSF attachment protein (SNAB_MOUSE)	5	5	0

P35951	Low-density lipoprotein receptor (LDLR_MOUSE)	5	5	0
P47758	Signal recognition particle receptor subunit beta (SRPRB_MOUSE)	5	5	0
P61804	Dolichyl-diphosphooligosaccharide--protein glycosyltransferase subunit DAD1 (DAD1_MOUSE)	5	4	1
P62878	E3 ubiquitin-protein ligase RBX1 (RBX1_MOUSE)	5	5	0
P63271	Transcription elongation factor SPT4-A (SPT4A_MOUSE)	5	5	0
P80313	T-complex protein 1 subunit eta (TCPH_MOUSE)	5	4	1
Q3UI43	BRISC and BRCA1-A complex member 1 (BABA1_MOUSE)	5	5	0
Q3UL36	Arginine and glutamate-rich protein 1 (ARGL1_MOUSE)	5	0	5
Q60930	Voltage-dependent anion-selective channel protein 2 (VDAC2_MOUSE)	5	5	0
Q61137	Astrotactin-1 (ASTN1_MOUSE)	5	5	0
Q61701	ELAV-like protein 4 (ELAV4_MOUSE)	5	5	0
Q62425	Cytochrome c oxidase subunit NDUFA4 (NDUA4_MOUSE)	5	4	1
Q6DYE8	Ectonucleotide pyrophosphatase/phosphodiesterase family member 3 (ENPP3_MOUSE)	5	5	0
Q7TMQ7	WD repeat-containing protein 91 (WDR91_MOUSE)	5	5	0
Q80VL1	Tudor and KH domain-containing protein (TDRKH_MOUSE)	5	5	0
Q8BHX1	HAUS augmin-like complex subunit 1 (HAUS1_MOUSE)	5	5	0
Q8BIA4	F-box/WD repeat-containing protein 8 (FBXW8_MOUSE)	5	5	0
Q8BMC4	Nucleolar protein 9 (NOP9_MOUSE)	5	5	0
Q8BMS1	Trifunctional enzyme subunit alpha, mitochondrial (ECHA_MOUSE)	5	4	1
Q8BQX5	Transmembrane and coiled-coil domain-containing protein 6 (TMCO6_MOUSE)	5	5	0
Q8BT07	Centrosomal protein of 55 kDa (CEP55_MOUSE)	5	5	0
Q8C5L3	CCR4-NOT transcription complex subunit 2 (CNOT2_MOUSE)	5	5	0
Q8CFI7	DNA-directed RNA polymerase II subunit RPB2 (RPB2_MOUSE)	5	5	0
Q8K3J1	NADH dehydrogenase [ubiquinone] iron-sulfur protein 8, mitochondrial (NDUS8_MOUSE)	5	5	0
Q8VE99	Coiled-coil domain-containing protein 115 (CC115_MOUSE)	5	5	0
Q91WD5	NADH dehydrogenase [ubiquinone] iron-sulfur protein 2, mitochondrial (NDUS2_MOUSE)	5	5	0
Q91YT0	NADH dehydrogenase [ubiquinone] flavoprotein 1, mitochondrial (NDUV1_MOUSE)	5	5	0
Q99M87	DnaJ homolog subfamily A member 3, mitochondrial (DNJA3_MOUSE)	5	4	1
Q99PM9	Uridine-cytidine kinase 2 (UCK2_MOUSE)	5	5	0
Q9CPP6	NADH dehydrogenase [ubiquinone] 1 alpha subcomplex subunit 5 (NDUA5_MOUSE)	5	5	0

Q9CQA9	Cancer-related nucleoside-triphosphatase homolog (NTPCR_MOUSE)	5	5	0
Q9CWX2	Complex I intermediate-associated protein 30, mitochondrial (CIA30_MOUSE)	5	5	0
Q9CZA6	Nuclear distribution protein nudE homolog 1 (NDE1_MOUSE)	5	5	0
Q9D0F3	Protein ERGIC-53 (LMAN1_MOUSE)	5	5	0
Q9D483	DNA-directed RNA polymerase III subunit RPC3 (RPC3_MOUSE)	5	5	0
Q9D6Z1	Nucleolar protein 56 (NOP56_MOUSE)	5	0	5
Q9DCH2	Ribonuclease P protein subunit p20 (POP7_MOUSE)	5	5	0
Q9EQS3	c-Myc-binding protein (MYCBP_MOUSE)	5	5	0
Q9JHS4	ATP-dependent Clp protease ATP-binding subunit clpX-like, mitochondrial (CLPX_MOUSE)	5	4	1
Q9JKX4	Protein AATF (AATF_MOUSE)	5	5	0
Q9JMH9	Unconventional myosin-XVIIIa (MY18A_MOUSE)	5	0	5
O35465	Peptidyl-prolyl cis-trans isomerase FKBP8 (FKBP8_MOUSE)	4	4	0
O70439	Syntaxin-7 (STX7_MOUSE)	4	4	0
O88952	Protein lin-7 homolog C (LIN7C_MOUSE)	4	4	0
P01897	H-2 class I histocompatibility antigen, L-D alpha chain (HA1L_MOUSE)	4	4	0
P14901	Heme oxygenase 1 (HMOX1_MOUSE)	4	4	0
P17439	Lysosomal acid glucosylceramidase (GLCM_MOUSE)	4	4	0
P22437	Prostaglandin G/H synthase 1 (PGH1_MOUSE)	4	4	0
P40142	Transketolase (TKT_MOUSE)	4	4	0
P46460	Vesicle-fusing ATPase (NSF_MOUSE)	4	4	0
P51912	Neutral amino acid transporter B(0) (AAAT_MOUSE)	4	4	0
P59913	Protein-L-isoaspartate O-methyltransferase domain-containing protein 1 (PCMD1_MOUSE)	4	4	0
P62482	Voltage-gated potassium channel subunit beta-2 (KCAB2_MOUSE)	4	4	0
P63001	Ras-related C3 botulinum toxin substrate 1 (RAC1_MOUSE)	4	4	0
P63094	Guanine nucleotide-binding protein G(s) subunit alpha isoforms short (GNAS2_MOUSE)	4	4	0
P63213	Guanine nucleotide-binding protein G(I)/G(S)/G(O) subunit gamma-2 (GBG2_MOUSE)	4	4	0
P97300	Neuroplastin (NPTN_MOUSE)	4	4	0
Q02614	SAP30-binding protein (S30BP_MOUSE)	4	4	0
Q04750	DNA topoisomerase 1 (TOP1_MOUSE)	4	0	4
Q3TXT3	SOSS complex subunit C (SOSSC_MOUSE)	4	4	0
Q3UHX9	Putative methyltransferase C9orf114 homolog (CI114_MOUSE)	4	4	0
Q3URD3	Sarcolemmal membrane-associated protein (SLMAP_MOUSE)	4	4	0
Q3V009	Transmembrane emp24 domain-containing protein 1 (TMED1_MOUSE)	4	4	0
Q5U4D9	THO complex subunit 6 homolog (THOC6_MOUSE)	4	4	0

Q60931	Voltage-dependent anion-selective channel protein 3 (VDAC3_MOUSE)	4	4	0
Q69ZQ2	Pre-mRNA-splicing factor ISY1 homolog (ISY1_MOUSE)	4	4	0
Q6PHU5	Sortilin (SORT_MOUSE)	4	4	0
Q6PIP5	NudC domain-containing protein 1 (NUDC1_MOUSE)	4	4	0
Q80U04	E3 ubiquitin-protein ligase Praja-2 (PJA2_MOUSE)	4	4	0
Q80XN0	D-beta-hydroxybutyrate dehydrogenase, mitochondrial (BDH_MOUSE)	4	4	0
Q80YQ8	E3 ubiquitin-protein ligase RMND5A (RMD5A_MOUSE)	4	4	0
Q8BG30	Negative elongation factor A (NELFA_MOUSE)	4	4	0
Q8BG94	COMM domain-containing protein 7 (COMD7_MOUSE)	4	4	0
Q8BHE8	m-AAA protease-interacting protein 1, mitochondrial (MAIP1_MOUSE)	4	4	0
Q8BIQ5	Cleavage stimulation factor subunit 2 (CSTF2_MOUSE)	4	4	0
Q8CGZ0	Calcium homeostasis endoplasmic reticulum protein (CHERP_MOUSE)	4	4	0
Q8K0H5	Transcription initiation factor TFIID subunit 10 (TAF10_MOUSE)	4	4	0
Q8VBT0	Thioredoxin-related transmembrane protein 1 (TMX1_MOUSE)	4	4	0
Q8VED2	Biogenesis of lysosome-related organelles complex 1 subunit 4 (BL1S4_MOUSE)	4	4	0
Q8VI33	Transcription initiation factor TFIID subunit 9 (TAF9_MOUSE)	4	4	0
Q99JY0	Trifunctional enzyme subunit beta, mitochondrial (ECHB_MOUSE)	4	4	0
Q9CQA5	Mediator of RNA polymerase II transcription subunit 4 (MED4_MOUSE)	4	4	0
Q9CRD2	ER membrane protein complex subunit 2 (EMC2_MOUSE)	4	4	0
Q9CSN1	SNW domain-containing protein 1 (SNW1_MOUSE)	4	4	0
Q9CWZ7	Gamma-soluble NSF attachment protein (SNAG_MOUSE)	4	4	0
Q9CX56	26S proteasome non-ATPase regulatory subunit 8 (PSMD8_MOUSE)	4	4	0
Q9CY50	Translocon-associated protein subunit alpha (SSRA_MOUSE)	4	4	0
Q9D0R4	Probable ATP-dependent RNA helicase DDX56 (DDX56_MOUSE)	4	4	0
Q9D2V5	Protein AAR2 homolog (AAR2_MOUSE)	4	4	0
Q9D706	RNA polymerase II-associated protein 3 (RPAP3_MOUSE)	4	4	0
Q9D818	Suppressor APC domain-containing protein 2 (SAPC2_MOUSE)	4	4	0
Q9D8W5	26S proteasome non-ATPase regulatory subunit 12 (PSD12_MOUSE)	4	4	0
Q9DBR3	Armadillo repeat-containing protein 8 (ARMC8_MOUSE)	4	4	0
Q9EPL8	Importin-7 (IPO7_MOUSE)	4	4	0
Q9ER00	Syntaxin-12 (STX12_MOUSE)	4	4	0

Q9JJZ4	Ubiquitin-conjugating enzyme E2 J1 (UB2J1_MOUSE)	4	4	0
Q9JKK1	Syntaxin-6 (STX6_MOUSE)	4	4	0
Q9JKL5	Calcineurin B homologous protein 3 (CHP3_MOUSE)	4	4	0
Q9QXN3	Activating signal cointegrator 1 (TRIP4_MOUSE)	4	4	0
Q9WTZ1	RING-box protein 2 (RBX2_MOUSE)	4	4	0
Q9WVE8	Protein kinase C and casein kinase substrate in neurons protein 2 (PACN2_MOUSE)	4	4	0
Q9Z1D1	Eukaryotic translation initiation factor 3 subunit G (EIF3G_MOUSE)	4	4	0
Q9Z2G6	Protein sel-1 homolog 1 (SE1L1_MOUSE)	4	4	0

Table 32 b: Relative Abundance of Mouse Proteins in the SAFit1 Dependent Eluate.

The enrichment factor (EF) comparing the relative protein abundance in both samples of the SAFit1 dependent eluate, the supernatant (4th column) and the dissolved pellet (5th column) with the relative protein abundance in the control samples (all 4 wash fraction pools, mock eluate pool) is given. The average enrichment factor is given in the 3rd column. The relative protein abundance in the mock eluate (6th column) was also compared with the relative abundance in all 4 wash fraction pools as an internal control.

Accession Number (UniProtKB)	Description	EF SAFit1 Dependent Eluate			EF Mock Eluate
		Mean	Supernatant	Pellet	
P20152	Vimentin (VIME_MOUSE)	97.1	25.5	168.8	0.0
P57784	U2 small nuclear ribonucleoprotein A' (RU2A_MOUSE)	92.7	78.1	107.4	0.0
Q60605	Myosin light polypeptide 6 (MYL6_MOUSE)	77.4	93.3	61.4	0.0
O55029	Coatomer subunit beta' (COPB2_MOUSE)	70.5	95.0	46.0	0.0
P31230	Aminoacyl tRNA synthase complex-interacting multifunctional protein 1 (AIMP1_MOUSE)	69.8	52.6	87.0	0.0
O35345	Importin subunit alpha-7 (IMA7_MOUSE)	68.0	79.8	56.3	0.0
P60229	Eukaryotic translation initiation factor 3 subunit E (EIF3E_MOUSE)	63.8	76.4	51.2	0.0
P63037	DnaJ homolog subfamily A member 1 (DNJA1_MOUSE)	56.1	56.0	56.3	0.0
Q7TMK9	Heterogeneous nuclear ribonucleoprotein Q (HNRPQ_MOUSE)	45.9	38.2	53.7	0.0
O89079	Coatomer subunit epsilon (COPE_MOUSE)	37.4	39.0	35.8	0.0
Q8QZY1	Eukaryotic translation initiation factor 3 subunit L (EIF3L_MOUSE)	35.7	45.8	25.6	0.0
Q9CWF2	Tubulin beta-2B chain (TBB2B_MOUSE)	35.5	37.3	33.6	0.0

Q9JHE7	Protein TSSC4 (TSSC4_MOUSE)	28.9	17.0	40.9	0.0
Q64337	Sequestosome-1 (SQSTM_MOUSE)	28.9	37.3	20.5	0.0
P68372	Tubulin beta-4B chain (TBB4B_MOUSE)	27.2	27.8	26.6	0.0
Q9ERD7	Tubulin beta-3 chain (TBB3_MOUSE)	25.6	25.7	25.6	0.0
Q9CQF3	Cleavage and polyadenylation specificity factor subunit 5 (CPSF5_MOUSE)	24.7	8.5	40.9	0.0
P67871	Casein kinase II subunit beta (CSK2B_MOUSE)	24.7	28.9	20.5	0.0
Q99LL5	Periodic tryptophan protein 1 homolog (PWP1_MOUSE)	24.1	4.0	44.3	0.0
O35326	Serine/arginine-rich splicing factor 5 (SRSF5_MOUSE)	21.9	11.6	32.1	0.0
Q9JK92	Heat shock protein beta-8 (HSPB8_MOUSE)	21.3	27.2	15.3	0.0
Q8VBV7	COP9 signalosome complex subunit 8 (CSN8_MOUSE)	19.6	18.7	20.5	0.0
Q9JHJ0	Tropomodulin-3 (TMOD3_MOUSE)	19.6	23.8	15.3	0.0
P99024	Tubulin beta-5 chain (TBB5_MOUSE)	18.2	18.7	17.8	0.0
P61979	Heterogeneous nuclear ribonucleoprotein K (HNRPK_MOUSE)	17.8	35.6	0.0	0.0
P16858	Glyceraldehyde-3-phosphate dehydrogenase (G3P_MOUSE)	17.0	8.5	25.6	0.0
P05213	Tubulin alpha-1B chain (TBA1B_MOUSE)	16.3	16.4	16.2	0.0
Q9D7A6	Signal recognition particle 19 kDa protein (SRP19_MOUSE)	15.9	11.3	20.5	0.0
Q9CQI7	U2 small nuclear ribonucleoprotein B" (RU2B_MOUSE)	15.3	15.3	15.3	0.0
Q91YN9	BAG family molecular chaperone regulator 2 (BAG2_MOUSE)	14.4	18.7	10.2	0.0
Q99JX4	Eukaryotic translation initiation factor 3 subunit M (EIF3M_MOUSE)	14.4	23.8	5.1	0.0
Q8BL97	Serine/arginine-rich splicing factor 7 (SRSF7_MOUSE)	13.2	3.4	23.0	0.0
Q9CWK3	CD2 antigen cytoplasmic tail-binding protein 2 (CD2B2_MOUSE)	12.8	15.3	10.2	0.0
Q3THE2	Myosin regulatory light chain 12B (ML12B_MOUSE)	12.3	14.4	10.2	0.0
Q9DCH4	Eukaryotic translation initiation factor 3 subunit F (EIF3F_MOUSE)	12.2	10.7	13.6	0.0
P56480	ATP synthase subunit beta, mitochondrial (ATPB_MOUSE)	11.7	17.0	6.4	0.0
P84104	Serine/arginine-rich splicing factor 3 (SRSF3_MOUSE)	11.5	1.4	21.5	0.0
Q6PDM2	Serine/arginine-rich splicing factor 1 (SRSF1_MOUSE)	11.1	3.6	18.6	0.0
Q8VDI7	Ubiquitin-associated domain-containing protein 1 (UBAC1_MOUSE)	10.6	13.6	7.7	0.0
Q60932	Voltage-dependent anion-selective channel protein 1 (VDAC1_MOUSE)	10.2	15.3	5.1	0.0
Q9ERG2	Striatin-3 (STRN3_MOUSE)	10.2	15.3	5.1	0.0
Q8K0G5	EARP and GARP complex-interacting protein 1 (EIPR1_MOUSE)	10.2	20.4	0.0	0.0

Q8N7N5	DDB1- and CUL4-associated factor 8 (DCAF8_MOUSE)	9.8	11.9	7.7	0.0
Q9JKB3	Y-box-binding protein 3 (YBOX3_MOUSE)	9.6	4.2	14.9	0.0
Q9D9Z5	DET1- and DDB1-associated protein 1 (DDA1_MOUSE)	9.4	5.9	12.8	0.0
P08752	Guanine nucleotide-binding protein G(i) subunit alpha-2 (GNAI2_MOUSE)	9.4	8.5	10.2	0.0
Q8BV13	COP9 signalosome complex subunit 7b (CSN7B_MOUSE)	9.2	12.6	5.8	0.0
Q61074	Protein phosphatase 1G (PPM1G_MOUSE)	9.1	8.7	9.6	0.0
P62960	Y-box-binding protein 1 (YBOX1_MOUSE)	8.7	6.4	11.0	0.0
Q99KF1	Transmembrane emp24 domain-containing protein 9 (TMED9_MOUSE)	8.5	17.0	0.0	0.0
P29341	Polyadenylate-binding protein 1 (PABP1_MOUSE)	7.6	11.5	3.8	0.0
Q8R409	Protein HEXIM1 (HEXI1_MOUSE)	7.1	5.7	8.5	0.0
Q03265	ATP synthase subunit alpha, mitochondrial (ATPA_MOUSE)	6.8	8.5	5.1	0.0
Q3TWW8	Serine/arginine-rich splicing factor 6 (SRSF6_MOUSE)	6.4	2.5	10.2	0.0
P16254	Signal recognition particle 14 kDa protein (SRP14_MOUSE)	6.1	3.5	8.8	0.0
P10126	Elongation factor 1-alpha 1 (EF1A1_MOUSE)	6.0	3.4	8.6	0.0
Q9R020	Zinc finger Ran-binding domain-containing protein 2 (ZRAB2_MOUSE)	6.0	0.0	11.9	0.0
O35127	Protein C10 (C10_MOUSE)	6.0	6.8	5.1	0.0
Q60737	Casein kinase II subunit alpha (CSK21_MOUSE)	5.9	9.3	2.6	0.0
P70699	Lysosomal alpha-glucosidase (LYAG_MOUSE)	5.9	6.3	5.4	0.0
P70403	Protein CASP (CASP_MOUSE)	5.8	11.6	0.0	0.0
P60824	Cold-inducible RNA-binding protein (CIRBP_MOUSE)	5.7	1.1	10.2	0.0
P23198	Chromobox protein homolog 3 (CBX3_MOUSE)	5.5	5.9	5.1	0.0
P58252	Elongation factor 2 (EF2_MOUSE)	5.1	10.2	0.0	0.0
Q05816	Fatty acid-binding protein 5 (FABP5_MOUSE)	5.1	10.2	0.0	0.0
Q14AI0	Sister chromatid cohesion protein DCC1 (DCC1_MOUSE)	5.1	10.2	0.0	0.0
Q810D6	Glutamate-rich WD repeat-containing protein 1 (GRWD1_MOUSE)	5.1	10.2	0.0	0.0
Q9DBC7	cAMP-dependent protein kinase type I-alpha regulatory subunit (KAP0_MOUSE)	5.1	10.2	0.0	0.0
Q9WVA4	Transgelin-2 (TAGL2_MOUSE)	5.1	10.2	0.0	0.0
Q9CWV6	PRKR-interacting protein 1 (PKRI1_MOUSE)	4.9	3.1	6.8	0.0
Q9JJT9	Phosphorylated adapter RNA export protein (PHAX_MOUSE)	4.8	8.6	1.1	0.0
Q9DBZ5	Eukaryotic translation initiation factor 3 subunit K (EIF3K_MOUSE)	4.8	4.8	4.7	0.0
O35864	COP9 signalosome complex subunit 5 (CSN5_MOUSE)	4.7	6.8	2.6	0.0
O88544	COP9 signalosome complex subunit 4 (CSN4_MOUSE)	4.6	6.4	2.8	0.0

Q60865	Caprin-1 (CAPR1_MOUSE)	4.4	3.6	5.1	0.0
Q99KJ8	Dynactin subunit 2 (DCTN2_MOUSE)	4.2	5.9	2.6	0.0
O54833	Casein kinase II subunit alpha' (CSK22_MOUSE)	4.2	8.5	0.0	0.0
Q8R3Q0	Store-operated calcium entry-associated regulatory factor (SARAF_MOUSE)	4.2	8.5	0.0	0.0
Q91YJ3	Thymocyte nuclear protein 1 (THYN1_MOUSE)	4.2	8.5	0.0	0.0
Q9D2C6	DNA-directed RNA polymerase III subunit RPC8 (RPC8_MOUSE)	4.2	8.5	0.0	0.0
Q9QZH3	Peptidyl-prolyl cis-trans isomerase E (PPIE_MOUSE)	4.2	8.5	0.0	0.0
Q9R1K9	Centrin-2 (CETN2_MOUSE)	4.2	8.5	0.0	0.0
P07901	Heat shock protein HSP 90-alpha (HS90A_MOUSE)	4.1	4.8	3.5	0.0
P11499	Heat shock protein HSP 90-beta (HS90B_MOUSE)	4.0	3.7	4.2	0.0
P61164	Alpha-centractin (ACTZ_MOUSE)	3.8	7.6	0.0	0.0
Q9QZ88	Vacuolar protein sorting-associated protein 29 (VPS29_MOUSE)	3.7	5.5	1.9	0.0
Q9CR00	26S proteasome non-ATPase regulatory subunit 9 (PSMD9_MOUSE)	3.7	7.4	0.0	0.0
Q8VDM6	Heterogeneous nuclear ribonucleoprotein U-like protein 1 (HNRL1_MOUSE)	3.4	5.8	1.0	0.0
O35226	26S proteasome non-ATPase regulatory subunit 4 (PSMD4_MOUSE)	3.4	6.8	0.0	0.0
P20108	Thioredoxin-dependent peroxide reductase, mitochondrial (PRDX3_MOUSE)	3.4	6.8	0.0	0.0
Q64514	Tripeptidyl-peptidase 2 (TPP2_MOUSE)	3.4	6.8	0.0	0.0
Q8K2T8	RNA polymerase II-associated factor 1 homolog (PAF1_MOUSE)	3.4	6.8	0.0	0.0
Q99L47	Hsc70-interacting protein (F10A1_MOUSE)	3.4	6.8	0.0	0.0
Q8BFZ3	Beta-actin-like protein 2 (ACTBL_MOUSE)	3.2	0.0	6.4	0.0
P47757	F-actin-capping protein subunit beta (CAPZB_MOUSE)	2.9	5.0	0.8	0.0
Q9EQU5	Protein SET (SET_MOUSE)	2.9	1.6	4.1	1.6
P61219	DNA-directed RNA polymerases I, II, and III subunit RPABC2 (RPAB2_MOUSE)	2.8	4.0	1.7	0.0
P97822	Acidic leucine-rich nuclear phosphoprotein 32 family member E (AN32E_MOUSE)	2.8	3.0	2.6	0.0
Q9JHR7	Insulin-degrading enzyme (IDE_MOUSE)	2.7	2.6	2.8	0.0
P06151	L-lactate dehydrogenase A chain (LDHA_MOUSE)	2.7	2.4	2.9	0.0
Q9QZD9	Eukaryotic translation initiation factor 3 subunit I (EIF3I_MOUSE)	2.7	2.7	2.6	0.0
O70591	Prefoldin subunit 2 (PFD2_MOUSE)	2.5	5.1	0.0	0.0
P09055	Integrin beta-1 (ITB1_MOUSE)	2.4	4.8	0.0	0.0
Q9D0B6	Protein PBDC1 (PBDC1_MOUSE)	2.4	2.7	2.0	0.0
Q9D0T1	NHP2-like protein 1 (NH2L1_MOUSE)	2.3	2.3	2.3	0.0
P83940	Elongin-C (ELOC_MOUSE)	2.2	2.9	1.5	0.0
Q99MN1	Lysine--tRNA ligase (SYK_MOUSE)	2.2	1.9	2.4	0.0

P62317	Small nuclear ribonucleoprotein Sm D2 (SMD2_MOUSE)	2.1	1.7	2.5	0.0
Q9D8X2	Coiled-coil domain-containing protein 124 (CC124_MOUSE)	2.1	0.3	3.8	0.0
O55135	Eukaryotic translation initiation factor 6 (IF6_MOUSE)	2.0	4.0	0.0	0.0
P11031	Activated RNA polymerase II transcriptional coactivator p15 (TCP4_MOUSE)	2.0	0.6	3.3	0.0
P47753	F-actin-capping protein subunit alpha-1 (CAZA1_MOUSE)	2.0	3.9	0.0	0.0
P56959	RNA-binding protein FUS (FUS_MOUSE)	1.9	1.2	2.6	0.0
P14873	Microtubule-associated protein 1B (MAP1B_MOUSE)	1.9	1.3	2.6	0.0
P58774	Tropomyosin beta chain (TPM2_MOUSE)	1.9	3.8	0.0	0.0
Q62093	Serine/arginine-rich splicing factor 2 (SRSF2_MOUSE)	1.9	0.9	2.8	0.0
Q8R1B4	Eukaryotic translation initiation factor 3 subunit C (EIF3C_MOUSE)	1.7	3.4	0.0	0.0
Q9CQK7	RWD domain-containing protein 1 (RWDD1_MOUSE)	1.7	3.4	0.0	0.0
Q76MZ3	Serine/threonine-protein phosphatase 2A 65 kDa regulatory subunit A alpha isoform (2AAA_MOUSE)	1.6	3.1	0.0	0.0
P62257	Ubiquitin-conjugating enzyme E2 H (UBE2H_MOUSE)	1.5	2.4	0.7	0.0
Q9CY58	Plasminogen activator inhibitor 1 RNA-binding protein (PAIRB_MOUSE)	1.5	0.2	2.9	0.0
P40630	Transcription factor A, mitochondrial (TFAM_MOUSE)	1.5	2.1	0.9	0.0
Q8JZQ9	Eukaryotic translation initiation factor 3 subunit B (EIF3B_MOUSE)	1.5	3.0	0.0	0.0
Q9ERF3	WD repeat-containing protein 61 (WDR61_MOUSE)	1.3	2.1	0.4	0.0
P61202	COP9 signalosome complex subunit 2 (CSN2_MOUSE)	1.2	2.4	0.0	0.0
Q99LT0	Protein dpy-30 homolog (DPY30_MOUSE)	1.1	2.3	0.0	0.0

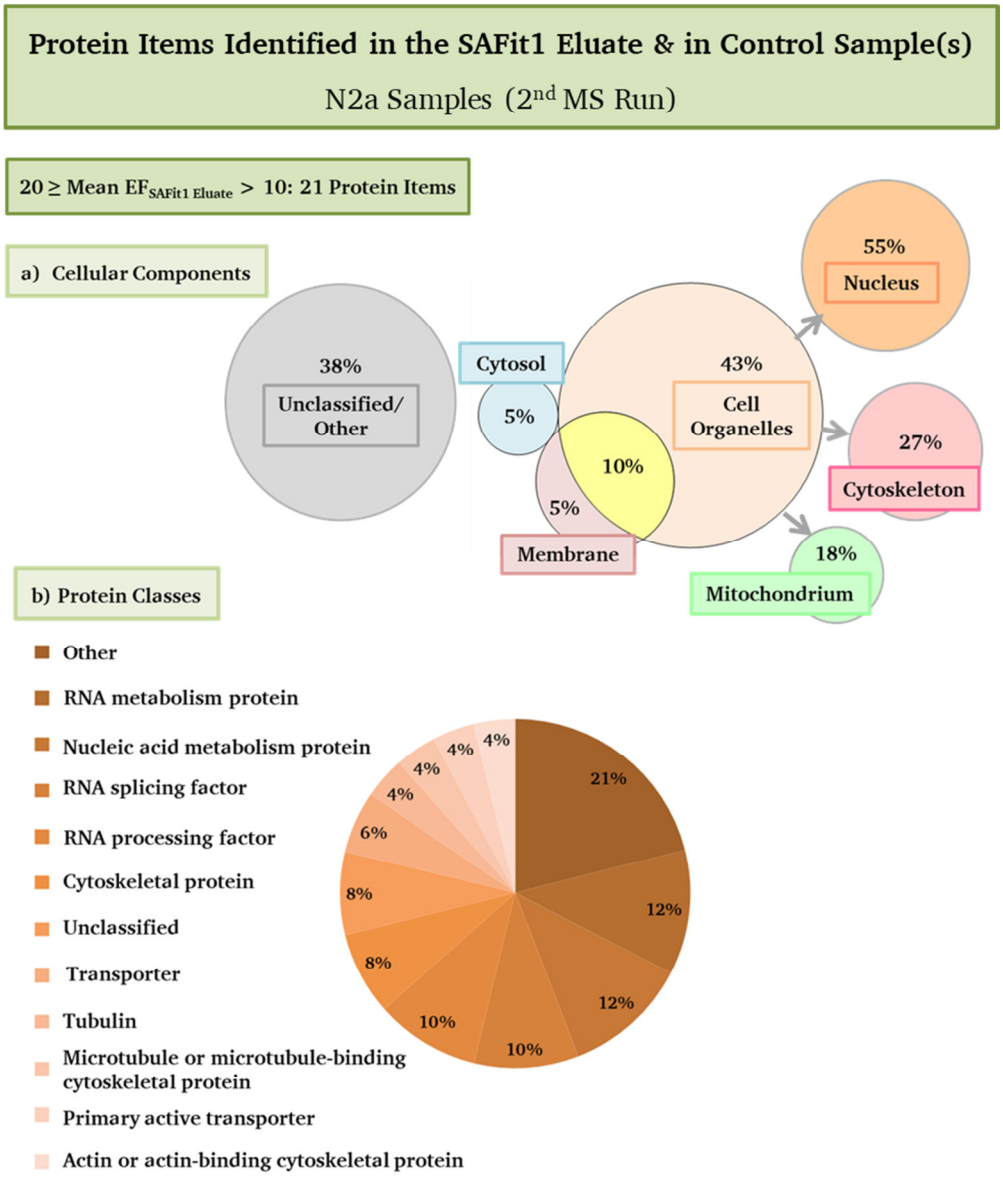

Figure 55: Assigning Mouse Protein Items Identified in the SAFit1 Dependent Eluate to Cellular Components and Protein Classes – "Intermediate/Low" Enrichment Factor.

Mouse protein items identified in the SAFit1 dependent eluate (sample C or/and sample D) and at least in one of the control samples with an enrichment factor (EF) between 10 and 20 (21 protein identifications) were assigned to cellular components (Figure a) and protein classes (Figure b) by PANTHER [4, 16, 61, 89].

Figure a: The relative cellular compartment distribution is given in %.

Figure b: The ratio of the identified protein classes is given in %. One protein item can be assigned to different protein classes.

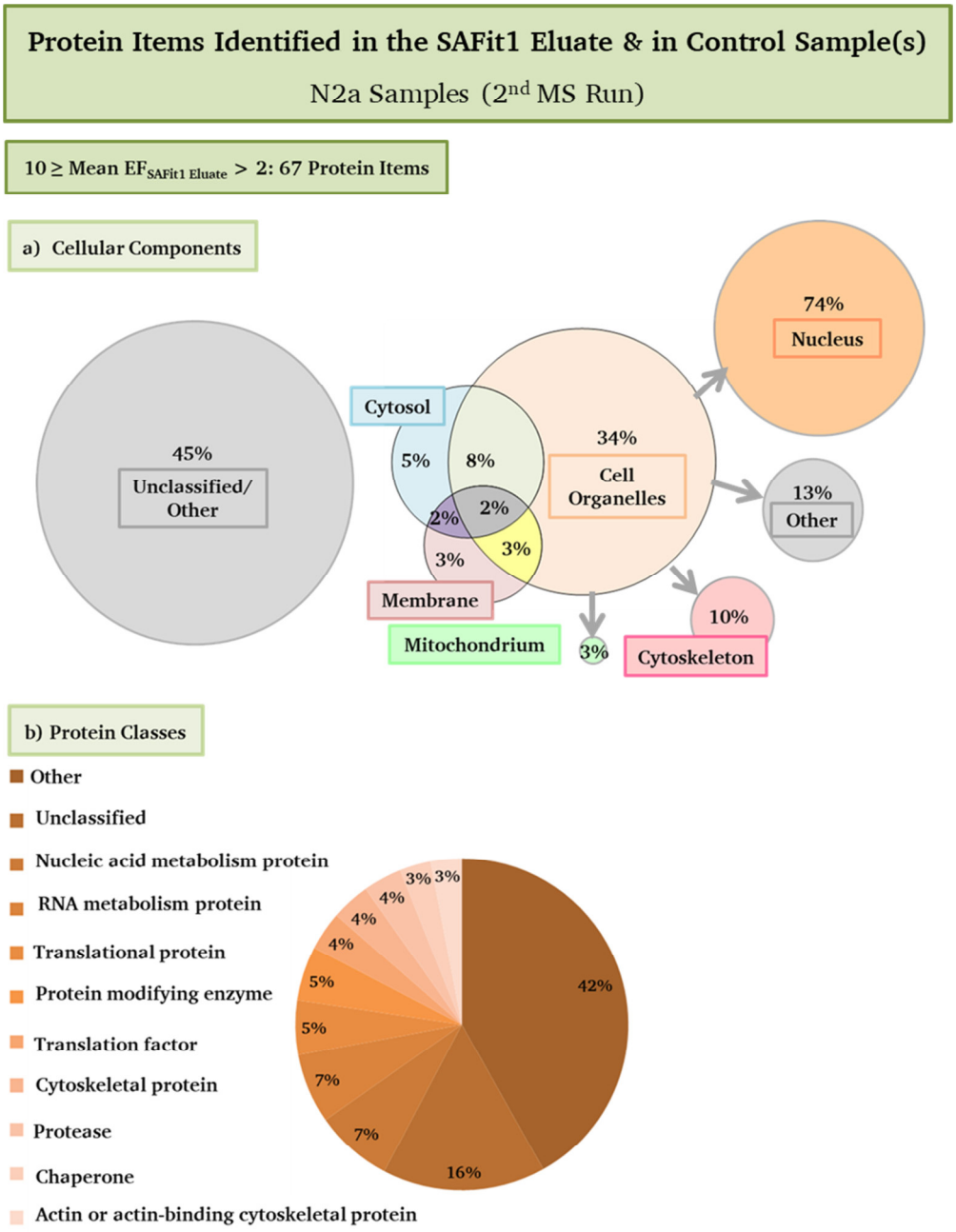

Figure 56: Assigning Mouse Protein Items Identified in the SAFit1 Dependent Eluate to Cellular Components and Protein Classes – "Low" Enrichment Factor.

Mouse protein items identified in the SAFit1 dependent eluate (sample C or/and sample D) and at least in one of the control samples with an enrichment factor (EF) between 10 and 2 (67 protein identifications) were assigned to cellular components (Figure a) and protein classes (Figure b) by PANTHER [4, 16, 61, 89].

Figure a: The relative cellular compartment distribution is given in %.

Figure b: The ratio of the identified protein classes is given in %. One protein item can be assigned to different protein classes.

6.2.3. Comparing the Protein Elution Profile from a High Density FKBP51FK1 Affinity Column and a Mock Column

The SAFit1 dependent eluates from two high density FKBP51FK1 affinity columns (final protein density: ~ 950 μM) and from two mock columns (- FKBP51FK1) were compared to identify enriched proteins. The relative protein abundance in the SAFit1 dependent eluate from a high density FKBP51FK1 affinity column was also compared with other samples carrying unspecific eluting proteins (wash fraction pools from the FKBP51FK1 affinity and the mock column) and with the complete cell lysate. Mouse protein items originating from N2a cell lysate exclusively identified in the SAFit1 dependent eluate from either both or one high density FKBP51FK1 affinity column(s) (sample 4 and/or sample 8, 3rd MS run) on the basis of at least 4 assigned spectra (mean of a technical duplicate) are listed in Table 33. These protein items were neither identified in the FKBP ligand dependent eluate (SAFit1, PPU339) nor in one of the corresponding control samples from a low density FKBP51FK1 affinity or control column (3rd MS run: samples 11 - 22). Mouse protein items identified in the SAFit1 dependent eluate from both columns, the high density FKBP51FK1 affinity and the mock column, were ranked regarding to the enrichment factor (EF) comparing the relative protein abundance in both samples (Table 34: protein items with an EF higher than 2 included). These protein items were assigned to cellular components and protein classes by PANTHER [4, 16, 61, 89] (Figure 57, Figure 58). Mouse protein items identified in the SAFit1 dependent eluate and the wash fraction pool from a high density FKBP51FK1 affinity column are also listed below (Table 35: protein items with an enrichment factor higher than 2 included).

Table 33: Mouse Protein Items Exclusively Identified in the SAFit1 Dependent Eluate from a High Density FKBP51FK1 Affinity Column – Comparing the Protein Elution Profile from a High Density FKBP51FK1 Affiniy and a Mock Column.

N2a cell lysate was loaded on two equilibrated high density FKBP51FK1 affinity columns (final protein density: about 950 µM). Two columns filled with blocked beads (- FKBP51FK1) were used as a control. All columns were washed with 50 CV buffer. 5 mM SAFit1 was added for elution. The last 20 wash fractions and the eluates from each column were pooled. Two samples of the complete N2a cell lysate were also analyzed. EF = Enrichtment factor.

Pull-down assay buffer, pH 8: 20 mM Tris, 100 mM NaCl, 0.5 mM EDTA, 1 mM PMSF, 1 mM DTT, Protease inhibitor cocktail (cOmplete mini, Roche, 1 tablet per 10 mL buffer).
Equilibration and cell lysis buffer, pH 8 = assay buffer + 0.5% (v/v) Nonidet-P40 substitute. Elution buffer, pH 8 = assay buffer ± 5 mM SAFit1.

Table 33: Mouse Protein Items Exclusively Identified in the SAFit1 Dependent Eluate from a High Density FKBP51FK1 Affinity Column – Comparing the Protein Elution Profile from a High Density FKBP51FK1 Affinity and a Mock Column.

The mouse protein items were identified in the SAFit1 dependent eluate from one or both high density FKBP51FK1 affinity columns (technical duplicate) but not in the control samples (wash fraction pools from two high density FKBP51FK1 affinity and two mock columns, SAFit1 dependent eluate from two mock columns) on the basis of at least 4 assigned spectra (5th column: mean of both SAFit1 dependent eluates, 6th column: absolute error). The relative number of identified spectra in the SAFit1 dependent eluate is given for each protein item (3rd column: mean in %, 4th column: absolute error in %). The protein abundance in the SAFit1 dependent eluate was also compared with the protein abundance in the complete cell lysate (7th column; n.a. = the protein item was not identified in the complete N2a cell lysate).

Accession Number (UniProtKB)	Description	Number of Identified Spectra (+51FK1+SAFit1)				EF = Eluate +51FK1+SAFit1 / Cell Lysate
		Relative		Absolute		
		Mean in %	Absolute Error in %	Mean	Absolute Error	
Q9QYI4	DnaJ homolog subfamily B member 12 (DJB12_MOUSE)	0.09	0.05	8	4	n.a.
Q9CQ19	Myosin regulatory light polypeptide 9 (MYL9_MOUSE)	0.06	0.06	6	6	n.a.
Q7TNC4	Putative RNA-binding protein Luc7-like 2 (LC7L2_MOUSE)	0.06	0.02	5	1	1
Q6ZQ58	La-related protein 1 (LARP1_MOUSE)	0.06	0.02	5	2	1
Q9D903	Probable rRNA-processing protein EBP2 (EBP2_MOUSE)	0.06	0.01	5	1	22
Q8K0V4	CCR4-NOT transcription complex subunit 3 (CNOT3_MOUSE)	0.05	0.01	4	1	20
Q7TSC1	Protein PRRC2A (PRC2A_MOUSE)	0.05	0.01	4	1	20
Q91W61	F-box/LRR-repeat protein 15 (FXL15_MOUSE)	0.04	0.03	4	3	18
Q9CYX7	RRP15-like protein (RRP15_MOUSE)	0.04	0.03	4	3	n.a.
Q8VE99	Coiled-coil domain-containing protein 115 (CC115_MOUSE)	0.04	0.02	4	2	n.a.
Q9QZ88	Vacuolar protein sorting-associated protein 29 (VPS29_MOUSE)	0.04	0.00	4	1	3
Q6P6I6	DNA-directed RNA polymerase II subunit GRINL1A (GRL1A_MOUSE)	0.04	0.00	4	1	n.a.
Q9D818	Suppressor APC domain-containing protein 2 (SAPC2_MOUSE)	0.04	0.00	4	1	n.a.

Table 34: Mouse Protein Items Identified in the SAFit1 Dependent Eluate from a High Density FKBP51FK1 Affinity and a Mock Column – N2a Samples 3rd MS Run.

The mouse protein items were identified in the SAFit1 dependent eluate from a high density FKBP51FK1 affinity and a mock column (- FKBP51FK1) as well. The protein items were not identified in the wash fraction pool from a high density FKBP51FK1 affinity column. Enrichment factors (mean of two pull-down assays) were calculated to compare the relative protein abundance in the SAFit1 dependent eluate from a high density FKBP51FK1 affinity column with the relative protein abundance in the complete N2a cell lysate (5th column), the SAFit1 dependent eluate (3rd column) and the wash fraction pool (4th column) from a mock column. n.a. = not available: the protein item was not identified in the wash fraction pool from a mock column (4th column) or in the complete cell lysate (5th column).

Accession Number (UniProtKB)	Description	Enrichment Factor		
		Eluate +51FK1+SAFit1 / Eluate -51FK1+SAFit1	Eluate +51FK1+SAFit1 / Wash -51FK1	Eluate +51FK1+SAFit1 / Cell Lysate
Q9QXE7	F-box-like/WD repeat-containing protein TBL1X (TBL1X_MOUSE)	28	n.a.	n.a.
Q6NVF9	Cleavage and polyadenylation specificity factor subunit 6 (CPSF6_MOUSE)	16	n.a.	8
Q8VDD8	WASH complex subunit 1 (WASH1_MOUSE)	15	n.a.	n.a.
Q9R0Q4	Mortality factor 4-like protein 2 (MO4L2_MOUSE)	14	n.a.	35
Q9CYH6	Ribosome biogenesis regulatory protein homolog (RRS1_MOUSE)	13	n.a.	32
Q14C51	Pentatricopeptide repeat domain-containing protein 3, mitochondrial (PTCD3_MOUSE)	13	n.a.	3
Q9D0B0	Serine/arginine-rich splicing factor 9 (SRSF9_MOUSE)	13	9	27
Q6NZL0	Protein SOGA3 (SOGA3_MOUSE)	12	n.a.	25
Q62318	Transcription intermediary factor 1-beta (TIF1B_MOUSE)	11	n.a.	0
Q8QZY9	Splicing factor 3B subunit 4 (SF3B4_MOUSE)	11	n.a.	10
Q60749	KH domain-containing, RNA-binding, signal transduction-associated protein 1 (KHDR1_MOUSE)	11	n.a.	n.a.
Q920E5	Farnesyl pyrophosphate synthase (FPPS_MOUSE)	11	n.a.	1
Q9JJF3	Ribosomal oxygenase 1 (RIOX1_MOUSE)	10	n.a.	20
Q62351	Transferrin receptor protein 1 (TFR1_MOUSE)	9	n.a.	1
Q91W59	RNA-binding motif, single-stranded-interacting protein 1 (RBMS1_MOUSE)	9	n.a.	n.a.
Q8BHJ5	F-box-like/WD repeat-containing protein TBL1XR1 (TBL1R_MOUSE)	9	n.a.	n.a.

Q9D554	Splicing factor 3A subunit 3 (SF3A3_MOUSE)	9	n.a.	7
Q9WV55	Vesicle-associated membrane protein-associated protein A (VAPA_MOUSE)	8	n.a.	3
Q8BTI8	Serine/arginine repetitive matrix protein 2 (SRRM2_MOUSE)	8	n.a.	1
Q3UMQ8	H/ACA ribonucleoprotein complex non-core subunit NAF1 (NAF1_MOUSE)	8	n.a.	n.a.
P70168	Importin subunit beta-1 (IMB1_MOUSE)	8	3	0
Q61029	Lamina-associated polypeptide 2, isoforms beta/delta/epsilon/gamma (LAP2B_MOUSE)	7	n.a.	12
Q8R1Q8	Cytoplasmic dynein 1 light intermediate chain 1 (DC1L1_MOUSE)	7	n.a.	1
Q9DBD5	Proline-, glutamic acid- and leucine-rich protein 1 (PELP1_MOUSE)	7	n.a.	4
Q9D6J6	NADH dehydrogenase [ubiquinone] flavoprotein 2, mitochondrial (NDUV2_MOUSE)	7	n.a.	6
O70252	Heme oxygenase 2 (HMOX2_MOUSE)	7	n.a.	1
O88522	NF-kappa-B essential modulator (NEMO_MOUSE)	6	n.a.	n.a.
Q9DCW4	Electron transfer flavoprotein subunit beta (ETFB_MOUSE)	6	n.a.	0
Q91XI1	tRNA-dihydrouridine(47) synthase [NAD(P)(+)]-like (DUS3L_MOUSE)	6	n.a.	12
P52503	NADH dehydrogenase [ubiquinone] iron-sulfur protein 6, mitochondrial (NDUS6_MOUSE)	6	n.a.	n.a.
Q99KS2	Neugrin (NGRN_MOUSE)	6	n.a.	n.a.
O54825	Bystin (BYST_MOUSE)	6	n.a.	9
Q8BHX1	HAUS augmin-like complex subunit 1 (HAUS1_MOUSE)	6	n.a.	n.a.
P60824	Cold-inducible RNA-binding protein (CIRBP_MOUSE)	6	n.a.	n.a.
Q99LF4	RNA-splicing ligase RtcB homolog (RTCB_MOUSE)	6	n.a.	3
Q91VD9	NADH-ubiquinone oxidoreductase 75 kDa subunit, mitochondrial (NDUS1_MOUSE)	6	n.a.	7
P60879	Synaptosomal-associated protein 25 (SNP25_MOUSE)	5	n.a.	4
Q3UL36	Arginine and glutamate-rich protein 1 (ARGL1_MOUSE)	5	n.a.	n.a.
Q9CYI4	Putative RNA-binding protein Luc7-like 1 (LUC7L_MOUSE)	5	n.a.	4
P56873	Protein ZNRD2 (ZNRD2_MOUSE)	5	10	5
Q9CQ25	Mitotic-spindle organizing protein 2 (MZT2_MOUSE)	5	n.a.	n.a.
Q91YT0	NADH dehydrogenase [ubiquinone] flavoprotein 1, mitochondrial (NDUV1_MOUSE)	5	n.a.	17
Q91XD7	Protein disulfide isomerase Creld1 (CREL1_MOUSE)	4	n.a.	9
Q923D5	WW domain-binding protein 11 (WBP11_MOUSE)	4	n.a.	n.a.
P63044	Vesicle-associated membrane protein 2 (VAMP2_MOUSE)	4	n.a.	n.a.
Q8C6B9	Active regulator of SIRT1 (AROS_MOUSE)	4	n.a.	n.a.
Q61137	Astrotactin-1 (ASTN1_MOUSE)	4	n.a.	n.a.
Q9DBR1	5'-3' exoribonuclease 2 (XRN2_MOUSE)	4	7	7

P40630	Transcription factor A, mitochondrial (TFAM_MOUSE)	3	n.a.	n.a.
Q91ZV0	Melanoma inhibitory activity protein 2 (MIA2_MOUSE)	3	7	n.a.
Q61249	Immunoglobulin-binding protein 1 (IGBP1_MOUSE)	3	n.a.	n.a.
Q64523	Histone H2A type 2-C (H2A2C_MOUSE)	3	n.a.	4
P62309	Small nuclear ribonucleoprotein G (RUXG_MOUSE)	3	n.a.	5
Q7TSI3	Serine/threonine-protein phosphatase 6 regulatory subunit 1 (PP6R1_MOUSE)	3	n.a.	27
Q9JKK1	Syntaxin-6 (STX6_MOUSE)	3	n.a.	n.a.
Q9EQS3	c-Myc-binding protein (MYCBP_MOUSE)	3	n.a.	7
O54908	Dickkopf-related protein 1 (DKK1_MOUSE)	3	n.a.	n.a.
Q9JLI8	Squamous cell carcinoma antigen recognized by T-cells 3 (SART3_MOUSE)	3	n.a.	7
Q9CPT5	Nucleolar protein 16 (NOP16_MOUSE)	3	n.a.	26
P25976	Nucleolar transcription factor 1 (UBF1_MOUSE)	3	n.a.	12
Q91YL2	E3 ubiquitin-protein ligase RNF126 (RN126_MOUSE)	3	n.a.	4
Q9D8C6	Mediator of RNA polymerase II transcription subunit 11 (MED11_MOUSE)	3	n.a.	n.a.
Q9JKX4	Protein AATF (AATF_MOUSE)	3	n.a.	27
Q9D7M1	Glucose-induced degradation protein 8 homolog (GID8_MOUSE)	3	n.a.	6
Q9DB42	Zinc finger protein 593 (ZN593_MOUSE)	3	n.a.	8
Q9CXL3	Uncharacterized protein C7orf50 homolog (CG050_MOUSE)	3	n.a.	6
Q9CQX2	Cytochrome b5 type B (CYB5B_MOUSE)	3	n.a.	3
Q9CZG3	COMM domain-containing protein 8 (COMD8_MOUSE)	3	n.a.	19
Q8VIJ6	Splicing factor, proline- and glutamine-rich (SFPQ_MOUSE)	3	8	7
P57784	U2 small nuclear ribonucleoprotein A' (RU2A_MOUSE)	3	n.a.	6
Q8K370	Acyl-CoA dehydrogenase family member 10 (ACD10_MOUSE)	3	n.a.	n.a.
Q9EP72	ER membrane protein complex subunit 7 (EMC7_MOUSE)	3	n.a.	n.a.
Q8BX10	Serine/threonine-protein phosphatase PGAM5, mitochondrial (PGAM5_MOUSE)	3	n.a.	33
Q7TMX5	Protein SHQ1 homolog (SHQ1_MOUSE)	3	n.a.	n.a.
Q8K3J1	NADH dehydrogenase [ubiquinone] iron-sulfur protein 8, mitochondrial (NDUS8_MOUSE)	3	n.a.	15
Q3TX08	tRNA (guanine(26)-N(2))-dimethyltransferase (TRM1_MOUSE)	3	n.a.	13
Q3TVI4	Protein HEXIM2 (HEXI2_MOUSE)	3	n.a.	n.a.
Q9CQ22	Ragulator complex protein LAMTOR1 (LTOR1_MOUSE)	3	n.a.	22
Q9D824	Pre-mRNA 3'-end-processing factor FIP1 (FIP1_MOUSE)	3	n.a.	18

Q8BMA6	Signal recognition particle subunit SRP68 (SRP68_MOUSE)	3	n.a.	18
Q60932	Voltage-dependent anion-selective channel protein 1 (VDAC1_MOUSE)	2	n.a.	1
Q99LL5	Periodic tryptophan protein 1 homolog (PWP1_MOUSE)	2	n.a.	n.a.
Q8N7N5	DDB1- and CUL4-associated factor 8 (DCAF8_MOUSE)	2	n.a.	n.a.
Q99104	Unconventional myosin-Va (MYO5A_MOUSE)	2	n.a.	n.a.
P61965	WD repeat-containing protein 5 (WDR5_MOUSE)	2	7	n.a.
Q9CR59	Growth arrest and DNA damage-inducible proteins-interacting protein 1 (G45IP_MOUSE)	2	n.a.	32
Q6PGL7	WASH complex subunit 2 (WASC2_MOUSE)	2	n.a.	18
Q8K2Q0	COMM domain-containing protein 9 (COMD9_MOUSE)	2	n.a.	n.a.
Q9JHJ0	Tropomodulin-3 (TMOD3_MOUSE)	2	n.a.	9
O35114	Lysosome membrane protein 2 (SCRB2_MOUSE)	2	n.a.	3
Q9CZA6	Nuclear distribution protein nudE homolog 1 (NDE1_MOUSE)	2	n.a.	n.a.
Q9QY76	Vesicle-associated membrane protein-associated protein B (VAPB_MOUSE)	2	n.a.	21
Q9CZT6	Protein CMSS1 (CMS1_MOUSE)	2	n.a.	22
P03975	IgE-binding protein (IGEB_MOUSE)	2	n.a.	3
Q9CQI7	U2 small nuclear ribonucleoprotein B" (RU2B_MOUSE)	2	n.a.	9
P97379	Ras GTPase-activating protein-binding protein 2 (G3BP2_MOUSE)	2	n.a.	8
Q60716	Prolyl 4-hydroxylase subunit alpha-2 (P4HA2_MOUSE)	2	n.a.	2
Q9D0I8	mRNA turnover protein 4 homolog (MRT4_MOUSE)	2	n.a.	2

Table 35: Mouse Protein Items Identified in the SAFit1 Dependent Eluate and in the Wash Fraction Pool from a High Density FKBP51FK1 Affinity Column.

The mouse protein items were identified in the SAFit1 dependent eluate and the wash fraction pool from a high density FKBP51FK1 affinity column. The relative protein abundance in the SAFit1 dependent eluate was compared with the relative protein abundance in the samples carrying unspecific eluting proteins (in the eluate from a mock column (- FKBP51FK1, 3rd column), in the wash fraction pool from a high density FKBP51FK1 affinity (4th column) or a mock (5th column) column) and with the complete N2a cell lysate. The enrichment factors are given as mean of two pull-down assays. n.a. = not available: the protein item was not identified in the corresponding sample.

Accession Number (UniProtKB)	Description	Enrichment Factor			
		Eluate +51FK1+SAFit1 / Eluate -51FK1+SAFit1	Eluate +51FK1+SAFit1 / Wash +51FK1	Eluate +51FK1+SAFit1 / Wash -51FK1	Eluate +51FK1+SAFit1 / Cell Lysate
Q8VDI7	Ubiquitin-associated domain-containing protein 1 (UBAC1_MOUSE)	n.a.	3	n.a.	n.a.
Q61112	45 kDa calcium-binding protein (CAB45_MOUSE)	n.a.	3	n.a.	15
Q8C3I8	Protein HGH1 homolog (HGH1_MOUSE)	10	5	5	2
Q9CQF3	Cleavage and polyadenylation specificity factor subunit 5 (CPSF5_MOUSE)	10	5	n.a.	1
P63280	SUMO-conjugating enzyme UBC9 (UBC9_MOUSE)	4	6	n.a.	3
Q8BFZ3	Beta-actin-like protein 2 (ACTBL_MOUSE)	3	4	11	2
P27048	Small nuclear ribonucleoprotein-associated protein B (RSMB_MOUSE)	3	5	7	6
Q9D1F4	Proline-rich AKT1 substrate 1 (AKTS1_MOUSE)	3	5	4	n.a.
Q9CR00	26S proteasome non-ATPase regulatory subunit 9 (PSMD9_MOUSE)	3	7	5	16
Q61584	Fragile X mental retardation syndrome-related protein 1 (FXR1_MOUSE)	2	2	n.a.	1
P62305	Small nuclear ribonucleoprotein E (RUXE_MOUSE)	2	7	n.a.	10
P62307	Small nuclear ribonucleoprotein F (RUXF_MOUSE)	2	3	6	12

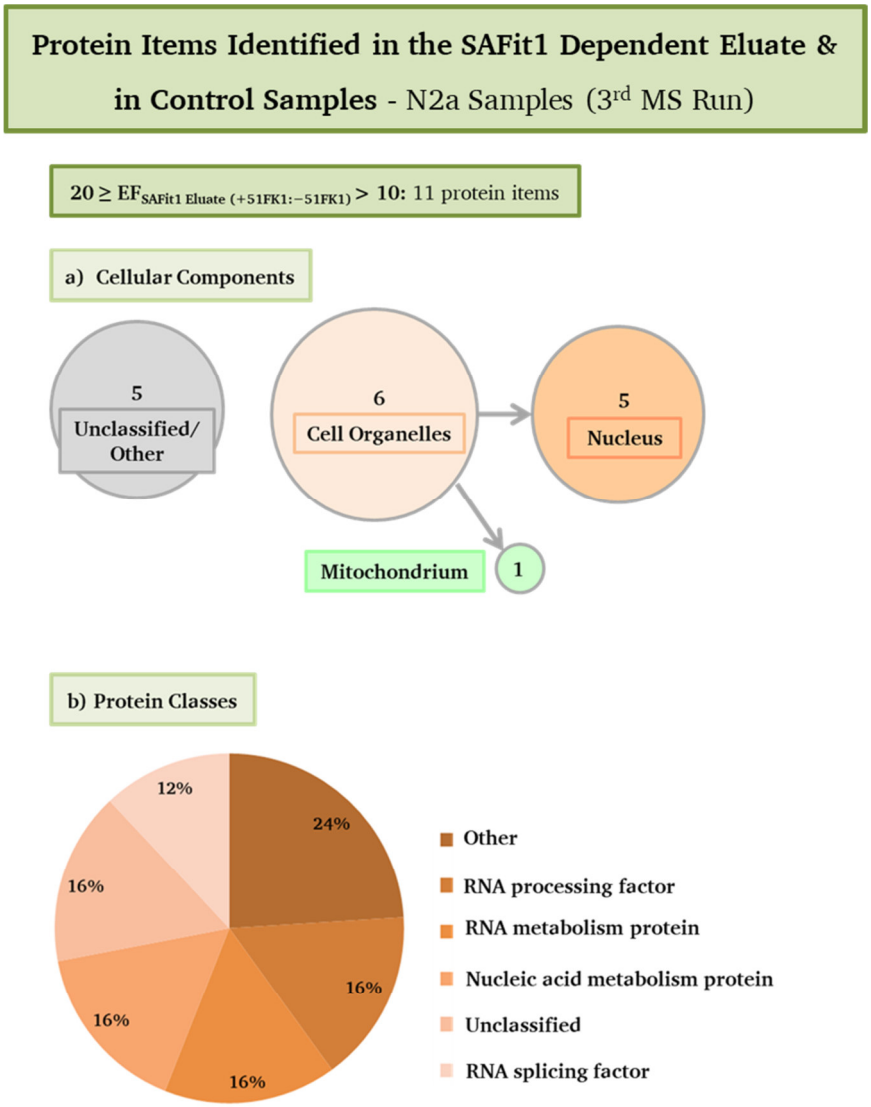

Figure 57: Assigning Mouse Protein Items Identified in the SAFit1 Dependent Eluate to Cellular Components and Protein Classes – Intermediate/Low Enrichment Factor.

The relative protein abundance in the SAFit1 dependent eluate from a high density FKBP51FK1 affinity column was compared with the SAFit1 dependent protein elution profile from a mock column (- FKBP51FK1). The protein items were not identified in the wash fraction pool from the high density FKBP51FK1 affinity column.

Mouse protein items (11 protein identifications) with an enrichment factor (EF) between 10 and 20 were assigned to cellular components (Figure a) and protein classes (Figure b) by PANTHER.

Figure a: The number of protein identifications is given for each subgroup.

Figure b: The distribution of the assigned protein classes is given in %. One protein item can be assigned to several protein classes.

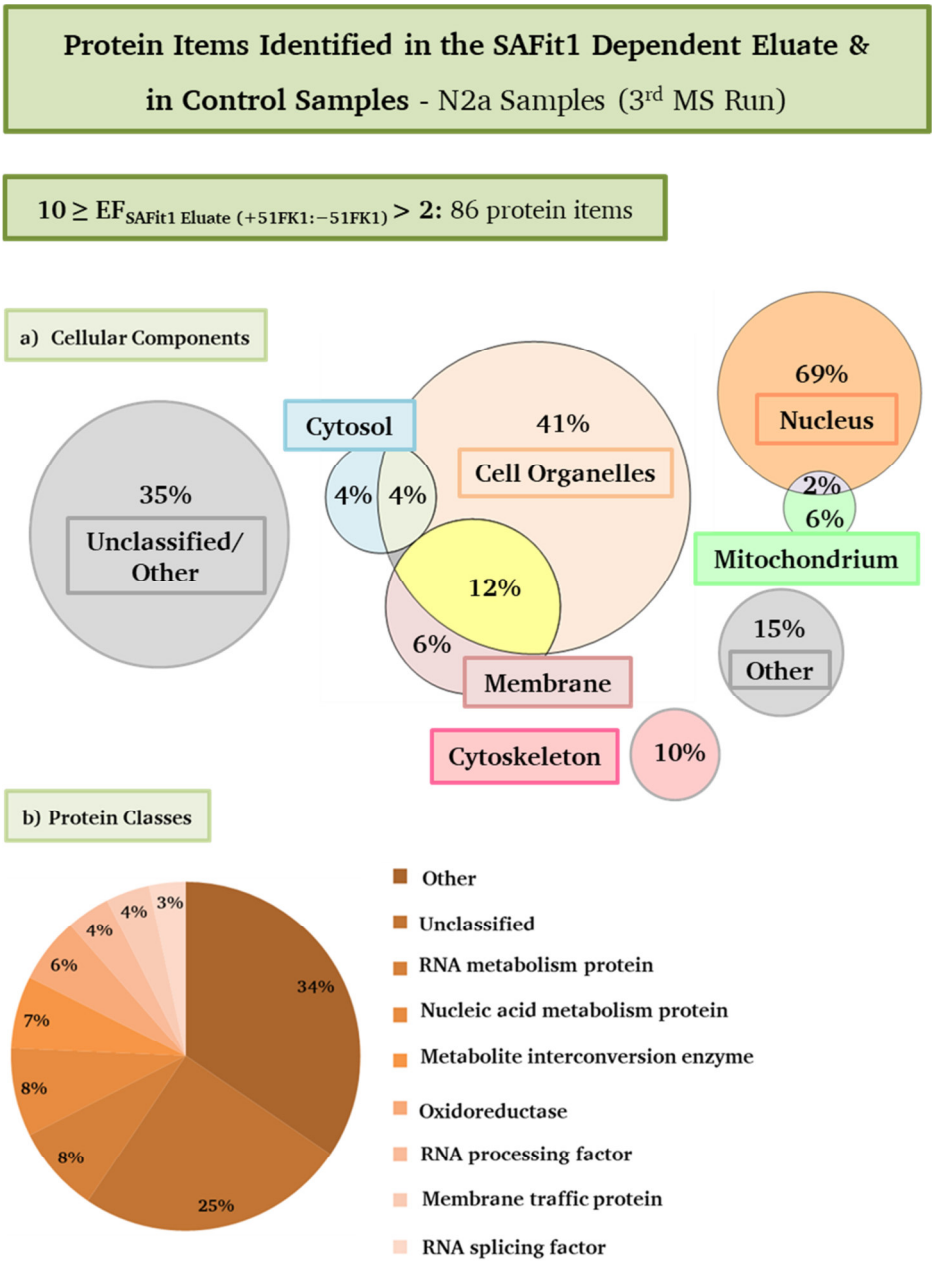

Figure 58: Assigning Mouse Protein Items Identified in the SAFit1 Dependent Eluate to Cellular Components and Protein Classes – Low Enrichment Factor.

The mouse protein elution profile in the SAFit1 dependent eluate from a high density FKBP51FK1 affinity and a mock column (- FKBP51FK1) were compared. The protein items were not identified in the wash fraction pool from the high density FKBP51FK1 affinity column.

Mouse protein items (86 protein identifications) with an enrichment factor (EF) between 2 and 10 were assigned to cellular components (Figure a) and protein classes (Figure b) by PANTHER.

Figure a: The cellular compartment distribution is given in %.

Figure b: The distribution of the assigned protein classes is given in %. One protein item can be related to different protein classes.

6.2.4. Elution from a Low Density FKBP51FK1 Affinity Column

Mouse proteins that showed the highest enrichment factors in the pull-down assay using a low density FKBP51FK1 affinity matrix are listed in Table 36. In contrast to the pull-down assays applying a high density FKBP51FK1 affinity matrix an assay buffer supplemented with 200 mM NaCl instead of 100 mM NaCl was used to decrease the background.

Table 36: Mouse Protein Items Identified in the FKBP Ligand Dependent Eluate from a Low Density FKBP51FK1 Affinity Matrix.

The mouse protein items originated from N2a cell lysate were identified in the FKBP ligand (SAFit1, PPU339) dependent eluate from a low density FKBP51FK1 affinity column. The relative protein abundance in the SAFit1 and PPU339 dependent eluate from a low density FKBP51FK1 affinity and a mock column were compared with each other (SAFit1: 4th column, PPU339: 7th column). The elution profile of SAFit1 and the non-binding SAFit1 analogue THE212P were also compared with each other (3rd column). The relative protein abundance in the FKBP ligand dependent eluates from a low density FKBP51FK1 affinity column was compared with the relative abundance in the wash fraction pools from a FKBP51FK1 affinity (SAFit1: 5th column, PPU339: 8th column)and a mock column (SAFit1: 6th, PPU339: 9th column).

Accession Number (UniProtKB)	Description	Enrichment Factor						
		Eluate +51FK1 +SAFit1 / Eluate +51FK1 +THE212P	Eluate +51FK1 +SAFit1 / Eluate -51FK1 +SAFit1	Eluate +51FK1 +SAFit1 / Wash +51FK1	Eluate +51FK1 +SAFit1 / Wash -51FK1	Eluate +51FK1 +PPU339 / Eluate -51FK1 +PPU339	Eluate +51FK1 +PPU339 / Wash +51FK1	Eluate +51FK1 +PPU339 / Wash -51FK1
P63038	60 kDa heat shock protein, mitochondrial (CH60_MOUSE)	n.a.	4	24	n.a.	n.a.	0	n.a.
P10126	Elongation factor 1-alpha 1 (EF1A1_MOUSE)	n.a.	4	5	13	n.a.	0	0
P06151	L-lactate dehydrogenase A chain (LDHA_MOUSE)	4	2	5	9	1	3	6
P09411	Phosphoglycerate kinase 1 (PGK1_MOUSE)	n.a.	0	0	0	n.a.	2	1
Q9R0P9	Ubiquitin carboxyl-terminal hydrolase isozyme L1 (UCHL1_MOUSE)	n.a.	0	1	1	4	3	1
P08249	Malate dehydrogenase, mitochondrial (MDHM_MOUSE)	n.a.	0	1	0	4	3	1
P05064	Fructose-bisphosphate aldolase A (ALDOA_MOUSE)	n.a.	0	0	0	2	3	1
P17751	Triosephosphate isomerase (TPIS_MOUSE)	1	0	1	1	2	3	2

7. Appendix

7.1. List of Figures

7.2. List of Tables

7.3. Abbreviations

A

aa	Amino acid
ACN	Acetonitrile
Amp	Ampicillin
APS	Ammonium peroxydisulphate
AR	Androgen receptor
AS160	AKT substrate of 160 kDa
AST	Active-site-titration
AU	Absorbance unit

B

BCA	Bicinchoninic acid assay

C

Cdc37	Cell division cycle protein 37
CDK	Cyclin-dependent kinase
CID	Collision-induced dissociation
CK	Christian Kozany
ClS	Claudia Sippel
cp.	Compare
Cpd	Compound
CV	Column volume

D

DMEM	Dulbecco´s Modified Eagle Medium
DMSO	Dimethyl sulfoxide
DNA	Deoxyribonucleic acid
DNAseI	Desoxyribonuclease I
DPBS	Dulbecco´s phosphate buffered saline
DTT	1,4-Dithiothreitol

E

E. coli	Escherichia coli
EC_{50}	Half maximal effective concentration

ECD	Electron-capture dissociation
EDTA	Ethylenediaminetetraacetic acid
EF	Enrichment factor
e.g.	For example
Eq.	Equivalents
ER	Estrogen receptor
ETD	Electron-transfer dissociation
EtOH	Ethanol
Exp.	Experiment(s)
Exp. No.	Experimental number

F

FA	Formic acid
FASP	Filter aided sample preparation
FBS	Fetal bovine serum
FDR	False discovery rate
FH	Felix Hausch
FI	Fluorescence intensity
FKBP	FK506 binding protein
FPA	Fluorescence polarization assay
FRAP	FKBP12-Rapamycin associated protein
FT-MS	Fourier transform ion cyclotron

G

GO	GeneOntology
GR	Glucocorticoid receptor
GSK3β	Glycogen synthase kinase 3-beta

H

HCD	Higher-energy collisional dissociation
HEK Cells	Human embryonic kidney cells
HG	Hausch glycerol stock
HP	Hausch plasmid stock
HPLC	High performance liquid chromatography
Hsp	Heat shock protein

Hs	Homo sapiens
hTERT	Human telomerase reverse transcriptase

I

IAM	Iodoacetamide
ICAT	Isotope-coded affinity tag
ICPL	Isotope coded protein labeling
$IKK_{\alpha/\beta/\gamma/\varepsilon}$	Inhibitor of nuclear factor kappa-B kinase subunit alpha/beta/gamma/epsilon
IPTG	Isopropyl β-D-1-thiogalactopyranoside
IRF	Interferon regulatory factor
iTRAQ	Isobaric tags for relative and absolute quantification

J

JBa	Johanna Bartmuß
JK	Jürgen Kolos
JPK	Jan-Philip Kahl

K

Kan	Kanamycin
Kd	Dissociation constant

L

LC	Liquid chromatography

M

MALDI	Matrix-assisted laser desorption ionization
MAVS	Mitochondrial antiviral signaling protein
MBA	Michael Bauder
ß-Me	ß-Mercaptoethanol
mgf	Mascot Generic Format
MP-H_2O	Millipore water
MR	Mineralcorticoid receptor
MS	Mass spectrometry
mTOR	Mammalian target of rapamycin

MTQ	Tianqi Mao
MWCO	Molecular weight cut-off

N

N2a Cells	Murine neuroblastoma cells
NEMO	NF-kappa-B essential modulator
NF-AT	Nuclear factor of activated T-cells
Ni	Nickel
NTA	Nitrilotriacetic acid

O

OD	Optical density
ON	Overnight

P

PDB	Protein data bank
pH	Pondus/Potentia hydrogenii
PHLPP	PH domain leucine-rich repeat-containing protein phosphatase
PLL	Poly-L-lysine
PMSF	Phenylmethylsulfonyl fluoride
PPIase	Peptidyl-prolyl *cis-trans* isomerase
$PPAR_{\gamma}$	Peroxisome proliferator-activated receptor γ
PPU	Patrick Purder
PR	Progesterone receptor
PSM	Peptide-spectrum match
PTMs	Post-translational protein modifications

R

Rap	Rapamycin
RELA	Transcription factor p65
RNA	Ribonucleic acid
RNS	Relative number of spectra
RT	Room temperature

S

SDS	Sodium dodecyl sulfate
SDS-PAGE	Sodium dodecyl sulfate polyacrylamide gel electrophoresis
SEC	Size exclusion chromatography
SHR	Steroid hormone receptor
SILAC	Stable isotope labeling by amino acids in cell culture
SIRT	NAD-dependent protein deacetylase sirtuin-7
SP3	Single-pot solid-phase-enhanced preparation
S-Trap	Suspension trapping

T

TBK1	TANK-binding kinase 1
TC	Tissue culture
TCEP	Tris(2-carboxyethyl)phosphine hydrochloride
TDS	Target-decoy search strategy
TEMED	N, N, N', N'-Tetramethylethylenediamine
TFA	Trifluoroacetic acid
TFE	2,2,2-Trifluoroethanol
THE	Tim Heymann
TMT	Tandem mass tags
TOF	Time of flight
TPR	Tetratricopeptide repeat domain
TRAF	TNF receptor associated factor

U

UPLC	Ultra-performance liquid chromatography
UV	Ultraviolet

V

VE-H_2O	Desalted tap water

7.4. Physical Units

Unit

Da	Dalton, 1 Da = 1 g/mol
g	Gram
h	Hour
L	Liter
M	Mol, 1 M = 1 mol/L
m	Meter
min	Minute
rcf	Relative centrifugal force
rpm	Revolutions per minute
v/v	Volume per volume
w/v	Weight per volume

Prefix

k	Kilo
m	Milli
μ	Micro
n	Nano
p	Pico

8. References

[1] Advanced Chemistry Development, Inc. www.acdlabs.com, 2021. *ACD/ChemSketch, version 2020.2.1*, Toronto, On, Canada.

[2] Ahern, G. P., Junankar, P. R., and Dulhunty, A. F. 1997. Subconductance states in single-channel activity of skeletal muscle ryanodine receptors after removal of FKBP12. *Biophysical Journal* 72, 1, 146–162.

[3] Akiyama, T., Shiraishi, T., Qin, J., Konno, H., Akiyama, N., Shinzawa, M., Miyauchi, M., Takizawa, N., Yanai, H., Ohashi, H., Miyamoto-Sato, E., Yanagawa, H., Yong, W., Shou, W., and Inoue, J.-I. 2014. Mitochondria-nucleus shuttling FK506-binding protein 51 interacts with TRAF proteins and facilitates the RIG-I-like receptor-mediated expression of type I IFN. *PLoS ONE* 9, 5, e95992.

[4] Ashburner, M., Ball, C. A., Blake, J. A., Botstein, D., Butler, H., Cherry, J. M., Davis, A. P., Dolinski, K., Dwight, S. S., Eppig, J. T., Harris, M. A., Hill, D. P., Issel-Tarver, L., Kasarskis, A., Lewis, S., Matese, J. C., Richardson, J. E., Ringwald, M., Rubin, G. M., and Sherlock, G. 2000. Gene ontology: tool for the unification of biology. The Gene Ontology Consortium. *Nature genetics* 25, 1, 25–29.

[5] Avila, G., Lee, E. H., Perez, C. F., Allen, P. D., and Dirksen, R. T. 2003. FKBP12 binding to RyR1 modulates excitation-contraction coupling in mouse skeletal myotubes. *The Journal of biological chemistry* 278, 25, 22600–22608.

[6] Balakrishnan, R., Harris, M. A., van Huntley, R., van Auken, K., and Cherry, J. M. 2013. A guide to best practices for Gene Ontology (GO) manual annotation. *Database: The Journal of Biological Databases and Curation* 2013.

[7] Balsevich, G., Häusl, A. S., Meyer, C. W., Karamihalev, S., Feng, X., Pöhlmann, M. L., Dournes, C., Uribe-Marino, A., Santarelli, S., Labermaier, C., Hafner, K., Mao, T., Breitsamer, M., Theodoropoulou, M., Namendorf, C., Uhr, M., Paez-Pereda, M., Winter, G., Hausch, F., Chen, A., Tschöp, M. H., Rein, T., Gassen, N. C., and Schmidt, M. V. 2017. Stress-responsive FKBP51 regulates AKT2-AS160 signaling and metabolic function. *Nature Communications* 8, 1, 1725.

[8] Barent, R. L., Nair, S. C., Carr, D. C., Ruan, Y., Rimerman, R. A., Fulton, J., Zhang, Y., and Smith, D. F. 1998. Analysis of FKBP51/FKBP52 chimeras and mutants for Hsp90 binding and association with progesterone receptor complexes. *Molecular endocrinology (Baltimore, Md.)* 12, 3, 342–354.

[9] Barg, S., Copello, J. A., and Fleischer, S. 1997. Different interactions of cardiac and skeletal muscle ryanodine receptors with FK-506 binding protein isoforms. *The American journal of physiology* 272, 5 Pt 1, C1726-33.

[10] Bartmuß, J. 2017. *Kovalente Immobilisierung des Proteins FKBP51FK1 an einer Gelmatrix unter Funktionserhalt Funktionserhalt*. Bachelor Thesis, TU Darmstadt.

[11] Bauder, M., Meyners, C., Purder, P. L., Merz, S., Sugiarto, W. O., Voll, A. M., Heymann, T., and Hausch, F. 2021. Structure-Based Design of High-Affinity Macrocyclic FKBP51 Inhibitors. *Journal of medicinal chemistry* 64, 6, 3320–3349.

[12] Baughman, G., Wiederrecht, G. J., Chang, F., Martin, M. M., and Bourgeois, S. 1997. Tissue distribution and abundance of human FKBP51, and FK506-binding protein that can mediate calcineurin inhibition. *Biochemical and biophysical research communications* 232, 2, 437–443.

[13] Bouwmeester, T., Bauch, A., Ruffner, H., Angrand, P.-O., Bergamini, G., Croughton, K., Cruciat, C., Eberhard, D., Gagneur, J., Ghidelli, S., Hopf, C., Huhse, B., Mangano, R., Michon, A.-M., Schirle, M., Schlegl, J., Schwab, M., Stein, M. A., Bauer, A., Casari, G., Drewes, G., Gavin, A.-C., Jackson, D. B., Joberty, G., Neubauer, G., Rick, J., Kuster, B., and Superti-Furga, G. 2004. A physical and functional map of the human TNF-alpha/NF-kappa B signal transduction pathway. *Nature cell biology* 6, 2, 97–105.

[14] Brown, E. J., Albers, M. W., Shin, T. B., Ichikawa, K., Keith, C. T., Lane, W. S., and Schreiber, S. L. 1994. A mammalian protein targeted by G1-arresting rapamycin-receptor complex. *Nature* 369, 6483, 756–758.

[15] Brown, E. J., Beal, P. A., Keith, C. T., Chen, J., Shin, T. B., and Schreiber, S. L. 1995. Control of p70 s6 kinase by kinase activity of FRAP in vivo. *Nature* 377, 6548, 441–446.

[16] Carbon, S., Ireland, A., Mungall, C. J., Shu, S., Marshall, B., and Lewis, S. 2009. AmiGO: online access to ontology and annotation data. *Bioinformatics (Oxford, England)* 25, 2, 288–289.

[17] Cheung-Flynn, J., Roberts, P. J., Riggs, D. L., and Smith, D. F. 2003. C-terminal sequences outside the tetratricopeptide repeat domain of FKBP51 and FKBP52 cause differential binding to Hsp90. *The Journal of biological chemistry* 278, 19, 17388–17394.

[18] Chevallet, M., Luche, S., and Rabilloud, T. 2006. Silver staining of proteins in polyacrylamide gels. *Nature protocols* 1, 4, 1852–1858.

[19] Chin, J. W., Martin, A. B., King, D. S., Wang, L., and Schultz, P. G. 2002. Addition of a photocrosslinking amino acid to the genetic code of Escherichiacoli. *Proceedings of the National Academy of Sciences of the United States of America* 99, 17, 11020–11024.

[20] Cigler, M., Müller, T. G., Horn-Ghetko, D., Wrisberg, M.-K. von, Fottner, M., Goody, R. S., Itzen, A., Müller, M. P., and Lang, K. 2017. Proximity-Triggered Covalent Stabilization of Low-Affinity Protein Complexes In Vitro and In Vivo. *Angewandte Chemie (International ed. in English)* 56, 49, 15737–15741.

[21] Condelli, V., Crispo, F., Pietrafesa, M., Lettini, G., Matassa, D. S., Esposito, F., Landriscina, M., and Maddalena, F. 2019. HSP90 Molecular Chaperones, Metabolic Rewiring, and Epigenetics: Impact on Tumor Progression and Perspective for Anticancer Therapy. *Cells* 8, 6.

[22] Des Georges, A., Clarke, O. B., Zalk, R., Yuan, Q., Condon, K. J., Grassucci, R. A., Hendrickson, W. A., Marks, A. R., and Frank, J. 2016. Structural Basis for Gating and Activation of RyR1. *Cell* 167, 1, 145-157.e17.

[23] Duncan, M. W., Aebersold, R., and Caprioli, R. M. 2010. The pros and cons of peptide-centric proteomics. *Nature biotechnology* 28, 7, 659–664.

[24] Dupree, E. J., Jayathirtha, M., Yorkey, H., Mihasan, M., Petre, B. A., and Darie, C. C. 2020. A Critical Review of Bottom-Up Proteomics: The Good, the Bad, and the Future of this Field. *Proteomes* 8, 3.

[25] Ebong, I., Beilsten-Edmands, V., Patel, N. A., Morgner, N., and Robinson, C. V. 2016. The interchange of immunophilins leads to parallel pathways and different intermediates in the assembly of Hsp90 glucocorticoid receptor complexes. *Cell Discov* 2, 1, 16002.

[26] Fabian, A.-K., März, A., Neimanis, S., Biondi, R. M., Kozany, C., and Hausch, F. 2013. InterAKTions with FKBPs--mutational and pharmacological exploration. *PLoS ONE* 8, 2, e57508.

[27] Gaali, S., Feng, X., Hähle, A., Sippel, C., Bracher, A., and Hausch, F. 2016. Rapid, Structure-Based Exploration of Pipecolic Acid Amides as Novel Selective Antagonists of the FK506-Binding Protein 51. *Journal of medicinal chemistry* 59, 6, 2410–2422.

[28] Gaali, S., Kirschner, A., Cuboni, S., Hartmann, J., Kozany, C., Balsevich, G., Namendorf, C., Fernandez-Vizarra, P., Sippel, C., Zannas, A. S., Draenert, R., Binder, E. B., Almeida, O. F. X., Rühter, G., Uhr, M., Schmidt, M. V., Touma, C., Bracher, A., and Hausch, F. 2015. Selective inhibitors of the FK506-binding protein 51 by induced fit. *Nature chemical biology* 11, 1, 33–37.

[29] Gasteiger E., Hoogland C., Gattiker A., Duvaud S., Wilkins M.R., Appel R.D., Bairoch A. 2005. Protein Identification and Analysis Tools on the ExPASy Server. (In) John M. Walker (ed): The Proteomics Protocols Handbook. *Humana Press Inc.*, 571–607.

[30] Gaudet, P. and Dessimoz, C. 2017. Gene Ontology: Pitfalls, Biases, and Remedies. In *The Gene Ontology Handbook*, C. Dessimoz and N. Škunca, Eds. Springer New York, New York, NY, 189–205. DOI=10.1007/978-1-4939-3743-1_14.

[31] Genest, O., Wickner, S., and Doyle, S. M. 2018. Hsp90 and Hsp70 chaperones: Collaborators in protein remodeling. *The Journal of biological chemistry* 294, 6, 2109–2120.

[32] Gibieža, P. and Petrikaitė, V. 2021. The regulation of actin dynamics during cell division and malignancy. *American Journal of Cancer Research* 11, 9, 4050–4069.

[33] Glatter, T., Ahrné, E., and Schmidt, A. 2015. Comparison of Different Sample Preparation Protocols Reveals Lysis Buffer-Specific Extraction Biases in Gram-Negative Bacteria and Human Cells. *Journal of proteome research* 14, 11, 4472–4485.

[34] Gnatzy, M. T., Geiger, T. M., Kuehn, A., Gutfreund, N., Walz, M., Kolos, J. M., and Hausch, F. 2021. Development of NanoBRET-Binding Assays for FKBP-Ligand Profiling in Living Cells. *Chembiochem : a European journal of chemical biology*.

[35] Goldman, A. R., Beer, L. A., Tang, H.-Y., Hembach, P., Zayas-Bazan, D., and Speicher, D. W. 2019. Proteome Analysis Using Gel-LC-MS/MS. *Current protocols in protein science* 96, 1, e93.

[36] Hähle, A., Geiger, T. M., Merz, S., Meyners, C., Tianqi, M., Kolos, J., and Hausch, F. 2019. FKBP51 and FKBP12.6-Novel and tight interactors of Glomulin. *PLoS ONE* 14, 9, e0221926.

[37] Hähle, A., Merz, S., Meyners, C., and Hausch, F. 2019. The Many Faces of FKBP51. *Biomolecules* 9, 1.

[38] HaileMariam, M., Eguez, R. V., Singh, H., Bekele, S., Ameni, G., Pieper, R., and Yu, Y. 2018. S-Trap, an Ultrafast Sample-Preparation Approach for Shotgun Proteomics. *Journal of proteome research* 17, 9, 2917–2924.

[39] Harding, M. W., Galat, A., Uehling, D. E., and Schreiber, S. L. 1989. A receptor for the immunosuppressant FK506 is a cis-trans peptidyl-prolyl isomerase. *Nature* 341, 6244, 758–760.

[40] Haslene-Hox H., Norborg A., Klinkenberg G. 2021. *Identification of protein interaction partners for the protein FKBP51 blocked by SAFit1 binding. Proteomic evaluation of samples from affinity chromatography of HEK293 cell lysate with FKBP51 and SAFit1*. Report Draft, SINTEF Industry.

[41] Haslene-Hox H., Norborg A., Klinkenberg G., Bravo S. B., Dominguez E. 2021. *Identification of protein interaction partners for the protein FKBP51 blocked by SAFit1 binding*. *Proteomic evaluation of samples from affinity chromatography of N2a cell lysate with FKBP51 and SAFit1*. Report Draft, SINTEF Industry.

[42] Heberle, H., Meirelles, G. V., da Silva, F. R., Telles, G. P., and Minghim, R. 2015. InteractiVenn: a web-based tool for the analysis of sets through Venn diagrams. *BMC bioinformatics* 16, 169.

[43] Hilario, E. C., Stern, A., Wang, C. H., Vargas, Y. W., Morgan, C. J., Swartz, T. E., and Patapoff, T. W. 2017. An Improved Method of Predicting Extinction Coefficients for the Determination of Protein Concentration. *PDA journal of pharmaceutical science and technology* 71, 2, 127–135.

[44] Hino, N., Okazaki, Y., Kobayashi, T., Hayashi, A., Sakamoto, K., and Yokoyama, S. 2005. Protein photo-cross-linking in mammalian cells by site-specific incorporation of a photoreactive amino acid. *Nature methods* 2, 3, 201–206.

[45] Jayaraman, T., Brillantes, A. M., Timerman, A. P., Fleischer, S., Erdjument-Bromage, H., Tempst, P., and Marks, A. R. 1992. FK506 binding protein associated with the calcium release channel (ryanodine receptor). *The Journal of biological chemistry* 267, 14, 9474–9477.

[46] Jeong, Y. Y., Her, J., Oh, S.-Y., and Chung, I. K. 2016. Hsp90-binding immunophilin FKBP52 modulates telomerase activity by promoting the cytoplasmic retrotransport of hTERT. *The Biochemical journal* 473, 20, 3517–3532.

[47] Jiang, W., Cazacu, S., Xiang, C., Zenklusen, J. C., Fine, H. A., Berens, M., Armstrong, B., Brodie, C., and Mikkelsen, T. 2008. FK506 binding protein mediates glioma cell growth and sensitivity to rapamycin treatment by regulating NF-kappaB signaling pathway. *Neoplasia (New York, N.Y.)* 10, 3, 235–243.

[48] Jin, L., Bi, Y., Hu, C., Qu, J., Shen, S., Wang, X., and Tian, Y. 2021. A comparative study of evaluating missing value imputation methods in label-free proteomics. *Scientific reports* 11, 1, 1760.

[49] Junttila, M. R., Saarinen, S., Schmidt, T., Kast, J., and Westermarck, J. 2005. Single-step Strep-tag purification for the isolation and identification of protein complexes from mammalian cells. *Proteomics* 5, 5, 1199–1203.

[50] Kästle, M., Kistler, B., Lamla, T., Bretschneider, T., Lamb, D., Nicklin, P., and Wyatt, D. 2018. FKBP51 modulates steroid sensitivity and NFκB signalling: A novel anti-inflammatory drug target. *European journal of immunology* 48, 11, 1904–1914.

[51] Kolos, J. M., Pomplun, S., Jung, S., Rieß, B., Purder, P. L., Voll, A. M., Merz, S., Gnatzy, M., Geiger, T. M., Quist-Løkken, I., Jatzlau, J., Knaus, P., Holien, T., Bracher, A., Meyners, C., Czodrowski, P., Krewald, V., and Hausch, F. 2021. Picomolar FKBP inhibitors enabled by a single water-displacing methyl group in bicyclic 4.3.1 aza-amides. *Chemical science* 12, 44, 14758–14765.

[52] Kolos, J. M., Voll, A. M., Bauder, M., and Hausch, F. 2018. FKBP Ligands-Where We Are and Where to Go? *Frontiers in pharmacology* 9, 1425.

[53] Kozany, C., März, A., Kress, C., and Hausch, F. 2009. Fluorescent probes to characterise FK506-binding proteins. *Chembiochem : a European journal of chemical biology* 10, 8, 1402–1410.

[54] Kumar, R., Moche, M., Winblad, B., and Pavlov, P. F. 2017. Combined x-ray crystallography and computational modeling approach to investigate the Hsp90 C-terminal peptide binding to FKBP51. *Scientific reports* 7, 1, 14288.

[55] Lagadari, M., Zgajnar, N. R., Gallo, L. I., and Galigniana, M. D. 2016. Hsp90-binding immunophilin FKBP51 forms complexes with hTERT enhancing telomerase activity‡. *Molecular Oncology* 10, 7, 1086–1098.

[56] Liu, J., Albers, M. W., Wandless, T. J., Luan, S., Alberg, D. G., Belshaw, P. J., Cohen, P., MacKintosh, C., Klee, C. B., and Schreiber, S. L. 1992. Inhibition of T cell signaling by immunophilin-ligand complexes correlates with loss of calcineurin phosphatase activity. *Biochemistry* 31, 16, 3896–3901.

[57] Liu, J., Farmer, J. D., Lane, W. S., Friedman, J., Weissman, I., and Schreiber, S. L. 1991. Calcineurin is a common target of cyclophilin-cyclosporin A and FKBP-FK506 complexes. *Cell* 66, 4, 807–815.

[58] Ludwig, K. R., Schroll, M. M., and Hummon, A. B. 2018. Comparison of In-Solution, FASP, and S-Trap Based Digestion Methods for Bottom-Up Proteomic Studies. *Journal of proteome research* 17, 7, 2480–2490.

[59] Luo, K., Li, Y., Yin, Y., Li, L., Wu, C., Chen, Y., Nowsheen, S., Hu, Q., Zhang, L., Lou, Z., and Yuan, J. 2017. USP49 negatively regulates tumorigenesis and chemoresistance through FKBP51-AKT signaling. *The EMBO journal* 36, 10, 1434–1446.

[60] Maiarù, M., Tochiki, K. K., Cox, M. B., Annan, L. V., Bell, C. G., Feng, X., Hausch, F., and Géranton, S. M. 2016. The stress regulator FKBP51 drives chronic pain by modulating spinal glucocorticoid signaling. *Science translational medicine* 8, 325, 325ra19.

[61] Mi, H., Muruganujan, A., Ebert, D., Huang, X., and Thomas, P. D. 2019. PANTHER version 14: more genomes, a new PANTHER GO-slim and improvements in enrichment analysis tools. *Nucleic Acids Res* 47, D1, D419-D426.

[62] Ohama, T. 2019. The multiple functions of protein phosphatase 6. *Biochimica et biophysica acta. Molecular cell research* 1866, 1, 74–82.

[63] O'Keefe, S. J., Tamura, J., Kincaid, R. L., Tocci, M. J., and O'Neill, E. A. 1992. FK-506- and CsA-sensitive activation of the interleukin-2 promoter by calcineurin. *Nature* 357, 6380, 692–694.

[64] Oroz, J., Chang, B. J., Wysoczanski, P., Lee, C.-T., Pérez-Lara, Á., Chakraborty, P., Hofele, R. V., Baker, J. D., Blair, L. J., Biernat, J., Urlaub, H., Mandelkow, E., Dickey, C. A., and Zweckstetter, M. 2018. Structure and pro-toxic mechanism of the human Hsp90/PPIase/Tau complex. *Nature Communications* 9.

[65] *PANTHER Class Information. Membrane, GO:0016020. http://pantherdb.org/panther/category.do?categoryAcc=GO:0016020, 09/01/2022.*

[66] *PANTHER Class Information. Cytosol, GO:0005829. http://pantherdb.org/panther/category.do?categoryAcc=GO:0005829, 09/01/2022.*

[67] *PANTHER Class Information. Organelle, GO:0043226. http://pantherdb.org/panther/category.do?categoryAcc=GO:0043226, 09/01/2022.*

[68] Pei, H., Li, L., Fridley, B. L., Jenkins, G. D., Kalari, K. R., Lingle, W., Petersen, G., Lou, Z., and Wang, L. 2009. FKBP51 affects cancer cell response to chemotherapy by negatively regulating Akt. *Cancer cell* 16, 3, 259–266.

[69] Perez-Riverol, Y., Wang, R., Hermjakob, H., Müller, M., Vesada, V., and Vizcaíno, J. A. 2014. Open source libraries and frameworks for mass spectrometry based proteomics: a developer's perspective. *Biochimica et biophysica acta* 1844, 1 Pt A, 63–76.

[70] Pomplun, S., Sippel, C., Hähle, A., Tay, D., Shima, K., Klages, A., Ünal, C. M., Rieß, B., Toh, H. T., Hansen, G., Yoon, H. S., Bracher, A., Preiser, P., Rupp, J., Steinert, M., and Hausch, F. 2018. Chemogenomic Profiling of Human and Microbial FK506-Binding Proteins. *Journal of medicinal chemistry* 61, 8, 3660–3673.

[71] Prasad, B., Achour, B., Artursson, P., Hop, C. E. C. A., Lai, Y., Smith, P. C., Barber, J., Wisniewski, J. R., Spellman, D., Uchida, Y., Zientek, M. A., Unadkat, J. D., and Rostami-Hodjegan, A. 2019. Toward a Consensus on Applying Quantitative Liquid Chromatography-Tandem Mass Spectrometry Proteomics in Translational Pharmacology Research: A White Paper. *Clinical pharmacology and therapeutics* 106, 3, 525–543.

[72] Reynolds, P. D., Ruan, Y., Smith, D. F., and Scammell, J. G. 1999. Glucocorticoid resistance in the squirrel monkey is associated with overexpression of the immunophilin FKBP51. *The Journal of clinical endocrinology and metabolism* 84, 2, 663–669.

[73] Riggs, D. L., Roberts, P. J., Chirillo, S. C., Cheung-Flynn, J., Prapapanich, V., Ratajczak, T., Gaber, R., Picard, D., and Smith, D. F. 2003. The Hsp90-binding peptidylprolyl isomerase FKBP52 potentiates glucocorticoid signaling in vivo. *The EMBO journal* 22, 5, 1158–1167.

[74] Romano, S., D'Angelillo, A., Pacelli, R., Staibano, S., Luna, E. de, Bisogni, R., Eskelinen, E.-L., Mascolo, M., Calì, G., Arra, C., and Romano, M. F. 2010. Role of FK506-binding protein 51 in the control of apoptosis of irradiated melanoma cells. *Cell death and differentiation* 17, 1, 145–157.

[75] Romano, S., Di Pace, A., Sorrentino, A., Bisogni, R., Sivero, L., and Romano, M. F. 2010. FK506 binding proteins as targets in anticancer therapy. *Anti-cancer agents in medicinal chemistry* 10, 9, 651–656.

[76] Sabers, C. J., Martin, M. M., Brunn, G. J., Williams, J. M., Dumont, F. J., Wiederrecht, G., and Abraham, R. T. 1995. Isolation of a protein target of the FKBP12-rapamycin complex in mammalian cells. *The Journal of biological chemistry* 270, 2, 815–822.

[77] Scheufler, C., Brinker, A., Bourenkov, G., Pegoraro, S., Moroder, L., Bartunik, H., Hartl, F. U., and Moarefi, I. 2000. Structure of TPR domain-peptide complexes: critical elements in the assembly of the Hsp70-Hsp90 multichaperone machine. *Cell* 101, 2, 199–210.

[78] Schülke, J.-P., Wochnik, G. M., Lang-Rollin, I., Gassen, N. C., Knapp, R. T., Berning, B., Yassouridis, A., and Rein, T. 2010. Differential impact of tetratricopeptide repeat proteins on the steroid hormone receptors. *PLoS ONE* 5, 7, e11717.

[79] Sergei Saveliev, Daniel Simpson, William Daily, Carolyn Woodroofe, Dieter Klaubert, Grzegorz Sabat, Robert Bulliet, Keith V.Wood. 2008. *Improve Protein Analysis with the New, Mass Spectrometry-Compatible ProteasMAX™ Surfactant*.

[80] Shevchenko, A., Tomas, H., Havlis, J., Olsen, J. V., and Mann, M. 2006. In-gel digestion for mass spectrometric characterization of proteins and proteomes. *Nature protocols* 1, 6, 2856–2860.

[81] SIB Swiss Institute of Bioinformatics. *Expasy ProtParam Tool*.

[82] Siekierka, J. J., Hung, S. H., Poe, M., Lin, C. S., and Sigal, N. H. 1989. A cytosolic binding protein for the immunosuppressant FK506 has peptidyl-prolyl isomerase activity but is distinct from cyclophilin. *Nature* 341, 6244, 755–757.

[83] Sinars, C. R., Cheung-Flynn, J., Rimerman, R. A., Scammell, J. G., Smith, D. F., and Clardy, J. 2003. Structure of the large FK506-binding protein FKBP51, an Hsp90-binding protein and a component of steroid receptor complexes. *Proceedings of the National Academy of Sciences of the United States of America* 100, 3, 868–873.

[84] Stechschulte, L. A., Hinds, T. D., Ghanem, S. S., Shou, W., Najjar, S. M., and Sanchez, E. R. 2014. FKBP51 reciprocally regulates GRα and PPARγ activation via the Akt-p38 pathway. *Molecular endocrinology (Baltimore, Md.)* 28, 8, 1254–1264.

[85] Stechschulte, L. A., Qiu, B., Warrier, M., Hinds, T. D., Zhang, M., Gu, H., Xu, Y., Khuder, S. S., Russo, L., Najjar, S. M., Lecka-Czernik, B., Yong, W., and Sanchez, E. R. 2016. FKBP51 Null Mice Are Resistant to Diet-Induced Obesity and the PPARγ Agonist Rosiglitazone. *Endocrinology* 157, 10, 3888–3900.

[86] Steele, T. W. E. and Samsó, M. 2019. The FKBP12 subunit modifies the long-range allosterism of the ryanodine receptor. *Journal of structural biology* 205, 2, 180–188.

[87] Szklarczyk, D., Gable, A. L., Lyon, D., Junge, A., Wyder, S., Huerta-Cepas, J., Simonovic, M., Doncheva, N. T., Morris, J. H., Bork, P., Jensen, L. J., and Mering, C. von. 2019. STRING v11: protein-protein association networks with increased coverage, supporting functional discovery in genome-wide experimental datasets. *Nucleic Acids Res* 47, D1, D607-D613.

[88] The, M., Tasnim, A., and Käll, L. 2016. How to talk about protein-level false discovery rates in shotgun proteomics. *Proteomics* 16, 18, 2461–2469.

[89] 2021. The Gene Ontology resource: enriching a GOld mine. *Nucleic Acids Res* 49, D1, D325-D334.

[90] The UniProt Consortium. 2019. UniProt: a worldwide hub of protein knowledge. *Nucleic Acids Res* 47, D1, D506-D515.

[91] Tianqi Mao. 2020. *Development of Novel Small-Molecule Degraders of FK506-Binding Protein 51*. PhD Thesis.

[92] Timerman, A. P., Ogunbumni, E., Freund, E., Wiederrecht, G., Marks, A. R., and Fleischer, S. 1993. The calcium release channel of sarcoplasmic reticulum is modulated by FK-506-binding protein. Dissociation and reconstitution of FKBP-12 to the calcium release channel of skeletal muscle sarcoplasmic reticulum. *The Journal of biological chemistry* 268, 31, 22992–22999.

[93] Tyanova, S., Temu, T., Sinitcyn, P., Carlson, A., Hein, M. Y., Geiger, T., Mann, M., and Cox, J. 2016. The Perseus computational platform for comprehensive analysis of (prote)omics data. *Nature methods* 13, 9, 731–740.

[94] 2021. UniProt: the universal protein knowledgebase in 2021. *Nucleic acids research* 49, D1, D480-D489.

[95] van Duyne, G. D., Standaert, R. F., Karplus, P. A., Schreiber, S. L., and Clardy, J. 1991. Atomic structure of FKBP-FK506, an immunophilin-immunosuppressant complex. *Science (New York, N.Y.)* 252, 5007, 839–842.

[96] Vaudel, M., Burkhart, J. M., Zahedi, R. P., Oveland, E., Berven, F. S., Sickmann, A., Martens, L., and Barsnes, H. 2015. PeptideShaker enables reanalysis of MS-derived proteomics data sets. *Nature biotechnology* 33, 1, 22–24.

[97] Venturi, E., Galfré, E., O'Brien, F., Pitt, S. J., Bellamy, S., Sessions, R. B., and Sitsapesan, R. 2014. FKBP12.6 Activates RyR1: Investigating the Amino Acid Residues Critical for Channel Modulation. *Biophysical Journal* 106, 4, 824–833.

[98] Verdier-Pinard, P., Pasquier, E., Xiao, H., Burd, B., Villard, C., Lafitte, D., Miller, L. M., Angeletti, R. H., Horwitz, S. B., and Braguer, D. 2008. TUBULIN PROTEOMICS: TOWARDS BREAKING THE CODE1. *Analytical biochemistry* 384, 2, 197–206.

[99] Vermeer, H., Hendriks-Stegeman, B. I., van der Burg, B., van Buul-Offers, S. C., and Jansen, M. 2003. Glucocorticoid-induced increase in lymphocytic FKBP51 messenger ribonucleic acid expression: a potential marker for glucocorticoid sensitivity, potency, and bioavailability. *The Journal of clinical endocrinology and metabolism* 88, 1, 277–284.

[100] Voll, A. M., Meyners, C., Taubert, M. C., Bajaj, T., Heymann, T., Merz, S., Charalampidou, A., Kolos, J., Purder, P. L., Geiger, T. M., Wessig, P., Gassen, N. C., Bracher, A., and Hausch, F. 2021. Macrocyclic FKBP51 Ligands Define a Transient Binding Mode with Enhanced Selectivity. *Angewandte Chemie (International ed. in English)* 60, 24, 13257–13263.

[101] Wang, Z. X. 1995. An exact mathematical expression for describing competitive binding of two different ligands to a protein molecule. *FEBS letters* 360, 2, 111–114.

[102] Wang, Z. X., Kumar, N. R., and Srivastava, D. K. 1992. A novel spectroscopic titration method for determining the dissociation constant and stoichiometry of protein-ligand complex. *Analytical biochemistry* 206, 2, 376–381.

[103] Witte, C.-P., Noël, L. D., Gielbert, J., Parker, J. E., and Romeis, T. 2004. Rapid one-step protein purification from plant material using the eight-amino acid StrepII epitope. *Plant molecular biology* 55, 1, 135–147.

[104] Wu, B., Li, P., Liu, Y., Lou, Z., Ding, Y., Shu, C., Ye, S., Bartlam, M., Shen, B., and Rao, Z. 2004. 3D structure of human FK506-binding protein 52: implications for the assembly of the glucocorticoid receptor/Hsp90/immunophilin heterocomplex. *Proceedings of the National Academy of Sciences of the United States of America* 101, 22, 8348–8353.

[105] Yan, Z., Bai, X., Yan, C., Wu, J., Li, Z., Xie, T., Peng, W., Yin, C., Li, X., Scheres, S. H. W., Shi, Y., and Yan, N. 2015. Structure of the rabbit ryanodine receptor RyR1 at near-atomic resolution. *Nature* 517, 7532, 50–55.

[106] Yanagisawa, T., Hino, N., Iraha, F., Mukai, T., Sakamoto, K., and Yokoyama, S. 2012. Wide-range protein photo-crosslinking achieved by a genetically encoded N(ε)-(benzyloxycarbonyl)lysine derivative with a diazirinyl moiety. *Molecular bioSystems* 8, 4, 1131–1135.

[107] Zissimopoulos, S. and Lai, F. A. 2005. Interaction of FKBP12.6 with the cardiac ryanodine receptor C-terminal domain. *The Journal of biological chemistry* 280, 7, 5475–5485.

9. Publication

Bauder, M., Meyners, C., Purder, P. L., **Merz, S.**, Sugiarto, W. O., Voll, A. M., Heymann, T., and Hausch, F. 2021. Structure-Based Design of High-Affinity Macrocyclic FKBP51 Inhibitors. *Journal of medicinal chemistry* 64, 6, 3320–3349.

Kolos, J. M., Pomplun, S., Jung, S., Rieß, B., Purder, P. L., Voll, A. M., **Merz, S.**, Gnatzy, M., Geiger, T. M., Quist-Løkken, I., Jatzlau, J., Knaus, P., Holien, T., Bracher, A., Meyners, C., Czodrowski, P., Krewald, V., and Hausch, F. 2021. Picomolar FKBP inhibitors enabled by a single water-displacing methyl group in bicyclic 4.3.1 aza-amides. *Chemical science* 12, 44, 14758–14765.

Voll, A. M., Meyners, C., Taubert, M. C., Bajaj, T., Heymann, T., **Merz, S.**, Charalampidou, A., Kolos, J., Purder, P. L., Geiger, T. M., Wessig, P., Gassen, N. C., Bracher, A., and Hausch, F. 2021. Macrocyclic FKBP51 Ligands Define a Transient Binding Mode with Enhanced Selectivity. *Angewandte Chemie (International ed. in English)* 60, 24, 13257–13263.

Hähle, A., Geiger, T. M., **Merz, S.**, Meyners, C., Tianqi, M., Kolos, J., and Hausch, F. 2019. FKBP51 and FKBP12.6-Novel and tight interactors of Glomulin. *PLoS ONE* 14, 9, e0221926.

Hähle, A., Merz, S., Meyners, C., and Hausch, F. 2019. The Many Faces of FKBP51. *Biomolecules* 9, 1.

Roos WP, Quiros S, Krumm A, **Merz S**, Switzeny OJ, Christmann M, Loquai C, Kaina B. B-Raf inhibitor vemurafenib in combination with temozolomide and fotemustine in the killing response of malignant melanoma cells. Oncotarget. 2014 Dec 30;5(24):12607-20.

10. Acknowledgement

I thank:

- Professor Felix Hausch for giving me the opportunity to complete my PhD under his supervision
- Christian Schimsheimer and my family for their mental support
- Tim Heymann for the synthesis of SAFit1 and THE212P
- Patrick Purder for the synthesis of PPU339
- Hanne Haslene-Hox, Anna Nordborg and Geir Klingenberg for the proteomic MS analysis
- Especially Hanne Haslene-Hox for answering all my questions about proteomic analysis and her supervision
- Michael Bauder, Jürgen Kolos, Tianqi Mao, Patrick Purder and Andreas Voll for the synthesis of chemical compounds
- All my former colleagues for making me smile in the lab and scientific discussions
- Claudia Sippel for being our “telephone joker” after laboratory relocation.

The proteomic analysis has received funding from the European Union´s Horizon 2020 research and innovation program under grant agreement No 823893 (EU-OPENSCREEN-DRIVE).